

**CHARACTERIZATION OF CHOLESTEROL-FREE LIPOSOMES FOR
USE IN DELIVERY OF ANTI-CANCER DRUGS**

by

NANCY DOS SANTOS

B.Sc. (Pharmacology and Therapeutics, Hons),
The University of British Columbia, 1999

A THESIS SUBMITTED IN PARTIAL FULFILLMENT OF THE
REQUIREMENTS FOR THE DEGREE OF

DOCTOR OF PHILOSOPHY

in

THE FACULTY OF GRADUATE STUDIES

Department of Pathology and Laboratory Medicine

We accept this thesis as conforming to the required standard

THE UNIVERSITY OF BRITISH COLUMBIA

September 2004

© Nancy Dos Santos, 2004

ABSTRACT

Improving existing therapies with lipid based carriers has been successfully applied to drugs that have narrow therapeutic indices, such as anti-cancer agents. It is known that the addition of cholesterol to a lipid matrix of gel phase lipids ($> C18$), increases the permeability of lipid membranes below the phase transition temperature (T_c) of the bulk phospholipid species used, and thus it is predicted that these formulations may retain drugs that are not compatible with conventional (cholesterol-containing) liposome formulations. Liposomes composed of 1,2-distearoyl-*sn*-phosphatidylcholine (DSPC), without added cholesterol, were effectively stabilized by incorporation of PEG-lipids, where stability was defined by parameters including prevention of surface-surface interactions and extending blood residence times.

Cholesterol-free liposomes as carriers for anti-cancer drugs are hampered, in part, because standard pH gradient-based loading methods rely on high temperatures ($> T_c$ of the phospholipids used), which can collapse the ion gradient and / or result in unstable loading. Doxorubicin, for example, could not be loaded efficiently into cholesterol-free DSPC liposomes, a problem that was circumvented by the addition of 10% (v/v) ethanol, as a permeability enhancer. Another more hydrophobic anthracycline, idarubicin, could be encapsulated in cholesterol-free liposomes without the aid of ethanol as a permeability enhancer. Cryo-transmission electron microscopic studies indicated that idarubicin formed a precipitate within the liposomes. Pharmacokinetic studies demonstrated that liposome encapsulation manifested a 66-fold increase ($1.97 \mu\text{mole h ml}^{-1}$) in the mean plasma area-under-the-curve (AUC) as compared to free idarubicin ($0.03 \mu\text{mole h ml}^{-1}$). Further alterations in lipid composition, including decreasing PEG-lipid and internal citrate (osmolarity) concentrations, resulted in stepwise improvements in drug retention and blood residence times. The optimized

lipid formulation, DSPC / DSPE-PEG₂₀₀₀ (98:2 mole ratio, 150 mM citrate), mediated a 175-fold ($7.0 \mu\text{mole h ml}^{-1}$) increase in mean plasma AUC and 5.5-fold (6.74 h) increase in the plasma half-life ($T_{1/2}$) when compared to free idarubicin. Antitumor activity of liposomal idarubicin was assessed in a P388 lymphocytic leukemia model, the median survival at the maximum tolerable dose (3 mg/kg) was 22 days (175 % ILS) for liposomal idarubicin and 19.5 days (144 % ILS) for free idarubicin. These results warranted further investigation to improve the therapeutic activity of liposomal idarubicin through use of combination drug treatments.

In order to assess this, a liposomal formulation of gemcitabine was prepared and the antitumor activity of a combination treatment consisting of liposomal gemcitabine and liposomal idarubicin was evaluated. Gemcitabine was passively encapsulated in DSPC / CH / DSPE-PEG₂₀₀₀ (50:45:5 mole ratio) at a 0.1 drug-to-lipid mole ratio. Pharmacokinetic studies indicated that encapsulation of gemcitabine in liposomes mediated a 135-fold ($15.4 \mu\text{mole h ml}^{-1}$) and 8-fold (14.3 h) increase in the mean plasma AUC and plasma half-life, respectively. An increase in median survival was observed in liposomal treatment groups of gemcitabine (3.4 mg/kg) / idarubicin (2 mg/kg) administered at 0.66 maximum tolerable doses for individual drugs. The median survival time was 30 days (281 % ILS) for liposomal gemcitabine / liposomal idarubicin, as compared to 16 days (100 % ILS) for 5 mg/kg liposomal gemcitabine, and 20.5 days (156 % ILS) for 2 mg/kg liposomal idarubicin. Assessment of the combination of these liposomal drugs yielded supra-additive effects.

TABLE OF CONTENTS

ABSTRACT	ii
TABLE OF CONTENTS	iv
LIST OF FIGURES	ix
LIST OF TABLES	xii
ABBREVIATIONS	xiii
ACKNOWLEDGEMENTS	xvi
DEDICATION	xvii
CHAPTER 1. INTRODUCTION	1
1.1. Cancer	1
1.1.1. Therapeutic interventions	2
1.1.2. Future treatment strategies	4
1.2. Drug Delivery	7
1.2.1. Liposomes	9
1.2.1.1. Liposome components	9
1.2.2. Classification of liposomes	16
1.2.3. Physicochemical properties of liposomes	19
1.2.3.1. Shape hypothesis of lipid polymorphism	19
1.2.3.2. Gel-to-liquid crystalline phase transition	21
1.2.4. Liposome formulations	23
1.2.4.1. Conventional liposomes	23
1.2.4.2. Sterically stabilized liposomes	24
1.2.5. Liposomes as drug carriers	24
1.2.5.1. Passive loading	26
1.2.5.2. Remote loading	26
1.2.6. Biological stability of liposomes	28
1.2.6.1. Plasma proteins	29
1.2.6.2. Mononuclear phagocytic system	31
1.2.7. Future directions of liposomal drug delivery	32
1.3. Thesis Rationale and Hypotheses	34
CHAPTER 2. MATERIALS AND METHODS	35
2.1. Materials	35

2.2.	Liposome Preparation	37
2.3.	Analytical Methods	37
2.3.1.	QELS liposome size analysis	37
2.3.2.	Trapped volume and lactose retention studies	39
2.3.3.	pH gradient determination	40
2.3.4.	Size exclusion chromatography	40
2.3.5.	Cryo-transmission electron microscopy	40
2.3.6.	Freeze fracture	41
2.3.7.	Drug and liposomal membrane association studies	44
2.3.8.	Liposomal plasma protein binding assay	45
2.4.	Drug Loading	48
2.4.1.	Remote loading of anthracyclines	48
2.4.2.	Passive loading of gemcitabine	49
2.5.	Pharmacokinetic Analysis	50
2.5.1.	Mice	50
2.5.2.	Plasma elimination of drugs	50
2.5.3.	Plasma elimination of liposomes	51
2.5.4.	Plasma elimination of liposomal drugs	52
2.5.5.	Anthracycline partitioning assay	52
2.5.6.	WinNonlin / pharmacokinetic modeling	53
2.6.	Cells and Culture	55
2.6.1.	Subculturing and trypan blue staining	55
2.6.2.	MTT cytotoxicity assay	56
2.6.3.	Calculusyn for analyzing drug combination treatments	57
2.7.	Animal Models	58
2.7.1.	Evaluation of antitumor activity in P388 lymphocytic leukemia model	58
2.7.2.	Evaluation of antitumor activity in MDA435/LCC6 human breast xenograft model	59
2.8.	Statistical Analysis	60

CHAPTER 3.IMPROVED RETENTION OF IDARUBICIN AFTER INTRAVENOUS INJECTION OBTAINED FOR CHOLESTEROL-FREE LIPOSOMES

61

3.1.	Introduction	61
3.2.	Hypothesis	63

3.3.	Results	63
3.3.1.	Circulation longevity of cholesterol-free liposomes	63
3.3.2.	Influence of poly(ethylene glycol) content and molecular weight on cholesterol-free liposome circulation longevity	66
3.3.3.	Optimal drug loading conditions for idarubicin	70
3.3.4.	Evaluation of liposomal idarubicin by cryo-transmission electron microscopy	72
3.3.5.	Pharmacokinetic analysis of liposomal idarubicin	74
3.4.	Discussion	74

CHAPTER 4. INFLUENCE OF POLY(ETHYLENE GLYCOL) GRAFTING DENSITY AND POLYMER LENGTH ON CHOLESTEROL-FREE LIPOSOMES: RELATING PLASMA CIRCULATION LIFETIMES TO PROTEIN BINDING

4.1.	Introduction	83
4.2.	Hypothesis	85
4.3.	Results	86
4.3.1.	Effect of DSPE-PEG ₂₀₀₀ grafting density on plasma circulation longevity of liposomes	86
4.3.2.	Factors limiting the amount of diacylphosphatidyl-ethanolamine-conjugated poly(ethylene glycol) lipid incorporation into DSPC liposomes	88
4.3.3.	Effect of PEG molecular weight on the circulation longevity of DSPC liposomes containing 5 and 2 mol% PEG-modified lipid	92
4.3.4.	Separation of liposomes from bulk plasma protein binding to liposomes and quantification of tightly adsorbed proteins both in vitro and in vivo	93
4.4.	Discussion	100

CHAPTER 5. pH GRADIENT LOADING OF ANTHRACYCLINES INTO CHOLESTEROL-FREE LIPOSOMES: ENHANCING DRUG LOADING RATES THROUGH USE OF ETHANOL

5.1.	Introduction	108
5.2.	Hypothesis	109
5.3.	Results	109

5.3.1.	Drug loading studies of anthracyclines in cholesterol-free liposomes	109
5.3.2.	Plasma elimination studies of anthracyclines encapsulated in cholesterol-free liposomes	110
5.3.3.	Drug and liposomal membrane association of anthracyclines	112
5.3.4.	Influence of ethanol on doxorubicin loading in liposomes	115
5.3.5.	Optimal ethanol concentration for drug loading in liposomes	117
5.3.6.	Influence of temperature, lipid concentration and phospholipid acyl chain length on ethanol-enhanced drug loading rates	121
5.3.7.	Influence of ethanol on release of entrapped doxorubicin in vivo	126
5.4.	Discussion	128
CHAPTER 6. DESIGNING A LIPOSOMAL CARRIER FOR THE HYDROPHOBIC ANTHRACYCLINE IDARUBICIN: SUBSTANTIAL INCREASES IN DRUG CONCENTRATIONS IN PLASMA ENHANCE THERAPEUTIC ACTIVITY IN A SENSITIVE, BUT NOT MULTIDRUG RESISTANT, MURINE LEUKEMIA MODEL		134
6.1.	Introduction	134
6.2.	Hypothesis	137
6.3.	Results	137
6.3.1.	Pharmacokinetics of free and liposomal idarubicin: effect of PEG concentration and internal citrate concentration	137
6.3.2.	Antitumor activity of single dose administration of free and liposomal idarubicin in the murine P388 leukemia model and MDA435/LCC6 (WT / MDR) breast xenograft model	144
6.3.3.	Evaluation of free and liposomal idarubicin in multidrug resistant MDA435/LCC6 (MDR) and P388 (ADR) tumor cells	150
6.4.	Discussion	153
CHAPTER 7. ACHIEVING SYNERGISTIC ANTITUMOR ACTIVITY IN VIVO: COMBINATION TREATMENT WITH LIPOSOMAL FORMULATIONS OF IDARUBICIN AND GEMCITABINE		161
7.1.	Introduction	161

7.2.	Hypothesis	163
7.3.	Results	164
7.3.1.	P388 lymphocytic leukemia cytotoxicity of gemcitabine and idarubicin used alone, and in combination	164
7.3.2.	Liposome encapsulation and plasma elimination of gemcitabine	166
7.3.3.	Antitumor activity of free and liposomal gemcitabine in P388 murine leukemia	172
7.4.	Discussion	177
CHAPTER 8. SUMMARIZING DISCUSSION		182
REFERENCES		191

LIST OF FIGURES

Figure 1.1.	Cancer: imbalance between survival and death signals	3
Figure 1.2.	Chemical structures of the anthracyclines and the cytidine analogues	6
Figure 1.3.	Structure of DSPE-PEG ₂₀₀₀ and the mushroom and brush conformations of PEG chains	14
Figure 1.4.	Lipid phase transition and influence of cholesterol on the phase transition temperature of DPPC liposomes	22
Figure 1.5.	Passive targeting of sterically stabilized liposomes	25
Figure 1.6.	An illustration of drug loading methods and drug distribution in liposomes	27
Figure 1.7.	An illustration of a multifunctional liposome	33
Figure 2.1.	Analysis of mean liposome diameter by quasielastic light scattering	38
Figure 2.2.	Cryo-transmission electron microscopy sample preparation stage	42
Figure 2.3.	Interpretation of 2-dimensional cryo-TEM images from 3-dimensional samples	43
Figure 2.4.	Flow chart: Separation of liposomes from bulk plasma proteins and quantitation of plasma protein adsorbed to liposomes	46
Figure 3.1.	Plasma elimination of liposome formulations in Balb/c mice	65
Figure 3.2.	Plasma elimination of liposomes prepared using phosphatidylcholine species with varying acyl chain lengths in the absence and presence of PE-PEG ₂₀₀₀	67
Figure 3.3.	Plasma elimination of DSPC liposomes containing increasing mol% PE-PEG ₂₀₀₀	68
Figure 3.4.	Plasma elimination of DSPC liposomes containing varying molecular weights of 5 mol% DSPE-PEG	69
Figure 3.5.	Remote loading of idarubicin into liposome formulations at 37°C and 65°C	71

Figure 3.6.	Cryo-transmission electron micrographs of “empty” and idarubicin-containing cholesterol-free and cholesterol-containing liposomes	73
Figure 3.7.	Plasma elimination of liposomal idarubicin following i.v. injection of cholesterol-free and cholesterol-containing liposomes	75
Figure 3.8.	Membrane partitioning of drugs encapsulated in liposomes through use of pH gradients and formation of a crystalline precipitate	81
Figure 4.1.	The effect of DSPE-PEG ₂₀₀₀ grafting density on the plasma elimination of cholesterol-free liposomes	87
Figure 4.2.	The effect of PEG-lipid concentration on liposome size as determined by QELS and freeze-fracture analysis	89
Figure 4.3.	Size exclusion chromatography analysis of DSPC liposomes prepared with 5 - 20 mol% DSPE-PEG ₂₀₀₀	91
Figure 4.4.	The effect of PEG-lipid molecular weight on the plasma elimination of DSPC liposomes	94
Figure 4.5.	Separation of DSPC liposomes containing 5 mol% DSPE-PEG ₂₀₀₀ from bulk mouse plasma proteins by size exclusion chromatography	96
Figure 4.6.	SDS-PAGE analysis of liposome-associated plasma proteins	99
Figure 5.1.	Time course of uptake of anthracyclines in cholesterol-free liposomes and the plasma elimination of anthracyclines encapsulated in DSPC / DSPE-PEG ₂₀₀₀ liposomes	111
Figure 5.2.	Influence of drug hydrophobicity on the liposomal membrane association in cholesterol-free and cholesterol-containing liposomes	113
Figure 5.3.	Ethanol-enhanced increases in drug loading rates into liposomes	116
Figure 5.4.	Influence of ethanol concentration on the accumulation of doxorubicin in cholesterol-free liposomes	118
Figure 5.5.	Influence of ethanol on liposome structure	122
Figure 5.6.	Influence of temperature and lipid concentration on ethanol-enhanced loading of doxorubicin into cholesterol-free liposomes	123

Figure 5.7.	The effect of phospholipid acyl chain length on ethanol-enhanced loading of doxorubicin into cholesterol-free liposomes	125
Figure 5.8.	Plasma elimination of liposomal doxorubicin: comparison of drug release from samples prepared in the absence and presence of 10% (v/v) ethanol	127
Figure 6.1.	The effect of DSPE-PEG concentration on the plasma elimination of idarubicin encapsulated in DSPC / DSPE-PEG ₂₀₀₀ (95:5 mole ratio) liposomes	138
Figure 6.2.	The effect of drug loading on the transmembrane pH gradient in liposomes prepared with varying internal citrate concentrations and the effect of osmotic gradients on liposome structure	141
Figure 6.3.	The effect of citrate concentration on the plasma elimination of idarubicin encapsulated in DSPC / DSPE-PEG ₂₀₀₀ (98:2 mole ratio) liposomes	143
Figure 6.4.	Antitumor activity of free and liposomal idarubicin on the growth of MDA435/LCC6 WT breast cancer xenografts in SCID Rag 2M mice	146
Figure 6.5.	Antitumor activity of free and liposomal idarubicin in mice bearing murine P388 WT leukemia (ascites) model	148
Figure 6.6.	Cytotoxicity of idarubicin and doxorubicin on MDA435/LCC6 wild type / MDR and P388 wild type / ADR cell lines	151
Figure 7.1.	Cytotoxic activity of gemcitabine and idarubicin and combinations thereof on P388 lymphocytic leukemia cells	165
Figure 7.2.	Dose reduction index analysis at IC ₉₀ of idarubicin (IDA) and gemcitabine (GEM) used alone or in combination and the combination index of GEM / IDA (1:10) fixed molar ratio	167
Figure 7.3.	Plasma elimination of free and liposomal gemcitabine in Balb/c mice	170
Figure 7.4.	P388 antitumor activity of a single i.v. bolus injection of free and liposomal gemcitabine administered at the maximum tolerated dose (MTD)	173
Figure 7.5.	Antitumor activity of free and liposomal idarubicin and gemcitabine combination treatment	176

LIST OF TABLES

Table 1.1.	Some chemotherapeutic agents used in the treatment of cancer	5
Table 1.2.	List of FDA approved liposomal agents	8
Table 1.3.	List of synthetic phospholipids commonly used in liposomes	11
Table 1.4.	Calculated mole fraction of PEG-lipid in area occupied by one PEG chain of different molecular weights in DSPC / DSPE-PEG ₂₀₀₀ liposomes	17
Table 1.5.	The percentage of surface area covered in liposome formulations containing 2 and 5 mol% PEG of different molecular weights	18
Table 1.6.	Shape hypothesis of lipid polymorphism	20
Table 2.1.	Summary of pharmacokinetic parameters	54
Table 4.1.	Summary of protein binding values to liposomes determined using in vitro and in vivo methods	97
Table 5.1.	The influence of ethanol concentration on size, % lactose retained and pH gradient in DSPC / DSPE-PEG ₂₀₀₀ (95:5 mole ratio)	120
Table 6.1.	Summary of pharmacokinetic parameters of free and liposomal idarubicin	145
Table 6.2.	Antitumor activity of free and liposomal formulations of idarubicin in BDF-1 mice bearing P388 tumors	149
Table 6.3.	Cytotoxicity of idarubicin and doxorubicin in wild type and resistant cell lines	152
Table 7.1.	Effect of lipid composition on the drug-to-lipid mole ratio and encapsulation efficiency of passively loaded gemcitabine	169
Table 7.2.	Summary of pharmacokinetic parameters of free and liposomal gemcitabine	171
Table 7.3.	Antitumor activity of combinations of free and liposomal idarubicin / gemcitabine in BDF-1 mice bearing P388 tumors	175

ABBREVIATIONS

AFU	Arbitrary fluorescence units
AML	Acute myelogenous leukemia
ANOVA	Analysis of variance
AUC	Area-under-the-curve
BALB/c	Inbred strain of mice
BCA	Bicinchoninic acid
BDF-1	Hybrid strain of mice
BSA	Bovine serum albumin
^{14}C	Carbon 14 radiolabel
CH	Cholesterol
CHE	Cholesteryl hexadecyl ether
Cryo-TEM	Cryo-transmission electron microscopy
DAPC	1,2-diarachidoyl- <i>sn</i> -glycero-3-phosphatidylcholine
DAUN	Daunorubicin hydrochloride
DBPC	1,2-dibehenoyl- <i>sn</i> -glycero-3-phosphatidylcholine
DMEM	Dulbecco's modified Eagle's medium
DMPC	1,2-dimyristoyl- <i>sn</i> -glycero-3-phosphatidylcholine
DMSO	Dimethylsulfoxide
DNA	Deoxyribonucleic acid
DOX	Doxorubicin hydrochloride
DPM	Disintegrations per minute
DPPC	1,2-dipalmitoyl- <i>sn</i> -glycero-3-phosphatidylcholine
DPPE	1,2-dipalmitoyl- <i>sn</i> -glycero-3-phosphatidylethanolamine
DSC	Differential scanning calorimetry
DSPC	1,2-distearoyl- <i>sn</i> -glycero-3-phosphatidylcholine
DSPE	1,2-distearoyl- <i>sn</i> -glycero-3-phosphatidylethanolamine
EDTA	Ethylenediaminetetraacetic acid
EPI	Epirubicin hydrochloride
FBS	Fetal bovine serum
GEM	Gemcitabine

$^3\text{[H]}$	Tritium radiolabel
HEPES	N-[2-hydroxyethyl]piperazine-N'-[2-ethanesulfonic acid]
HBS	HEPES buffered saline
HBSS	Hanks balanced salt solution
H_2SO_4	Sulphuric acid
i.p.	Intraperitoneal
i.v.	Intravenous
IC_{50}	The concentration required to achieve 50% inhibition in cell proliferation
IC_{90}	The concentration required to achieve 90% inhibition in cell proliferation
IDA	Idarubicin hydrochloride
ILS	Increase in lifespan
LSC	Liquid scintillation counting
LUV	Large unilamellar vesicle
MDA435/LCC6	Human breast carcinoma cell line
MDA435/LCC6 MDR1	Human breast carcinoma subline transfected with human MDR1 gene
MDR	Multidrug resistance
MLV	Multilamellar vesicle
MPPC	1-palmitoyl-2-hydroxy- <i>sn</i> -glycero-3-phosphocholine
MPS	Mononuclear phagocytic system
MTD	Maximum tolerable dose
MTT	3-[4,5-dimethylthiazol-2-yl]-2,5-diphenyl tetrazolium bromide
MW	Molecular weight
MWCO	Molecular weight cut off
OGP	Octyl- β -D-glucopyranoside
P388	Murine lymphocytic leukemia cell line
P388/ADR	Murine lymphocytic leukemia cell line resistant to doxorubicin
P_B	Protein binding value (μg protein / μmole lipid)
PBS	Phosphate buffered saline

PC	Phosphatidylcholine
PAGE	Polyacrylamide gel electrophoresis
PE	Phosphatidylethanolamine
PEG	Poly(ethylene glycol)
PK	Pharmacokinetic
QELS	Quasielastic light scattering
RPM	Revolutions per minute
SCID	Severe combined immunodeficient (mouse strain)
S.D.	Standard deviation
SDS	Sodium dodecyl sulphate
S.E.M.	Standard error of the mean
SUV	Small unilamellar vesicle
T_c	Gel-to-liquid crystalline phase transition temperature
UV	Ultraviolet
VIS	Visible
v/v	Volume to volume ratio
WT	Wild type

ACKNOWLEDGEMENTS

First, and foremost, I would like to thank my supervisor, Dr. Marcel Bally, for taking me under his wing and taking a chance on me. I don't think words can express how much of an influence you have had on my life. Your accomplishments and overwhelming dedication to your work are truly motivating.

A special thanks to Sean Semple, Troy Harasym, Sandy Klimuk and Dawn Waterhouse for showing me the ropes and getting me "hooked on science".

I am also greatly indebted to the Department of Advanced Therapeutics. There are so many people who directly, and indirectly, helped in the preparation of this thesis. I will try my best to not forget anyone...

I'd like to thank my summer students Kelly Cox, Ryan Gallagher and the "Dutchies" Annemarie Dopen, Floris van Baarda and Alex van Hecke for showing such enthusiasm and dedication during their time with me. You guys really kept me on my toes!

My supervisory committee Dr. Don Brooks, Dr. Karen Gelmon, Dr. John Hill, and Dr. Wan Lam for all your advice and commitment.

To Gigi Chiu, Euan Ramsay, Gwyn Bebb, Spencer Kong, Ludger Ickenstein, Sharon Johnstone, Ghania Chikh, Paul Tardi, Yanping Hu and Margaret Kliman-Depa for all the laughs and the insightful (and not-so insightful) discussions.

I'd like to give a special thank you to "the gang", who made coming to work so much fun, Jennifer Shabbits, Sheela Abraham, Jason Sartor, Daniel Menezes, Frances Wong, Lincoln Edwards, Catherine Tucker, Michelle Wong and Kevin Bennewith. I'll never forget the lunch breaks at GGW and the nights at the Odyssey and Urban Well. Good times! I have built life-long friendships with all of you!

To my office mates Corinna Warburton and Janet Woo, for being great listeners, getting me out of the lab for coffee breaks and keeping me sane.

To my dear friends, Cristina Tsaparas, Christine Allen, Ivana Cecic, Michelle Mullen, Caroline Bodner, Diana Silva, and Rick McNee for all your love and support.

And to the new members who have recently joined Advanced Therapeutics, you are all in good hands!

DEDICATION

To my parents,

Fernando and Ermelinda Dos Santos,

for all their love and support

and for showing me that the only way to achieve your goals

is through hard work and dedication,

and even though it may not always be easy,

in the end you will always be grateful for what you have accomplished!

CHAPTER 1

INTRODUCTION

In recent years lipid-based carriers, such as liposomes, have successfully encapsulated chemotherapeutic agents ameliorating some toxicity issues, while enhancing the overall therapeutic activity in cancer patients. The goal of this thesis was to design and characterize cholesterol-free liposomal formulations for a hydrophobic anthracycline, idarubicin. Moreover, the antitumor activity of this liposomal formulation was evaluated when used alone and in combination with gemcitabine.

1.1. Cancer

Cancer is one of the leading causes of mortality in Canada with an estimated 182 deaths per 100,000 people. According to the National Cancer Institute of Canada, the probability of developing cancer in one's lifetime is between 38 - 41%, while the probability of dying is between 23 - 27% (National Cancer Institute of Canada, Canadian Cancer Statistics, 2003, Toronto, 2003). The most prevalent types of cancer are prostate cancer and breast cancer in men and women, respectively. Lung cancer is the most frequent cause of death for both sexes. As evidenced by the high incidence and mortality rates, novel treatments strategies for this formidable disease are warranted.

Cancer is defined by a continual proliferation of abnormal cells leading to the formation of a tumor mass (local disease), that can invade other tissues and spread throughout the body (systemic disease). It is believed that an underlying genetic instability initiates, directly or indirectly through interactions with environmental factors, the transformation from a normal to an abnormal cell. Over time, the acquisition of multiple genetic mutations affecting normal cell

processes such as cell cycle, apoptosis, DNA repair and cell proliferation culminates in transformed cells that are heterogeneous and difficult to control [1].

Hanahan and Weinberg summarized the “hallmarks of cancer”, describing cancer as a manifestation of alterations to the normal cell [2]. More specifically, these alterations include insensitivity to growth inhibitory signals, evasion of programmed cell death, self-sufficiency of growth signals, limitless replicative potential, sustained angiogenesis, tissue invasion and metastasis [2] and disrupt the delicate balance between survival and death signals as illustrated in Figure 1.1.

1.1.1. Therapeutic Interventions

Most often cancer is treated with a myriad of therapeutic interventions including surgery, ionizing radiation and chemotherapy, the combination of which depends on the type and stage of disease. The goal of treatment is to reduce local tumor burden and eliminate all malignant cells. Surgery and radiation therapy are effective for local or contained disease, and is often curative at early stages of disease, but not all types of cancer can be treated by these methods. Hence the important role of chemotherapy not only in terms of control of local disease and prevention of relapse but also in the treatment of systemic disease. Adjuvant or palliative chemotherapy is administered to further improve overall survival and reduce disease relapse.

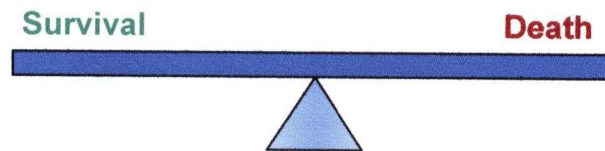
Since the first clinical trials for cancer investigating the application of nitrogen mustards [3], there has been a significant improvement in overall survival rates in select cancer patients. Once incurable cancers, such as childhood leukemia, are now treated with an expectation of a 90% long term survival rate. The continual progress in survival outcomes and advancement in

Figure 1.1

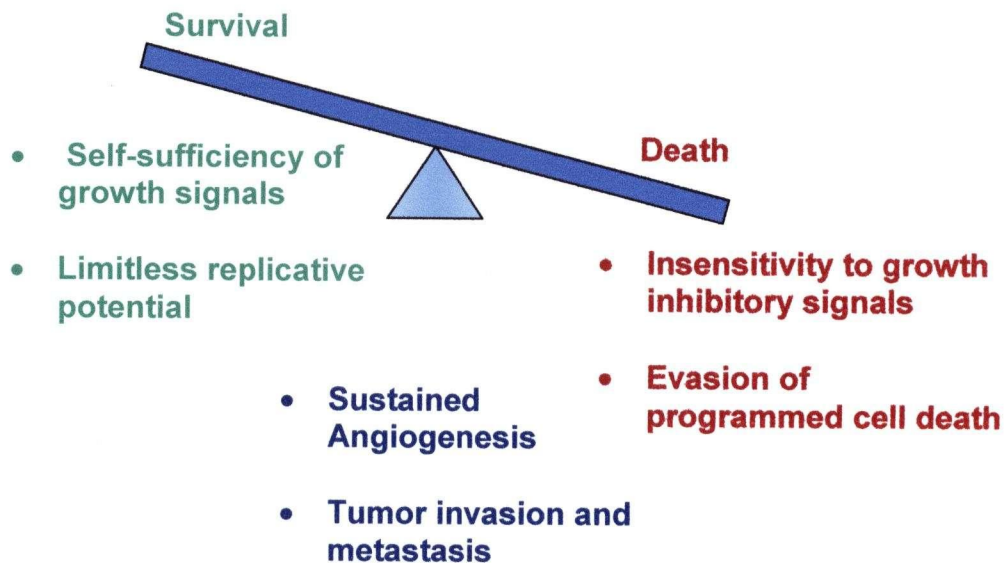
Cancer: imbalance between survival and death signals

(A) Normal cells have both survival and death signaling pathways in balance; however, (B) malignant cells aberrant cellular proliferation is achieved by enhancement in survival signals including “self sufficiency of growth signals and limitless replicative potential” and a reduction in death signals by “insensitivity to growth inhibitory signals and evasion of programmed cell death”. Other signaling processes are required to support the growth of a malignant tumor mass including “sustained angiogenesis and tumor invasion and metastasis”. The “hallmarks of cancer” was adapted from Hanahan D. *et al.* [2].

A. NORMAL CELL



B. MALIGNANT CELL



treatments have strongly paralleled the acquired scientific knowledge in tumor biology; and this is highlighted by the development of combination chemotherapy regimes that take into consideration mechanisms of drug action and developmental resistance [4].

Common classes of chemotherapeutic agents are listed in Table 1.1. Two drugs used in the thesis were idarubicin (an anthracycline antibiotic) and gemcitabine (a nucleoside analogue), which are reviewed in the introduction of Chapters 6 and 7, respectively, and the chemical structures are shown in Figure 1.2. Both idarubicin and gemcitabine interfere in the process of DNA synthesis for the intended purpose of targeting the rapidly dividing malignant cells. As not all cancer cells are rapidly proliferating and normal self-renewing cells are affected, these agents are very toxic, which is reflected by their narrow therapeutic indices. Note that the therapeutic index is a relative measure of a drug's toxic side effects (e.g., death, weight loss, myelosuppression) and therapeutic effects (e.g., antitumor activity or median survival).

1.1.2. Future Treatment Strategies

As the differences between normal and acquired malignant phenotypes and genotypes are understood, rational and targeted therapies are being developed and investigated in clinical trials. More recent novel treatments include manipulations of the immune system [5], stimulation of normal haematopoietic elements [6], induction of differentiation in tumor tissues [7], inhibition of angiogenesis [8] and delivery of genetic therapies [9].

The innovation in sequencing of the human genome and advancement in technologies to profile alterations in protein and genetic expression, coupled with the understanding of aberrant molecular signaling pathways and identification of target molecules, will significantly advance the treatment of cancer. One of the most recent accomplishments in targeted therapy, was

Table 1.1**Some chemotherapeutic agents used in the treatment of cancer**

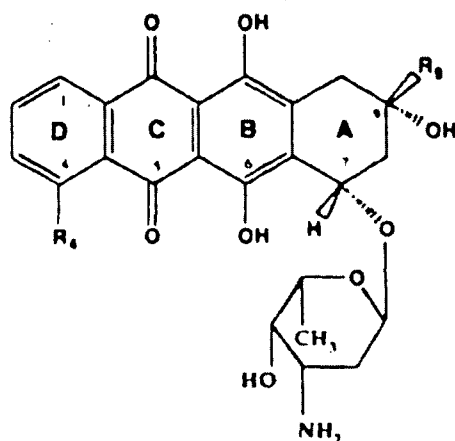
Drug Class	Chemical Name	Mechanism(s) of Action
Antitumor Antibiotics	Anthracyclines	Stabilize topoisomerase II-DNA cleavable complexes, DNA intercalation
	Actinomycin D	Inhibits DNA-directed RNA synthesis
Plant Alkaloids	Taxanes	Interfere with microtubules
	Vinca alkaloids	Bind tubulin, disrupt mitotic spindle formation
Nucleoside Analogues	Gemcitabine / Cytarabine	Inhibits DNA synthesis
	6-MP/ 6-TG	Inhibits DNA synthesis
Antimetabolites	Fludarabine / 2-CdA 5-Fluorouracil	Inhibits DNA synthesis Inhibits thymidylate synthase
	Methotrexate	Competitive inhibitor of DHFR, Inhibits DNA synthesis
Alkylating Agents	Cyclophosphamide	Intra-strand DNA crosslinker
	Temozolomide	Methylates guanine residues in DNA
Camptothecin Derivatives	Chlorambucil / Melphalan Topotecan / CPT-11	Intrastrand DNA crosslinker Stabilizes topoisomerase I-DNA complex
Epipodophyllotoxins	Etoposide	Stabilizes topoisomerase II-DNA cleavable complex
Platinum-Based Compounds	Cisplatin / Carboplatin	Intra-strand DNA crosslinker

Abbreviations: 6-MP, 6-mecaptopurine; 6-TG, 6-thioguanine; 2-CdA, 2-chlorodeoxyadenosine; DHFR, dihydrofolate reductase

Figure 1.2

Chemical structures of the anthracyclines and the cytidine analogues

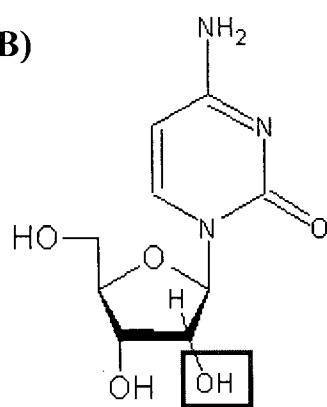
(A)



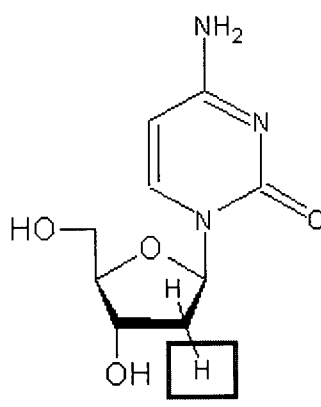
Anthracycline	R ₄	R ₉	relative lipophilicity Σf_i
Daunorubicin (DNR)	OCH ₃	C(=O)CH ₃	0
Doxorubicin (DOX)	OCH ₃	C(=O)CH ₂ OH	-1.67
Idarubicin (IDA)	H	C(=O)CH ₃	+1.05
Idarubicinol (IDOL)	H	CH(OH)CH ₃	+1.48

Adapted from Gallois et al. reference [142]

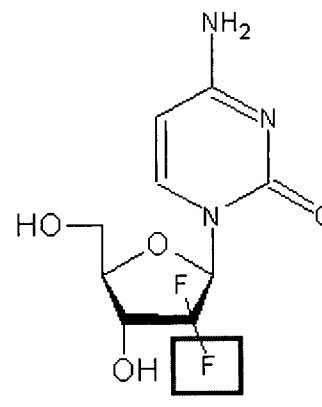
(B)



Cytidine



Cytarabine



Gemcitabine

Gleevec[®], which binds to the chimeric BCR-ABL fusion gene present in > 95% of chronic myelogenous leukemia patients. The significant increases in complete responses and median survival in patients enrolled in clinical trials evaluating Gleevec[®] compared to standard care, established a “proof of concept” for biological drugs. However, resistance and disease relapse have been observed [10], and thus it is believed that combination chemotherapeutic regimens will be the mainstay of cancer treatment. It is an exciting time in drug treatment for cancer; the era of administering standard chemotherapy treatment regimens for a particular type of cancer will be replaced with individualized treatment.

1.2. Drug Delivery

In view of the fact that many of the available chemotherapeutic agents have narrow therapeutic indices, drug delivery systems have been used as one strategy to improve the pharmacological effects of these drugs. Of the many delivery systems designed for intravenous use (micelles, lipid emulsions, liposomes, polymer-drug conjugates, polymer microspheres, nanoparticles, niosomes, and osmotic pumps), liposome technology has been successful with several products currently available for human use. These liposomal products encapsulate various drugs including the antifungal agent amphotericin B, and the anti-cancer agents daunorubicin, doxorubicin, and cytarabine and have been summarized in Table 1.2. Based on the success and versatility of lipid-based carriers for delivery of anti-cancer drugs, liposomes were utilized for the studies performed within the thesis for the delivery of idarubicin, as well as gemcitabine. Here, a brief review of this technology is provided with the aim of establishing a general understanding of the field as it relates to the research included in this thesis.

Table 1.2

List of FDA approved liposomal agents

Product Name	Therapeutic Agent	FDA Approval	Disease Treated	Company Name
Ambelcet [®]	Amphotericin B	1995/1996	Systemic fungal infections	Enzon
Ambisome [®]	Amphotericin B	1997	Systemic fungal infections	Gilead Sciences
Amphotec [®]	Amphotericin B	1997	Systemic fungal infections	Alza Corp.
DaunoXome [®]	Daunorubicin	1996	AIDS-related Kaposi's sarcoma	Gilead Sciences
DepoCyt [®]	Cytarabine	1999	Lymphomatoous meningitis	SkyePharma / Enzon
Doxil [®] / Caelyx [®]	Doxorubicin	1995/1999	AIDS-related Kaposi's sarcoma/ovarian and breast cancer	Alza Corp. (Sequus) / Schering-Plough
Myocet [®]	Doxorubicin	2000	Metastatic breast cancer	Elan Corp.
Visudyne [®]	Verteporfin	2000	Age-related macular degeneration	QLT / Novartis Ophthalmics

1.2.1. Liposomes

Dr. Alec Bangham was the first scientist to document the formation of closed spheres when phospholipids were shaken in water and to observe the resulting structures by optical and electron microscopes [11]. These closed vesicles were utilized as a model for the cell membrane [11], allowing scientists to study processes such as permeability and diffusion of molecules, the effect of anaesthetics on lipid membranes, and the reduction of surface tension by lung surfactant [12]. A few years later, liposomes were proposed as delivery vehicles [13]. Since the first record of liposomes in 1965, liposomes have been used in the pharmaceutical and cosmetics industries and for applications such as diagnostic imaging and cellular transfection.

Liposomes are spherical structures composed of a lipid bilayer or bilayers enclosing an aqueous core. For the purpose of drug delivery, liposomes are able to entrap water soluble (within the aqueous core), water insoluble (within the lipid bilayer) and amphipathic (partitioned between the lipid membrane and aqueous core) molecules. Liposomal drug delivery systems have been shown to improve the following drug characteristics; solubility [14], unfavorable pharmacokinetics (due to fast elimination rates), poor biodistribution, lack of selectivity for target tissues, and rapid degradation [15]. Overall, improvements to drug physicochemical characteristics can substantially enhance the therapeutic activity of some, but not all, encapsulated drugs.

1.2.1.1. Liposome components

Phospholipids

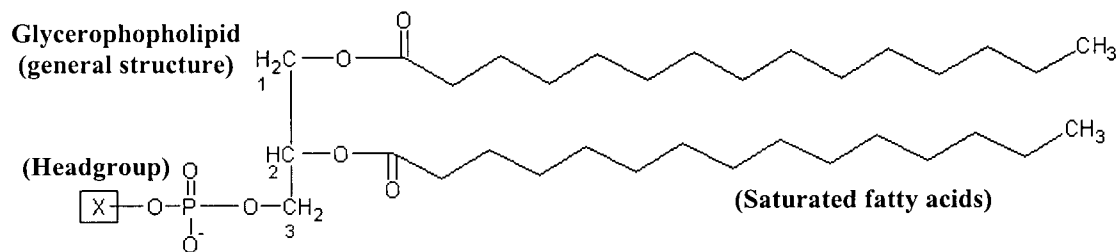
The bulk components of a liposomal lipid membrane are phosphatidylglycerides (phospholipids), amphipathic molecules that consist of a hydrophilic phosphate head group and

hydrophobic fatty acid chains bridged together by a glycerol backbone. The general structure of the phospholipid is illustrated in Table 1.3. In early studies, egg phosphatidylcholine (egg PC, egg lecithin) was used and these phospholipids, although exhibiting a single head group composition, contain various lipid species due to the presence of mixed and varying acyl chain lengths. More recently, highly purified phospholipids have been chemically synthesized consisting of saturated fatty acid species with the same number of carbons. The fatty acid chain can vary between 8 – 24 carbons (C8 – C24); among them, the most commonly used in liposomal drug delivery are myristic (C14), palmitic (C16) and stearic (C18). Aside from the fatty acid carbon length, the phosphate head group can be varied and include phosphatidylcholine (PC) and phosphatidylethanolamine (PE), which are zwitterionic (charges balanced with positive charge on head group and negative charge on phosphate group), and negatively charged phosphatidyl –serine, -glycerol and –inositol head groups. Phospholipids containing an even number of carbons are biodegradable and non-toxic for human use. Moreover, many of the physicochemical properties of liposomes such as stability, permeability, phase behaviour and membrane order depend on the fatty acid chain length and saturation and are further discussed in section 1.2.3.

Sphingolipids contain a sphingosine (instead of a glycerol) backbone and are also commonly used in lipid membranes. This phospholipid is more hydrophilic than glycerophospholipids (with the same head group), because the backbone contains two more electronegative hydroxyl and amino groups, and is incorporated to decrease the permeability of the lipid membrane [16].

Table 1.3

List of synthetic phospholipids commonly used in liposomes



Name of Glycerophospholipid	Head group (X)	Head group (X) Structure	Net Charge (at pH 7)
Phosphatidic acid	-	— H	-1
Phosphatidylethanolamine	Ethanolamine	— CH ₂ — CH ₂ — NH ₃ ⁺	zwitterionic
Phosphatidylcholine	Choline	— CH ₂ — CH ₂ — N ⁺ (CH ₃) ₃	zwitterionic
Phosphatidylserine	Serine	$\begin{array}{c} \text{— H}_3\text{C — CH — NH}_3^+ \\ \\ \text{O — C = O} \end{array}$	-1
Phosphatidylglycerol	Glycerol	— CH ₂ — CH(OH) — CH ₂ — OH	-1
Phosphatidylinositol	Inositol		-2

Cholesterol

Cholesterol has been deemed an essential component of lipid carriers, and one of the main aims of this thesis was to revisit cholesterol's role as a constituent of liposomal formulations developed for intravenous use. Cholesterol contains a four-membered sterol ring with a hydrocarbon chain (hydrophobic) and a hydrophilic hydroxyl group and is widely distributed in membranes of living cells. The use of cholesterol in membranes is reviewed within the introduction of Chapter 3. Cholesterol has significant implications in the gel-to-liquid phase transition temperature and protein binding discussed in sections 1.2.3.2 and 1.2.6.1, respectively.

Poly(ethylene glycol)-conjugated lipids

Poly(ethylene glycol) is a neutral, flexible [17], non-toxic, and non-antigenic polymer [18], that is soluble in water [19] and some organic solvents including toluene, methylene chloride, ethanol and acetone. PEG and water form a particularly "good structural fit" supported by hydrogen bonding to the ether oxygens of ethylene glycol ($-\text{CH}_2\text{-CH}_2\text{-O-}$) [19]. Water's close association with the PEG results in an excluded volume effect whereby other molecules are unable to directly interact with the polymer due to the "hydration shell" [20]. PEG's distinct physicochemical properties have been utilized for many applications including concentration and purification of nucleic acids or proteins [21, 22] and conjugation to proteins [23], peptides [24, 25], enzymes [26], monoclonal antibodies [27], lipids [28, 29] and drugs [30, 31] to increase blood residence times.

In drug delivery systems, particularly liposomes, PEG is most often conjugated to either a phospholipid or a sterol anchor. The orientation of the lipopolymer within the liposome is

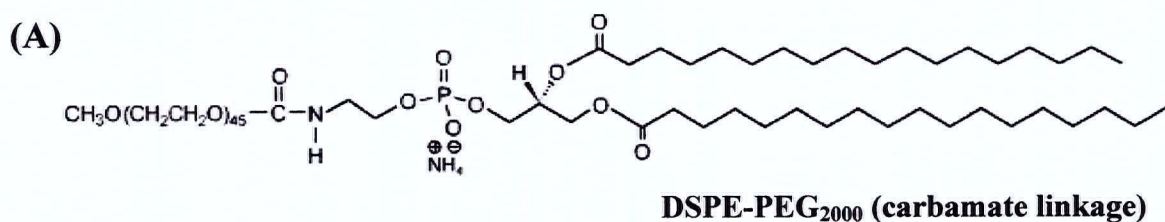
due, in part, to the hydrophobic effect, which results in the lipid anchor partitioning within the lipid bilayer and the PEG moiety extending from the liposome surface. There are currently a few methods used to incorporate PEG-lipids into lipid carriers including: (i) incorporation during the preparation of liposomes resulting in the presence of PEG on both the inner and outer leaflets of the lipid bilayer (the method used for the studies described in this thesis), and (ii) the addition of PEG-lipids to pre-formed liposomes, resulting in the presence of PEG exclusively on the outer monolayer of the liposome. For the latter procedure, there are two methods by which modification on the outer membrane was accomplished; (i) covalent attachment of PEG to PE incorporated in pre-formed vesicles [32] or (ii) mixing PEG-lipid micelles with pre-formed liposomes followed by spontaneous insertion of the PEG-lipids by physical adsorption [33-35]. One of the advantages of having PEG-lipids exclusively on the outer monolayer is that it is believed that the presence of PEG in the aqueous core of a liposome reduces the interior volume for encapsulation of drugs because of the exclusion volume effect [33]. In addition, the presences of PEG on the inner leaflet may increase drug release from liposomes, an effect that may be due to increased partitioning of the drug into the membrane interface [36].

Although many lipid anchors for PEG conjugation have been investigated, Parr *et al.* determined that phosphatidylethanolamine conjugated to PEG with a carbamate linkage, shown in Figure 1.3A, is the most chemically stable in a liposome when exposed to the biological milieu [28]. PEG is a neutral molecule, however, conjugation utilizing a carbamate linkage between ethanolamine group of phosphatidylethanolamine results in the generation of a lipid which has a net negative charge at physiological pH due to the phosphate group. Comparative electrophoretic studies by Webb *et al.*, indicated that the negative charge is not a typical “point” charge but a “shielded” (~ 80%) charge [37].

Figure 1.3

Structure of DSPE-conjugated PEG₂₀₀₀ and the mushroom and brush conformations of PEG chains

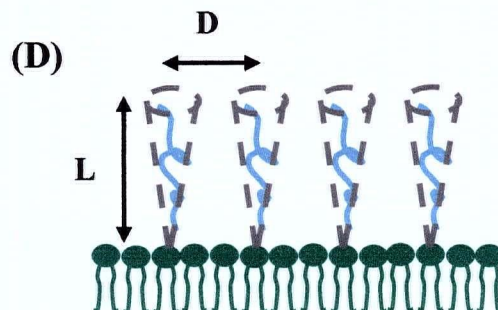
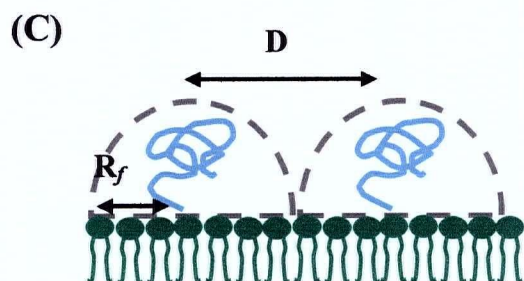
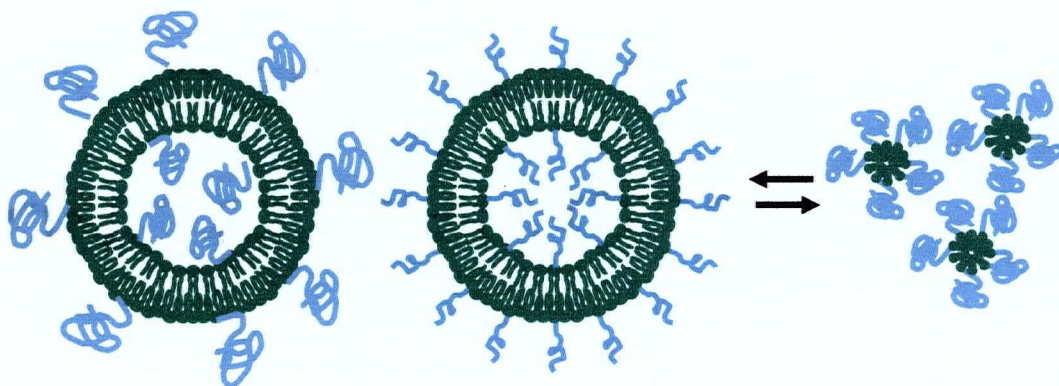
Structure of DSPE-PEG₂₀₀₀ (polymer chain repeating units = 45) incorporated into liposomes (A). The effect of PEG conjugated lipid grafting density on the structure of DSPC / DSPE-PEG₂₀₀₀ liposomes (B), < 5 mol% = mushroom regime, > 5 mol% = brush regime and > 10 mol%, mixed micelles are formed (refer to Chapter 4). The conformation of PEG is dependent on the grafting distance between the polymers (D) and the Flory radius (R_f) of the polymer (size is influenced by PEG MW). The mushroom conformation is adopted when D >> R_f (C), and the brush conformation is adopted when D < R_f (D).



(B) Mushroom Regime
DSPC/DSPE-PEG₂₀₀₀
< 5 mol% PEG

Brush Regime
DSPC/DSPE-PEG₂₀₀₀
> 5 mol% PEG

Mixed Micelle Formation
DSPC/DSPE-PEG₂₀₀₀
> 10 mol% PEG



It is known that the chain length of polymers (defined as the averaged MW of the PEG polymer used) and distance between grafting points (D) will affect the structure adopted by the polymer. In liposome formulations, the lipid matrix consists primarily of bulk phosphatidylcholine, having a molecular shape equated to a cylinder, where the area occupied by the head group is comparable to the area occupied by the acyl chain, which will pack together in a bilayer organization (see section 1.2.3.1 for review of the shape hypothesis). On the other hand, PEG polymers are conjugated to lipids and have an inverted cone shape (i.e., head group area \gg acyl chain area) and these lipids prefer to form micelle structures [38]. In fact it is reasonably well-established that PEG-lipids can act like detergents capable of disrupting liposome structure when added in sufficient concentrations. The concentration of PEG-lipid required to solubilize lipids organized in a bilayer structure is dependent on the chemical properties of PEG-lipid used as well as the lipid composition of the liposome.

At concentrations below those that induce liposome disruption, PEG-lipids are described to be either in a “mushroom” or in a “brush” regime [39, 40], shown in Figure 1.3. In the mushroom conformation, PEG has a high degree of rotational freedom (mobility) [17] and will move freely from a fixed point that encompasses a half-sphere which exhibits a defined radius referred to as the Flory radius (R_f). At low grafting densities ($D \gg R_f$), PEG is believed to exist in a mushroom configuration where the polymer-polymer interactions are minimal. At high PEG concentrations ($D \leq R_f$), polymer-polymer interactions (limited due to the volume exclusion effect) occur and the PEG polymers are extended (L) out from the lipid bilayer. This conformation has been referred to as the brush regime. At higher PEG concentrations, the micellar phase is formed in order to reduce lateral interactions between PEG chains [41]. In view of PEG’s predicted behaviour in the mushroom and brush regime, the mole fraction of

PEG-lipid and area occupied by one PEG chain can be calculated for different molecular weights (Table 1.4) when incorporated into a 100 nm liposome [42]. Based on the mole ratio of PEG-lipids incorporated into liposomes, assuming a homogenous distribution, the percent of total liposome surface area for a 100 nm liposome has been calculated in Table 1.5 [42].

1.2.2. Classification of liposomes

The amphipathic nature of phospholipids facilitates the formation of vesicular lipid bilayers (liposomes) in the presence of an excess amount of aqueous solvent. Liposomes are classified according to their size and number of lipid bilayers. Upon hydration of lipids in aqueous solutions, multilamellar vesicles (MLVs) are formed. MLVs have a large diameter (greater than 1 μm), and have been utilized as drug delivery vehicles, particularly for hydrophobic compounds such as amphotericin B. Small unilamellar vesicles (SUVs) contain a single bilayer surrounding an aqueous core, with diameters less than 100 nm. SUVs (approximate size is 50 nm) are formed from sonication of MLVs [43]; however, the major disadvantage for using these structures for delivery is their small size (small trapped volume) and, in turn, low encapsulation efficiencies, and instability in solution due to their high radius of curvature. Large unilamellar vesicles are most commonly used for drug delivery purposes and consist of one (or two) bilayer(s) surrounding an aqueous core. A standard way of preparing LUVs is by passing MLVs through a filtering (extruding) apparatus which houses filters exhibiting defined pore sizes, ranging between 0.05 – 0.2 μm . The extrusion method was preferred as it results in liposomes with relatively narrow size distributions. The resulting liposomes typically have a single bilayer surrounding the aqueous core and the trapped aqueous volume, depending on lipid composition, can range from 1 to 2.5 μl per μmole lipid.

Table 1.4

Calculated mole fraction of PEG-lipid in area occupied by one PEG chain of different molecular weights in DSPC / DSPE-PEG liposomes^a

PEG Molecular Weight	N^b	R_f (nm)^b	Protected Area (nm)² / PEG Molecule^c	Number of PEG Molecules Required to Cover Entire Surface	χ_p^b (X 100)
350	8	1.22	4.68	12393	10
550	13	1.63	8.35	6946	6
750	17	1.92	11.58	5009	4.3
2000	45	3.44	37.18	1560	1.4

^a Adapted from Allen C. *et al.* [42].

^b N = number of repeat units per polymer chain, R_f = Flory radius of PEG chain, χ_p = mole fraction of PEG-lipid in area occupied by one PEG chain.

The calculations of protected area are based on a simple model described elsewhere [17].

Table 1.5

The percentage of surface area covered in liposome formulations containing 2 and 5 mol% PEG of different molecular weights^a

Formulation	Mole Ratio (%)	Total Area of Liposome Covered by PEG (nm)	Percent of Total Surface Area of Liposome Covered (%)
DSPC / DSPE-PEG ₃₅₀	95 / 5	2.6×10^4	45
	98 / 2	1.0×10^4	17
DSPC / DSPE-PEG ₅₀₀	95 / 5	4.6×10^4	79
	98 / 2	1.8×10^4	31
DSPC / DSPE-PEG ₇₅₀	95 / 5	6.4×10^4	100
	98 / 2	2.5×10^4	43
DSPC / DSPE-PEG ₂₀₀₀	95 / 5	-	brush regime
	98 / 2	8.0×10^4	100

^a Adapted from Allen C *et al.* [42].

1.2.3. Physicochemical properties of liposomes



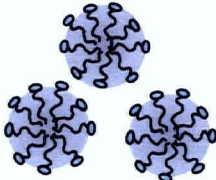


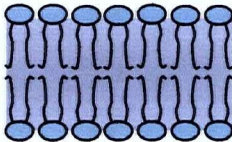

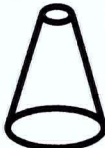
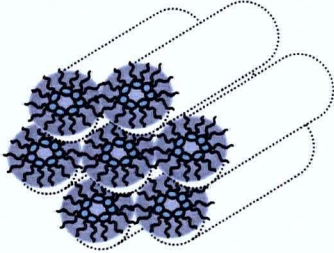
The physicochemical properties of a lipid membrane consist of cooperative interactions between the lipid components and include both the lipid bilayer and the interfacial water layer existing on the lipid surface. These interactions between lipid components and water will affect the shape of vesicles, gel-to-liquid phase transition temperature, membrane order, fluidity, and permeability. In addition, it is important to recognize that the presence of a drug in the membrane will influence the physicochemical properties of the liposome.

1.2.3.1. Shape hypothesis of lipid polymorphism

Not all lipids spontaneously form lipid bilayers, and this lipid polymorphism can be explained by the “shape hypothesis” [44], illustrated in Table 1.6. Aside from bilayers, which are formed from lipids exhibiting a cylindrical molecular shape, micelles and inverse micelles (which give rise to a hexagonal phase) are formed from lipids exhibiting inverted cone and cone-shapes, respectively. The predominant use of micelles and inverted micelles is in the formulation of detergents and transdermal delivery products, respectively. The polymorphic structure of lipids is mediated by other factors including lipid composition, salt concentration, pH and temperature. In general, the lipid species at highest concentration will predict the overall shape of the lipid membrane, for example the lipid composition used in many of the studies within the research component of the thesis was DSPC / DSPE-PEG₂₀₀₀ (95:5 mole ratio), a combination of cylindrical and inverted cone shaped lipids that form bilayers in

Table 1.6

Shape hypothesis of lipid polymorphism

Lipid	Molecular Shape	Aggregate Structure
Detergents Lysophospholipids PEG-conjugated lipids	  Inverted Cone	 Micelles
Phosphatidylcholine Phosphatidylglycerol Phosphatidylinositol Phosphatidylserine Sphingomyelin	  Cylinder	 Bilayer
Phosphatidylethanolamine Phosphatidylserine (pH < 4.0) Cholesterol	  Cone	 Reverse Micelles

solution. In addition, equal combinations of inverted cone and cone species will form bilayers leading to the interesting observation that two non-bilayer forming lipids exhibiting complementary shapes can be mixed together to achieve a bilayer structure [38]. The ability to trigger polymorphic liposome structural changes (e.g., fusogenic liposomes) has been exploited for drug delivery purposes and this is briefly reviewed in section 1.2.6.

1.2.3.2. Gel-to-liquid crystalline phase transition

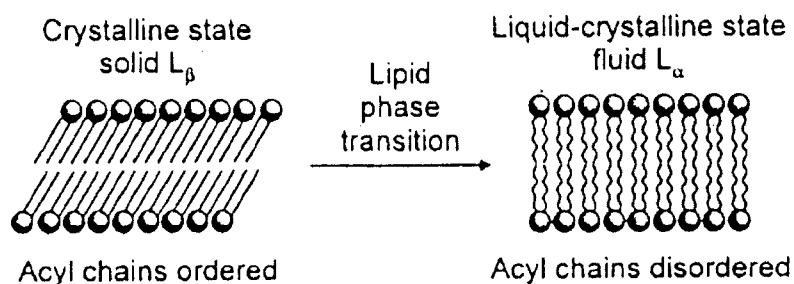
Colloidal systems, such as liposomes, have a distinct phase transition (T_c) from a gel state to a liquid crystalline state (Figure 1.4A). The phospholipid's fatty acyl chains exhibit a well-ordered conformation within the gel phase and become significantly more disordered above the critical temperature. The T_c is the critical temperature at which point there are equal proportions of the two phases, and coincides with a membrane structure that is most permeable [45]. This cooperative change is measured by differential scanning calorimetry (DSC), which can record changes in heat absorbance by a sample (Figure 1.4B). DSC studies have determined that the specific T_c is dependent on the length and saturation of the phospholipid's hydrocarbon chains, head group composition and cholesterol content. As a general rule, factors that increase the packing of the lipid membranes results in a higher T_c . Thus a higher T_c is observed when increasing hydrocarbon chain length (DSPC > DMPC), increasing hydrocarbon saturation (DSPC > DOPC) and reducing head group size (DSPE > DSPC). For the purposes of the thesis, the T_c for phosphatidylcholine species containing increasing chain length are 23°C (C14), 41°C (C16), 55°C (C18), 65°C (C20) and 74°C (C22).

The effect of cholesterol on the phase transition temperature has been thoroughly investigated [46]. In fluid membranes, cholesterol increases order and packing density within

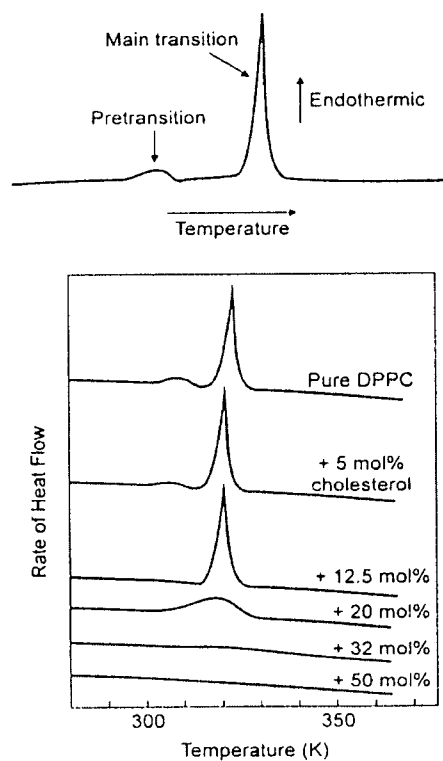
Figure 1.4

Lipid phase transition and influence of cholesterol on the phase transition temperature of DPPC liposomes

(A)



(B)



Figures A and B were adapted from references [44] and [47], respectively.

the lipid membrane, known as a “condensing” effect. In gel membranes, cholesterol decreases order and packing density within the lipid membrane, referred to as a “liquifying” effect. At high cholesterol concentrations (> 30 mol%) the measured phase transition is eliminated (shown in Figure 1.4) and the membrane is present in a liquid-ordered phase [47].

1.2.4. Liposome Formulations

1.2.4.1. Conventional liposomes

Lipid compositions containing phospholipids and cholesterol are often referred to as conventional (or first generation) formulations. The success of these lipid formulations as drug delivery vehicles in vivo was largely attributed to incorporation of > 30 mol% cholesterol to reduce the release of entrapped drugs or water-soluble markers and prevention of phospholipid transfer to plasma lipoproteins. Although neutral liposomes prepared of phosphatidylcholine species and cholesterol are effective as drug carriers, there remained perceived drawbacks to the technology. In particular, the rapid elimination of the liposomes following i.v. injection, an observation associated with liposome accumulation in the mononuclear phagocytic system (MPS), needed to be overcome if extended circulation lifetimes was to be obtained. Although appropriately designed formulations prepared of phospholipids and cholesterol did provide substantial improvements in drug delivery to diseased sites residing in non-MPS organs [48], it was believed that even better distribution attributes could be achieved if the uptake by cells of the MPS could be reduced. Further, it was proposed that additional therapeutic benefits could be achieved if the rate of liposome elimination could be reduced. It was already established that this could be achieved by saturating macrophages with high lipid doses [49] or by impairing macrophages with drugs (e.g., doxorubicin) [50, 51]. However other approaches were

considered, as outlined in the following section.

1.2.4.2. Sterically stabilized liposomes

Second generation liposomes, termed “sterically stabilized” or Stealth[®] liposomes, incorporate a surface coating consisting of ganglioside G_{M1} or poly(ethylene glycol)-conjugated lipids [52, 53]. These novel formulations significantly advanced and broadened the application of cholesterol-containing liposome formulations. Sterically stabilized liposomes exhibited significantly greater circulation half-lives [29, 32, 54, 55] and the elimination behaviour of these liposomes was no longer as sensitive to liposomal lipid dose [56, 57]. Subsequent studies illustrated that a longer circulation half-life could facilitate higher levels of drug accumulation within sites of tumor growth [58-60] associated with improved antitumor activity [61-63]. The mechanism by which increased liposome accumulation occurred was referred to as passive targeting, illustrated in Figure 1.5, and relies on several factors including “leaky” capillaries, such as those typically observed in sites of infection, inflammation and tumor growth [64], and small liposome size (< 200 nm) allowing the carriers to extravasate from the blood compartment into the interstitial space of these sites [59].

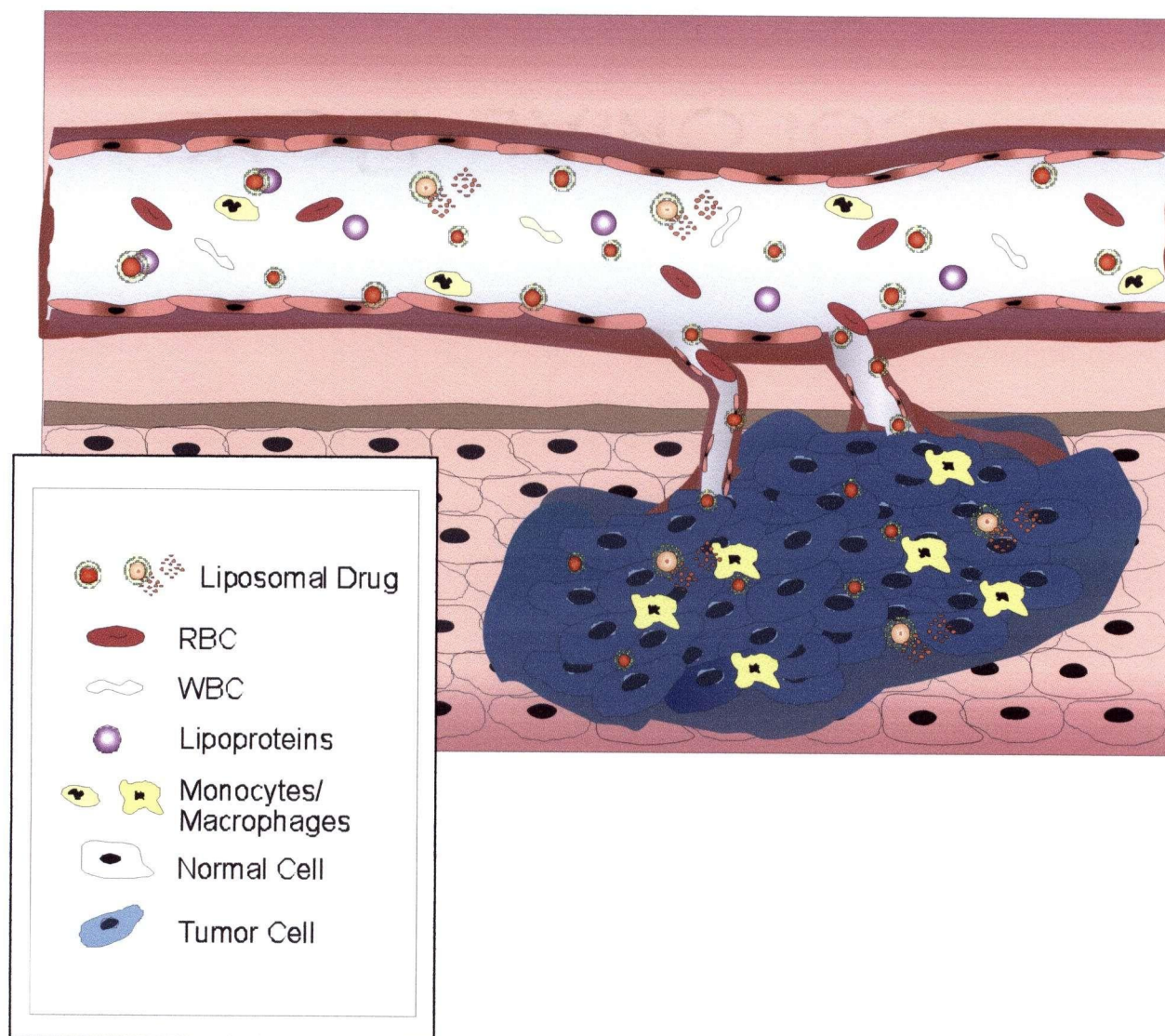
1.2.5. Liposomes as drug carriers

In the early 1970s, it was proposed that liposomes could potentially retain entrapped pharmaceuticals for treatment of diseases [65]. Within this thesis two anti-cancer drugs, idarubicin and gemcitabine, were encapsulated in liposomes. The advantages and disadvantages of different loading methods used to encapsulate these drugs will be discussed below.

Figure 1.5

Passive targeting of liposomes

Passive accumulation at the tumor site is obtained with appropriately designed liposomal carriers. These liposomes are retained within the blood compartment for extended time periods and have limited interactions with serum proteins. Discontinuous vascular endothelium is present at sites of infection, inflammation and tumor growth, permitting the extravasation of circulating macromolecules, such as liposomes, into these areas.



1.2.5.1. Passive loading

Hydrophobic drugs (e.g., taxol and amphotericin B) or water soluble drugs (e.g., cytarabine and gemcitabine) may be passively entrapped within liposomes during hydration of lipid and liposome formation, shown in Figure 1.6. Encapsulation efficiencies up to 100% may be achieved for hydrophobic drugs when exhibiting favourable drug-lipid interactions and drug solubility. Passive loading of water soluble drugs is typically very low (< 30%) and is dependent on the trapped volume of the liposome and liposomal lipid concentration. If drugs have to be encapsulated using passive loading methods it is more difficult to control parameters such as drug-to-lipid ratios and trapping efficiency. In the case of cytotoxic drugs, passive trapping also means that careful methods must be in place during liposome preparation and following preparation to remove the unencapsulated drug.

1.2.5.2. Remote loading

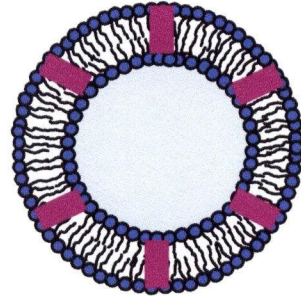
Drugs, such as anthracycline antibiotics, can alternatively be loaded into pre-formed liposomes containing a pH gradient (pH 4.0 inside, pH 7.4 outside), shown in Figure 1.6. This method is limited to drugs having an ionizable amine function, and results in encapsulation efficiencies of > 98%. For anthracyclines, the encapsulation efficiencies are much higher than predicted by the Henderson-Hasselbach equation, and may be explained by the formation of drug microprecipitates [66, 67] and / or drug association with or partitioning into the lipid membrane [68]. Drug retention by this method is dependent on liposome composition including surface charge, phospholipid acyl chain length, cholesterol content, internal buffering capacity, drug-to-lipid ratio, pH gradient, and liposome size [69], parameters that can all be independently altered. Other active loading methodologies include the ammonium sulfate gradient method

Figure 1.6

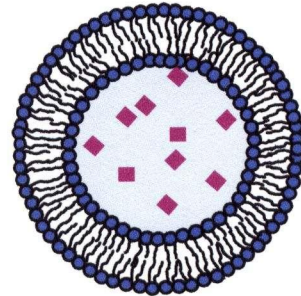
An illustration of drug loading methods and drug distribution in liposomes

Type of Drug Loading

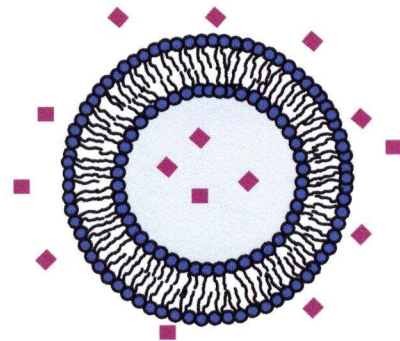
Passive association of a
hydrophobic drug



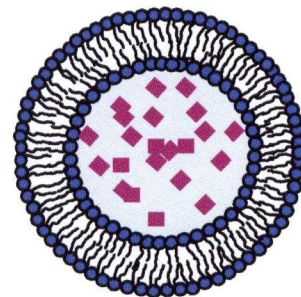
Passive encapsulation of a
hydrophilic drug



Drug distribution across the liposomal
membrane in the absence of a pH gradient



Active encapsulation of drug
(containing ionizable amine group)
in the presence of a pH gradient



[70] and metal complexation [71, 72]. The latter is of potential interest since drug loading may not be dependent on maintenance of an established pH gradient.

1.2.6. Biological stability of liposomes

The success of lipid-based carriers for anti-cancer drugs is dependent on their prolonged circulation longevity. The study of pharmacokinetics (“what the body does to the drug”) consists of absorption, distribution, metabolism and excretion processes. In many of the studies within the thesis, the rate of liposomal lipid and drug elimination were assessed. The elimination of liposomes was determined by measuring the liposomal lipid concentration in plasma over a defined time interval. These data, when combined with data obtained by measuring plasma drug levels, could be used together to follow changes in drug-to-lipid ratios over time, following administration. A reduction in the drug-to-lipid ratio provided an indication of drug release from the liposome in the plasma compartment.

Further analysis of the drug plasma concentration versus time curves with pharmacokinetic modeling may be used to determine the plasma half-life ($T_{1/2}$), clearance and volume of distribution. Pharmacokinetic models are mathematical relationships that are used to predict the behaviour of a drug in the body [73]. There are three types of modeling including physiologic, compartmental and non-compartmental. Physiologic models are based on disposition of a compound in anatomic regions within the body based on blood flow, tissue volumes, binding, transport and elimination parameters. Physiologic models are most often used when applying small vertebrate data to larger vertebrates, such as humans. Compartmental analysis is based on dividing the body into different homogenous compartments, not based on anatomic or physiological regions. For instance, a one compartment model assumes the

administered drug distributes quickly into a central compartment (consisting of the blood compartment and highly perfused organs). Sampling from the blood compartment is thus equivalent to the concentration within the central compartment from which the drug is eliminated by first-order kinetics. For multi-compartmental analysis the drug will distribute into the central compartment followed by a peripheral compartment(s) (which are less perfused tissues such as skin and muscle). Non-compartmental analysis is based on the statistical moment theory and does not have the assumptions that are present in compartmental models. Calculations of pharmacokinetic parameters are summarized in section 2.5.6. In general, changes in the pharmacokinetics of a liposome-encapsulated drug are reflected by delayed absorption, restricted biodistribution, decreased volume of distribution, delayed clearance and retarded metabolism relative to the non-encapsulated drug [74].

The plasma elimination of liposomes following i.v. administration is dependent on vesicle size [53], lipid composition and lipid dose [56, 75]. Prolonged circulation longevity is observed with liposomes exhibiting size distributions between 80 – 150 nm, prepared of neutral phospholipids, and is further improved by incorporation of ganglioside GM₁ or PEG-derivatized lipids for surface stabilization. The pharmacokinetic behaviour of liposomes is also influenced by interactions with plasma proteins and cells of the mononuclear phagocytic system and these factors are briefly discussed in the following sections.

1.2.6.1. Plasma Proteins

Plasma proteins have been shown to interact with liposome membranes upon intravenous administration. Interactions that are dependent on the liposome surface attributes include charge and hydrophilicity [32, 76]. There are three consequences of plasma protein

adsorption on the liposome membrane; (i) destabilization of the lipid membrane and leakage of encapsulated contents and (ii) presentation to and subsequent endocytosis by the macrophages of the mononuclear phagocytic system (MPS), and (iii) adsorption of plasma proteins, that in turn, mediate changes in the properties of liposomes. The latter effect is less well defined but highlights the fact that physicochemical characteristics of liposomes in the absence of plasma protein may be remarkably different than the physicochemical characteristics of liposomes with adsorbed plasma proteins.

There are several supporting observations that demonstrate that the interaction between plasma proteins and liposomes results in phospholipid transfer from liposomes to high density lipoproteins (HDL) particles [77-81]; a process mediated in part by a phospholipid transfer protein (PLTP) [82]. Further, phospholipid transfer was not observed in lipoprotein deficient mice and when various lipoproteins were re-introduced, only HDL compromised liposome stability [83]. Moreover, the addition of cholesterol or lipids such as sphingomyelin (SM) or 1,2-distearoyl-*sn*-phosphatidylcholine (DSPC) reduced phospholipid loss [84, 85]. Other plasma proteins that interact with liposomes include lipoprotein β_2 -glycoprotein I (apolipoprotein H) [86] and complement proteins [87] which bind to negatively charged phospholipids. Albumin, the most abundant protein in serum, does not have a detrimental effect on the integrity of liposomes, while immunoglobulins, such as IgG and C-reactive protein [88], mediate uptake by macrophages. Fibronectin, a protein involved in cell adhesion, phagocytosis and cytoskeletal organization, induces liposome aggregation [89]. It is important to note that even long circulating liposomes have been shown to adsorb plasma proteins (see Chapter 4), and it is unknown whether complete abrogation of liposome-plasma protein interactions may further extend blood circulation times. It is also not well understood how protein binding ultimately

affects the fate of and biological response to injected liposomes. Some have even argued that plasma protein binding actually protects liposomes in the plasma compartment.

1.2.6.2. Mononuclear phagocytic system

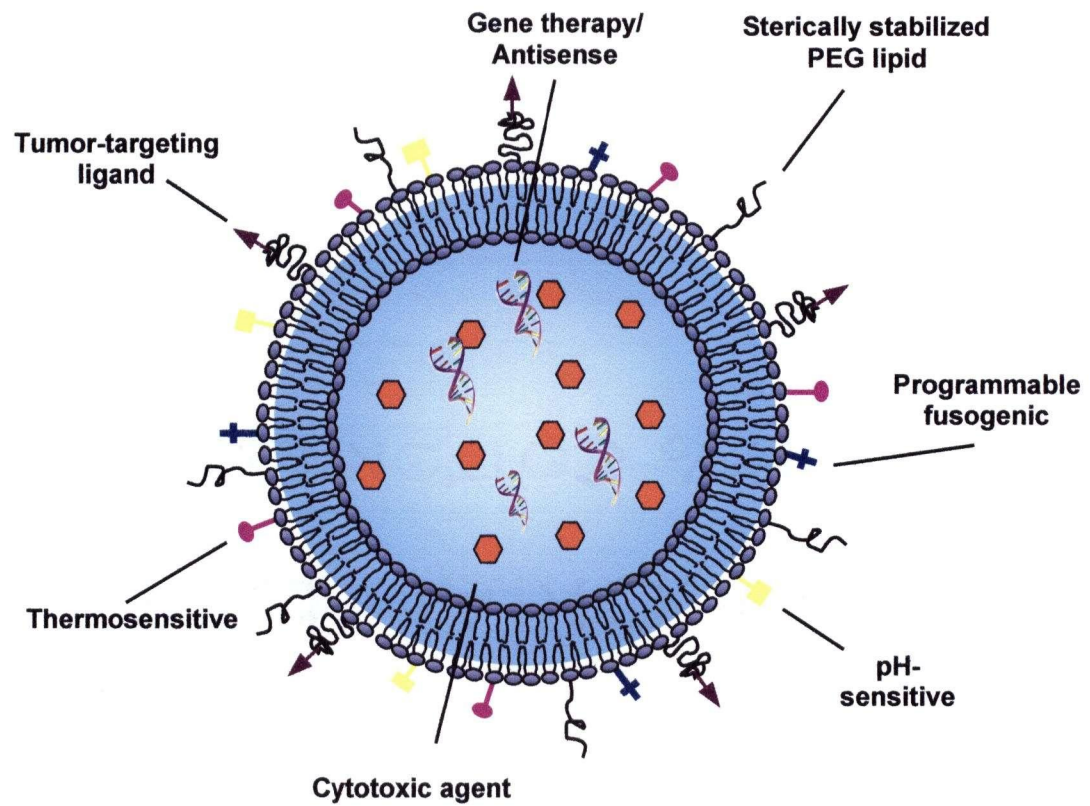
The mononuclear phagocytic system (MPS), also referred to as the reticuloendothelial system (RES), consists primarily of the macrophages in the liver (Kupffer cells), spleen and bone marrow as well as the circulating precursors to these cells, the blood monocytes. These cells are actively involved in the immune response to foreign matter in the body. Intravenous administration of liposomes leads to the predominant uptake of liposomes within tissues containing these phagocytic cells [48, 75, 90-93]. Plasma protein interactions with liposomes can facilitate endocytosis of the liposomes by macrophages or monocytes of the MPS system. The addition of cholesterol to liposome membranes was shown to moderately decrease accumulation within the liver and spleen [94]. Although delivery to macrophages has been exploited for vaccine development, it is considered not to be beneficial for liposomal antitumor agents and may be one factor that limits accumulation of drug-loaded carriers in tumor sites. As noted in section 1.2.4.2, the use of surface stabilizing polymers significantly delayed the rate of liposome uptake by the MPS and resulted in extended circulation lifetimes [29, 57]. Further investigation into strategies to reduce cell uptake have been successful in mediating improvements in the circulation longevity of liposomes. This may be achieved by preventing adsorption of proteins that facilitate (opsonins) phagocytosis and promoting adsorption of proteins that inhibit (dysopsonins) phagocytosis by macrophages of the MPS [95].

1.2.7. Future directions of liposomal drug delivery

When considering the use of liposomes to improve the therapeutic potential of existing drugs, increasing selectivity of a drug carrier for a target cell population and achieving controlled release rates are two of the goals for drug delivery systems. Increased selectivity for anti-cancer agents may be achieved by using strategies that extend the blood circulation lifetimes of liposomes by incorporation of surface stabilizing agents, such as PEG. Further strategies that increase carrier selectivity for malignant cells are being pursued and include development of ligand-targeted (immuno-) liposomes. It is anticipated, for example, that conjugation of novel tumor-specific monoclonal antibodies, such as Herceptin[®] (binds to HER2/Neu receptor) and Rituximab[®] (binds to CD20), will direct liposomes to malignant cells for local and systemic disease. Related efforts include those designed to promote localized drug release following passive targeting as well as more specific intracellular delivery and include pH-sensitive [96], programmable fusogenic [97] and thermosensitive [98] liposomes. pH-sensitive liposomes undergo a transition from a bilayer to a non-bilayer (hexagonal) phase that can result in loss of encapsulated contents and membrane fusion with nearby cells or membranes. This transition, as the name implies, occurs when the liposomes encounter an acidic environment, such as that which may be found within tumors or within cellular endosomal compartments. Programmable fusogenic liposomes exhibit a time-dependent destabilization based on the loss / exchange of liposome-associated PEG-derivatized lipids from the membrane surface. Thermosensitive liposomes exhibit membrane phase transition temperatures a few degrees above physiological body temperature, and site-specific drug accumulation can be triggered through mild heating of a tumor site. The use of multifunctional liposomes (illustration shown in Figure 1.7) utilizing a combination of these targeting and.

Figure 1.7

**An illustration of a multifunctional liposome
with multiple targets and triggered release mechanisms**



triggered release technologies may provide a superior approach to treat cancer.

1.3. Thesis Rationale and Hypotheses

It is generally accepted that > 30 mol% cholesterol is required to confer the biological stability to liposomal drug formulations. However, the addition of cholesterol to liposomes composed of gel phase lipids increases the overall permeability of the membrane (at temperatures $< T_c$). Thus, it was hypothesized that liposomes that do not contain cholesterol would exhibit improved drug retention attributes for drugs that are rapidly released from conventional formulations. It was anticipated that these formulations would be dependent on the use of surface stabilizing lipids, such as PEG-lipids, for biological stability.

Encapsulation of anti-cancer drugs in liposomes has been shown to improve the pharmacokinetic and biodistribution attributes of drugs, such as reducing toxicity and improving the therapeutic activity. Idarubicin, has improved pharmacological properties as compared to other anthracyclines (including reduced cardiac toxicity, less susceptibility to the activity of multidrug resistant proteins and pro-drug like characteristics due to its active metabolite), has not been successfully developed as a liposomal formulation in part because of rapid loss from liposomes prepared with cholesterol (Pai and Mayer, unpublished observations). It was hypothesized that extending the blood circulation lifetimes of idarubicin by liposome encapsulation will result in increased therapeutic activity. Moreover, it was anticipated that the therapeutic value of liposomal idarubicin would be optimal when used in combination with drugs exhibiting non-overlapping toxicities, proven efficacy and complementary mechanisms of action. In this respect, combining an agent that targets DNA repair (idarubicin poisons topoisomerase II) with an agent, such as gemcitabine, that promotes DNA damage may further increase antitumor activity.

CHAPTER 2

MATERIALS AND METHODS

2.1. Materials

Lipids. 1,2-dimyristoyl-*sn*-glycero-3-phosphatidylcholine (DMPC), 1,2-dipalmitoyl-*sn*-glycero-3-phosphatidylcholine (DPPC), 1,2-distearoyl-*sn*-glycero-3-phosphatidylcholine (DSPC), 1,2-diarachidoyl-*sn*-glycero-3-phosphatidylcholine (DAPC) and 1,2-dibehenoyl-*sn*-glycero-3-phosphatidylcholine (DBPC) phospholipids and 1,2-dimyristoyl-*sn*-glycero-3-phosphatidylethanolamine (DMPE), 1,2-dipalmitoyl-*sn*-glycero-3-phosphatidylethanolamine (DPPE) and 1,2-distearoyl-*sn*-glycero-3-phosphatidylethanolamine (DSPE)-conjugated poly(ethylene glycol) lipids (molecular weights 350, 550, 750, 2000 and 5000) were obtained from Avanti Polar Lipids, Inc. (Alabaster, AL, USA). Cholesterol (CH) was obtained from the Sigma-Aldrich Canada Ltd. (Oakville, ON, Canada). $^3\text{[H]}$ -cholesteryl hexadecyl ether (CHE) (51 Ci / mmole) and $^{14}\text{[C]}$ -CHE (50.6 mCi / mmole) were obtained from PerkinElmer, Inc. (Boston, MA, USA). $^3\text{[H]}$ -DSPE-PEG₂₀₀₀ was custom synthesized by Northern Lipids Inc. (Vancouver, BC, Canada). $^{14}\text{[C]}$ -DPPC (110 mCi / mmole) was purchased from Amersham Biosciences (Quebec City, QC, Canada).

Chemicals. Ethyl alcohol (99.9% v/v) was manufactured by Commercial Alcohols, Inc. (Chatham, ON, Canada). HEPES (N-[2-hydroxyethyl] piperazine-N'-[2-ethanesulfonic acid]), citric acid, Sephadex G-50 (medium), Sepharose CL-4B beads, OGP (octyl- β -D-glucopyranoside) detergent, MTT (3-(4, 5-dimethylthiazol-2-yl)-2,5-diphenyl tetrazolium bromide) reagent, and all other chemicals were obtained from Sigma-Aldrich Canada Ltd. (Oakville, ON, Canada). $^{14}\text{[C]}$ -lactose (54.3 mCi / mmole) were obtained from PerkinElmer, Inc. (Boston, MA, USA). $^{14}\text{[C]}$ -methylamine hydrochloride (56 mCi / mmole) was obtained

from Amersham Biosciences, (Quebec City, QC, Canada). Picofluor-15 and Picofluor-40 scintillation fluids were obtained from Packard Bioscience (Groningen, The Netherlands). Triton X-100 detergent was purchased from Bio-Rad Laboratories (Richmond, CA, USA). Sodium dodecyl sulphate (SDS 10% w/v) detergent was obtained from Gibco BRL (Life Technologies, Burlington, ON, Canada).

Drugs. The anthracyclines idarubicin hydrochloride (10 mg idarubicin; 100 mg lactose; MW 533.97; Pharmacia and Upjohn, Boston, MA, USA), epirubicin hydrochloride (50 mg epirubicin / 25 ml sodium chloride and sterile water, MW 579.95; Pharmacia and Upjohn, Boston, MA, USA), doxorubicin hydrochloride (10 mg doxorubicin and 52.6 mg lactose; MW 579.99; Faulding, Inc., Montreal, QC, Canada), daunorubicin hydrochloride (20 mg daunorubicin, 100 mg mannitol; MW 563.99; Novopharm, Ltd., Toronto, ON, Canada) and gemcitabine hydrochloride (200 mg gemcitabine, 200 mg mannitol, 12.5 mg sodium acetate; MW 299.5; Eli Lilly Canada, Inc. Toronto, Ontario, Canada) were manufactured by the indicated companies and obtained from British Columbia Cancer Agency (Vancouver, BC, Canada). $^3\text{[H]}$ -gemcitabine (11 Ci / mmole) was obtained from Moravek Biochemicals Inc. (Brea, CA, USA).

Cell Culture. Mouse serum was obtained from Cedarlane (Hornby, Ontario, Canada). Dulbecco's modified Eagle's medium (DMEM), RPMI 1640 and Hank's balanced salt solution (HBSS) were obtained from StemCell Technologies Inc. (Vancouver, BC, Canada). Fetal bovine serum (FBS) was obtained from Hyclone (Logan, UT, USA). L-glutamine and trypsin-ethylenediaminetetraacetic acid (trypsin-EDTA) were purchased from Gibco BRL (Life Technologies, Burlington, ON, Canada). Microtitre (96-well) Falcon[®] plates, culture flasks and blood collection tubes containing liquid EDTA were obtained from Becton-Dickinson

Biosciences (Mississauga, Ontario, Canada). Microfuge tubes were obtained from VWR (West Chester, PA, USA).

2.2. Liposome Preparation

All liposome formulations were prepared by the extrusion technique [99, 100]. Briefly, lipids were dissolved in chloroform and mixed together in a test tube at the indicated mole ratios. $^3\text{[H]}$ -cholesteryl hexadecyl ether (CHE) was added as a non-exchangeable, non-metabolizable lipid marker [101, 102]. The chloroform was evaporated under a stream of nitrogen gas and the sample was placed under high vacuum overnight to remove residual solvent. The lipid films were rehydrated in either citrate (300 mM citric acid, pH 4.0; with pH gradient for remote loading) or HBS (HEPES buffered saline, 20 mM HEPES, 150 mM NaCl, pH 7.4; no pH gradient) by gentle mixing and heating. Cholesterol-containing formulations were subjected to five cycles of freeze (liquid nitrogen) and thaw (65°C) prior to extrusion. The newly formed multilamellar vesicles (MLVs) were passed 10 times through an extruding apparatus (Northern Lipids Inc., Vancouver, BC, Canada) containing two stacked 100 nm Nucleopore[®] polycarbonate filters (Northern Lipids Inc., Vancouver, BC, Canada).

2.3 Analytical Methods

2.3.1. QELS liposome size analysis

The mean diameter and size distribution of each liposome preparation (prior to addition of ethanol or drugs), shown in Figure 2.1, was analyzed by a NICOMP model 270 submicron particle sizer (Pacific Scientific, Santa Barbara, CA, USA) operating at 632.8nm, and was typically 100 ± 30 nm by volume-weighting.

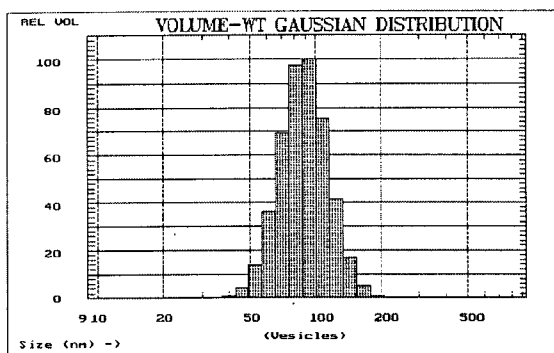
Figure 2.1

Analysis of mean liposome diameter by quasielastic light scattering

Mean liposome diameters of 91.7 ± 23.7 nm for DSPC / DSPE-PEG₂₀₀₀ (95:5 mole ratio; **A**) and 99.8 ± 29.0 nm for DSPC / CH / DSPE-PEG₂₀₀₀ (50:45:5 mole ratio; **B**) liposomes as measured by quasi-elastic light scattering using NICOMP submicron particle sizer model 370. Samples were diluted in sterile saline, pH 7.4.

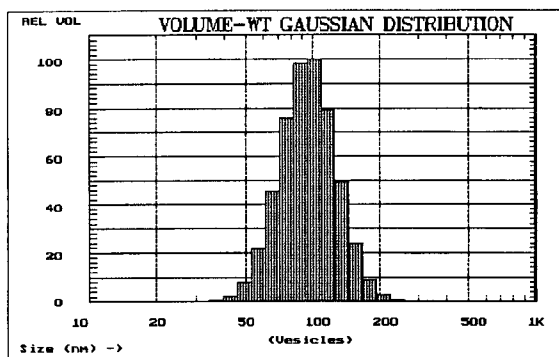
A

GAUSSIAN SUMMARY:
 Mean Diameter = 91.7 nm Chi Squared = 0.723
 Stnd. Deviation = 23.7 nm (25.8 %) Baseline Adj. = 0.000 %
 Coeff. of Var'n = 0.258 Mean Diff. Coeff. = 5.00E-08 cm²



B

GAUSSIAN SUMMARY:
 Mean Diameter = 99.8 nm Chi Squared = 0.247
 Stnd. Deviation = 29.0 nm (29.0 %) Baseline Adj. = 0.008 %
 Coeff. of Var'n = 0.290 Mean Diff. Coeff. = 4.60E-08 cm²



2.3.2. Trapped volume and lactose retention studies

To determine the trapped volume, lipids were prepared hydrated in HBS (pH 7.4) containing ^{14}C -lactose (54.3 mCi / mmole). Following extrusion and sizing, 100 μl aliquots were passed down Sephadex G-50 mini spin columns. Trapped volume was determined from the following equation:

$$\text{Trapped volume} = \frac{(A / B)}{(C / D)} \times (\text{Sample Volume}) \quad (1)$$

A = ^{14}C -lactose dpm eluted from spin column (100 μl of initial sample)

B = ^{14}C -lactose dpm of initial suspension prior to gel filtration / sample volume

C = ^3H -CHE dpm eluted (100 μl of initial sample)

D = specific activity of lipid stock (dpm / μmole total lipid)

For experiments in Chapter 3, lactose release over 48 hour time interval was determined following passive encapsulation of ^{14}C -lactose liposomes and removal of external lactose by size exclusion chromatography, samples (10 mM lipid) were placed in dialysis membrane (Spectrum Laboratories, Inc., Rancho Dominguez, CA, USA) in HBS buffer (pH 7.4) and solutions were incubated at 37°C. Aliquots were removed at various time points and passed down Sephadex G-50 mini spin columns to assess lactose release.

To determine the percent lactose retained after short incubations in Chapter 5, lipid films were hydrated in HBS (pH 7.4) containing tracer quantities of ^{14}C -lactose. Following extrusion, liposomes were incubated at 40°C with increasing ethanol concentrations (0 - 30% v/v) for 60 minutes and 100 μl aliquots were passed down Sephadex G-50 mini spin columns. Both lipid and lactose concentrations were determined using specific activity counts of ^3H -

CHE (51 Ci / mmole) and ^{14}C -lactose.

2.3.3. pH gradient determination

To measure the transmembrane pH gradient in Chapter 5, ^{14}C -methylamine was added to liposomes containing varying concentrations of ethanol (0, 5, 10, 20, and 30 % v/v) and incubated for 60 minutes. Samples were passed down Sephadex G-50 mini spin columns to separate liposome-encapsulated ^{14}C -methylamine. The pH gradient was calculated as previously determined [103] from the following equation:

$$\Delta\text{pH} = -\frac{\log [\text{H}]^+ \text{ in}}{[\text{H}]^+ \text{ out}} = -\log \frac{(\text{CH}_3\text{NH}_3)^+ \text{ in}}{(\text{CH}_3\text{NH}_3)^+ \text{ out}} \quad (2)$$

2.3.4. Size exclusion chromatography

For evaluating the mean diameter and structure of liposomes containing increasing concentrations of DSPE-PEG lipids in Chapter 4, DSPC / DSPE-PEG₂₀₀₀ (20 mM lipid) liposome formulations were dually radiolabeled with ^{14}C -CHE and ^3H -DSPE-PEG₂₀₀₀ and passed down a Sepharose CL-4B column (40 ml, 22 cm x 1.5 cm) at a flow rate of 0.5 ml/min. ^3H -DSPE-PEG₂₀₀₀ micelles were passed down the Sepharose CL-4B column as a reference for the elution volume of pure micelles.

2.3.5. Cryo-transmission electron microscopy

Liposomes were analyzed by cryo-transmission electron microscopy (cryo-TEM) in Chapters 3, 4, 5 and 6. Cryo-TEM is a specialized technique used for visualizing aggregate structures in surfactant-water solutions. The method employed and interpretation of liposome

images has been previously described [104, 105]. The samples were prepared in a controlled environment vitrification system (CEVS), a chamber that maintains high humidity (to avoid water evaporation) at constant temperature (~ 100 K), as illustrated in Figure 2.2. A drop of the liposome solution was placed on a copper grid containing a polymer film and blotted, forming a thin aqueous layer on the membrane. The sample was flash frozen in ethane (~ 100 K) allowing the film to vitrify, an essential step to prevent crystal formation. The copper grid containing the sample was transferred to an electron microscope at liquid nitrogen temperature ($\sim -160^{\circ}\text{C}$) where it was analyzed. The resolution is 4 – 5 nm, thus the lipid bilayer can be distinguished, and vesicle diameter is limited to 500 nm lipid aggregates. This method avoids staining, drying and chemical fixation in sample preparation and thus minimal artefacts are reported. Two examples of known artefacts include osmotic stress and size-sorting, the former occurs when solutions of liposomes prepared in buffers containing salt evaporate, invagination occurs and the latter occurs following blotting of the copper grid and rearranging of larger aggregates at the edge of the perforation whereas smaller aggregates are present in the centre of the perforation. Thus special attention must be made during preparation and interpretation of the 2-dimensional micrograph from the 3-dimensional vitrified liposome sample, illustrated in Figure 2.3.

2.3.6. Freeze fracture

The structure of DSPC liposomes containing increasing concentrations of DSPE-PEG₂₀₀₀ lipids was analyzed in Chapter 4. Aliquots of each specimen were mixed with glycerol (25% v/v) as a cryoprotectant and incubated for 30 min. A small droplet of sample was loaded into the well of a Balzers gold freeze fracture specimen holder (BAL-TEC, BU 012 130-T) such that the sample protruded 2 mm above the top of the holder. The holder was inverted and plunged

Figure 2.2

Cryo-transmission electron microscopy sample preparation stage

In a climate chamber (maintained at ~ 100 K and high humidity) a drop of the liposome solution was placed on a copper grid containing a polymer film and blotted. The sample was flash frozen in liquid ethane allowing the film to vitrify. The copper grid containing the sample was transferred to an electron microscope at liquid nitrogen temperature (~ -160 K) where it was analyzed. Figure was adapted from Almgren M. *et al.* [104].

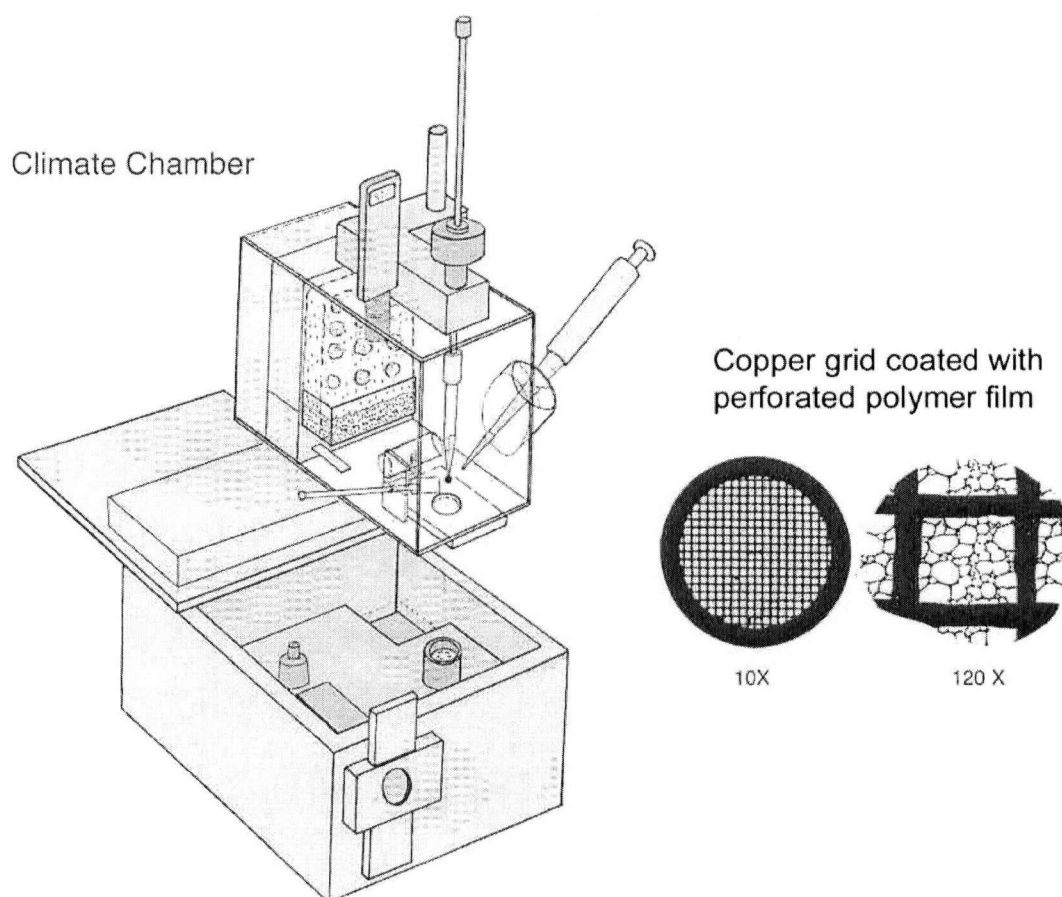
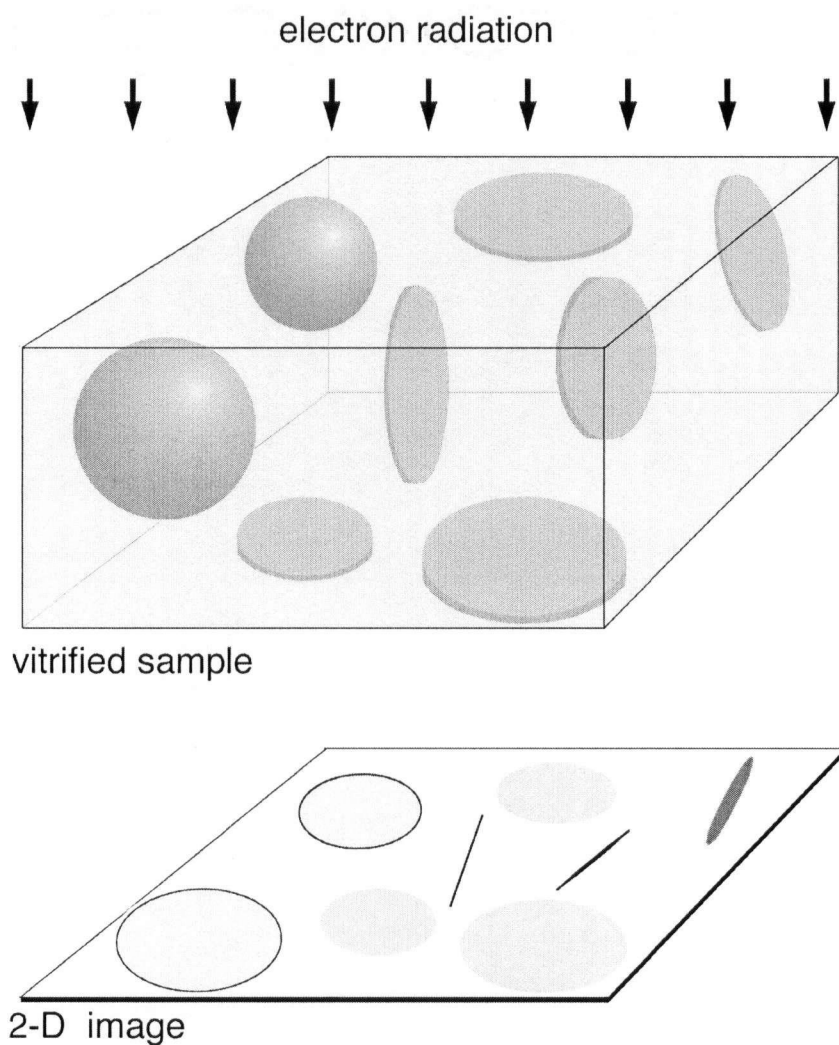


Figure 2.3

Interpretation of 2-dimensional cryo-TEM images from 3-dimensional samples

Liposomes and circular disks show differences in 2-dimensional image. Liposomes appear spherical (or with faceted edges) with a dense bilayer. Depending on the orientation of the circular disks, images appearing “face-on” will be circular without the dense outer member, and disks appearing “edge-on” will appear as a dense line as shown in the illustration adapted from reference [104].



into liquid propane (cooled to $\sim -160^{\circ}\text{C}$ with liquid nitrogen). After immersion, specimens were transferred to dry liquid nitrogen cooled cryovials and stored in liquid nitrogen. For freeze fracture, specimens were loaded onto the freeze fracture specimen table under liquid nitrogen, then inserted into a Balzers BAF 060 freeze fracture apparatus equipped with a quartz thin-film monitor (BAL-TEC, Balzers, Liechtenstein, Germany), which had been pre-cooled to -170°C . Specimens were then warmed to -110°C to -115°C and fractured without etching, followed immediately by replication using unidirectional platinum / carbon shadowing at 45 degrees (2.3 nm) and carbon backing at 90 degrees (2.2 nm). The holders containing the replicated samples were removed from the freeze fracture unit, thawed and slid gently into commercial bleach in the wells of a porcelain spotting plate. Cleaning required 48 hours in bleach at room temperature, with 3 changes of bleach. Replicas were then washed extensively with NANOpure water (Barnstead / Thermolyne, Dubuque, IA, USA) mounted on Formvar-coated 100 / hex copper grids and viewed at an accelerating voltage of 80 kV in a Hitachi H7600 transmission electron microscope (Tokyo, Japan) equipped with an AMT Advantage HR digital CCD camera (Advanced Microscopy Techniques Corp., Danvers, MA, USA).

2.3.7. Drug and liposomal membrane association studies

The amount of drug associated with liposomes prepared without a pH gradient was determined in Chapter 5. These studies were performed to ascertain the effect of drug hydrophobicity and the presence of ethanol on drug association with lipid membranes. Based on the experimental design, the drug concentration is a collective measurement of drug that has equilibrated across the lipid membrane into the aqueous space (or precipitated), drug associated with the lipid membrane through partitioning, hydrophobic and electrostatic interactions. In the

absence of a pH gradient, it is believed that most of the drug is associated with the membrane, although drug precipitation in the aqueous space cannot be disregarded. DSPC / DSPE-PEG₂₀₀₀ (95:5 mole ratio) and DSPC / CH / DSPE-PEG₂₀₀₀ (50:45:5 mole ratio) liposomes were prepared as described in Section 2.2. Lipids were hydrated in HBS, pH 7.4, and passed through an extruding apparatus. Drugs (idarubicin, daunorubicin, doxorubicin or epirubicin) and / or ethanol were combined with liposomes (5 mM total lipid concentration) at a 0.2 drug-to-lipid mole ratio and incubated at 40°C for 60 minutes. 100 µl aliquots were passed down Sephadex G-50 mini spin columns (680 X g, 2 min) and both lipid and drug concentrations were measured by radioactive counts (TriCarb[®] Model 1900TR liquid scintillation analyzer, Meriden, CT, USA) and an anthracycline extraction assay (section 2.5.2) followed by luminescence spectrometer detection, respectively.

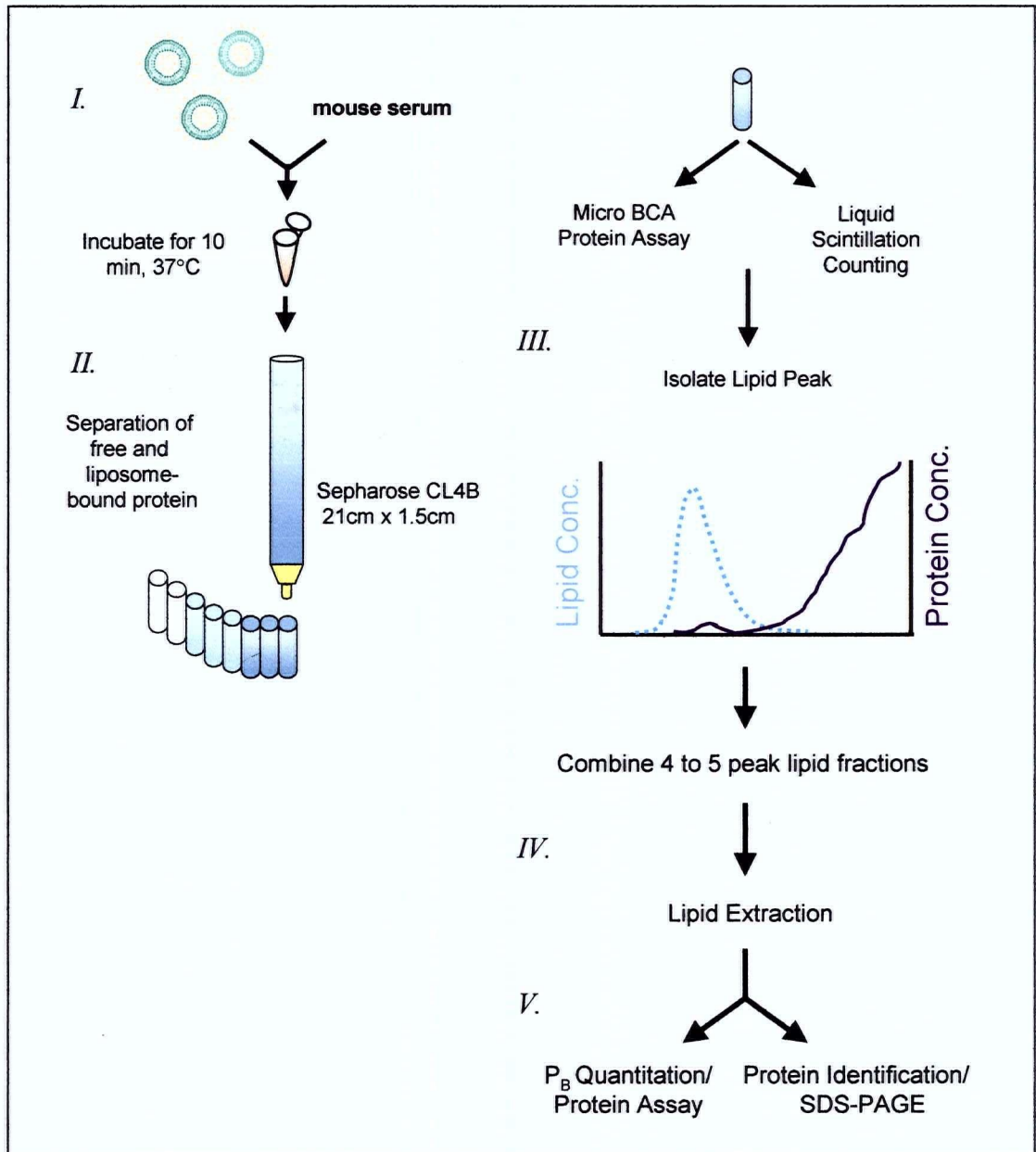
2.3.8. Liposomal plasma protein binding assay

For in vivo plasma protein binding studies performed in Chapter 4, Balb/c mice were administered 165 µmole/kg liposomal lipid intravenously in the lateral tail vein. Five minutes post-injection, a blood sample was obtained by cardiac puncture. Serum was isolated from whole blood by centrifugation for 10 minutes at 1000 X g, after allowing the blood to clot for 30 minutes. An aliquot of 500 µl plasma was separated by size exclusion chromatography as described below. For in vitro plasma protein binding studies, mouse serum (400 µl) and liposomes (7 mM lipid; 100 µl) were incubated at 37°C for 10 minutes. The lipid concentration was chosen to approximate 100 mg/kg lipid dose in vivo. The flow chart of methods used in determining liposomal plasma protein binding is shown in Figure 2.4.

Separation by size exclusion chromatography. The samples were separated by size on

Figure 2.4

Flow chart: Separation of liposomes from bulk plasma proteins and quantitation of plasma protein adsorbed to liposomes



a Sepharose CL-4B column (40 ml, 22 cm x 1.5 cm) with HBS (pH 7.4) at a flow rate of 0.5 ml/min. The first 8 ml was collected in a graduated cylinder and 0.5 ml fractions collected. From each sample, 25 μ l was utilized for scintillation counting (to determine lipid concentration) and 20 μ l for micro BCA assay (to determine protein concentration). This initial analysis was performed to discern the lipid and protein peaks to verify that there was complete separation between the two peaks.

Quantification of liposome-bound plasma proteins (P_B value). Providing that there was good separation between lipid and bulk plasma proteins, 3-5 fractions were pooled from the lipid peak. Due to the fact that lipid tends to interfere with many protein assays, a lipid extraction was performed to isolate the protein for quantification by micro-bicinchoninic acid (BCA) assay as described previously [106]. In brief, 20 μ l (in triplicate) of pooled sample was measured by liquid scintillation counting to determine the lipid concentration of the pooled sample. For lipid extraction 400 μ l of cold methanol was added to 100 μ l of pooled sample (in triplicate) in 1.5 ml microfuge tubes. The samples were vortexed and centrifuged at 9000 X g for 3 minutes. A 200 μ l aliquot of chloroform was added to the samples followed by vortexing and centrifuging at 9000 X g for 3 minutes. A 300 μ l aliquot of dH₂O was added to each sample, followed by vortexing and centrifuging at 9000 X g for 4 minutes. The upper phase was discarded (approximately 700 μ l) and 300 μ l of methanol was added, the sample was subsequently vortexed and centrifuged at 9000 X g for 4 min. Most of the supernatant was removed and the residual supernatant was dried down with nitrogen for 2 hours. Protein was present as a dry pellet at the bottom of the microfuge tube and resuspended in 110 μ l water at 50°C – 60°C. For protein concentration determination, 110 μ l of micro BCA working reagent (Pierce, Rockford, IL, USA) was added to each sample and measured at 570 nm on MRX

microplate reader (Dynex Technologies, Inc., Chantilly, VA, USA) and compared to a bovine serum albumin standard curve. The amount of lipid in the recovered sample was calculated from the specific activity. Protein binding values (P_B) were measured as $\mu\text{g protein} / \mu\text{mole liposomal lipid}$, values represented average and standard deviations from three experiments.

Electrophoretic analysis of liposome-bound proteins. Following separation of liposomes from bulk plasma proteins and delipidation (lipid extraction / protein precipitation), samples were solubilized in SDS-reducing buffer (0.0625 M Tris-HCl, 10% (v/v) glycerol, 2% (w/v) SDS, 5% (v/v) β -mercaptoethanol, 0.125% (w/v) bromophenol blue) heated to 95°C, cooled and centrifuged. Approximately 0.1 μmole of total lipid was loaded on a SDS-polyacrylamide gel (PAGE) prepared on a Mini Protean II electrophoretic apparatus (Bio-Rad Laboratories, Richmond, CA, USA). Proteins were visualized by silver staining. Silver stain SDS-PAGE molecular weight standards (Bio-Rad Laboratories, Richmond, CA, USA) were used to estimate the molecular weights of proteins.

2.4. Drug Loading

2.4.1. Remote loading of anthracyclines

The remote loading procedure has been well characterized for weak bases such as anthracyclines [107]. Following hydration of lipid films in citrate (300 mM citric acid; pH 4.0), extrusion and size determination, liposomes were passed down a Sephadex G-50 column (10 cm x 1.5 cm) equilibrated with HBS (HEPES buffered saline; 20mM HEPES, 150 mM NaCl, pH 7.4) to exchange the external buffer. The eluted liposomes had a transmembrane pH gradient, pH 4.0 inside and pH 7.4 outside. Drugs, and / or ethanol used in Chapter 4 (note that in all cases, ethanol was added following drug addition to prevent exposure of liposomes to

excessively high ethanol concentrations) were added to the liposome preparation (5 mM total lipid concentration) at a 0.2 drug-to-lipid mole ratio at varying incubation temperatures.

For determination of the rate of drug loading of anthracyclines into liposomes (used in Chapters 3 and 4), 100 μ l aliquots were added to mini spin columns at 1, 2, 5, 10, 15, 30, 60 and 120 minutes following remote loading. Spin columns were prepared by adding glass wool to a 1 cc syringe, followed by adding hydrated Sephadex G-50 beads that were packed by centrifugation (680 X g, 2 min). Following addition of the sample to the column, the liposome fraction was collected in the void volume (centrifugation 680 X g, 2 min) and both lipid and drug content were analyzed. The lipid concentration was determined from the specific activity of the $^3\text{[H]}$ -CHE radioactive counts and drug concentration was determined by measuring the absorbance at 480 nm (HP 8453 UV-visible spectroscopy system, Agilent Technologies Canada, Inc., Mississauga, ON, Canada) in a 1% Triton X-100 solution and compared to a standard curve. Prior to absorbance analysis, samples were heated in boiling water to the cloud point of the detergent and cooled to room temperature.

2.4.2. Passive loading of gemcitabine

Gemcitabine hydrochloride (200 mg) was rehydrated in HBS (HEPES buffered saline, 20 mM HEPES, 150 mM NaCl, pH 7.4) at a concentration of 50 mg/ml. A lipid film (150 μ mole lipid) containing trace quantities of $^3\text{[H]}$ -CHE radiolabel was prepared (as mentioned in section 2.2), and rehydrated with 1.6 ml (214 μ mole gemcitabine) solution at 40°C for 60 min. The samples were passed through an extruding apparatus containing 2 stacked 100 nm polycarbonate filters at 65°C. The mean diameter and size distribution of each liposome preparation was determined by quasielastic light scattering. Lipid and gemcitabine

concentrations were measured to estimate the encapsulation efficiency and final drug-to-lipid mole ratio. Lipid concentrations were determined by measuring radioactivity by liquid scintillation counting and gemcitabine concentration was determined by absorbance spectrophotometry with samples diluted with 10 mM OGP (octyl- β -D-glucopyranoside) detergent, measured at 268 nm and compared to a standard curve.

2.5. Pharmacokinetic Analysis

2.5.1. Mice

Balb/c mice breeders, 20-22g, were purchased from Charles River Laboratories (St. Constant, QC, Canada) and bred in house. Mice were housed in microisolator cages and given free access to food and water. All animal studies were conducted according to procedures approved by the University of British Columbia's Animal Care Committee and in accordance with the current guidelines established by the Canadian Council of Animal Care.

2.5.2 Plasma elimination of drugs

The rate of plasma elimination of idarubicin (Chapters 3 and 4) and gemcitabine containing tracer quantities of ^3H -gemcitabine (Chapter 7) was assessed. Mice were injected with 33 $\mu\text{mole/kg}$ (18 mg/kg) idarubicin or 16.5 $\mu\text{mole/kg}$ (5 mg/kg) gemcitabine administered intravenously into the lateral tail vein of Balb/c mice. At various time points up to 4 hours post-drug administration, blood was collected by tail nick (collected in microfuge tubes) or cardiac puncture (collected in liquid EDTA coated tubes), centrifuged at 1000 X g for 10 min to isolate the plasma fraction. The plasma was placed in a separate microfuge tube and vortexed to ensure a homogenous distribution.

The tail nick procedure for obtaining blood samples was used to minimize the number of mice sacrificed. In this way, three blood samples could be obtained from a single mouse within a 24 hour time interval. In brief, the lateral tail vein of mice was nicked with a small sharp blade. A 25 μ l glass pipet, pre-washed with EDTA, was used to withdraw blood. The blood was expelled into a microfuge tube containing 200 μ l of 5% (w/v) EDTA and thoroughly mixed. Blood / EDTA samples were centrifuged for 10 minutes at 1000 X g. The supernatant was transferred to a 1.5 ml microfuge tube. 250 μ l Hank's balanced salt solution (HBSS) was added to the pellet, resuspended and centrifuged for 10 minutes at 1000 X g. The supernatants were mixed together. Assuming a 48% haematocrit for a 20 gram Balb/c mice [101], approximately 13 μ l plasma was obtained from a 25 μ l blood sample. From the recovered plasma samples, aliquots were used to measure drug (and / or lipid) concentrations.

2.5.3. Plasma elimination of liposomes

The plasma elimination of liposomes containing tracer quantities of radiolabel (3 [H]-CHE or 14 [C]-CHE) was assessed. When required, samples were concentrated with cross-flow cartridges (500,000 MWCO) manufactured by A/G Technology Corp. (Needham, MA, USA) prior to i.v. administration. This method, tangential flow dialysis, was also used to remove residual ethanol in samples prepared in Chapter 5. Mice were injected with 165 μ mole/kg liposomal lipid administered intravenously into the lateral tail vein of Balb/c mice. At various time points up to 24 hours post-drug administration, blood was collected by tail nick (collected in microfuge tubes) and cardiac puncture (collected in liquid EDTA coated tubes) and centrifuged at 1000 X g for 10 min to isolate the plasma fraction. Studies assessing two radiolabels, 3 [H]-CHE and 3 [H]-DPPC, were completed and the results demonstrated that the

recovered plasma lipid concentrations were not significantly different.

2.5.4. Plasma elimination of liposomal drugs

The plasma elimination of liposomal drugs containing doxorubicin, daunorubicin, idarubicin, or gemcitabine samples administered intravenously into the lateral tail vein of Balb/c female mice was assessed. Mice were injected with 33 $\mu\text{mole/kg}$ drug and 165 $\mu\text{mole/kg}$ lipid (0.2 drug-to-lipid ratio). For liposomal gemcitabine samples, mice were injected with 16.5 $\mu\text{mole/kg}$ gemcitabine (0.1 drug-to-lipid mole ratio). At various time points post-drug administration, blood was collected by tail nick or cardiac puncture. Plasma lipid and $^3\text{[H]}$ -gemcitabine were quantified by liquid scintillation counting. Anthracyclines were extracted from plasma with a partitioning assay, described in section 2.5.5, followed by fluorescence spectrophotometer detection.

2.5.5. Anthracycline partitioning assay

Doxorubicin, daunorubicin, epirubicin and idarubicin were extracted from plasma or buffer samples with a standard partitioning assay [51], to determine total drug plasma concentration including possible metabolites. Briefly, an aliquot of plasma was added to a 16 x 100 mm test tube and made up to 800 μl with distilled water. Subsequently, 100 μl of both SDS and 10 mM H_2SO_4 were added, vortexed, and followed by the addition of 2 ml of 1:1 isopropanol / chloroform mixture. Samples were placed in -80°C for 1 hour. All tubes were equilibrated to room temperature. The bottom organic phase was carefully transferred into a clean test tube and samples were measured on an LS 50B luminescence spectrophotometer (Perkin-Elmer, Beaconsfield, Buckinghamshire, England) using an excitation wavelength of 480

nm (5 nm bandpass) and an emission wavelength of 550 nm (10 nm bandpass). The extraction efficiency for plasma samples was > 90%.

2.5.6 WinNonlin / pharmacokinetic modeling

The plasma elimination data was modeled using WinNonlin (version 1.5) pharmacokinetic software (Pharsight Corporation, Mountain View, CA, USA) to calculate pharmacokinetic parameters, listed in Table 2.1. As the plasma elimination data was not obtained from a single mouse (i.e., blood samples from 2 mice were required to measure the drug and lipid concentrations over a 24 hour time interval) the values were reported as mean plasma area under the time versus concentration curve (AUC) without standard deviations, thus statistical analysis could not be performed.

The mean plasma AUC for a defined time interval was determined from the concentration versus time curves and subsequent calculation by the standard trapezoidal rule, extrapolated to the last time point (Tlast). The drug concentration – time curves were applied to a pharmacokinetic (compartmental or non-compartmental) model and the best-fit was chosen. For plasma elimination studies in Chapters 4, 6 and 7, data fit a mono-exponential curve representing a one compartment model and thus the pharmacokinetic parameters were calculated as follows: plasma half-life was calculated from the formula $T_{1/2} = 0.693 / k_{elm}$, where k_{elm} is derived from the best fit line of the data represented as a semi-log plot (i.e., log drug plasma concentration versus time); clearance (CL) was calculated from the equation $CL = \text{dose}_{i.v.} / AUC$, where AUC is the area-under-the curve; volume of distribution (Vd) was calculated from the formula $Vd = \text{dose}_{i.v.} / C_p$, where C_p is the concentration in the plasma at time zero.

Table 2.1

Summary of pharmacokinetic parameters

AUC_{0-t}	<p>Area-Under-the-Curve of plasma concentration versus time plot from time zero to a defined time interval.</p> <p>This value is determined by integrating drug concentration in plasma versus time. <i>Units: $\mu\text{mole h ml}^{-1}$</i></p>
$T_{1/2}$	<p>Plasma Half-Life.</p> <p>The time required for the drug concentration in plasma to decrease by 50%. <i>Units: time (i.e., h).</i></p>
V_d	<p>Apparent Volume of Distribution.</p> <p>The volume of bodily fluid into which the drug dose is dissolved</p> <p>This value is calculated by dividing the dose (mg or mole) by the plasma drug concentrations (mg or mole/ unit volume). <i>Units: unit volume (e.g., L or ml).</i></p>
Cl	<p>Clearance.</p> <p>The volume of blood which is completely cleared of drug per unit time.</p> <p>This value is calculated by dividing the dose (mg or mole) by the AUC (mg or mole h ml^{-1}) or multiplying the V_d with $(0.693 / T_{1/2})$. <i>Units: volume/ time (i.e., ml h^{-1})</i></p>
$AUMC_{0-t}$	<p>Area-Under-the-Moment Curve of plasma concentration-time plot from time zero to a defined time interval.</p> <p>This value is determined by integrating area under the concentration-time versus time. <i>Units: $\mu\text{mole h}^2\text{ml}^{-1}$</i></p>
MRT_{last}	<p>Mean Residence Time. The time required for elimination of 63% of the injected dose from the plasma.</p> <p>Ratio of $(AUMC_{0-t}) / (AUC_{0-t})$. <i>Units: time (i.e., h)</i></p>

The area-under-the-moment (AUMC) is calculated from the first-moment curve of the plasma drug concentration versus time curve, which is the plasma concentration multiplied by the corresponding time point and plotted at the same time point [73]. The time constant (or time taken to eliminate 63% of the injected dose) is known as the mean residence time (MRT) was calculated as $MRT = 1 / k_{elm} = T_{1/2} / 0.693 = AUMC / AUC$. The pharmacokinetic parameters AUMC and MRT are based on the statistical moment theory (non-compartmental analysis).

2.6. Cells and Culture

2.6.1. Subculturing and trypan blue staining

P388 wild type and doxorubicin resistant (ADR) cells were obtained from the National Cancer Institute tissue repository (Bethesda, Maryland, USA) and were propagated *in vivo*. In brief, one vial of frozen ascites was removed from the nitrogen tank and thawed at 37°C and cells were injected *i.p.* into female BDF-1 mice (6-8 weeks old, 20-22 g, Charles River Laboratories, St. Constant, QC, Canada). Tumor-bearing mice were euthanized and a peritoneal lavage was performed. With a 1 cc syringe with 20 gauge needle, 0.5 – 1.0 ml of peritoneal fluid was removed and aliquoted into a 15 ml falcon tube containing 5 ml of Hank's Balanced Salt Solution (HBSS, no calcium or magnesium). A 0.5 ml aliquot was transferred into another 15 ml conical sterile tube containing 5 ml HBSS. The cells were exposed to plastic culture ware (for adherence of monocytes) and Ficoll-Paque density centrifugation (red blood cell removal). For cell counting, an aliquot (0.1 ml) of P388 cell suspension was diluted 1:1 with trypan blue (2%), stain and counted using the haemocytometer, only cells with > 90% cell viability were used for experimentation. For each passage, 2 female BDF-1 mice were injected *i.p.* with 1×10^6 cells in 0.5 ml (2×10^6 cells/ml) of P388 cell suspension. This was repeated every 6 - 8

days to a maximum of 18 passages. For tissue culture experiments such as MTT cytotoxicity assays, P388 cells were obtained following peritoneal lavage and treatment to remove red blood cells and peritoneal macrophages. P388 cells were maintained in RPMI culture media containing 10% FBS and 1% L-glutamine as a cell suspension in 25 cm² culture flasks maintained at 37°C in humidified air with 5% CO₂ and subcultured by dilution daily for no more than one week.

MDA435/LCC6 wild type and MDR1-transfected are human estrogen receptor negative breast cancer cells and were a generous gift from Dr. Robert Clarke (Georgetown University, Washington, D.C., USA). Cells were grown as adherent monolayer cultures in 25 cm² culture flasks in DMEM culture medium supplemented with 10% fetal bovine serum and 1% L-glutamine. Cells were maintained at 37°C in humidified air with 5% CO₂ and were subcultured weekly using 0.25% trypsin with 1 mM ethylenediaminetetraacetic acid (EDTA).

2.6.2. MTT cytotoxicity assay

In order to assess cytotoxicity the MTT (3-(4,5-dimethylthiazol-2-yl)-2,5-diphenyl tetrazolium bromide) assay was utilized [108]. Cells were counted by trypan blue staining (> 90% cell viability for experiments) and seeded in 96 well microtiter plates at 1500 cells / 0.1 ml diluted in medium. The wells in the perimeter of the 96 well microtiter plates contained 0.2 ml sterile water. After 24 hours at 37°C, serial dilutions of drugs (including doxorubicin, idarubicin or gemcitabine) were added to the plate (100 µl/well). Control wells consisted of media only (200 µl/well), or cells and media (no treatment). There were 6 replicates (per plate) for all control and treatment groups. Following 72 hours incubation at 37°C, MTT stock solution (5 mg/ml PBS; phosphate buffered saline, pH 7.4) was diluted 1:4 with media and 50 µl

was added to each well. Plates were incubated for 4 hours in humidified air with 5% CO₂ at 37°C. The P388 non-adherent cells were spun down for 10 minutes at 1800 RPM. The media was aspirated off and 0.15 ml DMSO was added per well and resuspended on a plate shaker (5 – 10 min). The absorbance was measured at 570 nm on a MRX microplate reader (Dynex Technologies, Inc., Chantilly, VA, USA). The cytotoxicity upon drug exposure was quantified by expressing the percent cell viability for each treatment relative to untreated control cells (% control). For multiple drug exposure studies (used in Chapter 7), the drug concentration required to inhibit 50% (IC₅₀) and 90% (IC₉₀) of cell growth, was compared between single and combination drug treatments. This was further analyzed by the median effect equation of Chou and Talalay [109], described in section 2.6.3.

2.6.3. Calcsyn for analyzing drug combination treatments

The method of Chou and Talalay was used to distinguish between synergy, antagonism and additive effects of combined drug treatments from in vitro MTT cytotoxicity assays. This method, now provided in a software package (Calcsyn; Biosoft, Cambridge, UK), derives a median effect equation (3) to correlate drug dose and effect.

$$fa/fu = (D/Dm)^m \quad (3)$$

A dose–effect plot is generally a sigmoidal relationship and the above symbols represent the following: D, dose of drug; Dm, median effect dose; fa, fraction affected dose; fu, fraction unaffected dose and m, an exponent signifying the sigmoidicity of the dose-effect curve. The mathematical equation above forms a linear relationship known as the median effect equation [109].

$$\log (fa/fu) = m \log (D) - m \log (Dm) \quad (4)$$

Fixed ratio combinations of idarubicin and gemcitabine were initially selected on the basis of the IC_{50} of each drug. It was assumed that idarubicin and gemcitabine have mutually exclusive mechanisms of action and thus for two drugs D_1 and D_2 (doses of drug 1 and 2 when used in combination for a specific fractional effect) divided by their D_x (dose of drug for a specific fractional effect when administered as a single agent), their “combination index” or additive effect is equal to 1.

$$(D)_1/(D_x)_1 + (D)_2/(D_x)_2 = 1 \quad (5)$$

Thus synergy was defined by a combination index (CI) of < 1 and antagonism was defined as > 1 . Data were reported as mean \pm S.D. from three separate experiments, performed in triplicate.

2.7. Animal Models

2.7.1. Evaluation of antitumor activity in P388 lymphocytic leukemia model

Dose range finding studies of free and liposomal idarubicin (Chapter 6 and 7) and / or gemcitabine (Chapter 7) were performed in non-tumor bearing female BDF-1 mice. Mice were weighed daily and monitored for signs of stress or toxicity (e.g., lethargy, scruffy coat, and ataxia). The maximum tolerable dose (MTD) was defined as the dose that no animal in a given group exhibited signs of significant toxicity for 30 days post-drug treatment.

Efficacy studies were conducted in female BDF-1 mice injected i.p. with 10^6 P388 cells. Treatments commenced 24 hours post tumor cell inoculation. Treatment groups consisted of saline (control) and 0.5, 1, 2 and 3 mg/kg doses of free or liposomal idarubicin administered as a single i.v. bolus injection and between 100 to 500 mg/kg gemcitabine and 1 to 5 mg/kg liposomal gemcitabine (selected on the basis of dose range finding studies). In Chapter 7, fixed

dose ratios for combination treatments were defined on the basis of 0.66 MTD [110] when used as a single agent. Mice were monitored daily for signs of stress and toxicity as detailed in the previous paragraph. Median survival time (MST) and percent weight loss was determined for each treatment. Although death was indicated as an end point, animals that showed signs of illness due to tumor progression were terminated, and the day of death was recorded as the following day.

2.7.2. Evaluation of antitumor activity in a MDA435/LCC6 human breast xenograft model

MDA435/LCC6 was established as a novel ascites model from the estrogen receptor negative MDA-MB-435 human breast cancer cell line. The cells were isolated from exponentially growing MDA-MB-435 cells inoculated in the mammary fat pads of NCr *nu/nu* athymic mice. Cells from a subsequent spontaneous ascites were removed and transplanted i.p. into NCr *nu/nu* athymic mice. The full length human MDR1 cDNA was transduced into MDA435/LCC6 cells and selected in the presence of colchicine for 3 months as described previously [111]. Both WT and MDR1-transfected MDA435/LCC6 cells were a generous gift from Dr. Robert Clarke (Georgetown University, Washington DC, USA)

Both MDA435/LCC6 WT and MDR1 transfected cell lines were maintained and passaged in culture in DMEM medium containing 10% FBS and 1% L-glutamine in incubators with humidified air and 5% CO₂. For in vivo animal model studies, SCID/Rag 2M mice were injected i.p. (0.5 ml) with 5 million MDA435/LCC6 WT or MDR1-transfected cells. After 20 - 25 days ascites were removed via peritoneal lavage and placed in 15 ml sterile falcon tube with 5 ml HBSS (no calcium or magnesium salts). The ascites suspension was further diluted to 25 -

30 ml in a 50 ml sterile falcon tube. Cell concentration was determined by trypan blue staining using a haemocytometer and cells were resuspended in HBSS (following centrifugation) at concentration of 40 million cells/ml. Using a 27G needle, 50 μ l of the cell suspension (2 million cells) was injected subcutaneously in the back of SCID/Rag 2M mice. When tumors were palpable, treatments were administered i.v. and tumors were measured with callipers.

2.8. Statistical Analysis

All data values are reported as mean \pm standard deviation (S.D.). A standard one-way analysis of variance (ANOVA) was used to determine statistically significant differences of the means. For multiple comparisons, Post-hoc analysis using the Tukey-Kramer test was performed. Survival curves were computed using the Kaplan-Meier method. Long-term survivors (survival time > 60 days) were censored, and assigned a survival time of 61 days. Treatment groups were subsequently analyzed using SPSS statistics software (SPSS Inc., Chicago, IL, USA) and compared using a two sample log-rank test. $P < 0.05$ was considered significant for all statistical tests.

CHAPTER 3

IMPROVED RETENTION OF IDARUBICIN AFTER INTRAVENOUS INJECTION OBTAINED FOR CHOLESTEROL-FREE LIPOSOMES*

3.1 Introduction

The development of liposomes as effective drug delivery systems was achieved, in part, as a consequence of improved properties obtained following incorporation of membrane rigidifying agents such as cholesterol. In fact, some of the early research on liposomes as delivery systems for i.v. applications demonstrated that the presence of cholesterol (i) enhanced retention of entrapped solutes [45, 46, 112-114], (ii) diminished interaction with plasma proteins [115, 116], (iii) reduced phospholipid loss by phospholipases and lipoproteins [79, 81, 117], (iv) reduced macrophage digestion [94] and (v) maintained membrane fluidity over a wide temperature range. It is believed that a combination of these factors collectively yielded lipid carriers that were resilient within the biological milieu in terms of both liposome structure stability and retention of entrapped solutes.

Given the progress in liposome technology as a delivery strategy for anti-cancer drugs, some may find it surprising that this simple methodology is not applied more generically to other cancer drugs. In principle, liposomes must be developed with desirable and controlled release properties that are selected on the basis of the drug being entrapped. More specifically, the lipid composition of liposomes cannot be viewed in generic terms, where one liposome formulation is suitable for all drugs. Rather it is critical for the liposome to be designed around the drug of interest. The suitability of a liposome formulation is determined by an iterative process that correlates pharmacodynamic behaviour of the encapsulated drug with the plasma

* Adapted from Dos Santos, N. et al. (2002) Improved retention of idarubicin after intravenous injection obtained for cholesterol-free liposomes. *Biochimica et Biophysica Acta*, 1561: 188-201.

elimination and biodistribution behaviour of the liposomal carrier. A critical parameter measured in these studies is the in vivo drug release rate that, in turn, is dependent on lipid composition. It is well understood that liposomal formulations prepared using zwitterionic lipids, such as diacylphosphatidylcholine, and cholesterol are effective as drug carriers, but the benefits for a given anti-cancer drug depend on the ability of the carrier to retain drug following i.v. administration, and to release it at an appropriate rate. Further, simple changes in phospholipid acyl chain length can have dramatic effects on in vivo drug release rates [118]. In general, as acyl chain length increases, drug retention increases [119]. There are some drugs, however, which are simply not retained well in these phospholipid / cholesterol formulations, even when the acyl chain length increases to C22 and the bilayer exhibits gel-to-liquid crystalline transitions above 100°C.

Another solution to improve the retention of certain drugs is based on the preparation of liposomes without cholesterol. This has not been explored thoroughly, but there are now compelling reasons to consider the potential of cholesterol-free liposomes as carriers. As a direct consequence of cholesterol's interactions with phospholipids, the permeability of a liposome increases at temperatures below the phase transition temperature of the bulk lipid component [47, 120]. Thus, membranes (absent of cholesterol) consisting of gel phase lipids ($T_c > 40^\circ\text{C}$) will form a more rigid membrane capable of retaining entrapped contents for in vivo administration. Additional incorporation of surface stabilizing PEGs will further prevent surface-surface interactions and facilitate prolonged circulation lifetimes. To date little is known about the application of cholesterol-free liposomes for retention of entrapped solutes and these reasons, alone, were sufficient to propose that cholesterol-free liposomes may be relevant carriers for hydrophobic agents that are not currently retained in conventional formulations.

3.2 Hypothesis

Liposomes composed of gel phase phospholipids, in particular distearoylphosphatidylcholine, and PEG-conjugated lipids will have prolonged circulation longevity and will be suitable for delivery of a hydrophobic anthracycline, idarubicin.

3.3 Results

3.3.1 Circulation longevity of cholesterol-free liposomes

Given that the pharmacokinetic behaviour of an encapsulated drug will be dependent on the pharmacokinetic characteristics of the drug carrier, studies were completed to assess circulation longevity of various liposome formulations. The cholesterol-free liposome formulation composed of DSPC / DSPE-PEG₂₀₀₀ (95:5 mole ratio) was compared with cholesterol-containing formulations consisting of DSPC / CH (55:45 mole ratio) and DSPC / CH / DSPE-PEG₂₀₀₀ (50:45:5 mole ratio). Each liposome formulation was injected intravenously into the lateral tail vein of mice (~ 3.3 μmole / mouse for a 20 g mice) and at various time points aliquots of EDTA-treated plasma were analyzed to determine total lipid/ml plasma. As shown in Figure 3.1, DSPC liposomes were rapidly eliminated from the circulation with less than 6% of the injected dose ($< 0.2 \mu\text{mole/ml}$ plasma) present at 1 hour post-administration and an estimated mean plasma area under the curve ($\text{AUC}_{0-24\text{h}}$) of $2.38 \mu\text{mole h ml}^{-1}$. Inclusion of cholesterol into the membrane resulted in a 10-fold increase in the mean plasma $\text{AUC}_{0-24\text{h}}$; however, at 24 hours post-administration less than 1% of the injected dose remained in the plasma compartment. Inclusion of 5 mol% DSPE-PEG₂₀₀₀ into the DSPC / CH formulation resulted in a 2-fold increase in the mean plasma AUC in comparison to DSPC / CH

(55:45 mole ratio), a result which is consistent with other reports demonstrating that incorporation of PEG-modified lipids can enhance the circulation lifetime of liposomes [29, 57].

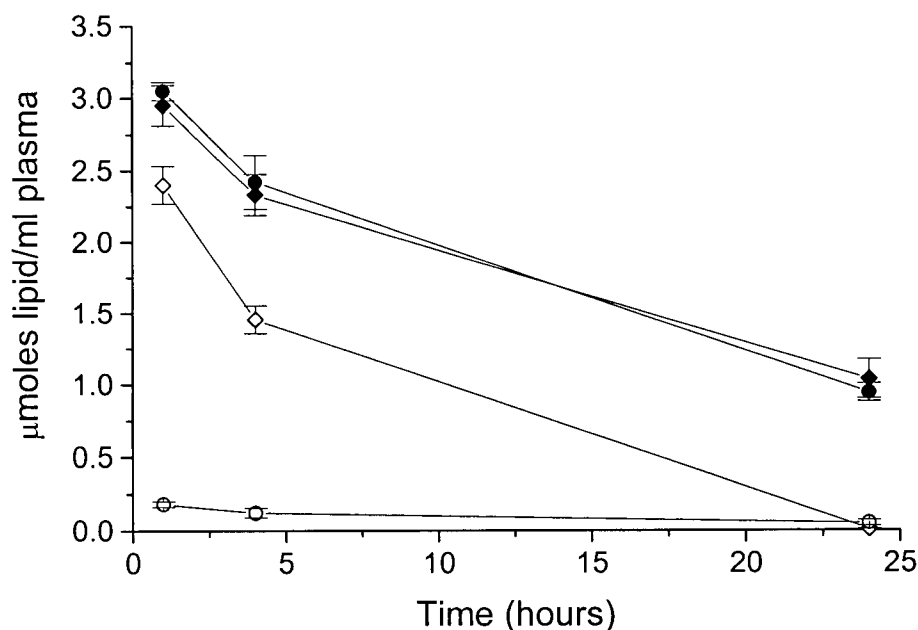
Inclusion of 5 mol% DSPE-PEG₂₀₀₀ into DSPC liposomes without cholesterol engendered significant increases in circulation lifetimes when compared to DSPC formulations without stabilizing lipids. There was a 19-fold increase in mean plasma AUC_{0-24h}, and 29% of the injected dose was present in the circulation after 24 hours. This result demonstrated that poly(ethylene glycol)-conjugated lipids are an essential component of cholesterol-free liposomes if they are to be used as systemically viable drug carriers. It should be noted that the data are consistent with results obtained by Woodle *et al.* who first demonstrated that the presence of PEG-conjugated lipids enhanced circulation longevity of liposomes in a manner that was independent of lipid composition [57].

While characterizing cholesterol-free liposome formulations it was of importance to decide which formulation would be optimal for application as a delivery system for a relatively hydrophobic anti-cancer agent, such as idarubicin. The influence of 5 mol% PE-PEG on the plasma elimination of liposomes containing various acyl chain lengths of phosphatidylcholine; DSPC (C18), DPPC (C16) and DMPC (C14) was evaluated. In these studies the acyl chain length of the bulk phospholipid (PC) in the lipid bilayer was incorporated with the corresponding PE-conjugated PEG containing the same number of carbons in order to ensure optimal mixing conditions, however, it is now well established that the short chain (C14 and less) PEG-modified PEs, are rapidly exchanged out of liposomal membranes after i.v. administration [97, 121]. Thus the effects of PEG-lipid incorporation may be influenced by this parameter.

Figure 3.1

Plasma elimination of liposome formulations in Balb/c mice

Large unilamellar liposomes radiolabeled with ^3H -cholesteryl hexadecyl ether (CHE) were administered intravenously via the dorsal tail vein of female Balb/c mice at a dose of 165 $\mu\text{mole/kg}$ total lipid. Blood was collected at 1, 4 and 24 hours by tail nick and cardiac puncture procedures (injected dose = 3.3 $\mu\text{mole lipid / ml plasma}$). An aliquot of plasma was used to determine liposomal lipid content as described in Chapter 2. The liposome formulations comprised of DSPC / DSPE-PEG₂₀₀₀ (95:5 mole ratio, ●), DSPC / CH / DSPE-PEG₂₀₀₀ (50:45:5 mole ratio, ◆), DSPC / CH (55:45 mole ratio, ◇), and DSPC (100 mole ratio, ○). Each data point represents the average lipid plasma concentration \pm S.D. for four mice.



Data used to assess the circulation longevity of DSPC, DPPC and DMPC liposomes in the absence and presence of 5 mol% PE-PEG₂₀₀₀ is summarized in Figure 3.2. There was no significant difference in the circulation longevity between DMPC (100 mole ratio) and DMPC / DMPE-PEG₂₀₀₀ (95:5 mole ratio) liposomes; however, as the acyl chain length of the phospholipid increased, a more significant difference in circulation longevity between the various PCs and PC / PE-PEG₂₀₀₀ (95:5 mole ratio) liposomes was observed. As suggested above, differences in the PEG-lipid induced effects on the liposomal systems may be attributed to the phase state of the liposomes whereby a more liquid-crystalline phase lipid may facilitate rapid exchange of lipid components out of and into the liposomal membrane following i.v. injection. For example, it has been demonstrated that egg phosphatidylcholine rapidly accumulates cholesterol following i.v. injection [122], therefore the slow plasma elimination rate observed for DMPC liposomes (without PEG-modified lipids) may be attributed to the accumulation of cholesterol into this formulation and / or to the transfer of the ³[H]-radiolabel to lipoproteins. Studies evaluating the retention of ¹⁴[C]-lactose indicated that both DMPC and DPPC liposomes lost encapsulated contents rapidly in vitro and thus DSPC liposomes were utilized in subsequent studies.

3.3.2 Influence of poly(ethylene glycol) content and molecular weight on cholesterol-free liposome circulation longevity

Previous studies have demonstrated that the elimination rate of cholesterol-containing systems decreases following PEG incorporation, a result that is dependent on both PEG content and molecular weight [123-125]. As shown in Figures 3.3 and 3.4, variations in PEG-lipid

Figure 3.2

Plasma elimination of liposomes prepared using phosphatidylcholine species with varying acyl chain lengths in the absence and presence of PE-PEG₂₀₀₀

Large unilamellar liposomes radiolabeled with ^3H -cholesteryl hexadecyl ether (CHE) were administered intravenously via the dorsal tail vein of female Balb/c mice at an approximate dose of 165 $\mu\text{mole/kg}$ total lipid. Blood was collected at 1, 4 and 24 hours by tail nick and cardiac puncture procedures (injected dose = 3.3 $\mu\text{mole lipid / ml plasma}$). An aliquot of plasma was used to determine liposomal lipid content as described in Chapter 2. Liposomes of varying acyl chain lengths DMPC / DMPE-PEG₂₀₀₀ (**A**, squares), DPPC / DPPE-PEG₂₀₀₀ (**B**, triangles) and DSPC / DSPE-PEG₂₀₀₀ (**C**, circles) in the absence (open symbols) and the presence (closed symbols) of 5 mol% PE-PEG₂₀₀₀ were evaluated. Each data point represents the average lipid plasma concentration \pm S.D. for four mice.

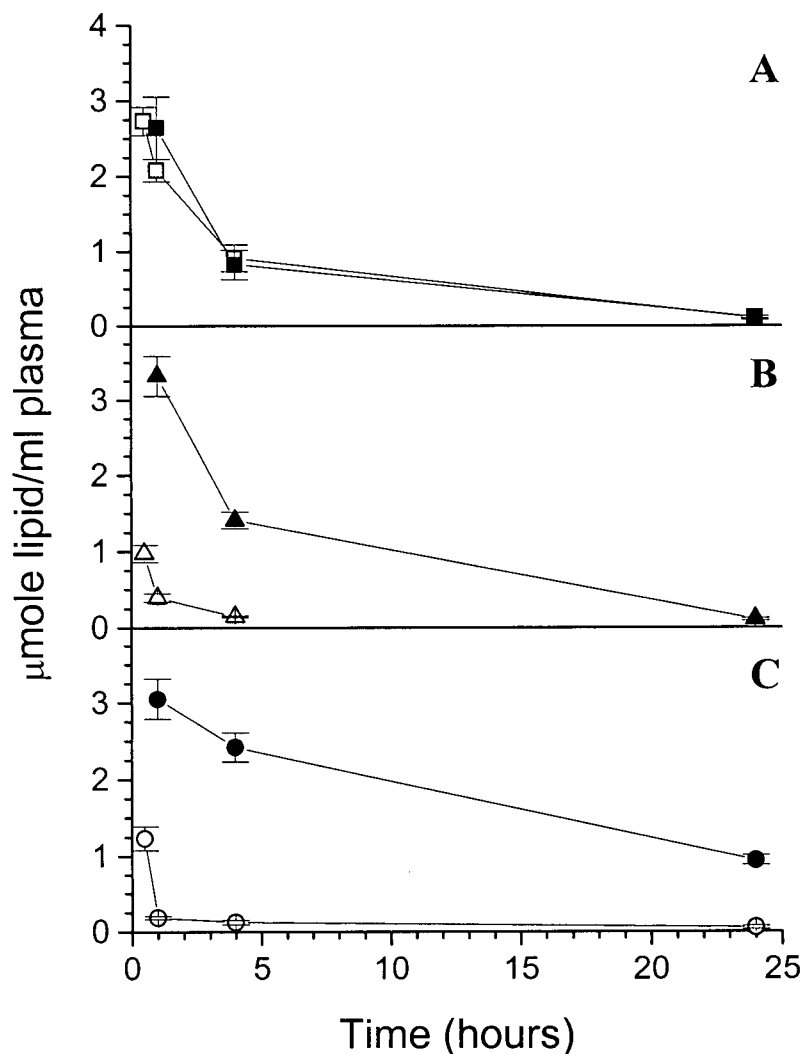


Figure 3.3

Plasma elimination of DSPC liposomes containing increasing mol % PE-PEG₂₀₀₀

Large unilamellar liposomes radiolabeled with ^3H -cholesteryl hexadecyl ether (CHE) were administered intravenously via the dorsal tail vein of female Balb/c mice at an approximate dose of $165\text{ }\mu\text{mole/kg}$ total lipid. Blood was collected at 1, 4 and 24 hours by tail nick and cardiac puncture procedures (injected dose = $3.3\text{ }\mu\text{mole lipid / ml plasma}$). An aliquot of plasma was used to determine liposomal lipid content as described in Chapter 2. DSPC liposomes containing 2 mol% (filled circles, dotted line), 5 mol% (filled circles), 10 mol% (open circles), and 15 mol% (open circles, dotted line) PEG were evaluated. Each data point represents the average total lipid plasma concentration \pm S.D. for four mice.

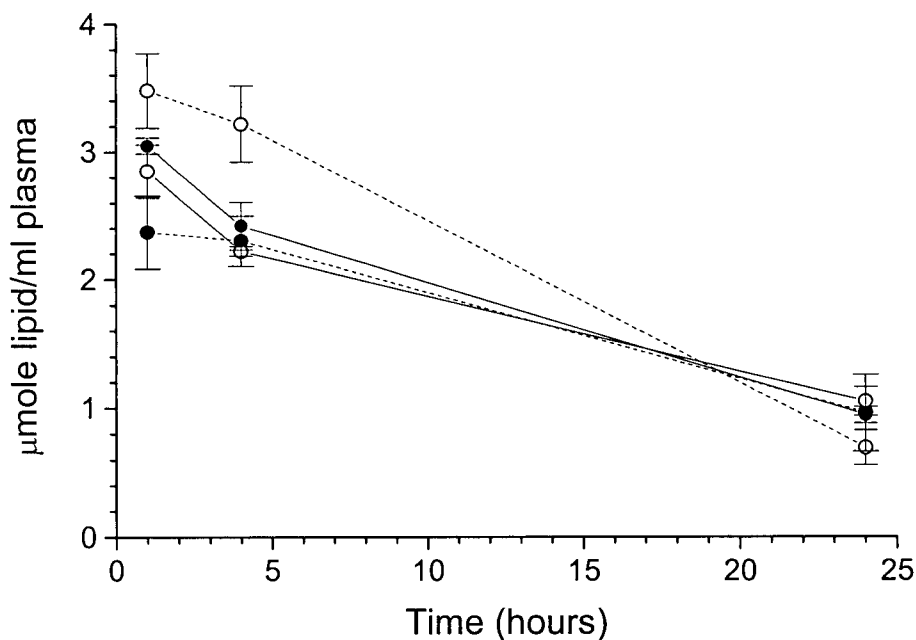
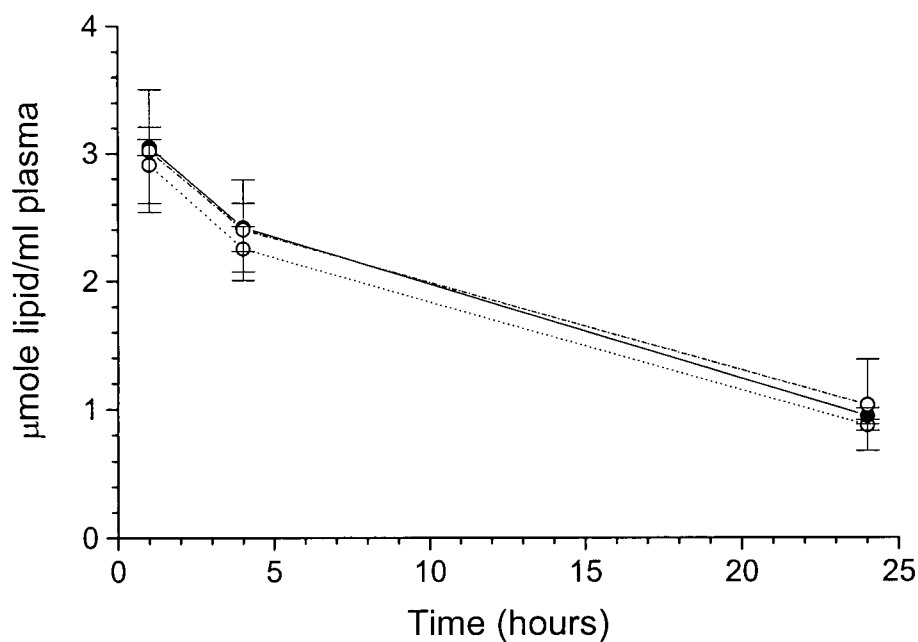


Figure 3.4

Plasma elimination of DSPC liposomes containing varying molecular weights of 5 mol% DSPE-PEG

Large unilamellar liposomes radiolabeled with ^3H -cholesteryl hexadecyl ether (CHE) were administered intravenously via the dorsal tail vein of female Balb/c mice at an approximate dose of $165\ \mu\text{mole/kg}$ total lipid. Blood was collected at 1, 4 and 24 hours by tail nick and cardiac puncture procedures (injected dose = $3.3\ \mu\text{mole lipid / ml plasma}$). An aliquot of plasma was used to determine liposomal lipid content as described in Chapter 2. DSPC liposomes containing 5 mol% DSPE-PEG where the PEG molecular weight was 750 (open circles, dotted line), 2000 (filled circles) and 5000 (open circles, dashed line). Each data point represents the average total lipid plasma concentration \pm S.D. for four mice.



content from 2 - 15 mol%, and PEG molecular weight, from 750 to 5000, had no significant impact on altering the plasma elimination circulation longevity of DSPC liposomes. It should be noted that as PEG concentration was increased to levels in excess of 15 mol% in DSPC liposomes, the solution became clear indicative of non-liposomal micelles or bilayer disc formation [126], a result which is consistent with other reports [29, 127, 128].

3.3.3 Optimal drug loading conditions for idarubicin

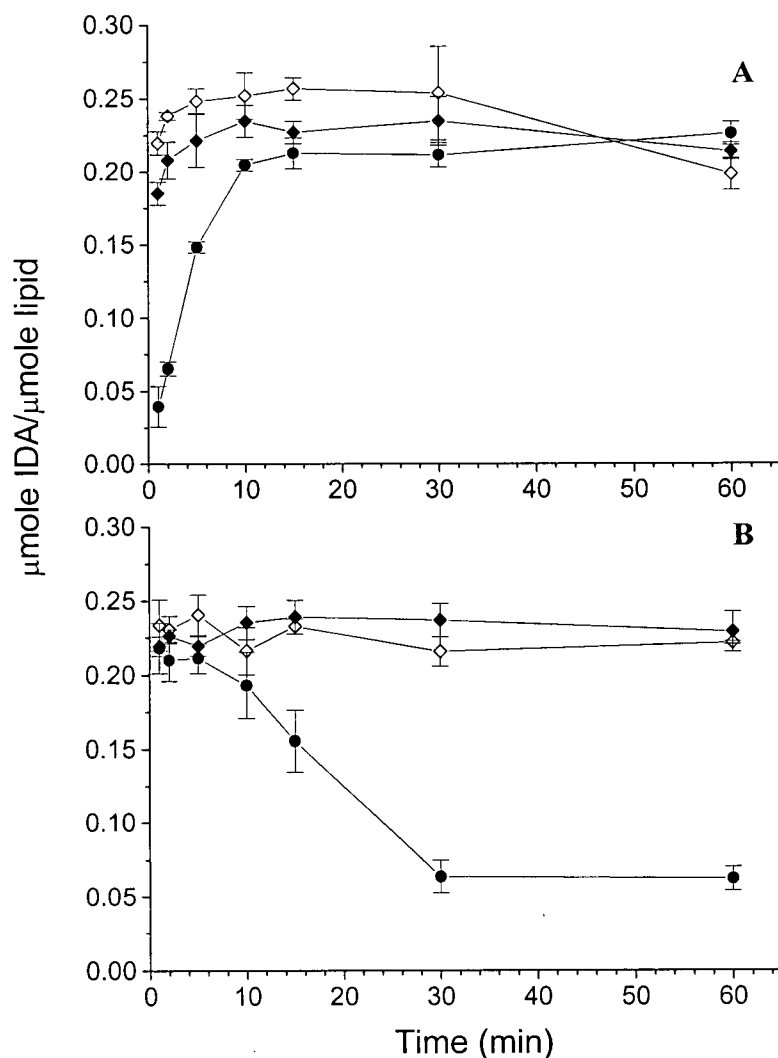
The primary purpose of evaluating the pharmacokinetic behaviour of the cholesterol-free liposomes was to determine whether in the absence of cholesterol, the *in vivo* retention of drugs poorly retained by cholesterol-containing formulations could be improved. Since the drug retention attributes of anthracycline derivatives may be correlated to their hydrophobicity, the DSPC / DSPE-PEG₂₀₀₀ liposome formulation was assessed to enhance the drug retention of the hydrophobic anthracycline idarubicin [129]. A liposomal formulation of idarubicin displaying enhanced drug circulation lifetimes has not been obtained to date, presumably because the idarubicin is rapidly released from cholesterol-containing systems.

The first step was to establish whether idarubicin could be encapsulated in liposomes. The studies described here have used the well-established pH gradient-based loading technique. In particular idarubicin was loaded into liposomes exhibiting an approximate 3.5 unit transmembrane pH gradient at a 0.2 drug-to-lipid ratio incubated at 37°C and 65°C. As indicated in Figure 3.5, idarubicin displayed optimal loading in cholesterol-free liposomes at 37°C. At this incubation temperature, the accumulation of idarubicin into the liposomes was rapid, with > 95% encapsulation observed in 15 minutes, however, the drug loading rate was slower than for cholesterol-containing liposomes. At 65°C, a temperature higher than the phase

Figure 3.5

Remote loading of idarubicin into liposome formulations at 37°C and 65°C

Liposomes (5 mM) were incubated with 1 mM idarubicin (0.2 drug-to-lipid ratio) at 37°C (**A**) and 65°C (**B**). At various time points, 100 μ l of the incubating mixture was passed down mini Sephadex G-50 spin columns and subsequently analyzed for lipid and drug concentrations by liquid scintillation counting and a standard anthracycline partitioning assay as described in the Chapter 2. Drug loading was compared between DSPC / DSPE-PEG₂₀₀₀ (95:5 mole ratio, closed circles), DSPC / CH (55:45 mole ratio, open diamonds) and DSPC / CH / DSPE PEG₂₀₀₀ (50:45:5 mole ratio, filled diamonds) liposome formulations. Each data point represents the average μ mole IDA / μ mole lipid \pm S.D. for 3 experiments.



transition of the liposomes, drug loading was instantaneous for all formulations (100% encapsulation efficiency at 1 minute post-drug loading) but idarubicin was rapidly released from cholesterol-free liposomes with approximately 25% of the drug remaining in the liposomes 30 minutes post-drug loading.

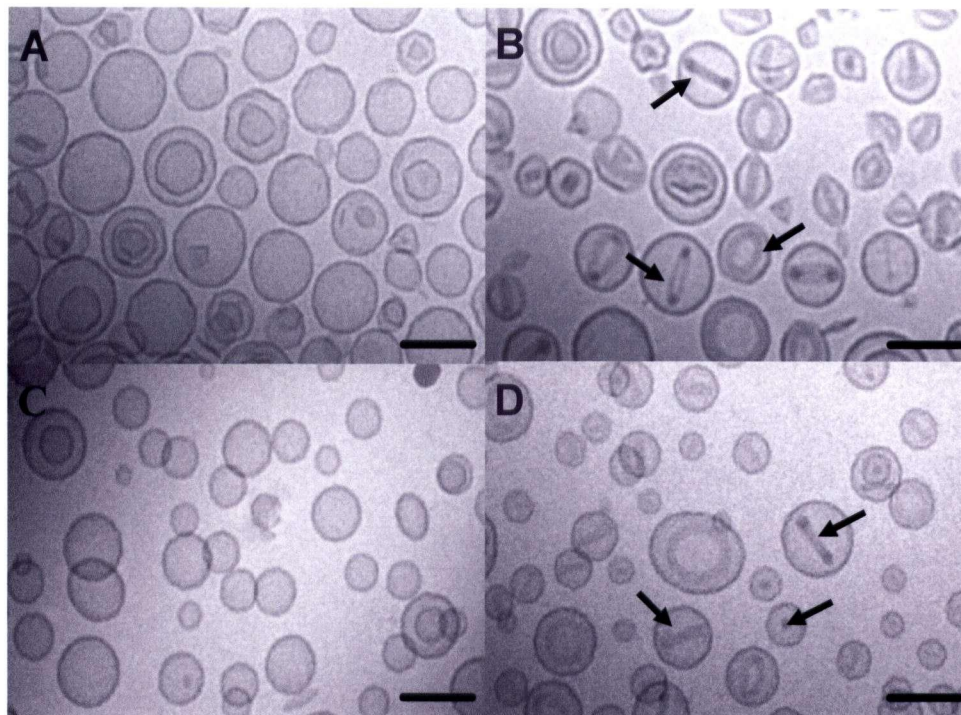
3.3.4 Evaluation of liposomal idarubicin by cryo-transmission electron microscopy

Previous studies have explored the structure of doxorubicin within liposomes, linking the formation of citrate doxorubicin precipitates to improved retention [67]. To assess the physical state of encapsulated idarubicin, cryo-transmission electron microscopy (cryo-TEM) was used. “Empty” and drug-loaded DSPC / DSPE-PEG₂₀₀₀ (95:5 mole ratio) liposomes were analyzed and the resulting cryo-TEM images have been summarized in Figure 3.6. As shown by the representative micrographs in Figures 3.6A and 3.6C, there was an observed difference in structure between “empty” cholesterol-free and cholesterol-containing liposomes. DSPC / DSPE-PEG₂₀₀₀ (95:5 mole ratio) liposomes have angular surface features whereas DSPC / CH / DSPE-PEG₂₀₀₀ (50:45:5 mole ratio) liposomes consisted primarily of smooth and rounded membranes. In both cholesterol-free (Figure 3.6B) and cholesterol-containing liposomes (Figure 3.6D) with encapsulated idarubicin, a precipitate was evident inside the liposomes, resulting in the “coffee bean” structure observed by others for liposomal formulations of doxorubicin. Although these cryo-TEM images do not eliminate the possibility of idarubicin’s interaction with the lipid membrane, it can be concluded that both cholesterol-containing and cholesterol-free formulations have some of the entrapped idarubicin present as a precipitate in the aqueous core of the liposome.

Figure 3.6

Cryo-transmission electron micrographs of “empty” and idarubicin-containing cholesterol-free and cholesterol-containing liposomes

DSPC / DSPE-PEG₂₀₀₀ (95:5 mole ratio, **A, B**) and DSPC / CH / DSPE-PEG₂₀₀₀ (50:45:5 mole ratio, **C, D**) liposomes were prepared and cryo-transmission electron micrographs were obtained after establishment of a transmembrane pH gradient, but prior to drug loading. Cryo-transmission electron micrographs of idarubicin-loaded liposomes demonstrated precipitation (see arrows) of idarubicin in cholesterol-free (**B**) and cholesterol-containing liposomes (**D**). Bar represents 100 nm.



3.3.5 Pharmacokinetic analysis of liposomal idarubicin

Pharmacokinetic studies were performed to determine the idarubicin retention attributes of the cholesterol-free formulation in vivo. Liposomes were prepared at a 0.2 drug-to-lipid mole ratio and subsequently injected i.v. in Balb/c mice at a dose of 165 $\mu\text{mole/kg}$ lipid and 33 $\mu\text{mole/kg}$ idarubicin. The plasma elimination profile of idarubicin and lipid, as well as the calculated drug-to-lipid ratio in the plasma compartment are shown in Figure 3.7. In the absence of a drug carrier, idarubicin was rapidly eliminated with $< 3\%$ of the injected dose present after 15 minutes. This is in sharp contrast to the results obtained when idarubicin was administered encapsulated in DSPC / DSPE-PEG₂₀₀₀ (95:5 mole ratio). The mean plasma AUC_{0-4h} for free idarubicin was 0.04 $\mu\text{mole h ml}^{-1}$ in comparison to 1.97 $\mu\text{mole h ml}^{-1}$ for cholesterol-free liposomes. The greatest retention of idarubicin was achieved using cholesterol-free liposomes, resulting in a mean plasma AUC_{0-4h} that was 66-fold higher than free idarubicin. The lipid elimination profiles were consistent with the total lipid plasma concentrations shown in Figures 3.1 and 3.2 suggesting that unlike vincristine and doxorubicin [16, 51], idarubicin encapsulation did not cause a significant change in liposome elimination. The calculated changes in drug-to-lipid ratios indicate that the drug retention attributes of the cholesterol-free formulation is the best, and the data support the contention that cholesterol-free liposomes provide a format to be used to deliver drugs not well retained in cholesterol-containing liposomes.

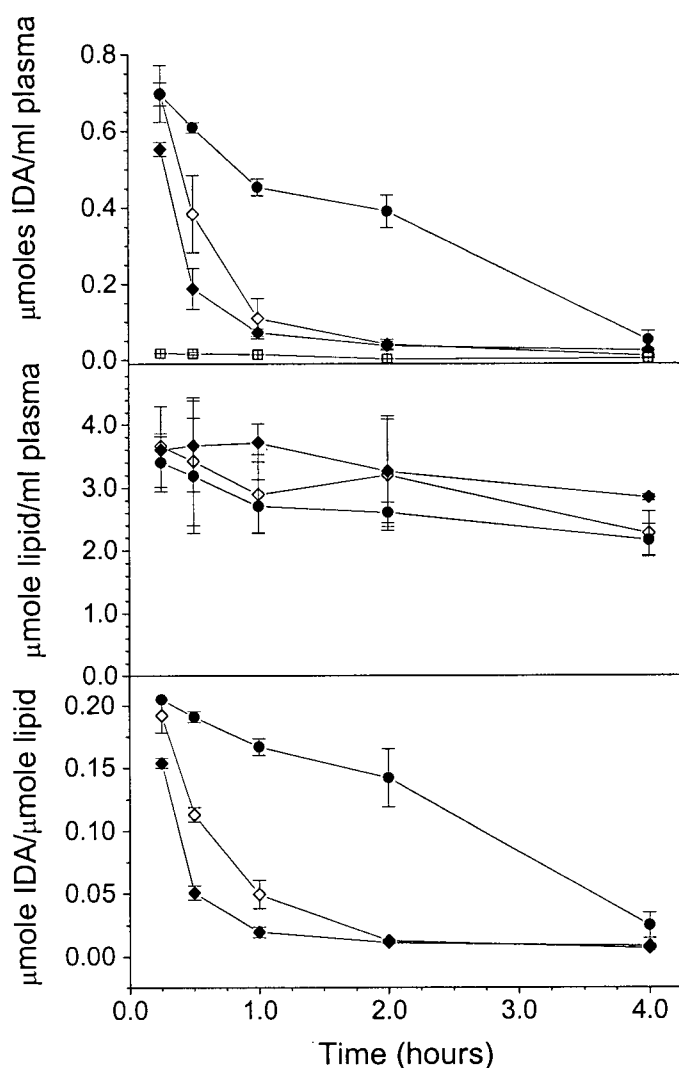
3.4 Discussion

These studies have focused on cholesterol-free liposome delivery systems, with the aim of establishing their utility for delivery of hydrophobic drugs, such as idarubicin. Prior to

Figure 3.7

Plasma elimination of liposomal idarubicin following i.v. injection of cholesterol-free and cholesterol-containing liposomes

Large unilamellar liposomes radiolabeled with [^3H]-cholesteryl hexadecyl ether (CHE) were administered intravenously via the dorsal tail vein of female Balb/c mice at an approximate dose of 165 $\mu\text{mole/kg}$ total lipid and 33 $\mu\text{mole/kg}$ idarubicin. Blood was collected at 0.25, 0.5, 1, 2 and 4 hours post-drug administration. Plasma was prepared and aliquots were assayed for lipid and idarubicin concentration as described in Chapter 2. Prolonged circulation longevity of idarubicin was observed in DSPC / DSPE-PEG₂₀₀₀ (95:5 mole ratio, filled circles) in comparison to DSPC / CH / DSPE-PEG₂₀₀₀ (50:45:5 mole ratio, filled diamonds), DSPC / CH (55:45 mole ratio, open diamonds), and free idarubicin (open squares). Each data point represents the average drug / lipid plasma concentration \pm S.D. for four mice.



establishment of liposome formulations designed for drug delivery applications [79, 85, 113, 130], cholesterol-free vesicles were the standard model for biological membranes. Thus there is a great deal of existing literature on the in vitro physical and chemical properties of liposomes prepared without cholesterol. This existing literature provides a solid foundation on which to support the development of cholesterol-free liposomes as intravenous delivery systems. Despite extensive studies of cholesterol-free formulations, there has been little emphasis on their application as drug carriers other than DPPC lipid compositions used for thermosensitive formulations [131-133]. Others have focused on the physicochemical and biological attributes of cholesterol-free liposomes including phase transition temperature determination by differential scanning calorimetry [128], x-ray diffraction [134], and protein binding [135, 136], permeability [137] and pharmacokinetic studies [55, 123]. Collectively these studies provide conclusive evidence that cholesterol-free liposomes have distinct properties that may be beneficial for drug carriers.

However when this information has been applied to drugs, such as doxorubicin, the cholesterol-free formulation, even when stabilized by PEG-lipid incorporation, exhibit poor drug retention when compared to cholesterol-containing formulations [133]. It is believed that this is due, in part, to the chemical attributes of the drug used and the phase transition temperature of DPPC ($T_c \sim 41^\circ\text{C}$). For a temperature sensitive carrier, it may be advantageous to select lipids that have a characteristic T_c just above body temperature considering that lipids become more permeable near their phase transition temperature. Therefore selection of lipids with a higher T_c than 40°C may facilitate greater retention of entrapped solutes. This report provides evidence that cholesterol-free liposomes can exhibit improved drug retention attributes, thus providing the opportunity to develop such formulations for drugs that are poorly retained in

cholesterol-containing liposomes.

Within the context of this chapter, a direct comparison of cholesterol-free DSPC / DSPE-PEG₂₀₀₀ (95:5 mole ratio) liposomes with other successful drug carrier formulations including conventional DSPC / CH (55:45 mole ratio) and sterically stabilized DSPC / CH / DSPE-PEG₂₀₀₀ (50:45:5 mole ratio) liposomes is provided. There are two important observations pertaining to cholesterol-free liposomes that warrant further discussion. First and foremost, PEG is an essential component of cholesterol-free liposomes. Its presence engenders enhanced circulation longevity, apparently in a manner that is independent of PEG concentration and molecular weight. Secondly, idarubicin encapsulated in cholesterol-free liposomes demonstrated greater retention *in vivo*, independent of the formation of a precipitate structure within liposomes.

The results indicate that DSPC / DSPE-PEG₂₀₀₀ (95:5 mole ratio) liposomes exhibit circulation lifetimes comparable to sterically stabilized liposome formulations (DSPC / CH / DSPE-PEG₂₀₀₀; 50:45:5 mole ratio). Woodle *et al.* have also demonstrated that PEG-PE / PC / CH (1:10:5 mole ratio) and PEG-PE / PC (0.15:0.85 mole ratio) liposomes exhibited similar circulation lifetimes, with circulation half-lives of 15.8 h and 14.9 h, respectively [57]. In the absence of surface-grafted PEGs, cholesterol-free DSPC liposomes were rapidly eliminated, an observation that is likely due to either protein binding or liposome aggregation. As noted during the course of these studies, both DPPC and DSPC liposomes aggregate rapidly when cooled to a temperature below the *T_c* of the acyl chain. In fact, in order to investigate the properties of pure PC systems, at least 0.5 mol% PE-PEG₂₀₀₀ is required (for further analysis refer to Chapter 4). Importantly, the circulation longevity of cholesterol-free DSPC / DSPE-PEG₂₀₀₀ liposomes following *i.v.* administration was not influenced by the amount of PEG-modified lipid (2 - 15

mol%), or the PEG molecular weight (750 - 5000). This is in contrast to previous studies investigating cholesterol-containing liposomes where PEG content and molecular weight are important considerations when optimizing the circulation lifetime of these liposomes [125, 138].

Several investigators have demonstrated that cholesterol is required to maintain stability of liposomes in the plasma compartment [79, 85, 113, 139]. Many of these studies were completed with small unilamellar liposomes prepared using lipids that exhibited a T_c below 37°C, and thus were likely in a fluid phase when injected into mammals. Bedu-Addo *et al.* and others have demonstrated that cholesterol-free liposomes exhibit a phase transition temperature [128], but this transition broadens and becomes difficult to measure when the cholesterol level increases [140]. Heating liposomes prepared of defined acyl length PCs above the phase transition temperature and subsequently cooling them below the T_c causes membrane defects (grain boundaries) to form. The appearance of defects is clearly evident in the cryo-TEM shown in Figure 3.6 and these membrane defects are believed to be the source of non-specific protein binding [139] which, in turn, may define whether the carrier is recognized by the cells of the MPS system. Addition of surface stabilizing compounds such as PEG may shield these defects from recognition by plasma proteins, rendering them more stable than liposomes composed exclusively of saturated phospholipids. An inherent attribute of such a conclusion is that pure PC liposomes may display reduced protein binding attributes provided that the membrane defects are shielded by PEGs. The results suggest that this can be achieved for a broad range of PEG molecular weight species and surface grafting densities.

The entrapment of idarubicin into cholesterol-free DSPC / DSPE-PEG₂₀₀₀ liposomes with an established pH gradient proved to be as effective with cholesterol-free liposomes when compared to cholesterol-containing formulations. As expected, however, the drug loading

attributes of the cholesterol-free formulation were more dependent on the temperature used for loading and idarubicin could not be encapsulated at 65°C in cholesterol-free liposomes, a temperature higher than its phase transition temperature. Similarly, Unezaki *et al.* loaded thermosensitive (cholesterol-free) DSPC / DPPC / DSPE-PEG (9:1:0.61 mole ratio) liposomes with doxorubicin by the remote loading procedure at 60°C for 10 minutes and only achieved 65% encapsulation efficiency [133]. Reduced loading may be a consequence of membrane destabilization at temperatures above the T_c of the bulk membrane component.

The studies demonstrated that > 95% of idarubicin was loaded into the PEG-PE stabilized DSPC liposomes at 37°C. The ability to load idarubicin into liposomes at a lower temperature than the phase transition temperature may be directly attributed to idarubicin's hydrophobicity [141]. Consistent with cholesterol-containing liposomes, drug loading for the cholesterol-free liposomes is dependent on liposome composition as well as the specific physicochemical properties of the drug being used. Importantly, the cholesterol-free formulations may be particularly well suited for the more hydrophobic drugs.

Upon drug loading, cryo-TEM images indicated that idarubicin was present in a precipitated form. This observation is consistent with other anthracyclines that have been encapsulated in liposomes by loading methods relying on the use of citrate or ammonium sulfate [70]. It is interesting that Gallois *et al.* have specifically studied idarubicin's interaction with phospholipid membranes concluding that idarubicin embeds within the bilayer forming a complex with phosphatidic acid and cholesterol [142]. Considering that neither cholesterol nor phosphatidic acid were present within the liposomes, the remote loading procedure allows idarubicin to be present at concentrations high enough for the anthracyclines to stack and self-associate [67]. Self-association may be more energetically favourable than interactions

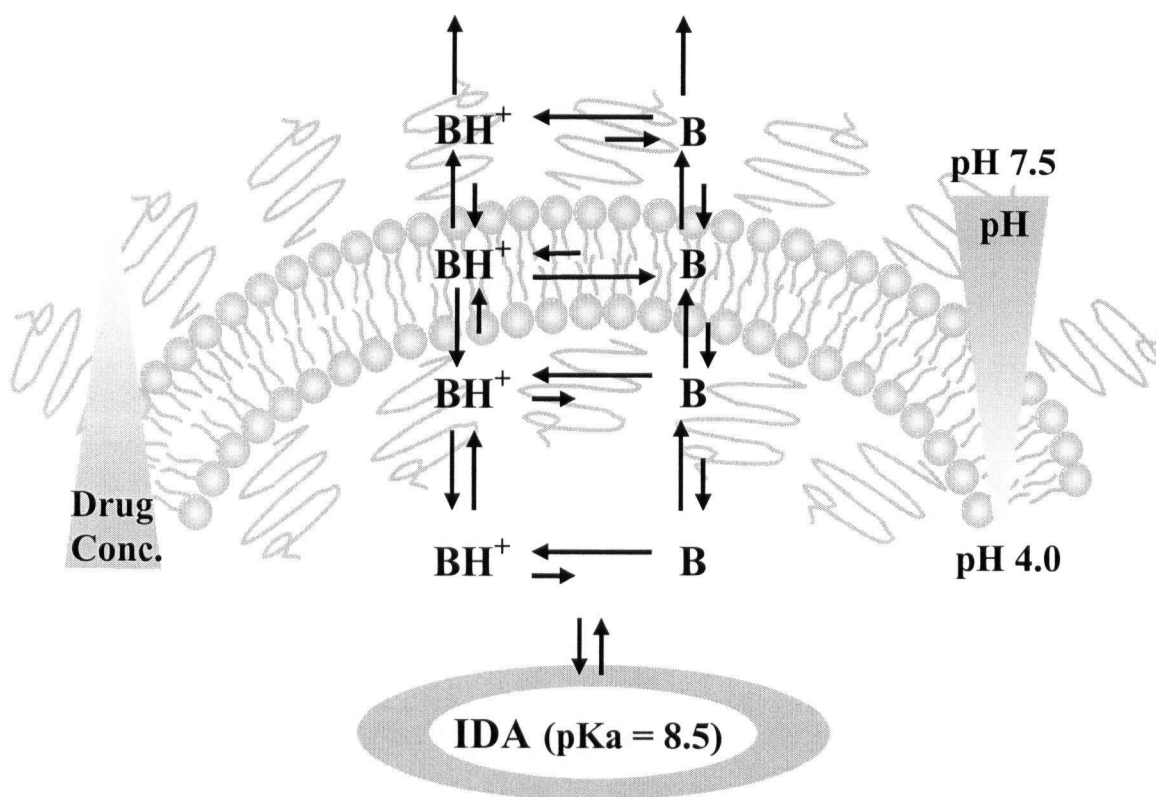
dependent on membrane partitioning, although the membrane partitioning behaviour of idarubicin may play a direct role in enhancing the drug retention attributes observed here for DSPC / PE-PEG formulations. As shown clearly in Figure 3.6, idarubicin was present in a precipitated form within cholesterol-containing liposomes, as well as cholesterol-free liposomes. This result suggests that enhanced retention within cholesterol-free liposomes was not solely a consequence of precipitate formation. The studies demonstrated that membrane composition also governs drug release kinetics, which is believed to be the most important factor governing the release characteristics of a liposomally-encapsulated drug.

As modeled in Figure 3.8, the release of entrapped idarubicin (present in both free and precipitated forms) from the aqueous core of a liposome to the external environment is dependent on the partitioning behaviour of the drug. This, in turn, is dependent on pH, membrane surface charge and the chemical attributes of the lipid acyl chains. Although the initial rationale for employing cholesterol-free liposomes for retention was simple, the model suggests that release due to the interaction of the drug with components of the liposome is complex. For example, the chemical reaction used to prepare PEG-modified phospholipids results in the generation of an anionic lipid from a zwitterionic lipid. The presence of this charged lipid will influence drug release properties, as noted by others [37], and this is presumably due to enhanced partitioning of the encapsulated drug. Drug partitioning behaviour will be dependent on a number of processes which are dictated, in part, by the equilibrium between protonated and unprotonated drug forms as they transfer from the precipitated complex trapped in the core of the liposome through the bilayer interface and the bilayer itself. Note that even though the unprotonated form of the drug will cross the membrane faster than the protonated form, there is evidence to suggest that the protonated form of a drug can cross the

Figure 3.8

Membrane partitioning of drugs encapsulated in liposomes through use of pH gradients and formation of a crystalline precipitate

Idarubicin (IDA), protonated (BH^+) and unprotonated (B) forms, are present in a dynamic equilibrium as they transfer from the precipitated complex trapped in the aqueous core of the liposome, through the bilayer interface and the bilayer itself. The release of IDA is dependent on the partitioning behaviour of the drug, which is dependent on pH, membrane surface charge, and the chemical attributes of the lipid acyl chains. It is assumed that the rate limiting step in drug release is governed by permeation through the membrane rather than dissolution of the drug precipitate.



lipid bilayer [143]. Although the degree of partitioning of idarubicin within cholesterol-free and cholesterol-containing liposomes was not investigated in this chapter (refer to Chapter 5), it is believed that membrane interactions are the most critical determinant of drug release.

Woodle *et al.* hypothesized that by adding PEG to a membrane, one could eliminate the requirement of lipids with high phase transition temperature to allow greater control of leakage rates and other important bilayer properties [57]. Removing cholesterol from the membrane may facilitate even greater flexibility and control of drug leakage rates, when combined with the stabilization effects of PEGs.

In conclusion, it was demonstrated that cholesterol-free liposomes with surface-grafted PEG may have unforeseen advantages over cholesterol-containing formulations. Inclusion of surface-stabilizing components such as PEG eliminates the requirement of cholesterol within a membrane that exhibits very different drug release properties. In this case, enhanced retention of idarubicin was achieved.

CHAPTER 4

INFLUENCE OF POLY(ETHYLENE GLYCOL) GRAFTING DENSITY AND POLYMER LENGTH ON CHOLESTEROL-FREE LIPOSOMES: RELATING PLASMA CIRCULATION LIFETIMES TO PROTEIN BINDING

4.1. Introduction

When considering the development of liposomal drug delivery technology two factors are worth further consideration. First, it has been established that the presence of certain encapsulated drugs (e.g., clondronate, doxorubicin, vincristine) can have a toxic effect on cells of the MPS, leading to dramatic increases in liposome circulation longevity regardless of the presence of surface-grafted PEG's [50, 144]. Second, the functional role of incorporated PEG-lipids and cholesterol has not been clearly delineated. In this context, both lipids have been categorized as "stabilizing" components. Stabilization refers to retention of encapsulated contents, prevention of protein binding following intravenous injection, as well as an associated increase in plasma circulation lifetime. In total, these attributes can help to achieve maximum delivery of encapsulated contents to disease sites that exhibit poorly formed or "leaky" blood vessel structures, as is observed in sites of tumor growth.

The focus of studies encompassed in this thesis is on the use of lipid-based carriers to deliver encapsulated chemotherapeutic agents to tumor sites, but as noted in Chapter 3, this work has questioned the role that cholesterol plays in the development of therapeutically interesting formulations of certain drugs, such as idarubicin. As demonstrated in Chapter 3, liposomes prepared with gel phase lipids such as DSPC ($T_c = 55^\circ\text{C}$) and surface stabilizing PEG-conjugated lipids have long plasma circulation lifetimes, essentially identical to sterically stabilized cholesterol-containing liposomes. Further, removal of cholesterol was associated with dramatic improvements in retention of the hydrophobic anthracycline idarubicin. These

data clearly indicate that stable liposomal formulations can be designed without added cholesterol. Importantly the pharmaceutical viability of these cholesterol-free formulations appears to be much more dependent on the presence of surface-grafted PEGs.

The mechanistic role of PEG-conjugated lipids in liposomes designed for systemic drug delivery has not been fully elucidated. There are a number of plausible hypotheses to explain PEG's role in prolonging blood residence times of liposomes; the most widely acknowledged is PEG's role in steric stabilization [41, 127, 134, 145]. The most compelling evidence for this hypothesis included measurements of the repulsive pressure in lipid membranes with and without polymers that demonstrated that there was a larger interbilayer spacing (4 nm) in membranes containing polymers as compared to unmodified bilayers [146]. Kenworthy *et al.* analyzed electron density profiles to show the distance between apposing DSPC / DSPE-PEG lipid bilayers as a function of concentration of PEG-lipid in bilayer and size of the grafted PEG chain. The extension of the PEG chain from the bilayer surface was 10, 28, 60 and 100 angstroms for PEG molecular weights 350, 750, 2000 and 5000, respectively [134]. It is believed that steric stabilization can lead to reductions in liposome aggregation events [54, 147] and plasma protein adsorption [136, 148].

In view of PEG's behaviour in lipid membranes, the optimal amount of PEG to be incorporated to protect or shield the entire surface area of liposomes can be predicted. It is interesting, however, that optimal amounts of PEG-lipid incorporation have typically been defined empirically and optimal concentrations appear to be highly dependent on liposomal lipid composition. Based on calculated surface coverage estimations for DSPE-PEG (molecular weight 2000) for 100 nm liposomes, the recommended amount of this polymer is 5 mol% [17, 42, 135]. However, given the known and anticipated effects of PEG on encapsulation of drugs

and the pharmacokinetic behaviour of the lipid carriers, both PEG molecular weight and grafting density must be optimized when designing a specific drug carrier.

It should also be recognized that most evidence for reduction of protein binding has been observed when PEG is grafted on solid surfaces or biomaterials such as artificial organs, limbs, contact and intraocular lenses for humans [149]. Further, there has been a growing body of evidence suggesting that PEG engrafted on liposome surfaces can reduce specific protein interactions [150, 151], while having little impact on total plasma protein binding. In view of these recent findings, the purpose of the research summarized in this chapter was to understand the role of PEG-lipid incorporation into cholesterol-free liposomes in terms of surface-surface interactions including self-association (aggregation) and plasma protein adsorption, and in turn, how these interactions may influence the elimination rate of these liposomes.

4.2. Hypothesis

It is hypothesized that increases in the circulation longevity of PEG-engrafted cholesterol-free liposomes can be attributed to PEG's role in inhibiting surface-surface interactions that engender aggregation of liposomes. It is anticipated that this effect would be accentuated in cholesterol-free liposomes in part because of the inherent tendency of these formulations to self-associate and due to differences in the PEG anchors existing in a mobile versus an immobile phase.

4.3. Results

4.3.1. Effect of DSPE-PEG₂₀₀₀ grafting density on plasma circulation longevity of liposomes

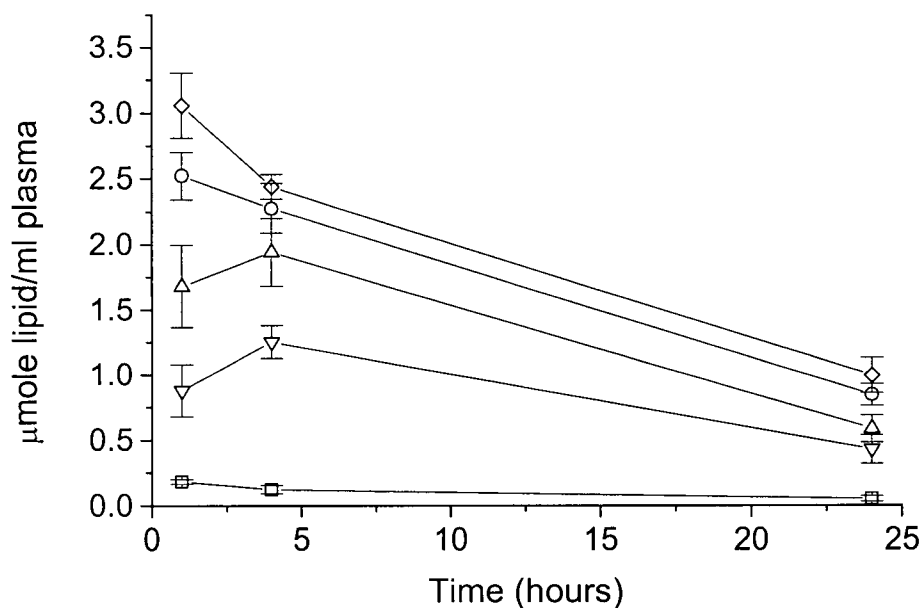
Data presented in chapter 3 (Figure 3.3) suggested that there was no significant difference in the circulation longevity of DSPC liposomes prepared with 2 - 10 mol% PEG-lipids (molecular weight 2000), yet previous studies have suggested that at least 5 mol% of the PEG-modified lipid is required to provide optimal surface protection for a 100 nm liposome [17, 42, 135]. Pharmacokinetic studies were performed as a functional test for assessing the minimal amount of surface-grafted PEG required to achieve enhanced circulation lifetimes in vivo. DSPC cholesterol-free liposomes were prepared with varying concentrations of PEG-conjugated to DSPE (DSPE-PEG₂₀₀₀). Samples were injected into the lateral tail vein of female Balb/c mice at a dose of 165 $\mu\text{mole/kg}$ (approximately 100 mg/kg). At 1, 4 and 24 hours, blood was collected by either tail nick or cardiac puncture and plasma was analyzed for liposomal lipid as described in the Chapter 2.

The results, summarized in Figure 4.1, indicate that PEG grafting densities as low as 0.5 mol% could significantly enhance liposome circulation longevity. The mean plasma area-under-the-curve ($\text{AUC}_{0-24\text{h}}$) was 5.6-fold higher for these liposomes when compared to 100 mol% DSPC liposomes. This effect could be attributed to the ability of low levels of DSPE-PEG₂₀₀₀ to prevent aggregation / self-association of the DSPC liposomes after the extrusion. Further increases in mean plasma $\text{AUC}_{0-24\text{h}}$ were observed as the DSPE-PEG₂₀₀₀ concentration increased and these values plateaued for liposomes prepared with 2 and 5 mol% DSPE-PEG₂₀₀₀, which exhibited a mean plasma $\text{AUC}_{0-24\text{h}}$ of 41.3 and 45.8 $\mu\text{mole h ml}^{-1}$, respectively. The percent of injected lipid dose remaining 24 hours post-injection was 30%, 26%, 18% and 13%

Figure 4.1

The effect of DSPE-PEG₂₀₀₀ grafting density on the plasma elimination of cholesterol-free liposomes

Liposome formulations composed of DSPC and varying amount of DSPE-PEG-conjugated lipids (MW 2000); 0 mol% (\square), 0.5 mol% (∇), 1 mol% (\triangle), 2 mol% (\circ), and 5 mol% (\diamond) were administered as a single i.v. bolus injection of 165 $\mu\text{mole/kg}$ total lipid ($\sim 100 \text{ mg/kg}$, injected dose = 3.3 $\mu\text{mole lipid / ml plasma}$) in female Balb/c mice. Plasma concentrations of liposomal lipid were measured as described in Chapter 2, using radiolabeled ^3H -CHE as a non-exchangeable non-metabolizable liposome marker. Each data point represents the average total lipid plasma concentration \pm S.D. of 3 mice.



for liposomes containing 5, 2, 1 and 0.5 mol% DSPE-PEG₂₀₀₀, respectively. All of these values were significantly higher than those observed for liposomes prepared in the absence of added DSPE-PEG₂₀₀₀.

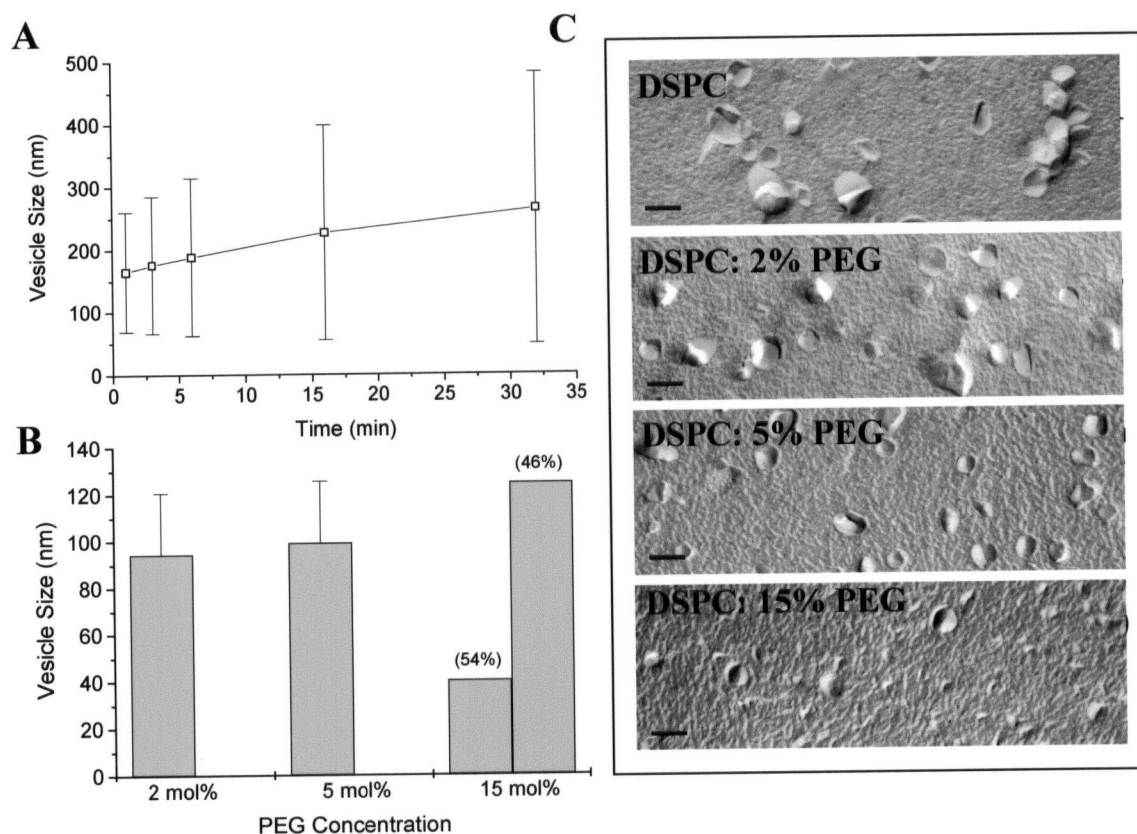
4.3.2. Factors limiting the amount of diacylphosphatidylethanolamine-conjugated poly(ethylene glycol) lipid incorporation into DSPC liposomes

Although the studies presented in Figure 4.1 suggest that DSPE-PEG₂₀₀₀ incorporation at levels of 2 mol% is sufficient to achieve enhanced circulation lifetimes, it was important to determine what factors may limit the amount of PEG-lipid incorporation in these cholesterol-free liposomes. The effect of PEG lipid incorporation on liposome vesicle diameter and structure was determined by quasielastic light scattering (QELS) and freeze fracture analysis; as summarized in Figure 4.2. In the absence of DSPE-PEG₂₀₀₀, there was a time dependent increase in vesicle size over a time course of 30 minutes following extrusion. These liposomes were prepared at 65°C and were diluted in saline at room temperature. Even when working as rapidly as possible, the liposome size determined within minutes of extrusion, was greater than the expected 100 nm size range. The aggregation was immediate as indicated by a mean vesicle diameter at 1 minute post extrusion of 164.7 ± 96 nm (chi-squared 0.435) (Figure 4.2A). The vesicle size increased to 263.8 ± 216.9 nm (chi-squared 2.990, suggestive of a multimodal size distribution) after 32 minutes. When these liposomes were heated to 65°C, the vesicle size returned to mean diameters between 100 – 200 nm, suggesting that aggregation / self association, and not fusion, caused the increase vesicle size. A representative freeze fracture electron micrograph of DSPC liposomes (Figure 4.2C) supports the conclusion that vesicle-vesicle association occurs in the preparations that lack DSPE-PEG₂₀₀₀. DSPC liposomes

Figure 4.2

The effect of PEG-lipid concentration on liposome size as determined by QELS and freeze-fracture analysis

(A) The vesicle diameter (bars represent standard deviation of population) of DSPC liposomes following extrusion through 2 stacked 100 nm polycarbonate filters was measured by QELS analysis over a 30 minute time course. (B) The effect of DSPE-PEG₂₀₀₀ on the vesicle diameter of DSPC liposomes. The size of DSPC liposomes containing 2, 5 and 15 mol% DSPE-PEG₂₀₀₀ was determined by QELS analysis (bars represent standard deviation of population). Liposomes containing 15 mol% DSPE-PEG₂₀₀₀ exhibited a bimodal distribution with % of total liposome population indicated in parentheses. (C) Freeze-fracture micrographs of DSPC cholesterol-free liposomes composed of 0 - 15 mol% DSPE-PEG₂₀₀₀. The freeze fracture technique is outlined in Chapter 2. Bar indicates 100 nm.



containing 2 and 5 mol% DSPE-PEG₂₀₀₀ exhibited mean diameters of between 95 and 100 nm (with a standard deviation of > 20% and a chi-squared value of 0.250 indicative of a unimodal vesicle population) (Figure 4.2B). The size of these liposomes was confirmed by freeze fracture analysis (Figure 4.2C).

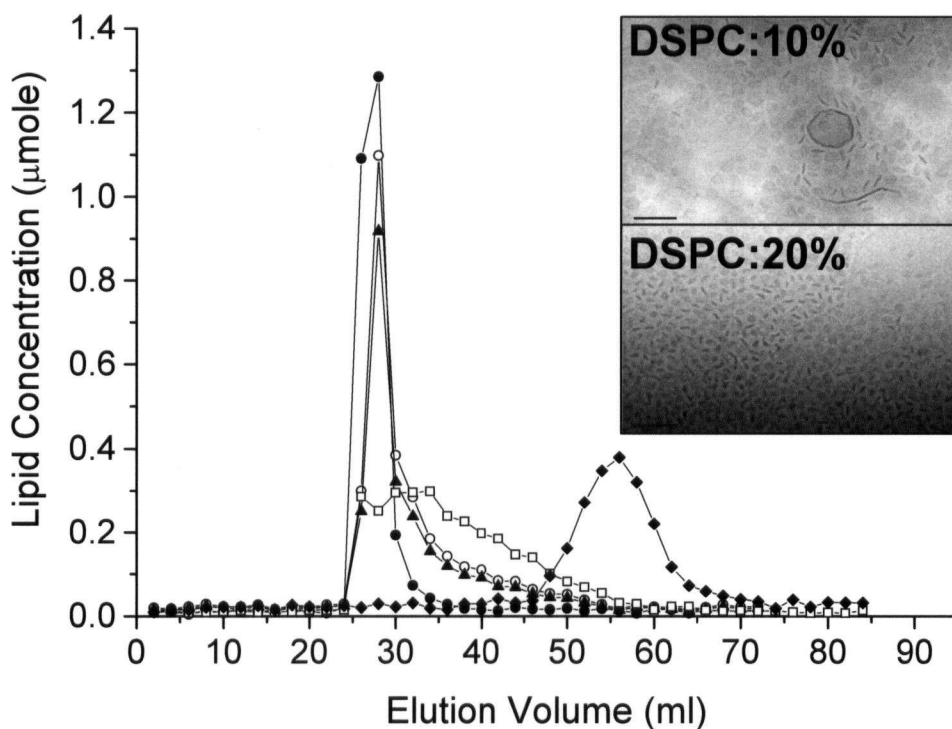
When DSPC liposomes were prepared with 15 mol% DSPE-PEG₂₀₀₀, QELS analysis indicated a bimodal distribution with structures exhibiting a mean diameter of 40 nm (54% of the liposome population) and 125 nm (46% of the liposome population). The existence of the smaller vesicle population represents bilayers disks and / or mixed micelles and is consistent with the bilayer destabilizing effects of PEG-modified lipids. Freeze fracture electron micrographs of these formulations (Figure 4.2D) suggest that there were fewer liposomes present within a given fracture plane when compared to samples prepared from liposomes composed of 2 and 5 mol% DSPE-PEG₂₀₀₀ (note that all samples were prepared with 10 mM total lipid concentration). Previous studies have indicated that it is difficult to distinguish micelles by freeze fracture techniques due to the lack of a fraction plane between an inner and outer leaflet which comprises the lipid bilayer [152].

To further assess whether the presence of DSPE-PEG₂₀₀₀ at levels in excess of 5 mol% led to the formation of mixed micelles, DSPC liposomal formulations composed of 5 – 20 mol% DSPE-PEG₂₀₀₀ were analyzed by size exclusion chromatography. The elution profiles were compared to those observed using 100 nm DSPC / cholesterol liposomes and to pure DSPE-PEG₂₀₀₀ micelles. For size exclusion chromatography studies (Figure 4.3), dual-labelled DSPC liposomes with increasing levels of DSPE-PEG₂₀₀₀ were passed down a Sepharose CL-4B column at a flow rate of 0.5 ml/min. One peak eluted between 24 - 30 ml for liposomes composed of 5 mol% PEG, the same elution profile observed for control DSPC / cholesterol

Figure 4.3

Size exclusion chromatography analysis of DSPC liposomes prepared with 5 - 20 mol% DSPE-PEG₂₀₀₀

DSPC liposomes (20 mM lipid) containing 5 - 20 mol% DSPE-PEG₂₀₀₀ were dual radiolabeled with tracer quantities of ¹⁴[C]-CHE and ³[H]-DSPE-PEG₂₀₀₀ were prepared and subsequently passed down a Sepharose CL-4B column (40 ml, 22 cm x 1.5 cm) at a flow rate of 0.5 ml/min. The formulations containing varying amounts of PEG conjugated lipids are indicated by the following symbols, 5 mol% (●), 10 mol% (○), 15 mol% (▲), 20 mol% (□). ³[H]-DSPE-PEG₂₀₀₀ micelles were passed down the column as a control (◆). **Inset:** Representative cryo-transmission electron micrographs of mixed micelles composed of DSPC and 10 or 20 mol% DSPE-PEG₂₀₀₀. Bar represents 100 nm.



liposomes. For formulations containing 10 mol% DSPE-PEG₂₀₀₀ the bulk of the lipid eluted between 24 - 30 ml (consistent with liposomes), however there was significant tailing in the elution profile. This tailing was augmented as the amount of DSPE-PEG₂₀₀₀ increased and appeared as a distinct peak in fraction 32 – 35 ml for those formulations prepared using 20 mol% DSPE-PEG₂₀₀₀. It should be noted that the second peak was distinct from that observed when using pure PEG micelles, which eluted in fractions 48 - 62 ml. For all elution peaks, both ³[H]-PEG-lipids and ¹⁴[C]-CHE were present, indicating that all liposome populations represented by the different elution peaks contained both the bulk phospholipids and PEG components.

To further characterize the mixed micelle peak present in DSPC liposomes prepared using 10 and 20 mol% DSPE-PEG₂₀₀₀, cryo-transmission electron micrographs of these samples were prepared. Representative micrographs of DSPC liposomes prepared with 10 mol% and 20 mol% DSPE-PEG₂₀₀₀ (Figure 4.3 inset) indicated that small structures were present. In particular, bilayer disks (indicated by many “edge on” orientations) were evident as described previously by Edwards *et al.* for cholesterol-containing systems [126] and Ickenstein *et al.* for cholesterol-free systems [153]. Taken together, these studies indicate that DSPC liposomes, incorporating between 2 - 5 mol% DSPE-PEG₂₀₀₀, can form stable preparations that exhibit extended circulation lifetimes. Bilayers disks or mixed micelles were present when the amount of DSPE-PEG₂₀₀₀ was equal to or greater than 10 mol%.

4.3.3. Effect of PEG molecular weight on the circulation longevity of DSPC liposomes containing 5 and 2 mol% PEG-modified lipid

It is known that the liposome surface coverage is dependent on both the PEG

concentration and polymer length (molecular weight). Results shown in Figure 4.1 indicated that 2 mol% DSPE-PEG₂₀₀₀ was sufficient to achieve increased circulation longevity for cholesterol-free liposomes prepared with DSPC, a grafting density that is less than what has been suggested as optimal for cholesterol-free liposomes. With this in mind, it was appropriate to assess whether optimal PEG chain length is also different for the cholesterol-free formulations.

The effect of PEG molecular weight was determined using circulation longevity of cholesterol-free liposomes as a functional assay of surface protection. As described previously, female Balb/c mice were injected with 165 μ mole/kg total lipid in the lateral tail vein and blood was removed at 1, 4 and 24 hour post-injection by tail nick or cardiac puncture. Blood plasma was analyzed for liposomal lipid and the results have been summarized in Figure 4.4. Although DSPC liposomes containing 5 and 2 mol% DSPE-PEG₂₀₀₀ exhibited higher levels of liposomal lipid in the plasma over the 24 h time course following i.v. administration, the differences between those formulations prepared with lower molecular weight PEGs were not significant. Liposomes containing DSPE-PEG₇₅₀, DSPE-PEG₅₅₀, or DSPE-PEG₃₅₀ had similar circulation lifetimes regardless of whether the level of incorporation was 5 mol% or 2 mol%, where ~18% and ~10% of the original lipid dose was recovered 24 hours post-injection, respectively.

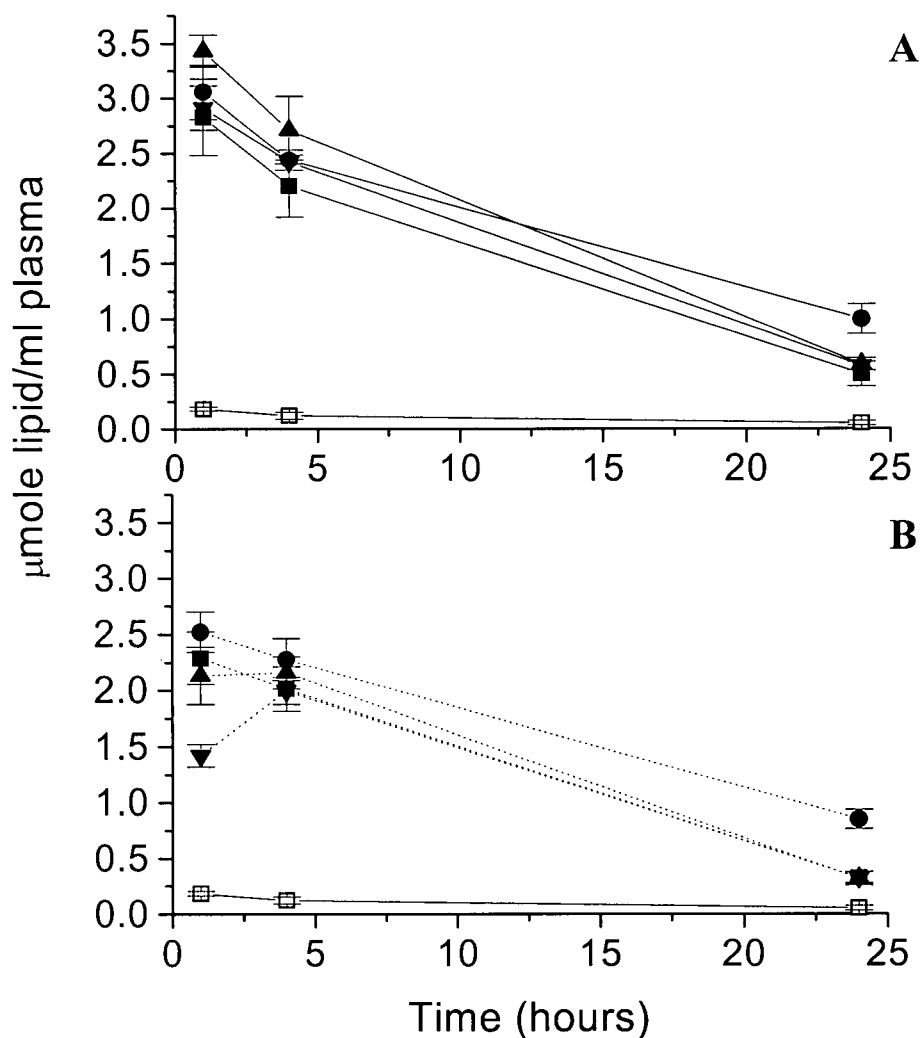
4.3.4. Separation of liposomes from bulk plasma protein binding to liposomes and quantification of tightly adsorbed proteins both in vitro and in vivo

Given the purported role of PEG as a surface component capable of blocking plasma protein binding, additional studies examined plasma protein binding to these long circulating cholesterol-free liposomes. It was anticipated that PEG, regardless of molecular weight (350 vs.

Figure 4.4

The effect of PEG-lipid molecular weight on the plasma elimination of DSPC liposomes

Female Balb/c mice were administered a single i.v. bolus injection of 165 $\mu\text{mole/kg}$ total lipid (injected dose = 3.3 $\mu\text{mole lipid / ml plasma}$). Liposomal formulations were composed of DSPC containing 5 mol% (A) and 2 mol% (B) PEG-lipids of varying molecular weights. Symbols represent DSPE-PEG₂₀₀₀ (●), DSPE-PEG₇₅₀ (■), DSPE-PEG₅₅₀ (▲), or DSPE-PEG₃₅₀ (▼). Unfilled squares indicate DSPC (100 mol%) liposomes. Plasma lipid was measured as described in Chapter 2. Each data point represents the average total lipid plasma concentration \pm S.D. for 3 mice.



2000 average MW) or grafting density (2 vs. 5 mol%), would reduce protein binding. Protein binding studies were completed using methods that evaluated liposomes exposed to plasma proteins in vivo and in vitro. The methods incorporated protocols characterized by others [32, 154-156] and are outlined in Chapter 2. For the in vivo studies, all groups with the exception of DSPC / DSPE-PEG₂₀₀₀ (99:1 mole ratio) had > 95% recovery in the plasma compartment 5 minutes after injection. For DSPC / DSPE-PEG₂₀₀₀ (99:1 mole ratio) ~ 75% of the injected liposomal lipid dose was recovered 5 minutes post-injection. The plasma was then fractionated on size exclusion column to separate free from liposome-associated proteins. The peak fractions of the eluted liposomes were pooled and the lipid was extracted to avoid interference in the micro BCA assay used to measure protein. Figure 4.5 represents a typical elution profile of liposomes (closed circles) and bulk plasma proteins (open squares). Peak lipid fractions, indicated between the arrows, were pooled and the total liposomal lipid concentration was quantified. This was followed by a lipid extraction [106] and protein precipitation step as outlined in Chapter 2.

The amount of protein bound (μg) per μmole lipid is summarized in Table 4.1 for DSPC liposome prepared with increasing amounts of DSPE-PEG₂₀₀₀. Protein binding values obtained with cholesterol-free liposomes were compared to conventional (DSPC / CH; 55:45 mole ratio) and sterically stabilized (DSPC / CH / PEG; 50:45:5 mole ratio) liposomes. The data presented in Table 4.1 emphasize three points. First, all liposome formulations evaluated, regardless of the level of PEG-modified lipids included in the preparations, exhibited comparable in vitro protein binding (P_B) values. The P_B values ranged from 29.86 ± 5.5 for DSPC / CH (55:45 mole ratio) liposomes to 39.91 ± 6.6 for DSPC / DSPE-PEG₂₀₀₀ (95:5 mole ratio). Second, the P_B values determined using in vitro methods were not

Figure 4.5

Separation of DSPC liposomes containing 5 mol% DSPE-PEG₂₀₀₀ from bulk mouse plasma proteins by size exclusion chromatography

Mouse serum and liposomes were incubated at 37°C for 10 minutes. The mixture was passed down a Sepharose CL-4B column (40 ml, 22 cm x 1.5 cm) with HBS (20 mM HEPES, 150 mM NaCl, pH 7.4) at a flow rate of 0.5 ml/min. Fractions (0.5 ml) were collected and assayed for liposomal lipid concentration (liquid scintillation counting) and protein concentration (micro BCA assay). Under these conditions, optimal separation of liposomes and bulk serum proteins was achieved. The peak fractions, indicated between the arrows, were pooled to determine amount of plasma protein bound to liposomes.

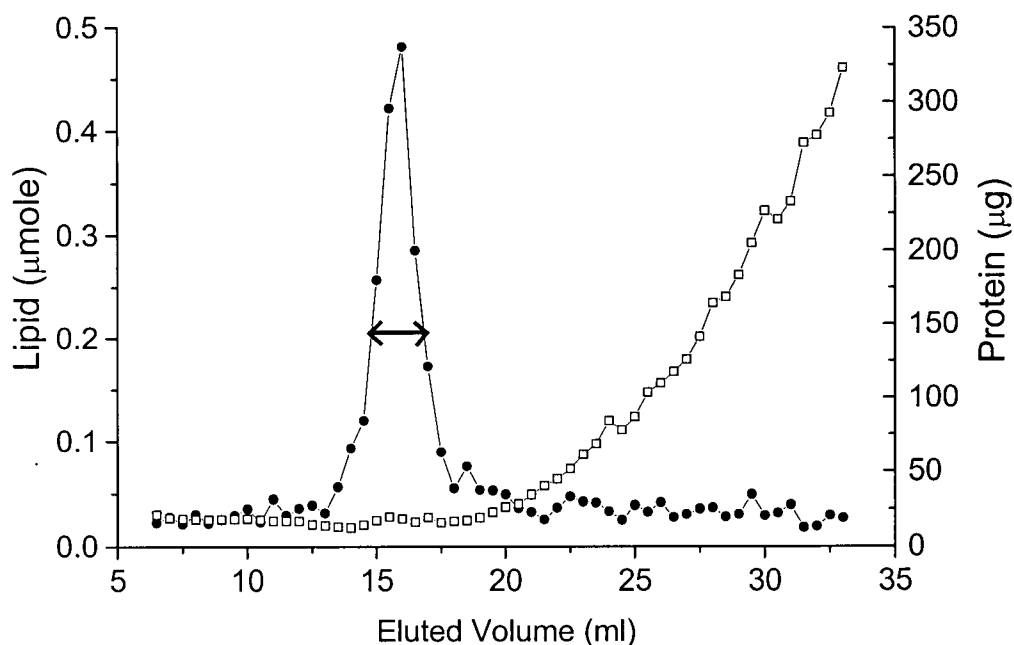


Table 4.1

Summary of protein binding values to liposomes determined using
in vitro and in vivo methods

Sample ^a	Protein Binding (P _B μ g protein/ μ mole lipid)	
	In Vitro ^b	In Vivo ^c
DSPC / CH (55/45)	29.86 \pm 5.5	29.91 \pm 5.7
DSPC / CH / DSPE-PEG ₂₀₀₀ (50/45/5)	34.18 \pm 8.7	23.79 \pm 3.6
DSPC / DSPE-PEG ₂₀₀₀ (99/1)	35.37 \pm 10.9	42.62 \pm 6.1
DSPC / DSPE-PEG ₂₀₀₀ (98/2)	39.40 \pm 5.4	N/D ^d
DSPC / DSPE-PEG ₂₀₀₀ (95/5)	39.91 \pm 6.6	29.46 \pm 6.6
DSPC / DSPE-PEG ₂₀₀₀ (90/10)	30.75 \pm 0.6	N/D ^d

^a Liposome formulations with mole ratios of lipid components indicated in parentheses

^b for in vitro groups, data represent averaged means of 3 - 5 experiments, S.D.

^c for in vivo groups, data represent the average of 3 mice for each group tested, S.D.

^d N/D, indicates not determined

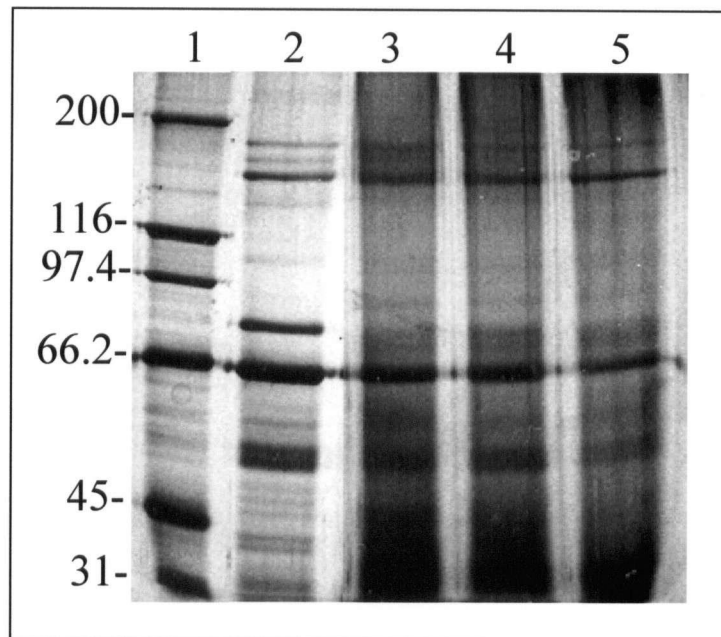
significantly different ($p > 0.05$) from those determined using the *in vivo* recovery method. Third, in light of data presented in Figure 4.1 where it was shown that DSPC / DSPE-PEG₂₀₀₀ (99:1 mole ratio) liposomes (P_B values of 35.37 ± 10.9) were eliminated more rapidly from the plasma than liposomes prepared with 2 (P_B values of 39.40 ± 5.4) and 5 (P_B values of 39.91 ± 6.6) mol% DSPE-PEG₂₀₀₀, it can be suggested that protein binding in these formulations does not correlate with liposome elimination behaviour.

Although the P_B values suggest that PEG incorporation does not have a significant impact of non-specific plasma protein adsorption as determined using the techniques described here, it is possible that the types of proteins bound were different, a parameter that could be qualitatively assessed by polyacrylamide gel electrophoresis (PAGE) analysis of the liposome associated proteins. Studies investigating protein binding profiles were initiated by recovering plasma proteins bound to DSPC / CH / DSPE-PEG₂₀₀₀ (50:45:5 mole ratio), DSPC / DSPE-PEG₂₀₀₀ (99:1 mole ratio) and DSPC / DSPE-PEG₂₀₀₀ (95:5 mole ratio). Subsequently the isolated proteins were separated on 7.5% acrylamide gel and visualized by silver stain. A representative study is shown in Figure 4.6, where it should be noted that loading was standardized on the basis of the amount of liposomal lipid from which the protein was isolated (i.e., protein loaded was isolated from 0.1 μ mole total lipid for all samples analyzed). The profiles suggest that proteins exhibiting molecular weights similar to serum albumin (\sim mol. wt. = 66,000) and IgG (mol. wt.=150,000) were bound at comparable levels for DSPC / CH / DSPE-PEG₂₀₀₀ (50:45:5 mole ratio) and DSPC / DSPE-PEG₂₀₀₀ (99:1 and 95:5 mole ratios) liposomes. In summary, these protein binding studies indicated that plasma proteins adsorb onto the liposome surface at comparable levels and in comparable patterns regardless of whether the liposome contain cholesterol or PEG-modified lipids.

Figure 4.6

SDS-PAGE analysis of liposome-associated plasma proteins

Protein was extracted by precipitation from column-purified liposomes (0.1 μ mole total lipid) and separated on 7.5% polyacrylamide gels. Proteins were visualized by silver stain. Lane 1, high molecular weight markers; Lane 2, total mouse serum (200x diluted); Lane 3, DSPC / CH / DSPE-PEG₂₀₀₀ (50:45:5 mole ratio); Lane 4, DSPC / DSPE-PEG₂₀₀₀ (99:1 mole ratio); Lane 5, DSPC / DSPE-PEG₂₀₀₀ (95:5 mole ratio).



4.4. Discussion

Incorporation of surface-grafted PEG on liposomes has had a significant impact on the development of this technology for use in the delivery of chemotherapeutic agents. However, there remains a great deal of speculation about how surface-grafted PEGs increase circulation lifetime of i.v.-administered liposomes. It is generally believed that the effect is attributed to PEG's ability to reduce plasma protein binding; an observation originally documented for solid surfaces with surface-grafted PEG moieties. Reducing plasma protein binding is believed to minimize recognition of the injected liposomes by cells of the mononuclear phagocytic system (MPS), which are known to play a significant role in the elimination of these particulate delivery systems from the blood compartment.

In recent years, however, there has been a growing body of evidence suggesting that PEG does not reduce plasma protein adsorption on liposomes [95]. Further, the benefits obtained through use of PEG-modified lipids appear to be highly dependent on liposomal lipid composition. For several reasons, including improved retention of certain encapsulated anti-cancer drugs, there is an interest in the development of liposomal formulations, which are prepared without added cholesterol. In this regard, few studies have characterized how PEG-modified lipids influence the behaviour of liposomes composed of gel phase lipids.

In this chapter, a functional assay measuring how PEG modification influenced the behaviour of DSPC liposomes was used to study PEG's role as a surface-stabilizing ligand. The functional assay was based on PEG-mediated increases in DSPC liposome circulation lifetime following i.v. administration in mice; however, the liposome characterization studies completed during the course of these experiments provided information on PEG's impact on surface-surface interactions including plasma protein adsorption and liposome aggregation. The results

identify three important points that warrant further discussion. First, since significant improvements in circulation longevity could be achieved with 100 nm DSPC liposomes prepared with PEG levels < 5 mol% when using PEGs with average molecular weights (chain length) of < 2000, the role of surface coverage by PEG and its correlation to plasma elimination of liposomes needs further consideration. A second and related point concerns the requirement of PEG-modified lipids to prevent liposome aggregation of DSPC liposomes. Third, since protein binding values were not significantly influenced by the presence of PEG-lipids, the role of protein binding in mediating liposome elimination must be contemplated.

The pharmacokinetic studies indicated that PEG grafting density and PEG molecular weight affects the circulation longevity of cholesterol-containing liposomes, however pharmacokinetic studies reported here and in Chapter 3, indicated that there were no significant differences in the circulation longevity of cholesterol-free liposomes composed of 2-10 mol% PEG (molecular weight 2000) or 5 mol% PEG molecular weights between 750 and 5000 [61]. There were no additional improvements in the circulation longevity of liposomes prepared with PEG (molecular weight 2000) concentrations greater than 2 mol%, a polymer concentration that is argued to provide sufficient surface coverage for a 100 nm liposome [42]. Assuming that the PEG-lipids homogenously distribute within the DSPC lipid matrix, surface coverage calculations in DSPC / DSPE-PEG₂₀₀₀ liposomes previously calculated [42], indicates that 100% surface coverage of a 100 nm liposome is obtained with both 2 mol% DSPE-PEG₂₀₀₀ and 5 mol% DSPE-PEG₇₅₀.

Although this data can be used to provide justification for levels of PEG incorporation sufficient to provide complete surface coverage of the liposomes, it is notable that PEG grafting densities between 0.5 – 5 mol% yielded stepwise improvements in mean plasma AUC_{0-24h} and

substantial decreases in DSPC liposome elimination were achieved using DSPE-PEG₂₀₀₀ at levels that were < 2 mol% and when using DSPE-PEG₃₅₀ at levels of 5 mol%. As indicated in Figure 4.4, liposomes containing 5 mol% PEG molecular weights 550 and 350 exhibited similar elimination profiles, yet calculations estimating surface coverage with these shorter length polymers would be > 50%. For example, liposomes composed of 2 mol% DSPE-PEG₃₅₀ have only 17% surface coverage, yet had a 5.6-fold increase in mean plasma AUC_{0-24h} as compared to 100 mol% DSPC liposomes [128, 157]. In view of these results, plasma elimination studies indicated that the incorporation of PEG-derivatized DSPE in DSPC liposomes, significantly prolonged the circulation longevity of liposomes. This effect cannot be explained fully on the basis of arguments relating surface coverage with enhanced circulation lifetime.

The most compelling evidence for the ability of PEG-lipids to prevent surface-surface interactions, in particular aggregation, was revealed by cryo-TEM micrographs and QELS analyses (see Figure 4.2). These studies demonstrate that 100 mol% DSPC liposomes can be prepared by extrusion methods, but the resulting liposomes rapidly coalesce and aggregate. This aggregation is apparent by eye, where the solution transitions from a translucent to an opaque appearance, and by light scattering methods which can measure a doubling in particle size within 30 minutes of preparation. Incorporation of as little as 0.5 mol% DSPE-PEG₂₀₀₀ prevented this aggregation. It is suggested that aggregation contributed to the rapid initial phase of elimination of the DSPC liposomes, and it can be suggested that aggregation was increased in the plasma compartment. Regardless, < 1.5% of the original lipid dose could be recovered in the plasma compartment 24 hours post-injection. PEG concentrations as low as 0.5 mol% DSPE-PEG₂₀₀₀ (Figure 4.1) and 2 mol% DSPE-PEG₃₅₀ (Figure 4.4) were sufficient to increase the circulation lifetime of liposomes and prevent aggregation. As mentioned above,

incorporation of these PEG-modified lipids was not sufficient to provide complete surface coverage. Thus, it can be argued that the dominant effect of PEG in these cholesterol-free liposomes was due to inhibition of liposome aggregation.

A similar conclusion was reached by Ahl *et al.*, when investigating the role of derivatives of PE on circulation longevity in DSPC liposomes [158]. The studies demonstrated that aggregation was prevalent in both rat serum and plasma, and in turn, the liposome aggregation level (measured by turbidity measurements) was inversely correlated with in vivo circulation lifetimes. Further, previous studies investigating the effects of PEG on preventing fusion of dioleoylphosphatidylethanolamine (DOPE) or didodecylphosphate (DDP) bilayers, also concluded that fusion inhibition was due to PEG-mediated inhibition of liposome association. PEG-lipids engrafted on liposomes prevents close interactions between liposomes, thus effectively ablating attractive Van der Waals short range forces that may occur to promote aggregation [159, 160]. Since cholesterol-free liposomes have a greater tendency to aggregate than cholesterol-containing liposomes, the effects of short chain PEGs and low levels of PEG incorporation are much more apparent in these formulations.

Current trends in the development of liposomal delivery vehicles are moving towards the inclusion of gel phase lipids as the lipid matrix. In the absence of cholesterol, these formulations contain membrane defects (also known as grain boundaries) that have a higher propensity for adsorption of plasma proteins. Further, it is conceivable that in gel phase lipids, PEG-lipids are not homogeneously distributed. Evidence in support of this statement was provided by studies performed by Bedu-Addo *et al.* These studies demonstrated the presence of a “shoulder” in DSC thermograms of DSPC / DSPE-PEG₂₀₀₀ lipid mixtures, indicating phase separation of the two components [128, 157]. For these reason, it was rational to suggest that

PEG-lipid incorporation into cholesterol-free DSPC liposomes reduced protein adsorption at these membrane defects.

As indicated in the plasma protein binding studies (Table 4.1) and SDS PAGE analysis (Figure 4.6), there were no significant differences in the amount of protein bound to DSPC liposomes, independent of PEG concentration. The studies demonstrated that cholesterol-free formulations with adsorbed plasma proteins ($\geq 35.4 \mu\text{g protein} / \mu\text{mole lipid}$) had long circulation lifetimes [83, 161, 162]. The absolute protein binding values obtained in these studies correlated well with previous studies. Plasma protein binding values ranged between 29 – 49 $\mu\text{g protein} / \mu\text{mole lipid}$. Studies performed by Chonn *et al.* indicated that neutral liposomes bound 30 $\mu\text{g protein} / \mu\text{mole lipid}$ [163], while the addition of cholesterol reduced protein binding to 22 – 27 $\mu\text{g protein} / \mu\text{mole lipid}$ [116]. It is notable in the studies of Chonn *et al.* that liposomes composed of bulk phospholipid $> \text{C16}$ exhibited protein binding values of 90 $\mu\text{g protein} / \mu\text{mole lipid}$ [163], which was attributed to the presence of membrane packing defects present when these liposomes were below the T_c of the bulk phosphatidylcholine.

The protein binding to DSPC formulation, which did not have some level of incorporated PEG, was not evaluated because of their rapid aggregation after preparation. It should be noted, as well, that the protein binding values reported here were higher [42, 154] and lower [164] than other reported studies. Variability in protein binding values arise when different separation techniques (of liposomes and bulk plasma proteins) and protein quantitation methods are utilized and for this reason it is important to compare the relative changes in protein binding to different liposomes compositions within a given study.

A potential weakness in many of protein binding studies completed to date concerns the loss of loosely adsorbed proteins and changes in protein binding that occur as a function of time.

Using the methods described here, there was not a significant difference in protein binding values observed for liposomes recovered 10 or 30 minutes after addition to serum, in vitro (not shown). However, it is easy to recognize that the liposomes prior to injection are going to be different shortly after injection due to the adsorption of proteins. The Vroman effect suggests that protein adsorption to surfaces is a dynamic interaction and the first proteins to interact with surfaces are those that are most abundant followed by less abundant proteins [165-169]. It is also relatively unknown whether the initial proteins that interact with the liposome surface provide a scaffold to facilitate interactions with other proteins, known as the layering effect.

Short incubations, such as those utilized in these studies, could measure the predominant interactions with IgG and serum albumin, thereby no differences would be observed between the different lipid compositions. Further, due to the fact that both albumin and IgG are both large proteins that are found adsorbed to liposomes in large quantities; and would make up most of the weight or bands on a gel, minor but possibly significant changes in smaller proteins would be relatively hard to detect. Changes in protein binding may be more apparent when analyzing various incubation times and utilizing methodologies to identify (small) plasma proteins including 2D gel electrophoresis, MALDI-TOF spectroscopy and protein microarray technologies. In combination with better, less invasive separation techniques these methods may be able to identify both tightly and loosely bound proteins adsorbed to the liposome bilayer.

In view of the results, there are a number of factors to explain why PEG engrafted on liposomes did not reduce plasma protein binding. First, liposomes with surface-associated PEGs may interact with a defined pool of opsonins and when this pool is depleted, longer blood residency times are observed. The doses (liposomal lipid concentration) chosen for both in vitro

and in vivo protein quantification were comparable. In previous studies, a reduction in plasma protein binding to liposomes was observed with increased lipid doses [170] and others have shown that low doses of PEG-coated liposomes (20 nmol/kg body weight) were rapidly eliminated [171], results that could be attributed to having a limited pool of opsonins and / or saturation of MPS. Second, the signaling of particles for elimination by MPS may be under negative-selection suggesting that specific proteins, known as dysopsonins, block interactions with receptors that activate either macrophages or complement [154, 172, 173]. Third, protein binding to liposomes may result in the formation of protein / liposome complexes that are pharmacokinetically comparable even though they may have remarkably different liposomal lipid composition. In this context, PEG's role may be more defined in terms of preventing interaction with Fc receptors (IgG), receptors on macrophages or complement proteins [164, 174], or by directly inhibiting cell uptake. Profiles of adsorbed proteins may, therefore, be actually a relatively poor predictor of circulation longevity of lipid-based carriers [95].

In summary, the results from this chapter indicated that levels ≤ 5 mol% DSPE-PEG₂₀₀₀ can be incorporated into cholesterol-free DSPC liposomes. There was not a significant difference between plasma elimination of liposomes containing 5 and 2 mol% DSPE-PEG₂₀₀₀ and these grafting densities may be optimal for drug delivery. At concentrations > 10 mol% PEG, mixed micelles or bilayer disks were formed. Some mixed micelle formulations have already been investigated as potentially useful drug delivery systems [175-177], but it is important to be working with a well-defined single population of structures when developing formulations for pharmaceutical applications. In relating liposome circulating lifetimes to the role of PEG, it was demonstrated that liposomal formulations containing very low

concentrations of PEG-conjugated lipids prevented aggregation of liposomes and prolonged circulation longevity, not attributed to an overall reduction in plasma protein adsorption.

CHAPTER 5

pH GRADIENT LOADING OF ANTHRACYCLINES INTO CHOLESTEROL-FREE LIPOSOMES: ENHANCING DRUG LOADING RATES THROUGH USE OF ETHANOL*

5.1. Introduction

The studies described in this chapter investigated anthracycline encapsulation within DSPC / DSPE-PEG lipid mixtures through the use of transmembrane pH gradient-based loading methods. Although anthracyclines such as doxorubicin and idarubicin have a similar structure, they have significantly different octanol / buffer concentration ratios [178]. Increased idarubicin uptake in liposomes may be directly attributed to idarubicin's higher relative hydrophobicity [179], aiding in its transbilayer movement which, in turn, results in increased loading rates as well as efficient loading at lower temperatures when compared to doxorubicin. Although our rationale to characterize cholesterol-free liposomes composed of gel phase DSPC was to effectively improve retention of drugs that exhibit increased permeability across the bilayer, there is also an interest in assessing drugs that may exhibit decreased bilayer permeability. An approach to improve the loading efficiency of such drugs is to enhance the drug partitioning and / or permeability of the lipid bilayer.

Several methods have been shown to increase membrane permeability including incorporation of cholesterol below the T_c of the bulk phospholipid [180], poly(ethylene glycol) modified lipids [181, 182], and lysophospholipids [183]. Simpler methods, such as the addition of short chain alcohols [184-186] or surfactants, such as detergents [187], have also been applied. Considering that the interaction of short chain alcohols, such as ethanol, with lipid bilayers is well documented and is easily removed from samples, this was identified as a

*Adapted from: Dos Santos, N. *et al.* (2004) pH gradient loading of anthracyclines into cholesterol-free liposomes: enhancing drug loading rates through use of ethanol. *Biochimica et Biophysica Acta*, 1661 (1): 47-60.

preferred method.

Many groups have investigated the specific interaction of ethanol with lipid bilayers [188-191]. Addition of ethanol to lipid membranes results in an increase in the dielectric constant [192], dehydration of the phospholipid head groups [193], and an increase in ion permeability [186]. It should also be noted that ethanol has been extensively used in the preparation of liposomes for improving transdermal liposomal drug delivery [194], improving encapsulation of proteins [195], and gene-based agents [196, 197], increasing trapped volume [198], and ensuring compositional homogeneity [199].

In the studies described herein, doxorubicin's low membrane permeability made it difficult to effectively encapsulate the drug in cholesterol-free liposomes. Therefore ethanol was utilized, at concentrations well below that required to collapse the imposed pH gradient, in order to increase drug loading rates.

5.2. Hypothesis

Use of liposomes composed of DSPC without added cholesterol, have a reduced membrane permeability, which presents a problem for drug loading by the pH gradient method. Thus, enhancing drug permeability and partitioning by use of ethanol will increase the rate of doxorubicin loading into cholesterol-free liposomes.

5.3. Results

5.3.1. Drug loading studies of anthracyclines in cholesterol-free liposomes

Studies from Chapter 3 demonstrated that encapsulation of idarubicin in DSPC / DSPE-PEG₂₀₀₀ liposomes (prepared in pH 4.0 citrate buffer and exchanged into a pH 7.4 HBS buffer)

was optimal between 37 - 40°C, a temperature range below the phase transition temperature of DSPC. In contrast to idarubicin, doxorubicin could not be efficiently loaded under the same conditions (Figure 5.1A; open circles). In fact less than 25% of the added doxorubicin accumulated in DSPC / DSPE-PEG₂₀₀₀ liposomes over the 2 hour time course at 40°C. The rate of daunorubicin loading (open triangles) was faster than doxorubicin, but slower than idarubicin. It should be noted that the rate of drug loading in the cholesterol-free liposomes increased when the loading temperature was elevated. For idarubicin, daunorubicin and doxorubicin 100% loading was achieved in DSPC / DSPE-PEG₂₀₀₀ liposomes within 2 minutes when the incubation temperature was higher than the *T_c* of DSPC (55°C).

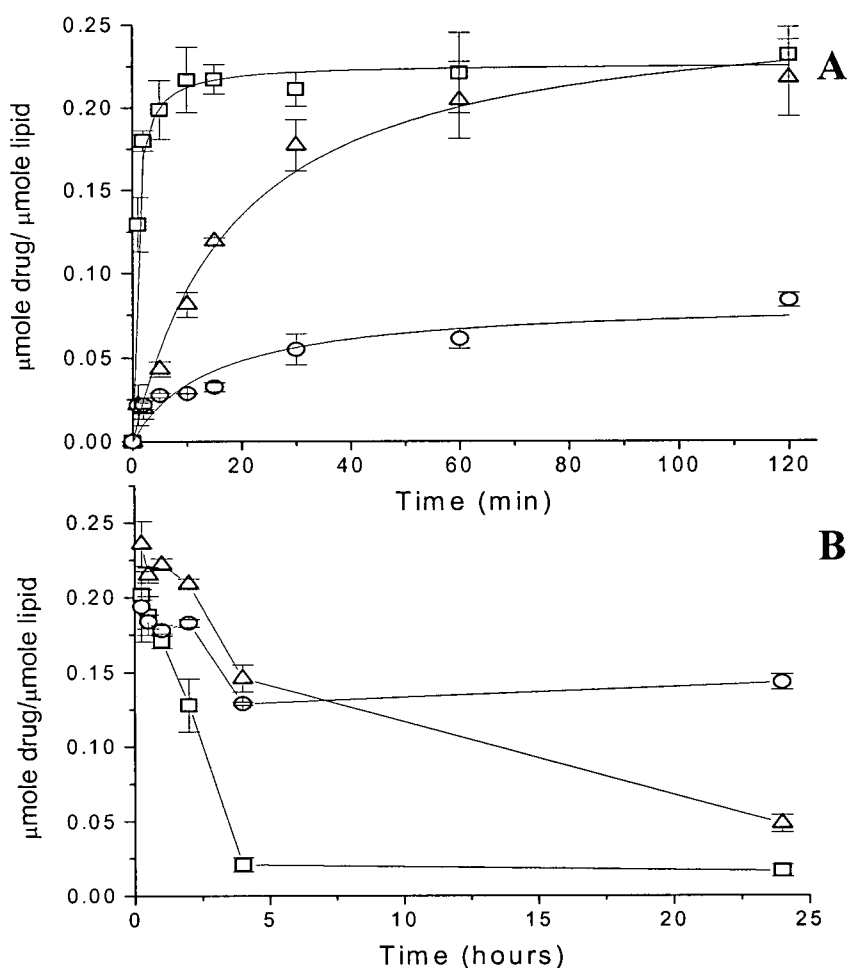
5.3.2. Plasma elimination studies of anthracyclines encapsulated in cholesterol-free liposomes

Lipid membranes are selectively permeable and permit the bidirectional flow of solutes, such as drugs, and thus we wanted to establish whether the observed differences in drug loading rates at 40°C would be an indication of drug elimination rates in vivo. Idarubicin, daunorubicin and doxorubicin were remotely loaded into DSPC / DSPE-PEG₂₀₀₀ (95:5 mole ratio) liposomes and injected into the lateral tail vein of female Balb/c mice at 33 µmole/kg drug and 165 µmole/kg lipid doses (0.2 drug-to-lipid ratio). Drug and lipid plasma concentrations were measured by standard procedures described in Chapter 2, and plotted as the µmole drug / µmole lipid ratio versus time post-administration (Figure 5.1B). Plasma lipid elimination profiles were similar for all samples and therefore the calculated drug-to-lipid mole ratio provides an indication of the amount of drug released from the liposomes over time after injection [200]. Significant differences ($p < 0.05$) in plasma drug-to-lipid mole ratios were observed at 24 hours

Figure 5.1

Time course of uptake of anthracyclines into cholesterol-free liposomes and the plasma elimination of anthracyclines encapsulated in DSPC / DSPE-PEG₂₀₀₀ liposomes

(A) DSPC / DSPE-PEG₂₀₀₀ (95:5 mole ratio) liposomes (with transmembrane pH gradient, pH 4 inside, 7.5 outside) were incubated with idarubicin (\square), daunorubicin (\triangle) or doxorubicin (\circ) at 40°C (0.2 drug-to-lipid mole ratio). At various time points, 100 μ l aliquots of sample were passed down mini spin columns and subsequently analyzed for drug and lipid concentrations as described in Chapter 2. Lipid and drug concentrations were 5 mM and 1 mM, respectively. Each data point represents the average μ mole drug / μ mole lipid \pm S.D. for 3 experiments. (B) Large unilamellar vesicles radiolabeled with 3 [H]-cholesteryl hexadecyl ether (CHE) were encapsulated with idarubicin (\square), daunorubicin (\triangle) or doxorubicin (\circ) by remote loading. Liposomal drugs were administered intravenously via the dorsal tail vein of Balb/c mice at a dose of 33 μ mole/kg drug and 165 μ mole/kg total lipid (0.2 drug-to-lipid mole ratio). Blood was collected at various time points following administration. Plasma was assayed for lipid and doxorubicin concentration as described in Chapter 2. Each data point represents the μ mole drug / μ mole lipid \pm S.D. for 3 mice.



post-drug administration. Values of 0.02, 0.05 and 0.14 $\mu\text{mole drug} / \mu\text{mole lipid}$ were measured for idarubicin, daunorubicin and doxorubicin encapsulated in cholesterol-free liposomes at the 24 hour time point. As predicted, the release of anthracyclines from liposomes could be related to drug loading rates.

5.3.3. Drug and liposomal membrane association of anthracyclines

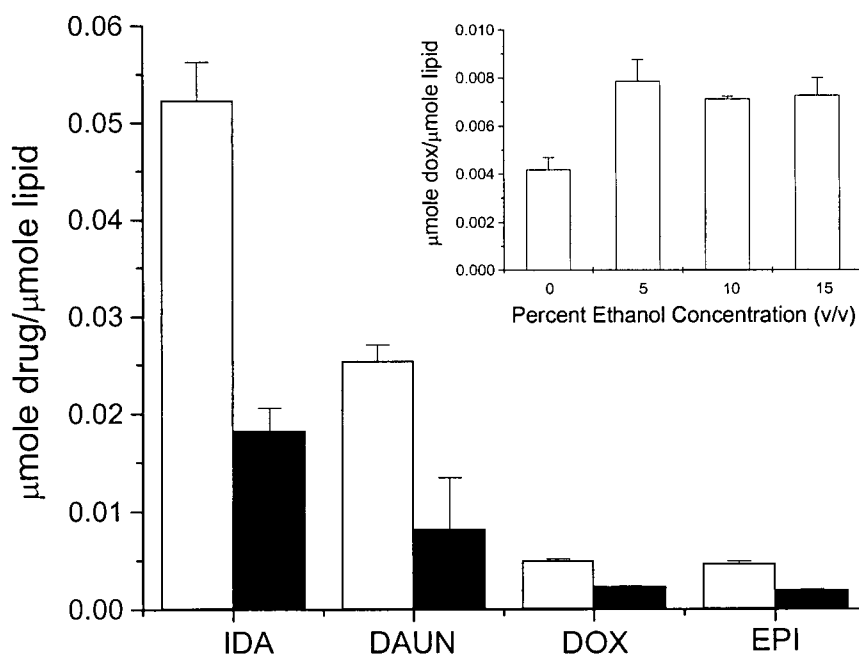
To this point a connection between anthracycline drug loading rates at 40°C, a temperature below the T_c of the bulk phospholipid, and the retention of anthracyclines encapsulated in cholesterol-free liposomes in vivo has been established. Doxorubicin's lower drug loading rate and increased retention in cholesterol-free liposomes as compared to both daunorubicin and idarubicin is consistent with doxorubicin's lower partition coefficient [179], as illustrated in Figure 5.2. The amount of drug associated with cholesterol-free (open bars) and cholesterol-containing (filled bars) liposomes, prepared without a pH gradient, was determined; the measured values should be taken to represent liposomal membrane association and it should not be viewed as a direct measurement of drug partitioning. Based on the experimental conditions, the amount of drug associated with the liposomes is a collective measurement of drug that has equilibrated across the lipid membrane in the aqueous space, drug associated with the lipid membrane through partitioning, hydrophobic and electrostatic interactions. In the absence of a pH gradient, it is believed that most of the drug is associated with the membrane, although drug equilibration into the aqueous space cannot be disregarded.

The results in Figure 5.2 demonstrate that the anthracycline liposomal membrane association is reduced by a factor of more than 2 when the DSPC / DSPE-PEG₂₀₀₀ liposomes are prepared with 45 mol% cholesterol. This result is consistent with the understanding that

Figure 5.2

Influence of drug hydrophobicity on the liposomal membrane association in cholesterol-free and cholesterol-containing liposomes

DSPC / DSPE-PEG₂₀₀₀ (95:5 mole ratio, open bars) and DSPC / CH / DSPE-PEG₂₀₀₀ (50:45:5 mole ratio, filled bars) liposomes exhibiting no pH gradient, were incubated with the anthracyclines idarubicin, daunorubicin, doxorubicin and epirubicin at 40°C for 60 minutes (lipid concentration was 5mM). 100 μ l aliquots were passed down mini spin columns and analyzed for lipid and drug concentrations by liquid scintillation counting and an anthracycline extraction assay (refer to Chapter 2) followed by fluorescence spectrometer detection. Each data point represents the μ mole drug / μ mole lipid \pm S.D. for 3 experiments. **Inset:** Influence of ethanol on doxorubicin liposomal membrane association. DSPC / DSPE-PEG₂₀₀₀ (95:5 mole ratio, open bars) liposomes exhibiting no pH gradient, were incubated with doxorubicin and increasing concentrations of ethanol (0 - 15% v/v) at 40°C for 60 minutes. Lipid and drug concentrations were measured as detailed above and in Chapter 2. Each data point represents the μ mole doxorubicin / μ mole lipid \pm S.D. for 3 experiments.



cholesterol decreases the partitioning of drugs into bilayers since cholesterol occupies space in the membrane that might otherwise be occupied by the hydrophobic drug, an effect that has been shown by others to be greater at lower temperatures [201]. For liposomes prepared without cholesterol, the drug liposomal membrane association data (shown as the amount of drug associated per μmole liposomal lipid) suggests that the level of idarubicin associated was almost 10-fold greater than that observed for doxorubicin or epirubicin, the most hydrophilic of the anthracyclines that were evaluated. The liposomal membrane association behaviour of daunorubicin is intermediate between idarubicin and doxorubicin.

These results have a number of interesting implications. The focus of these studies was based on the suggestion that enhancing doxorubicin membrane association and / or enhancing membrane permeability of the lipid bilayer, under conditions that do not affect the stability of the pH gradient, could increase drug loading rates of doxorubicin in cholesterol-free liposomes.

As the results from the drug liposomal membrane association assay are consistent with relative hydrophobicities of the anthracyclines [178, 179], this assay was utilized to evaluate whether doxorubicin membrane association could be enhanced with the addition of ethanol at 40°C . The results are summarized in the inset graph of Figure 5.2. In the presence of ethanol (0-15% v/v), the drug-to-lipid ratio was between 0.007 – 0.008 μmole doxorubicin / μmole lipid, approximately 2-fold higher than in the absence of ethanol, and considered statistically significant ($p < 0.01$). Note that calculations based on the equilibration of drug concentration across lipid membranes at 1 mM doxorubicin, assuming no membrane partitioning, was expected to yield 0.002 μmole doxorubicin / μmole lipid. Thus it can be suggested that the majority of the associated drug is membrane bound. The results indicated that there were no significant differences in doxorubicin membrane association as the ethanol concentrations

increased from 5 to 15% v/v. Note that non-equilibrium conditions were introduced during the separation of lipid-associated and free drug on the Sephadex G-50 spin columns. If membrane-associated ethanol is removed while being passed down the column, this may result in a loss in membrane-associated doxorubicin and an under-estimation of the level of membrane association.

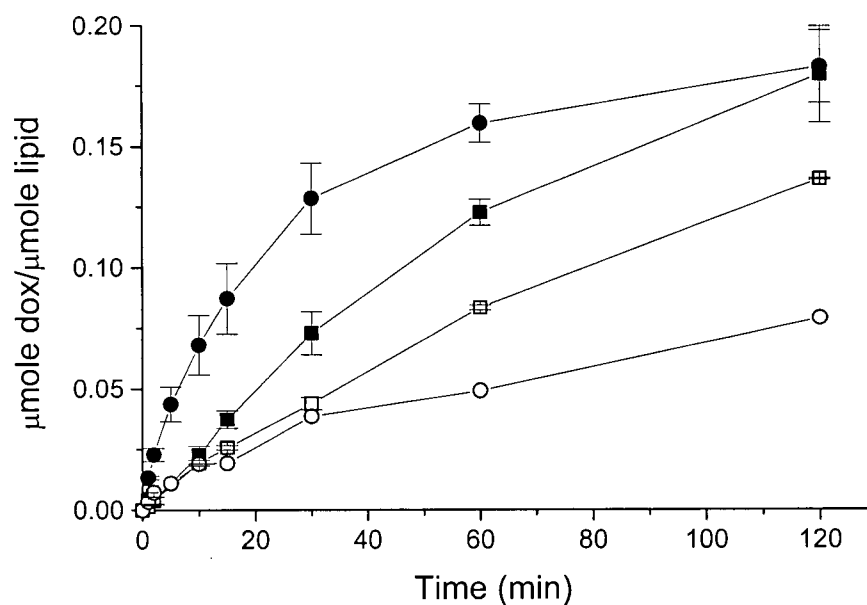
5.3.4. Influence of ethanol on doxorubicin loading in liposomes

As summarized in Figure 5.3, the rate and extent of doxorubicin loading at 37°C was significantly increased by the addition of ethanol (10%, v/v) to DSPC / DSPE-PEG₂₀₀₀ liposomes. Greater than 90% encapsulation efficiency was achieved following a 2 hour incubation at 37°C, a value that was 2.3-fold higher than that observed in the absence of ethanol. For DSPC / DSPE-PEG₂₀₀₀ liposomes the initial drug loading rates were 6.40 (nmole dox/μmole lipid) min⁻¹ as compared to 1.40 (nmole dox/μmole lipid) min⁻¹ in the presence and absence of ethanol, respectively. In the absence of ethanol, liposomes composed of DSPC / CH / DSPE-PEG₂₀₀₀ exhibited improved encapsulation efficiencies (72% at 2 hours) and faster initial drug loading rates (1.5 (nmole dox/μmole lipid) min⁻¹) as compared to liposomes prepared without cholesterol. It should be noted that previous studies have shown that cholesterol decreases the partitioning of ethanol in membranes, predominantly at lower temperatures [202] and thus addition of ethanol to liposomes prepared with 45 mol% cholesterol had a minimal effect on doxorubicin loading rates. In the presence of ethanol (10%, v/v) DSPC / CH / DSPE-PEG₂₀₀₀ liposomes exhibited an initial drug loading rate of 2.4 (nmole dox/μmole lipid) min⁻¹; a rate that was 3-fold lower than observed for DSPC / DSPE-PEG₂₀₀₀ liposomes.

Figure 5.3

Ethanol-enhanced increases in drug loading rates into liposomes

DSPC / CH / DSPE-PEG₂₀₀₀ (50:45:5 mole ratio, squares) and DSPC / DSPE-PEG₂₀₀₀ (95:5 mole ratio, circles) liposomes (with transmembrane pH gradient, pH 4 inside, 7.5 outside) were incubated at 37°C with doxorubicin (0.2 drug-to-lipid mole ratio) in the absence (open symbols) and presence (closed symbols) of 10% (v/v) ethanol. At various time points, 100 μ l aliquots of sample were passed down mini spin columns and subsequently analyzed for drug and lipid concentrations as described in Chapter 2. Each data point represents the μ mole doxorubicin / μ mole lipid \pm S.D. for 3 experiments.



5.3.5. Optimal ethanol concentration for drug loading in liposomes

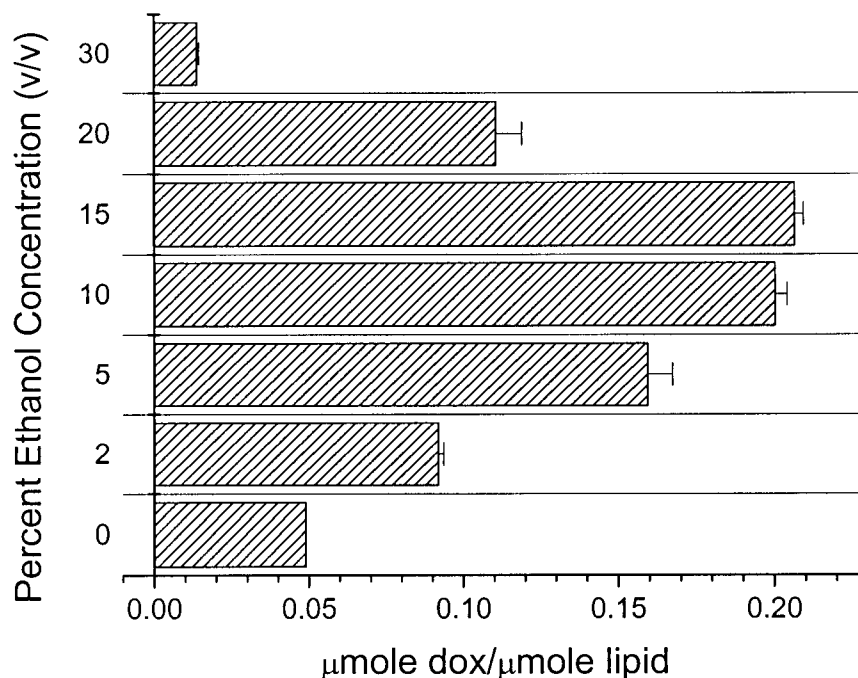
In order to determine the optimal ethanol concentration for doxorubicin loading into DSPC / DSPE-PEG₂₀₀₀ liposomes, the effect of increasing ethanol concentrations was investigated by measuring doxorubicin loading efficiency after a 1 hour incubation at 37°C (Figure 5.4). The highest encapsulation efficiencies were observed when the liposomes were incubated in 10 to 15% (v/v) ethanol. As shown in Figure 5.4, the encapsulation efficiency was reduced significantly when the concentration of ethanol was $\geq 20\%$ (v/v). When the DSPC / DSPE-PEG₂₀₀₀ liposomes were incubated in the presence of 40 and 50% (v/v) ethanol there was an observed increase in solution viscosity or “gelling” of the sample.

Since more subtle changes in liposome structure may occur in the presence of $\leq 20\%$ (v/v) ethanol, the effect of ethanol addition on liposome size, ¹⁴[C]-lactose retention and the pH gradient used to engender drug loading and promote drug retention was assessed (Table 5.1). DSPC / DSPE-PEG₂₀₀₀ liposomes were exposed to various concentrations of ethanol for 1 hour prior to measuring liposome size by quasielastic light scattering (QELS). DSPC / DSPE-PEG₂₀₀₀ liposomes exposed to increasing ethanol concentrations all exhibited minimal increases in mean diameter and polydispersity as judged by standard deviations. At ethanol concentrations $\leq 20\%$ (v/v) there was less than a 12% increase in liposome size. The particle size analysis data suggested that even at ethanol concentrations $\geq 20\%$ (v/v) the liposomes remained as a single population exhibiting a Gaussian distribution. However, a 35% increase in liposome size was observed at ethanol concentrations of 30% (v/v). Samples passed down Sephadex G-50 columns to remove residual ethanol exhibited a size that was not significantly different from the sample prior to chromatography.

Figure 5.4

Influence of ethanol concentration on the accumulation of doxorubicin into cholesterol-free liposomes

DSPC / DSPE-PEG₂₀₀₀ (95:5 mole ratio) liposomes (with transmembrane pH gradient, pH 4 inside, 7.5 outside) were incubated at 37°C with doxorubicin and increasing concentrations of ethanol. At 1 hour, post drug loading, aliquots were passed down mini spin columns and the eluted fraction was analyzed for drug and lipid concentration by methods outlined in Chapter 2. Each data point represents the $\mu\text{mole doxorubicin} / \mu\text{mole lipid} \pm \text{S.D.}$ for 3 experiments.



The permeability of DSPC / DSPE-PEG₂₀₀₀ lipid membranes in the presence of ethanol was determined using a radiolabeled ¹⁴[C]-lactose aqueous space marker (Table 5.1). Lipid films were rehydrated with HBS (pH 7.4) containing trace quantities of the radiolabeled lactose and then were extruded. Liposome samples were incubated with increasing concentrations of ethanol (0 - 30% v/v) for 60 minutes and passed down mini columns to separate retained and free lactose. When incubated with 30% ethanol (v/v), the % lactose retained decreased significantly ($p < 0.05$), consistent with the notion that ethanol at this concentration affected liposome permeability sufficiently to promote release of the entrapped marker. Radiolabeled markers, such as lactose, are also used to indicate liposome trapped volumes. In the absence of ethanol, DSPC / DSPE-PEG₂₀₀₀ liposomes prepared by the extrusion technique through 100 nm pore size filters exhibited a trapped volume of $1.94 \pm 0.11 \mu\text{l}/\mu\text{mole}$. This value was comparable to previously published trapped volumes for liposomes prepared by extrusion through 100 nm pore size filters [99].

Another indication of ethanol-induced increases in liposome permeability was provided by measuring the stability of an imposed transmembrane pH gradient. The DSPC / DSPE-PEG₂₀₀₀ liposomes used in these studies were prepared in a pH 4.0 citrate buffer and were subsequently exchanged into HBS at pH 7.4. The estimated pH gradient of > 3 units can be measured using radiolabeled methylamine as a probe [203]. A measured pH gradient of > 2.7 units was observed when ethanol concentrations were $\leq 10\%$ (v/v), however at higher ethanol concentration ($\geq 20\%$ v/v), there was a significant ($p < 0.05$) reduction in the measured transmembrane pH gradient. Previously published data have suggested that the magnitude of the pH gradient is important in terms of maximizing the efficiency of doxorubicin loading, as well as playing a critical role in governing drug retention [69]. The decreased loading

Table 5.1

Influence of ethanol concentration on size, % lactose retained and pH gradient in DSPC / DSPE-PEG₂₀₀₀ (95:5 mole ratio)

Ethanol Conc. (v/v)	Liposome Size (nm) ^a		Lactose Retained (%) ^b	pH Gradient ^c
	Precolumn	Postcolumn		
0%	107	109	100 ± 7	2.77 ± 0.23
5%	113	112	103 ± 9	2.80 ± 0.24
10%	116	112	97 ± 7	3.44 ± 0.50
20%	120	116	100 ± 6	1.89 ± 0.04
30%	144	133	74 ± 6	0.86 ± 0.01

^a liposome size determined by QELS before and after size exclusion chromatography

^b measurements determined by entrapped ¹⁴[C]-lactose added during sample rehydration. The values represent the average of 3 experiments ± S.D.

^c measurements determined by internal and external concentrations of ¹⁴[C]-methylamine after 1 hour incubation at 40°C. The values represent the average of 3 experiments ± S.D.

efficiencies noted in Figure 5.4 at ethanol concentrations $\geq 20\%$ (v/v) are likely due to ethanol's effect on collapsing the pH gradient.

Ethanol-induced changes in DSPC / DSPE-PEG₂₀₀₀ liposomes were also assessed by cryo-transmission electron microscopy. The representative photomicrographs shown in Figure 5.5 suggest that the integrity of liposome structure was maintained in the presence of 10% ethanol (v/v). However, the decreases in percent lactose retention and pH gradient at higher ethanol concentrations ($\geq 20\%$, v/v) could be directly attributed to a breakdown of liposome structure observed in the electron micrographs. This was evidenced by the presence of open liposomes (OL) seen when the liposomes were in 20% (v/v) ethanol as well as OL and bilayer sheets (S) observed when the ethanol concentration was increased to 30% (v/v).

5.3.6. Influence of temperature, lipid concentration and phospholipid acyl chain length on ethanol-enhanced drug loading rates

The results thus far indicate that increases in the rate of anthracycline loading into DSPC / DSPE-PEG₂₀₀₀ liposomes parallels increases in membrane association. Further, it is demonstrated that ethanol can be used to enhance the loading efficiency of doxorubicin, one of the anthracyclines that exhibits the lowest level of membrane partitioning. This effect is presumably the result of ethanol-mediated increases in doxorubicin partitioning. Ethanol-enhanced doxorubicin loading is dependent on temperature (Figure 5.6A) and lipid concentration (Figure 5.6B). Interestingly, the rate of drug loading was only enhanced when the temperature was higher than 37°C. No measurable drug uptake could be observed when the samples were incubated at 23 or 4°C (Figure 5.6A). Increased lipid concentration resulted in significantly reduced drug loading rates (Figure 5.6B). Further studies indicated that increasing

Figure 5.5

Influence of ethanol on liposome structure

Cryo-TEM electron micrographs were obtained of DSPC / DSPE-PEG₂₀₀₀ (95:5 mole ratio) liposomes after establishment of a transmembrane pH gradient (pH 4 inside, 7.5 outside). In the presence of 0 and 10% ethanol (v/v), lipid bilayers (B), described as intact vesicles with polyhedron shapes, were observed. At 20% ethanol, some open liposomes (OL) were present, however at 30%, open liposomes (OL) and bilayer sheets (S) were observed. Bar represents 200 nm.

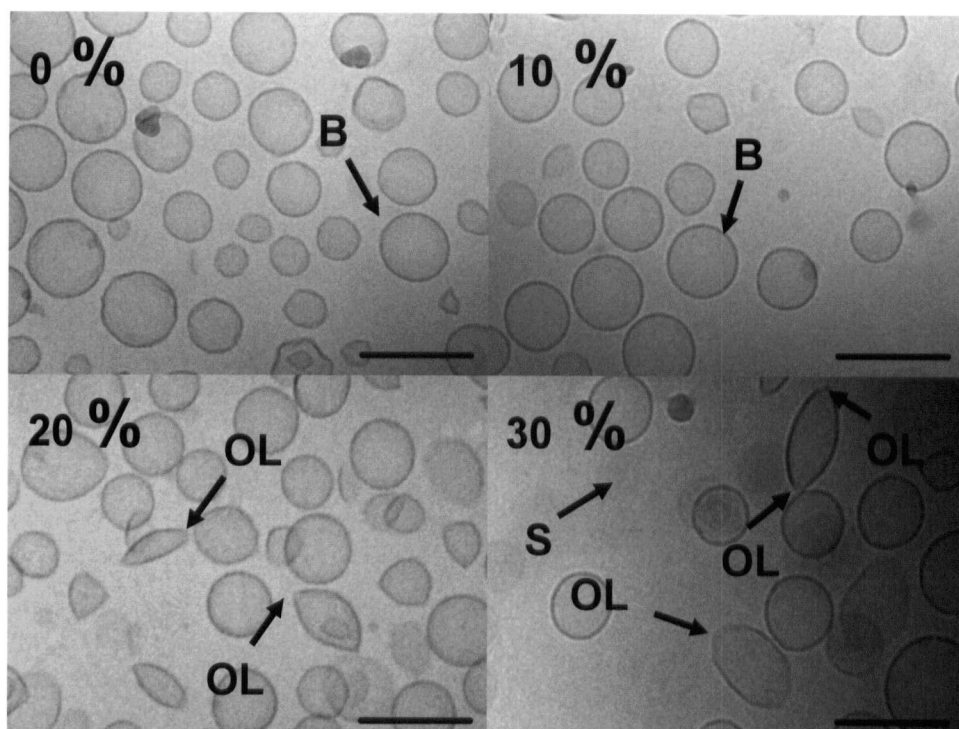
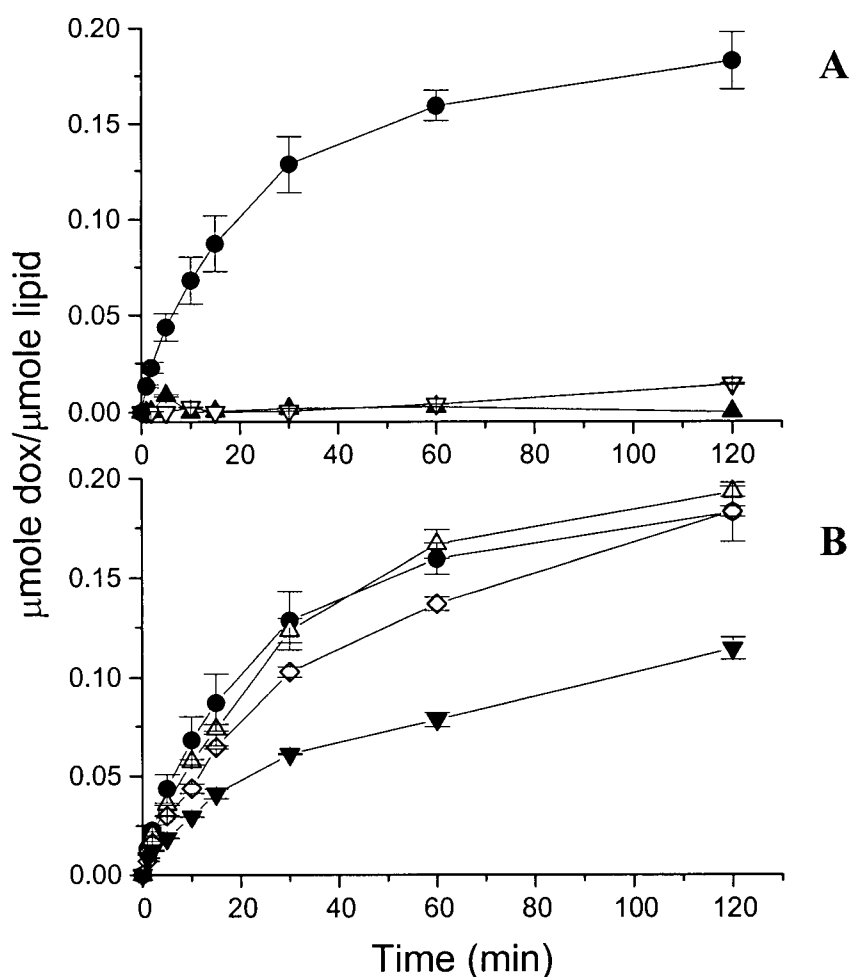


Figure 5.6

Influence of temperature and lipid concentration on ethanol-enhanced loading of doxorubicin into cholesterol-free liposomes

(A) DSPC / DSPE-PEG₂₀₀₀ (95:5 mole ratio) liposomes (with transmembrane pH gradient, pH 4 inside, 7.5 outside) and doxorubicin (0.2 drug-to-lipid mole ratio) were incubated at various temperatures; 4°C (▲), 23°C (▽) and 37°C (●). At various time points, 100 µl aliquots of sample were passed down mini spin columns and subsequently analyzed for drug and lipid concentrations as described in Chapter 2. (B) DSPC / DSPE-PEG₂₀₀₀ (95:5 mole ratio) liposomes (with transmembrane pH gradient, pH 4 inside, 7.5 outside) were prepared at various lipid concentrations, 5 mM (●), 10 mM (△), 15 mM (◇) and 20 mM (▼), and incubated with doxorubicin at 37°C. At various time points, 100 µl aliquots of sample were passed down mini spin columns and subsequently analyzed for drug and lipid concentrations as described in Chapter 2. Each data point represents the µmole doxorubicin / µmole lipid \pm S.D. for 3 experiments.



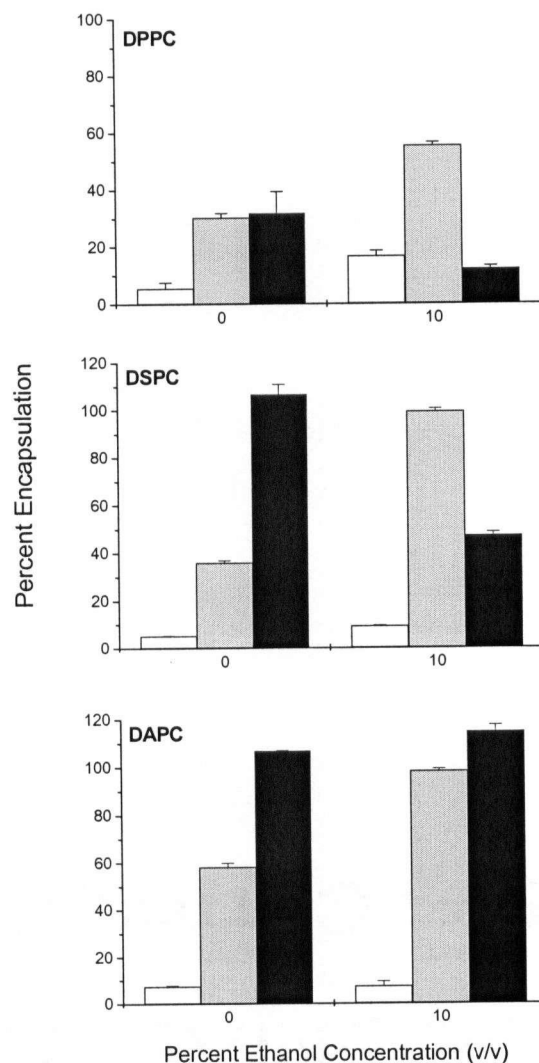
ethanol concentration at high lipid concentrations (20 mM) did not significantly improve drug loading rates (not shown), a result which suggests the importance of maintaining optimal ethanol concentrations, as well as, ethanol-to-lipid ratios.

Additional studies, shown in Figure 5.7, demonstrated that doxorubicin could be loaded into cholesterol-free liposomes prepared with phospholipids of varying acyl chain lengths. These results illustrate three important points. First, as indicated in Section 5.1 doxorubicin loading efficiencies in the absence of ethanol increase as the loading temperature increases. Thus, for DSPC / DSPE-PEG₂₀₀₀ and DAPC / DSPE-PEG₂₀₀₀ liposomes doxorubicin encapsulation efficiencies of > 95% were achieved when the incubation temperature is held at 60°C (filled bars). For DAPC / DSPE-PEG₂₀₀₀ liposomes, doxorubicin encapsulation efficiencies of 58% and 98% were achieved at 40°C (grey bars) and 60°C (filled bars), respectively. These temperatures are well below the T_c of DAPC and illustrate the importance of drug partitioning behaviour in determining drug loading attributes. Second, doxorubicin loading into the three liposomal formulations, DPPC / DSPE-PEG₂₀₀₀ ($T_c \sim 41^\circ\text{C}$), DSPC / DSPE-PEG₂₀₀₀ ($T_c \sim 55^\circ\text{C}$) and DAPC / DSPE-PEG₂₀₀₀ ($T_c \sim 66^\circ\text{C}$), increases as temperature is increased below the respective phase transition temperatures. When loading was completed in the presence of 10% (v/v) ethanol, encapsulation efficiencies of all three formulations significantly improved (2 - 3 fold) at 40°C (grey bars). Both DSPC and DAPC formulations achieved greater than 98% trapping efficiencies. Third, the loading efficiencies of doxorubicin into DPPC / DSPE-PEG₂₀₀₀ liposomes were in general poor. The addition of 10% (v/v) ethanol to the DPPC / DSPE-PEG₂₀₀₀ liposomes, however, did increase the encapsulated efficiencies more than 2-fold at both 20°C and 40°C. It is likely that improvements in doxorubicin loading into DPPC / DSPE-PEG₂₀₀₀ liposomes could be achieved if the loading temperature and ethanol

Figure 5.7

The effect of phospholipid acyl chain length on ethanol-enhanced loading of doxorubicin into cholesterol-free liposomes

Liposomes exhibiting a transmembrane pH gradient (pH 4 inside, pH 7.5 outside) composed of 95% mole ratio of DPPC, DSPC and DAPC and 5% mole ratio of DSPE-PEG₂₀₀₀ were incubated at 20°C (white bars), 40°C (grey bars) and 60°C (black bars) for 60 minutes. At various time points, 100 µl aliquots of sample were passed down mini spin columns and subsequently analyzed for drug and lipid concentrations as described in Chapter 2. Each data point represents the percent encapsulation \pm S.D. for 3 experiments.



concentration are carefully selected.

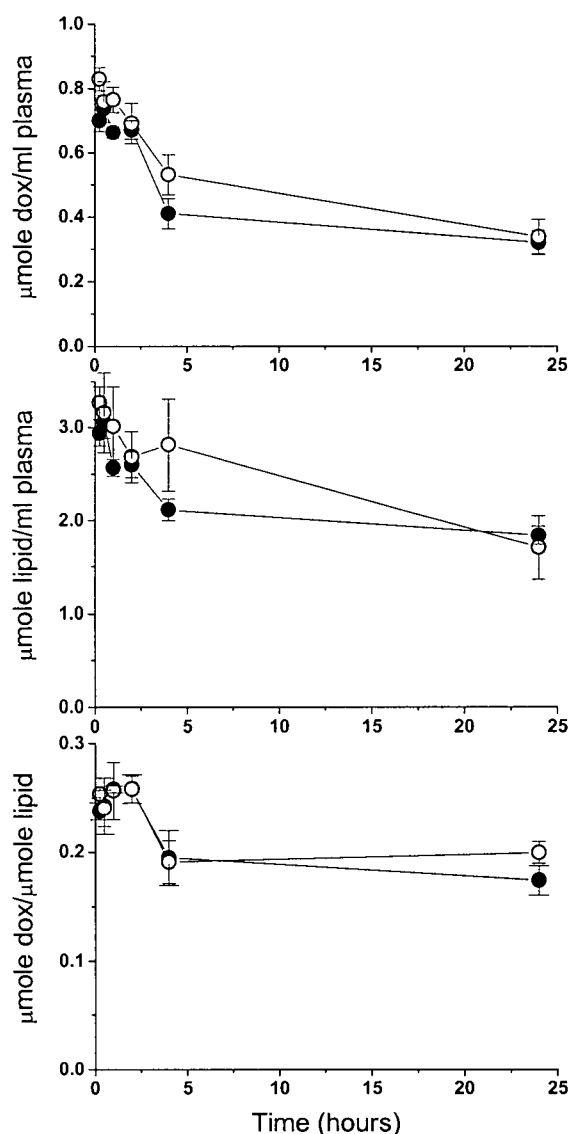
5.3.7. Influence of ethanol on release of entrapped doxorubicin in vivo

The use of ethanol to enhance doxorubicin loading into DSPC / DSPE-PEG₂₀₀₀ liposomes may be of limited interest if residual ethanol incorporation in the lipid bilayers adversely affects the release of entrapped agents in vivo. Thus, a pharmacokinetic study was completed to determine whether in vivo release of doxorubicin was altered when drug loading was completed in the presence of 10% (v/v) ethanol. Liposomes were prepared as described in Chapter 2 and loaded to achieve a 0.2 drug-to-lipid mole ratio. Prior to injection, the outside buffer was exchanged using tangential flow dialysis in an effort to remove as much of the residual ethanol as possible. Subsequently, the liposomes were injected intravenously in the lateral tail vein of female Balb/c mice at a dose of 165 $\mu\text{mole/kg}$ lipid and 33 $\mu\text{mole/kg}$ (19 mg/kg) doxorubicin. The plasma elimination profile of doxorubicin and lipid, as well as the calculated drug-to-lipid mole ratio in the plasma compartment are shown in Figure 5.8. Importantly, minimal differences were observed in the elimination profiles of the liposomal drugs prepared in the absence (open symbols) or presence (filled symbols) of ethanol. Calculated mean plasma $\text{AUC}_{0-24\text{h}}$ for doxorubicin encapsulated in liposomes prepared with and without ethanol were 9.8 $\mu\text{mole h ml}^{-1}$ and 11.4 $\mu\text{mole h ml}^{-1}$, respectively. Approximately 39% of the total injected doxorubicin remained in circulation 24 hours post-drug administration. Further, the measured drug-to-lipid mole ratios were not significantly different at any time points evaluated. These results clearly demonstrate that the use of ethanol to enhance loading of doxorubicin below the phase transition of the bulk phospholipid, is a potentially useful method that will not compromise in vivo drug release attributes.

Figure 5.8

Plasma elimination of liposomal doxorubicin: comparison of drug release from samples prepared in the absence and presence of 10% (v/v) ethanol

Large unilamellar liposomes radiolabeled with ^3H -cholesteryl hexadecyl ether (CHE) were administered intravenously via the dorsal tail vein of female Balb/c mice at an approximate dose 33 $\mu\text{mole/kg}$ doxorubicin and 165 $\mu\text{mole/kg}$ total lipid (0.2 drug-to-lipid mole ratio). Blood was collected at 0.25, 0.5, 1, 2, 4 and 24 hours. Plasma was prepared and aliquots were assayed for lipid and doxorubicin concentration as described in Chapter 2. No significant differences were observed in the elimination profiles of DSPC / DSPE-PEG₂₀₀₀ (95:5 mole ratio) prepared in the absence (○) and presence (●) of 10% (v/v) ethanol. Each data point represents the average plasma concentration \pm S.D. for three mice.



5.4. Discussion

The delicate balance between retention and release of therapeutic agents entrapped in liposomes is established as an important factor governing the therapeutic and toxic effects of liposomal drugs. Altering lipid membrane composition with the specific goal of optimizing permeability to achieve enhanced drug bioavailability following administration has been extensively explored. For example, liposomes have been engineered to undergo changes affecting drug release in response to pH [204], phospholipase exposure [205, 206] and temperature [98] in an effort to achieve improved local drug bioavailability. The behaviour of many of these formulations is dependent on use of liposomes with little or no cholesterol. Removal of cholesterol has introduced problems related to drug loading, liposome stability, liposome-protein binding, liposome elimination and in vivo drug release following i.v. injection. The incorporation of PEG-modified lipids into pure PC liposomes, effectively overcomes problems associated with liposome elimination [42, 55, 135].

It was also shown that certain drugs are actually better retained in liposomes that lack cholesterol (refer to Chapter 3). The general utility of such liposomes will depend, however, on defining methods which facilitate drug loading and manufacturing, particularly since the stability of these liposomes is much more dependent on temperature. If pH gradient-based drug loading methods are being considered, one obvious approach is to select a drug that loads efficiently into cholesterol-free liposomes at incubation temperatures below the T_c of the bulk phospholipids. For example, idarubicin loads efficiently into DSPC / DSPE-PEG₂₀₀₀ liposomes that exhibit a transmembrane pH gradient at 40°C (see Figure 5.1A). In contrast, doxorubicin, an anthracycline that partitions less efficiently into DSPC / DSPE-PEG₂₀₀₀ membranes, loads very slowly at 40°C. Loading of doxorubicin is improved as the incubation temperature

increases, however the stability of the cholesterol-free liposomes are compromised at temperatures above the T_c of the bulk phospholipids.

If effective drug loading at temperatures below the T_c of the bulk phospholipids is dependent in part on drug partitioning, then it is anticipated that improved loading could be achieved through use of agents that could enhance drug partitioning and / or membrane permeability, provided that this did not adversely affect liposome stability. In this study, increasing the doxorubicin liposomal membrane association with ethanol effectively improved doxorubicin uptake in DSPC liposomes stabilized with 5 mole % poly(ethylene glycol)-conjugated DSPE.

The rationale for using ethanol or other short chain alcohols during drug loading demonstrated by the studies in Chapter 5 is three-fold. First, to improve the loading rates of drugs that are not sufficiently hydrophobic to permeate the bilayer. Second, to increase permeability of lipid membranes composed of long acyl chains (greater than C18). Third, to increase the total drug encapsulation levels within liposomes (for example DPPC cholesterol-free liposomes) loaded at fixed temperatures well below the T_c of the bulk phospholipid.

The studies performed in this report confirmed that drug loading rates below the T_c of the bulk phospholipid were correlated with the hydrophobicity of the drug. Idarubicin, for example, was the most hydrophobic anthracycline and optimal loading of this drug could be achieved at 40°C degrees in DSPC / DSPE-PEG₂₀₀₀ liposomes. Less hydrophobic agents, such as doxorubicin, required higher temperatures to increase drug loading rates. The results clearly demonstrated that ethanol addition improved doxorubicin loading efficiencies at temperatures below the T_c of the bulk phospholipids (see Figures 5.2 – 5.4). This was even observed for both DSPC / DSPE-PEG₂₀₀₀ liposomes and DAPC / DSPE-PEG₂₀₀₀ liposomes (see Figure 5.7).

Liposomes composed of long acyl phospholipids are not commonly considered for drug delivery purposes in part because of difficulties in both preparation and drug loading. Based on these studies, the addition of ethanol will provide opportunities to investigate the applicability of novel drugs encapsulated within formulations containing long acyl chain phospholipids.

The studies indicated that DPPC cholesterol-free liposomes exhibited a lower capacity for doxorubicin encapsulation. Others have shown that the thermosensitive liposomal formulation, DPPC / DSPE-PEG₂₀₀₀ with small amounts of lyso-phosphatidylcholine (developed by Needham and associates) also have a low drug encapsulation capacity. Loading efficiencies of > 98% can only be achieved for 0.05 drug-to-lipid weight ratios when encapsulated below the T_c of the membrane and this formulation cannot be effectively loaded above the phase transition temperature due to instability of the liposomes [207, Ickenstein L, unpublished results]. It is believed that methods relying on use of ethanol to improve drug loading efficiencies may solve some of the problems that have been encountered when developing these drug-loaded thermosensitive liposomal formulations.

Concerns regarding the use of ethanol to improve pH gradient-based loading of the more hydrophilic drugs into DSPC / DSPE-PEG₂₀₀₀ have been addressed. At concentrations $\leq 15\%$ (v/v) ethanol liposome size, retention of a trapped aqueous marker, and stability of an imposed pH gradient were not significantly changed (see Table 5.1). At concentrations $\geq 20\%$ (v/v) the presence of open liposomes and bilayer sheets were evident by cryo-transmission electron microscopy (see Figure 5.5) and there was a significant reduction in the magnitude of an imposed 3.5 unit pH gradient. The reduction of the $[H^+]$ gradient at high ethanol concentrations, may be due to either an overall change in the membrane permeability of all liposomes or attributed to a decrease in the number of liposomes available to maintain a pH gradient due to

dissolution of the lipid bilayer. The most obvious change in DSPC / DSPE-PEG₂₀₀₀ liposomes occurred at ethanol concentrations > 30% (v/v).

The studies indicated that both drug loading rates and liposomal membrane association could predict the in vivo stability of a drug encapsulated in a particular liposome formulation. The relationships observed are qualified when drugs of a similar structure are compared and examined in the same lipid composition, however, there are some inconsistencies. For example, increased drug partitioning of idarubicin in cholesterol-free as compared to cholesterol-containing liposomes (Figure 5.2) would suggest that there would be increased drug loading rates and increased drug release in vivo for cholesterol-free liposomes, which is not the case. Faster drug loading rates were observed in cholesterol-containing liposomes (Figure 5.3) while enhanced retention of idarubicin in vivo was observed in cholesterol-free liposomes (shown in Chapter 3) as compared to cholesterol-containing lipid formulations. These particular inconsistencies can be explained by differences in membrane order and fluidity between DSPC cholesterol-free and cholesterol-containing liposomes. Furthermore, Madden *et al.* performed a survey of many drugs and analyzed drug accumulation into egg PC vesicles, and determined that drug uptake could not be predicted on log octanol / water partition coefficients alone [208].

These observations highlight the importance of other parameters involved in both drug uptake into, and release from, liposomes including lipid membrane order, drug solubility (aqueous and membrane), drug membrane partitioning, drug electrostatic and hydrophobic interactions. There should be a concerted effort to tease out each of these factors and their contribution to both drug loading and release from liposomes. It would be quite valuable if one could establish high through-put assays capable of predicting the stability of drug encapsulated in liposomes formulations in an effort to decrease the trial and error approach currently used.

One of the principal questions arising from these studies is how does ethanol enhance doxorubicin loading rates, allowing the transfer of doxorubicin from the external medium into the aqueous core of the membrane, while maintaining the proton gradient? One potential mechanism involves increasing the interaction of doxorubicin with liposomal membranes thereby improving drug loading rates. As the elimination profile of doxorubicin loaded with and without ethanol was not significantly different, it suggests that most of the residual ethanol was removed. Therefore, increased doxorubicin liposomal membrane association was preferentially introduced during drug loading but reduced (by the removal of ethanol) prior to pharmacokinetic analysis.

Ethanol-lipid membrane interactions have been extensively studied, however, there is still a debate on where ethanol resides in the membrane, and the nature of the interaction; binding or partitioning [209]. Studies completed to date indicate that ethanol resides at the lipid / water interface near the head groups, with a small amount partitioned in the bilayer core [186, 189]. Regarding lipid interdigitation, an increase in the incorporation of ethanol can induce this polymorphic change in membrane structure [198, 210-212]. Interdigitation is described as a consequence of the displacement of water from the interfacial region [193], resulting in a disordering effect on lipid packing [213] and intercalation of phospholipids acyl chains from opposing leaflets [214]. The presence of interdigitation domains would likely increase bilayer permeability in both directions and does not explain how the incorporation of low levels of ethanol in lipid membranes resulted in increased doxorubicin drug loading rates, while maintaining the pH gradient.

A plausible explanation for the effects of ethanol on selective increases in drug permeability pertains to asymmetric distribution of ethanol in lipid bilayers. Most studies have

clearly indicated that short chain alcohols are positioned at the lipid / water interface of the membrane [215]. Studies performed by Heerklotz *et al.* demonstrated that membrane stress and permeabilization of lipid bilayers by solutes was induced by asymmetric incorporation of compounds [216]. Asymmetric ethanol incorporation may explain why doxorubicin could permeate into the aqueous space of the liposomes, while proton permeability was not increased substantially. Furthermore, if the majority of ethanol partitioned within the outer leaflet of the bilayer, ethanol would be relatively easily removed and would not affect doxorubicin release from the liposomes.

In summary, the addition of ethanol to pre-formed liposomes is an effective strategy to increase drug membrane association and membrane permeability, allowing loading of drugs that are not sufficiently hydrophobic to cross lipid membranes on a practical time scale. At low ethanol concentrations, initial drug loading rates were significantly improved without affecting the *in vivo* behaviour of the resulting liposomes. Ethanol-enhanced drug loading will be of particular interest when utilizing thermosensitive liposomal formulations, heat labile drugs or conditions (such as acidic pH) that promote rapid phospholipid degradation at high temperatures. The studies reported here highlight a few advantages of this method. Importantly it is anticipated that similar approaches may be used to improve loading of other anti-cancer drugs into cholesterol-free liposomes.

CHAPTER 6

DESIGNING A LIPOSOMAL CARRIER FOR THE HYDROPHOBIC ANTHRACYCLINE IDARUBICIN: SUBSTANTIAL INCREASES IN DRUG CONCENTRATIONS IN PLASMA ENHANCE THERAPEUTIC ACTIVITY IN A SENSITIVE, BUT NOT MULTIDRUG RESISTANT, MURINE LEUKEMA MODEL

6.1. Introduction

During recent years, the potential for liposomes as drug delivery vehicles to improve the therapeutic index of anti-cancer drugs has been realized. Drugs within appropriately designed lipid-based carriers can exhibit an improved therapeutic index due to carrier-mediated decreases in drug toxicity without significant changes in antitumor activity and / or drug toxicity. Perhaps not surprisingly, not all anti-cancer drugs benefit through development of a liposomal carrier. It appears that the drug as well as the liposome needs to be carefully selected in order to achieve optimal therapeutic results, as judged by animal models of cancer. One of the most common classes of anti-cancer agents, the anthracycline antibiotics, appear to benefit from encapsulation in liposomes and there are clinically approved liposomal formulations for both doxorubicin and daunorubicin [217, 218], however, not all members of this drug family have been formulated successfully. The interest was to design a lipid formulation for idarubicin, an anthracycline that is garnering significant clinical interest.

Idarubicin is a hydrophobic daunorubicin analogue that is less cardiotoxic than daunorubicin or doxorubicin [129, 219]. More importantly, idarubicin has demonstrated a 10-fold higher cytotoxic activity than daunorubicin in cultured human cancer cells [220] and this increased activity has been attributed to its greater hydrophobicity [141], greater induction of DNA strand breaks (than daunorubicin) through the direct mechanism of inhibition of DNA topoisomerase II, generation of free radicals, and exhibition of G2 cell cycle arrest. From a mechanistic perspective it is also worth noting that idarubicin is metabolized in the liver to

idarubicinol by the enzyme aldoketoreductase, and this metabolite exhibits cytotoxic effects comparable to that achieved with the parent compound [220] that are significantly greater than other anthracycline metabolites [221, 222]. Finally, idarubicin is less susceptible to the activity of multidrug resistant proteins [221, 223-225].

Currently this drug is indicated for the treatment of acute myelogenous leukemia (AML), although it is not generally utilized as frontline therapy [226, 227]. Idarubicin has also demonstrated antitumor activity against other malignancies including melanoma, sarcoma, non-Hodgkin's lymphoma and lung, ovarian and advanced breast cancers [228].

When considering the development of an improved formulation for idarubicin it is important to recognize that, upon administration of idarubicin, there is less accumulation within the heart and spleen as compared to daunorubicin [229], therefore idarubicin is less cardiotoxic than the other analogues [230]. Thus, attempts to improve the therapeutic properties of this drug will rely on improving pharmacokinetics and altering the biodistribution of the drug in favour of achieving enhanced therapeutic effects.

Given that idarubicin exhibits many ideal pharmacological properties, the studies described herein have sought to demonstrate that its therapeutic activity could be improved when encapsulated within a liposomal carrier. In order to address this, an important dilemma had to be solved: How can a liposome be used to stably encapsulate a highly membrane permeant hydrophobic drug like idarubicin? This led to the consideration of cholesterol-free lipid-based carriers.

Idarubicin is more lipophilic than either daunorubicin or doxorubicin [178, 179] and is quickly released from conventional liposomal formulations prepared with cholesterol as a stabilizing component. Studies from Chapter 3 demonstrated that idarubicin was better retained

in cholesterol-free liposomes as compared to conventional cholesterol-containing liposomes. However, idarubicin plasma concentrations were below detectable limits 4 hours post-injection of these liposomal formulations. These results suggested that the formulation, albeit significantly more effective as a carrier for idarubicin than formulations where the liposomes were prepared with cholesterol, released > 90% of their encapsulated contents within 4 hours after i.v. injection.

The research objectives of the studies presented in this chapter were to evaluate whether further improvements in circulation longevity of idarubicin could be achieved by altering the composition of cholesterol-free liposomes (phospholipid acyl chain length, PEG content and PEG molecular weight) and / or by modification of the procedure used to encapsulate the drug.

The working hypothesis was that increases in plasma idarubicin levels and idarubicin circulation longevity would improve antitumor activity. Increases in plasma idarubicin levels mediated by the drug carrier will be a reflection of how fast the drug is released from the carrier after administration. If little or no drug is released from the injected liposomes, then the circulating drug levels will be dictated by the circulating levels of liposomal lipid. Conversely, if the encapsulated drug rapidly dissociates from the carrier, then the drug levels achieved would be comparable to those observed following administration of the drug without the carrier. In this regard, it is difficult to predict how the release rate of a given anti-cancer drug from liposomes influences therapeutic activity [200].

Previous studies have demonstrated that some drugs exhibit improved antitumor activity when encapsulated in lipid-based carriers that engender longer circulation lifetimes. For example, both vincristine and doxorubicin have demonstrated an increased antitumor activity when the plasma half-life is increased [60, 63, 231, 232]. In fact it has been shown that

increased drug release of doxorubicin from liposomes prepared of dimyristoylphosphatidylcholine (DMPC) / cholesterol actually results in an increase in toxicity and a decrease in therapeutic effects [233]. The studies outlined here were specifically designed to gain stepwise improvements in idarubicin retention in liposomes after i.v. administration, with the goal of achieving increased plasma drug levels over time and improving therapeutic activity.

6.2. Hypothesis

Further improvements in the in vivo retention of idarubicin in cholesterol-free liposomes will be achieved through use of decreased PEG concentrations and increased buffering capacity (internal citrate concentration) that will, in turn, improve the therapeutic activity.

6.3. Results

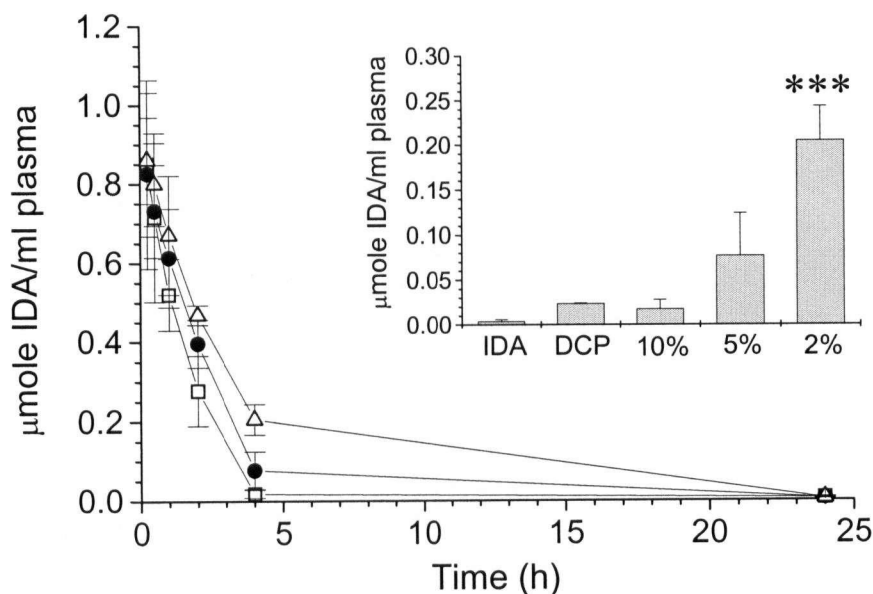
6.3.1. Pharmacokinetics of free and liposomal idarubicin: effect of PEG concentration and internal citrate concentration

The influence of altering lipid composition (phospholipids acyl chain length, mol% PEG-conjugated lipids and PEG molecular weight) and loading parameters (internal citrate concentration and pH) on the plasma circulation lifetimes of idarubicin in cholesterol-free liposomes exhibiting a transmembrane pH gradient (pH 4.0 inside, pH 7.4 outside) was evaluated. Female Balb/c mice were administered as a single i.v. injection of free idarubicin (33 μ mole/kg; 18 mg/kg) or liposomal idarubicin (33 μ mole drug/kg and 165 μ mole total lipid/kg; ~ 100 mg total lipid/kg). Both plasma lipid and drug levels were measured at 0.25, 0.5, 1, 2, 4 and 24 hours following drug administration. The results, shown in Figure 6.1, suggest that

Figure 6.1

The effect of DSPE-PEG concentration on the plasma elimination of idarubicin encapsulated in DSPC / DSPE-PEG₂₀₀₀ liposomes

Liposome formulations containing varying amounts of PEG-conjugated lipids; 10 mol% (\square), 5 mol% (\bullet) and 2 mol% (\triangle) were loaded with idarubicin at a 0.2 drug-to-lipid mole ratio and administered as a single i.v. bolus injection of 33 $\mu\text{mole/kg}$ idarubicin to female Balb/c mice. Plasma lipid and drug concentrations were measured as described in Chapter 2. **Inset:** Idarubicin plasma concentration at 4 hours post injection. Legend: IDA, free idarubicin ($n = 3$), DCP, DSPC / CH / DSPE-PEG₂₀₀₀ (50:45:5 mole ratio; $n = 6$), 10% ($n = 6$), 5% ($n = 24$) and 2% ($n = 6$), the latter numbers represent the mol% of PEG-lipid incorporated into DSPC / DSPE-PEG₂₀₀₀ liposomes. Liposomes were loaded and administered i.v. to female Balb/c mice as described above. Data points represent the average $\mu\text{mole idarubicin / ml plasma} \pm \text{S.D}$ for at least 3 mice. *** denotes that the $\mu\text{mole IDA / ml plasma}$ concentration for DSPC / 2 mol% DSPE-PEG₂₀₀₀ liposomes is statistically different from all other groups tested, as determined by one-way ANOVA and Tukey-Kramer test with $p < 0.001$.



increasing the mol% of DSPE-conjugated PEG resulted in more rapid elimination of idarubicin from the circulation. When using cholesterol-free liposomes with 10 mol% DSPE-PEG₂₀₀₀ the plasma levels of idarubicin 4 hours after administration were only 3-fold greater than that observed following injection of free idarubicin (Figure 6.1 inset). These values were not significantly different from results obtained with cholesterol-containing liposomes (results from Chapter 3).

In contrast, decreasing the PEG concentration to 2 mol% resulted in a 50-fold ($p < 0.001$) increase in idarubicin plasma concentrations at 4 hours post-drug administration (Figure 6.1 inset). Formulations prepared with DAPC (C20) and 5 mol% PEG-conjugated lipids did not significantly extend idarubicin circulation lifetimes and there were no marked increases of idarubicin plasma concentration at 4 hours post-drug administration ($p > 0.05$) (not shown). Formulations prepared with DBPC (C22) were relatively difficult to work with considering the high temperatures ($> 80^{\circ}\text{C}$) required for extrusion and inconsistent loading results.

Additional variables considered in these studies included varying PEG molecular weights (350 - 5000), which also did not result in a significant impact on the idarubicin plasma elimination profile (not shown). It is important to note that the changes in lipid composition described here did not significantly change the plasma elimination of the liposomes as reflected by the mean plasma liposomal lipid $\text{AUC}_{0-24\text{h}}$, liposome circulation lifetime and % injected dose remaining 24 hours after i.v. administration.

Studies described by Mui *et al.* concluded that osmotic gradients across lipid bilayers influence drug release [234], however these studies were completed in cholesterol-containing liposomal formulations. In an effort to determine whether the cholesterol-free formulations used in the studies described here exhibited sensitivity to transmembrane osmotic gradients,

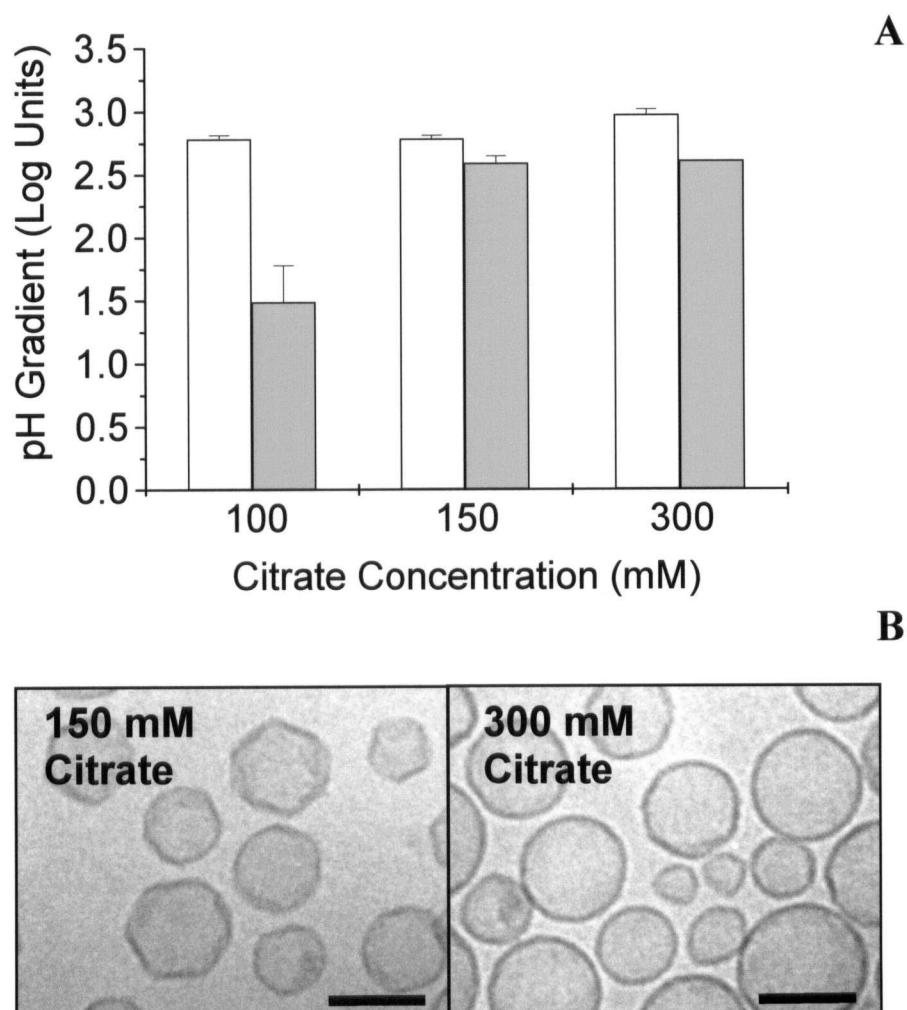
liposomes were prepared in hyper- and iso-osmotic citrate solutions. Prior to initiating plasma elimination studies with these formulations, however, it was important to determine whether decreases in citrate concentration (the method used to change internal osmolarity) decreased the transmembrane pH gradient after idarubicin loading. In general high citrate concentrations (≥ 300 mM) have been utilized to maintain a large buffering capacity such that following drug loading, the transmembrane pH gradient is maintained. It has been shown for other drugs loaded into liposomes through use of pH gradients that drug-mediated decreases in the magnitude of the transmembrane pH gradient after drug loading are associated with increases in the rate of drug release. The results from Figure 6.2A indicate that when liposomes were prepared with either 300 mM (573 mOsm/kg solution) or 150 mM (296 mOsm/kg solution) citrate the magnitude of the transmembrane pH gradient measured prior to (open bars) and following drug loading (grey bars) was not significantly different. When liposomes were prepared with 100 mM citrate (179 mOsm/kg solution), the pH gradient was significantly reduced following drug loading. For this reason plasma elimination studies were completed only with liposomes prepared with either 300 or 150 mM citrate.

The effect of varying internal citrate concentration, and hence osmolarity gradients established across the lipid membranes, on liposome structure was investigated by cryo-transmission electron microscopy. Representative micrographs of “empty” liposomes prepared with transmembrane gradients of 150 mM and 300 mM internal citrate concentrations are shown in Figure 6.2B. Liposomes prepared with 300 mM citrate (shown on the right) appear swollen or “rounded up”, a characteristic observed when enclosed lipid membranes are exposed to hypo-osmotic solutions. Liposomes prepared with 150 mM citrate (shown on the left) appear to be smaller and exhibit atypical (not smooth) surface features.

Figure 6.2

The effect of drug loading on the transmembrane pH gradient in liposomes prepared with varying internal citrate concentrations and the effect of osmotic gradients on liposome structure

(A) Liposomes contained a transmembrane gradient (inside pH 4.0, outside pH 7.5) with internal citrate concentrations of 300 mM, 150 mM and 100 mM. White and grey bars represent “empty” and drug-loaded (0.2 drug-to-lipid mole ratio, 1 mM : 5 mM) liposomes, respectively. (B) Cryo-TEM electron micrographs were obtained of DSPC / DSPE-PEG₂₀₀₀ (95:5 mole ratio) liposomes containing a transmembrane pH gradient with 150 mM and 300 mM citrate concentrations (pH 4.0) inside and HBS buffer (pH 7.4) outside. Osmolarity is indicated in parentheses for the different buffers; 100 mM citrate (179 mOsm/kg), 150 mM citrate (296 mOsm/kg), 300 mM citrate (573 mOsm/kg) and HBS (319 mOsm/kg). Bars represent 100 nm.



The plasma elimination profiles of idarubicin encapsulated in DSPC / DSPE-PEG₂₀₀₀ (98:2 mole ratio) liposomes with internal citrate concentrations of 300 mM (open triangles) and 150 mM (closed triangles) are provided in Figure 6.3. A reduction in the internal citrate concentration resulted in a significant increase in idarubicin plasma concentration. At 4 hours post-injection, there was a 2.4-fold increase in idarubicin concentration in the plasma of mice injected with liposomes containing 150 mM citrate as compared to those injected with liposomes containing 300 mM citrate. The changes in liposome shape noted in Figure 6.2B did not affect liposome elimination rates, thus the changes in drug levels in the plasma were attributed to increases in idarubicin retention in those liposomes prepared with 150 mM citrate buffer.

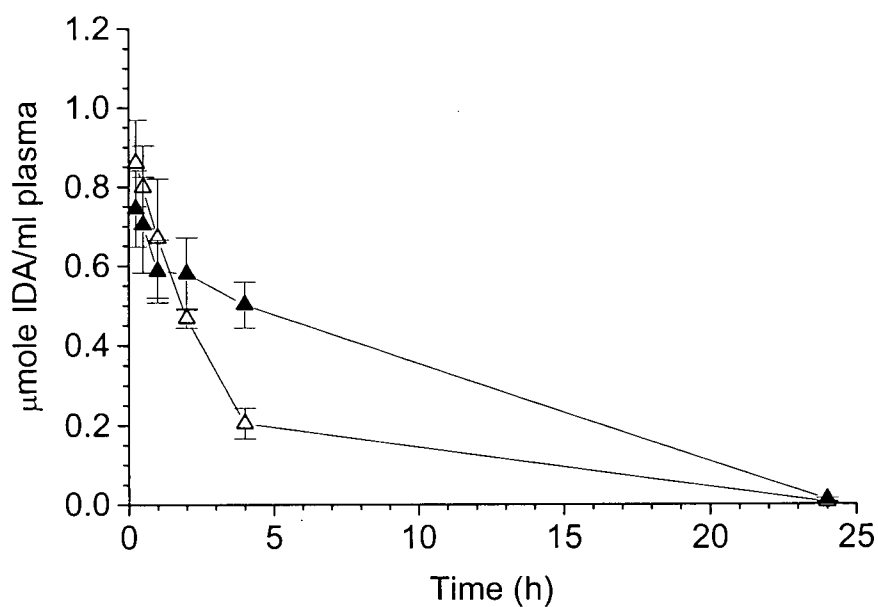
In summary, 63% of the injected drug dose remained in circulation when idarubicin was encapsulated in low PEG (150 mM citrate) cholesterol-free liposomes, as compared to 5% for free idarubicin at 4 hours post-drug administration. Further, the results suggest that cholesterol-free liposomes may be more sensitive to osmotic gradients than conventional cholesterol-containing lipid membranes.

Key pharmacokinetic parameters were calculated from the idarubicin plasma concentration versus time profiles shown in Figures 6.1 and 6.3 and are presented in Table 6.1. Both free and encapsulated idarubicin exhibited a monophasic elimination profile characteristic of a one compartment pharmacokinetic model ($R^2 \geq 0.922$ for all groups). In particular, area-under-the-curve (AUC), circulation half-life ($T_{1/2}$), area-under-the-moment-curve (AUMC) and mean residence time (MRT) increased upon encapsulation of idarubicin in lipid-based carriers, whereas plasma clearance (Cl) decreased. Further, the volume of distribution (Vd) was markedly lower (< 1.09 ml) for all liposomal idarubicin formulations as compared to free

Figure 6.3

Effect of citrate concentration on the plasma elimination of idarubicin encapsulated in DSPC/DSPE-PEG₂₀₀₀ (98:2 mole ratio) liposomes

Liposomes containing a transmembrane gradient (inside pH 4.0, outside pH 7.5) with internal citrate concentrations of 300 mM (\triangle , $n = 6$) and 150 mM (\blacktriangle , $n = 9$) were loaded with idarubicin at a 0.2 drug-to-lipid mole ratio and administered to Balb/c mice as a single i.v. bolus injection of 33 $\mu\text{mole/kg}$ idarubicin. Each data point represents the average $\mu\text{mole IDA/ml}$ plasma \pm S.D.



idarubicin (38.6 ml). Table 6.1 indicates that the lipid formulation demonstrating the highest drug AUC_{0-4h} in the plasma compartment following i.v. administration was DSPC / DSPE-PEG₂₀₀₀ (98:2 mole ratio, 150 mM citrate) and this formulation was used to assess idarubicin antitumor activity.

6.3.2. Antitumor activity of single dose administration of free and liposomal idarubicin in the murine P388 leukemia model and MDA435/LCC6 breast xenograft model

Prior to initiation of efficacy studies, routine limited dose range finding experiments in non-tumor bearing BDF-1 mice were performed. The maximum tolerable dose (MTD) was estimated as the dose that mice survived, without significant weight loss (less than 15%) or signs of stress or toxicity (e.g., lethargy, scruffy coat, laboured breathing), for 30 days following drug administration. For free and liposomal idarubicin the MTD was 4 mg/kg and 3 mg/kg, respectively, in BDF-1 mice. This indicates that the liposomal idarubicin was more toxic or potent than the free form. It should be noted that mice administered with high doses of either free or liposomal idarubicin developed a swelling on their face, specifically around the nose and these mice were terminated due to this unexpected adverse side effect. This side effect was observed in both normal (BDF-1) and immune-deficient (SCID Rag 2M) mice and compromised the dose range used for efficacy studies. For this reason, data summarized below has emphasized doses of idarubicin which provided the maximum therapeutic effects without observation of this toxicity in any of the mice within a given group.

The antitumor effect of free and liposomal idarubicin in SCID Rag 2M mice bearing MDA435/LCC6 human breast solid tumors are illustrated by the data summarized in Figure 6.4. Treatments consisting of a single i.v. bolus injection were administered 20 days after tumor cell

Table 6.1

Summary of pharmacokinetic parameters of free and liposomal idarubicin

Sample	AUC _{0-t} ^a ($\mu\text{mole}\cdot\text{h}\cdot\text{ml}^{-1}$)	T _{1/2} ^d (h)	Cl ($\text{ml}\cdot\text{h}^{-1}$)	AUMC ($\mu\text{mole}\cdot\text{h}^2\cdot\text{ml}^{-1}$)	MRT _{last} (h)
Free IDA	0.04	1.23	21.68	0.07	1.78
DSPC / CH / PEG (50:45:5) / 300 mM	0.37	0.18	2.15	0.1	0.26
DSPC / PEG (90:10) / 300 mM	1.48	1.01	0.54	2.16	1.46
DSPC / PEG (95:5) / 300 mM	1.97	1.44	0.41	4.09	2.08
DSPC / PEG (98:2) / 300 mM citrate	2.60	1.89	0.31	7.09	2.72
DSPC / PEG (95:5) / 150 mM	3.37	2.36	0.24	11.49	3.41
DSPC/PEG (98:2)/ 150 mM	7.04	6.74	0.11	68.41	9.72

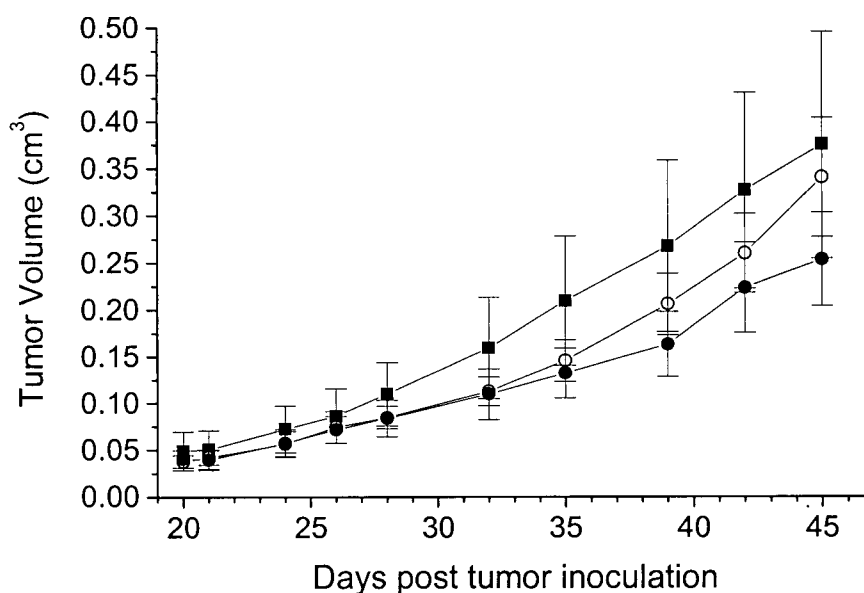
^a AUC was calculated using the trapezoidal rule (0-T_{last}), T_{last} was 4 hours

All PK elimination profiles were fit to iv-bolus one compartment model using WinNonlin Version 1.5 pharmacokinetic software; R², goodness of fit statistic for one compartment model > 0.92 for all groups. The calculations of each pharmacokinetics parameter is shown in Table 2.1.

Figure 6.4

Antitumor efficacy of free and liposomal idarubicin on the growth of MDA435/LCC6 WT breast cancer xenografts in SCID Rag 2M mice

MDA435/LCC6 tumors were grown on the backs of SCID Rag 2M mice. Mice were administered a single i.v. bolus injection of saline (filled squares), 1 (circles) mg/kg of free (open symbols) or liposomal (filled symbols) idarubicin initiated on day 20. Data are expressed as means \pm SEM (n = 4 mice/group). Comparison of tumor volumes on day 45 between groups was not statistically significant as determined by one-way ANOVA and Tukey-Kramer test.



inoculation. Free and liposomal idarubicin treatment groups were compared at equivalent doses, 1 mg/kg. This dose was well-tolerated and exhibited no signs of toxicity. For the MDA435/LCC6 WT tumor model liposomal idarubicin appeared to show a trend towards improved therapeutic activity, but the difference between the free drug and liposomal drug treatment groups was not significant. On day 45 (25 days after treatment was initiated), the mean tumor weight for saline, free drug and liposomal drug treated mice were 0.38 ± 0.24 , 0.34 ± 0.13 and 0.25 ± 0.10 g ($p = 0.589$).

The antitumor activity of free and liposomal idarubicin was also determined in BDF-1 mice with i.p. P388 ascitic tumors and these data have been summarized in Figure 6.5 and Table 6.2. Both, free and liposomal idarubicin increased the survival time in the P388 model in a dose-dependent manner. Saline-treated mice typically had to be terminated due to tumor growth between days 7 - 9 and this control group exhibited a median survival time of 8 days. Mice treated with equivalent doses of free and liposomal idarubicin between 0.5 and 3 mg/kg exhibited dose dependent increases in median survival time. Drug doses of 2 and 3 mg/kg of liposomal idarubicin resulted in % increase in lifespan (ILS) values of 156 and 175, respectively. Comparable doses of free idarubicin resulted in % ILS values of 113 and 144, respectively. It should be noted (see Table 6.2) that the highest dose of idarubicin, 3 mg/kg, administered for both free and liposomal drug was very well tolerated and caused a weight loss of 3.8% and 4.2%, respectively. Weight loss reached a nadir 5 days after drug administration and recovered to control values by day 11.

Treatment with liposomal idarubicin at doses of 0.5, 1 and 2 mg/kg resulted in significantly higher median survival times ($p < 0.005$) when compared to mice treated with the equivalent doses of free idarubicin. There was not a significant difference in the median

Figure 6.5

Antitumor activity of free and liposomal idarubicin in mice bearing murine P388 WT leukemia (ascites) model

Survival curves were derived from groups of 6 (0.5 mg/kg free and liposomal IDA), 12 (control and free IDA groups) and 14 (liposomal IDA groups) BDF-1 mice inoculated i.p. with 10^6 P388 cells and treated 24 hours later. Mice were administered a single i.v. bolus injection of saline (filled squares), 0.5 (down triangles), 1 (up triangles), or 2 mg/kg (circles) of free (open symbols) or liposomal (filled symbols, DSPC / DSPE-PEG₂₀₀₀, 98:2 mole ratio) idarubicin.

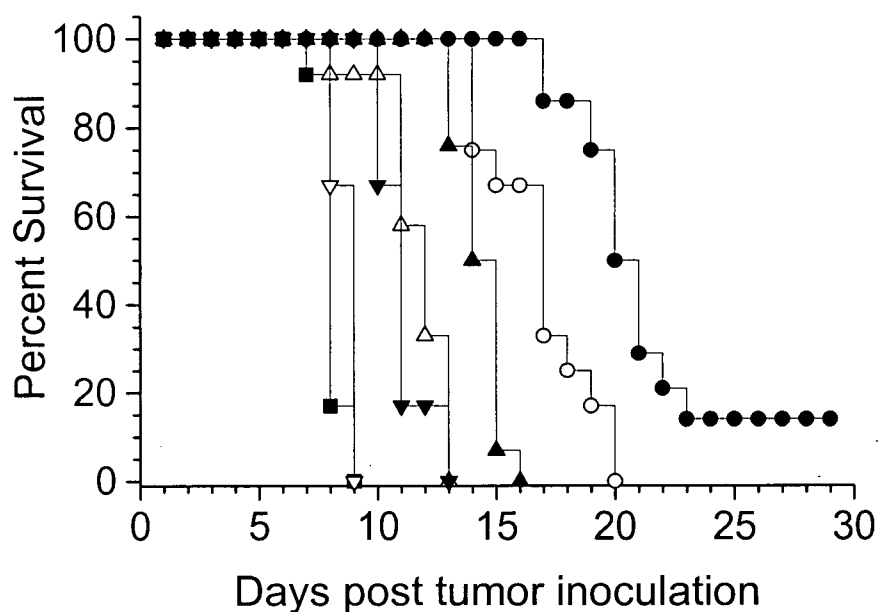


Table 6.2

Antitumor activity of free and liposomal formulations of idarubicin in BDF-1 mice bearing P388 tumors

Group	Drug Dose (mg/kg)	Percent Wt Change (day 5)	Median Survival Time (days)	ILS (%) ^a	L/F ^b
Control	-	11.8	8.0	-	-
Free Idarubicin	0.5	11.4	9.0	13	-
	1	2.1	12.0	50	-
	2	-1.4	17.0	113	-
	3	-3.8	19.5	144	-
DSPC/PEG (98:2)/	0.5	0.5	11.0	38	2.9
150 mM Citrate	1	2.4	14.5	81	1.6
	2	-1.9	20.5	156	1.4
	3	-4.2	22.0	175	1.2

^a Percent increase in lifespan (ILS) values were determined from median survival times comparing treated and saline control groups

^b L/F, liposomal/free median survival time; values were determined by dividing the median survival time of the liposomal group by the median survival time of mice administered an equivalent dose of free idarubicin

survival time of mice treated at the 3 mg/kg dose ($p > 0.05$). However three (out of 28) mice treated with liposomal idarubicin survived beyond 60 days after tumor cell inoculation as compared to one (out of 24) for mice treated with free idarubicin at 2 and 3 mg/kg doses. These data suggest that liposomal idarubicin was more efficacious than equivalent doses of free idarubicin, a result that is reflected in the L/F values shown in Table 6.2. The L/F value is the % ILS ratio obtained for animals treated with liposomal (L) and free (F) drug at an equivalent doses and this value was greater than 1 for all doses evaluated.

6.3.3. Evaluation of free and liposomal idarubicin in multidrug resistant MDA435/LCC6 (MDR) and P388 (ADR) tumor cells

As indicated in the introduction, one of the rationales for pursuing development of liposomal idarubicin was based on its potential to be more effective in treating multidrug resistant tumors. The cytotoxic effect of idarubicin and doxorubicin was evaluated in MDA435/LCC6 (WT / MDR) and P388 (WT / ADR) cell lines in vitro. MDA435/LCC6 MDR cells were transfected with the MDR1 gene and exhibited a 6.8-fold overexpression of p-glycoprotein [235]. P388 ADR cells were cultured in the presence of low levels of doxorubicin to induce resistance and it is known that these cells also have elevated levels of p-glycoprotein. Cytotoxic activity of the selected drugs was evaluated using the MTT assay [108, 236] following 72 hours exposure to drugs. Cytotoxicity was expressed as percent cell viability relative to untreated control cells (Figure 6.6).

There were two important observations from these studies. First, all cells lines were more sensitive to idarubicin than doxorubicin. Second, the log fold resistance (IC_{50} of resistant cells divided by IC_{50} of wild type cells) of MDA435/LCC6 cells was much lower for cells

Figure 6.6

Cytotoxicity of idarubicin and doxorubicin on MDA435/LCC6 wild type/MDR and P388 wild type/ADR cell lines

Cells were treated with varying concentrations of idarubicin (squares) and doxorubicin (circles). Wild type cells are represented by open symbols and resistant (ADR / MDR) sublines are represented by closed symbols. Cytotoxicity was evaluated by standard MTT assay as described in Chapter 2. Each value represents the mean from at least three independent experiments; bars, SD.

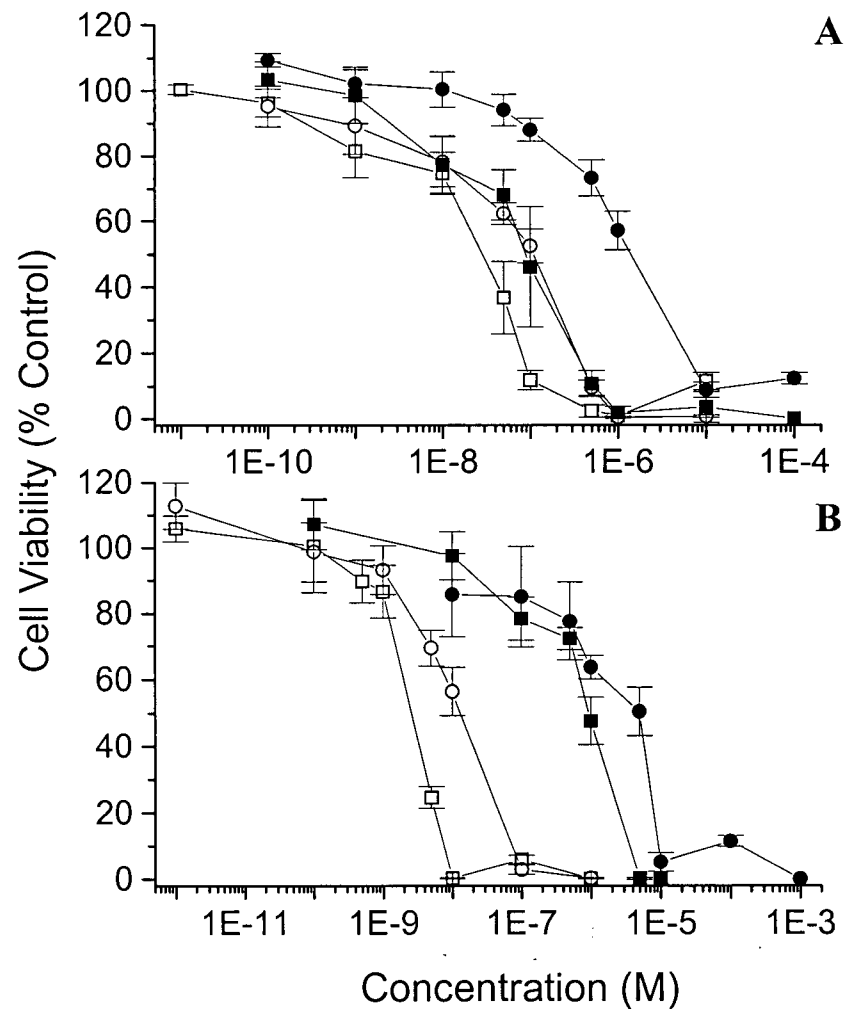


Table 6.3**Cytotoxicity of idarubicin and doxorubicin in wild type and resistant cell lines**

Cell Line	Drug	IC ₅₀ ^a		Log-Fold Resistance ^b
		WT	ADR/MDR	
P388	Idarubicin	2.5 nM	933.1 nM	373
P388	Doxorubicin	13.0 nM	5.0 µM	381
MDA435/LCC6	Idarubicin	27.9 nM	89.1 nM	3.2
MDA435/LCC6	Doxorubicin	115.4 nM	1.4 µM	12.3

^a IC₅₀ concentration of drug required to inhibit 50% of cell proliferation, determined in vitro with microculture tetrazolium (MTT) assay as described in Chapter 2.

^b Fold resistance calculated by dividing IC₅₀ of resistance cell line by IC₅₀ of wild type cell line.

treated with idarubicin than doxorubicin. No differences in log-fold resistance were observed in P388 cells (Table 6.3). The cytotoxicity studies demonstrated that both cell lines are sensitive to idarubicin and the P388 cells are approximately 10-fold more sensitive than the MDA435/LCC6 cells, consistent with the *in vivo* results shown in Figures 6.4 and 6.5. It should be noted that *in vitro* cytotoxicity data indicated that by increasing the exposure of P388 wild type cells to idarubicin from 24 to 72 hours, the concentration of idarubicin required to achieve a 50% cell kill (IC_{50}) decreased from 14.4 nM to 1.8 nM, suggesting improvements in therapeutic activity could be attributed to use of a formulation that extended the plasma circulation lifetime *in vivo*. *In vivo* efficacy studies were completed in mice bearing established MDA435/LCC6 MDR1 and P388 ADR tumors. Liposomal idarubicin treatment was not significantly more active than free idarubicin and neither drug formulation was judged to be significantly different than the saline treated controls (not shown). There was also no significant increase in survival times observed in mice bearing P388 ADR ascites tumors when treated with free or liposomal idarubicin as compared to controls (not shown). From these studies it was evident that the encapsulation of idarubicin did not provide additional therapeutic benefits in tumor models overexpressing p-glycoprotein.

6.4. Discussion

The intent of these studies was to assess the therapeutic potential of a liposomal formulation of the anti-cancer drug idarubicin. Prior to initiating studies in animals bearing sensitive and resistant tumors, changes in liposome composition and loading conditions were evaluated in an effort to achieve the highest idarubicin plasma concentrations over time. Importantly, previous research from this laboratory has already established that the hydrophobic

anthracycline idarubicin rapidly dissociates from liposomes that are prepared with cholesterol.

Although, the role of cholesterol in governing idarubicin release from liposomes and the development of cholesterol-free liposomes for drug delivery are of interest, the studies summarized in the report were conducted to establish whether simple changes in liposome composition and drug loading parameters would lead to further improvements in idarubicin retention in these cholesterol-free liposomes and whether the resulting formulation provided an additional therapeutic benefit when compared to free idarubicin. The results suggest that substantial (150-fold) increases in plasma idarubicin AUC can be achieved through simple changes in the liposome formulation and that the increase in AUC can result in improved therapeutic activity when using drug sensitive, as opposed to drug resistant, tumors.

Three observations in this study warrant discussion and further investigation. These will be discussed in turn and include: (i) development of cholesterol-free liposomes as drug carriers, (ii) why substantial increases in plasma AUC result in small, albeit, significant increases in therapeutic activity compared to free drug, and (iii) consideration of therapeutic strategies that incorporate liposomal idarubicin.

When considering strategies to optimize circulating drug levels through use of liposomal drug carriers, two factors appear to be crucial: (i) liposome circulation lifetime and (ii) drug release from those circulating liposomes. It is well established that improvements in liposome circulation can be achieved by incorporation of cholesterol and further increased by incorporation of PEG-modified phospholipids. More recently, the role of cholesterol in stabilizing liposomes containing PEG-modified lipids has been questioned. Results from these studies have clearly demonstrated that in terms of circulation lifetime, cholesterol is not required in liposomes that incorporate PEG-modified lipids. This observation has triggered a number of

separate studies investigating plasma protein binding to these liposomes optimized PEG-lipid levels in terms of grafting density and PEG chain length, use of alternative lipids that may achieve similar or improved properties in cholesterol-free liposomes which do not include PEG-modified lipids and potential therapeutic applications of these cholesterol-free liposomes. Regarding the latter, an excellent example includes the development of cholesterol-free DPPC liposomes as thermosensitive delivery systems which release contents following mild heating.

Another less well developed application concerns the use of cholesterol-free liposomes to achieve improvements in drug retention as illustrated in this thesis for idarubicin, a drug that is not well-retained in liposomes that contain cholesterol. Since all liposome compositions evaluated during the course of these investigations exhibited comparable plasma elimination rates, the reported highlights liposome-mediated increases in idarubicin circulation lifetime and plasma AUC. Thus, when reviewing the data it is important to recognize that observed increases in idarubicin levels in the plasma can be attributed to decreases in idarubicin release from the circulating liposomes.

It is reasonably well accepted that increases in membrane rigidity can increase drug retention in liposomes and this is exemplified by liposomal formulations utilizing SM or DSPC instead of EPC or DMPC as the bulk phospholipid component [16, 231, 232, 237]. In this context, changing the composition of the cholesterol-free liposomes by replacing DSPC (C18) with DAPC (C20) or DBPC (C22) did not significantly improve the circulation longevity of idarubicin and actually made it more difficult to manufacture and load the liposomes. It is acknowledged that changes in acyl chain composition did not improve the properties of liposomal idarubicin formulation, but increases in acyl chain length may prove to be of value for other drugs and it is important to recognize that these liposomes (without cholesterol) were

effectively stabilized (i.e., exhibited extended circulation lifetimes) by incorporation of PEG-conjugated lipids regardless of the bulk PC used.

It has been suggested and demonstrated that for certain drugs that surface-grafted PEG increases drug partitioning into the membrane interface, resulting in increased drug release [36, 181]. This effect of PEG has been attributed to the fact that PEG moieties are most frequently conjugated onto diacylphosphatidylethanolamine species and, when conjugated, the resulting PEG-modified lipid is anionic. It has been suggested that the anionic surface charge may facilitate binding and subsequently release of drugs, which are primarily in a cationic form when encapsulated using pH gradient (interior acidic) techniques. Studies completed here demonstrate that changes in PEG molecular weight did not significantly impact idarubicin plasma circulation lifetimes, however PEG grafting density had a significant impact. Incorporating 10 mol% PEG resulted in a liposomal idarubicin formulation that exhibited significantly faster drug elimination. Since the circulation lifetime of the DSPC liposome formulation containing 10 mol% PEG-lipid was not affected, changes in circulating drug levels were due to increased drug release from liposomes in the plasma compartment.

Consistent with this observation, reductions in PEG grafting density increased idarubicin circulation longevity and, in fact, for those formulations prepared with 300 mM citrate buffer incorporation of 2 mol% PEG provided a 2.1-fold increase in idarubicin plasma AUC_{0-4h} when compared to DSPC liposomes prepared with 5 mol% PEG-modified lipids and almost a 19-fold increase in AUC_{0-4h} when compared to DSPC / CH liposomes containing 5 mol% PEG-modified lipid (see Table 6.1). Again it should be noted that these liposomal formulations (prepared with 2 mol% PEG-modified lipid) exhibited circulation lifetimes that were not different from liposomes prepared with higher PEG grafting densities [42]. Further, in the studies reported

here the PEG-conjugated lipids were added prior to formation of the lipid film and thus were incorporated into both the outer and inner monolayers of the liposome. It can be suggested that further increases in idarubicin circulation levels could be achieved through use of liposomes where PEG-lipids are incorporated by an exchange process from micelles [33, 34].

Other than removal of cholesterol, the most significant increase in idarubicin plasma levels that were achieved following administration of the liposomal drug was due to use of liposome prepared in iso-osmotic (150 mM) pH 4.0 citrate buffer. It was recognized that reductions in citrate concentration would decrease entrapped buffering capacity and that drug loading induced decreases in the transmembrane pH gradient in these systems may cause an increase in idarubicin release and an associated decrease in plasma idarubicin levels. The studies summarized here indicate that a 2-fold decrease in entrapped buffer concentration could still engender efficient idarubicin loading (when the drug was added at a 0.2 drug-to-lipid ratio) and the transmembrane pH gradient following drug encapsulation was comparable to that observed in liposomes prepared in 300 mM pH 4.0 citrate buffer (see Figure 6.2).

When using idarubicin loaded liposomes (containing 2 mol% PEG-lipids) prepared using the 150 mM pH 4.0 citrate buffer, there was 2.7-fold increase in idarubicin AUC_{0-4h} when compared to the same liposomal formulation prepared in 300 mM pH 4.0 citrate. These results suggest that the cholesterol-free liposomes may be more sensitive to transmembrane osmotic gradients than cholesterol-containing formulations, which are not significantly affected by osmotic gradients in excess of 300 mOsm/kg [234]. It is not clear why cholesterol removal would increase osmotic fragility, but it is known that cholesterol-free membranes display grain boundaries (see cryo-TEM images in Figure 6.2) and these regions may increase the fragility of the these liposomes, particularly in the presence of plasma proteins.

For assessment of antitumor activity *in vitro* and *in vivo*, murine (P388 leukemia) and human (MDA435/LCC6) cell lines were used. The MDA435/LCC6 WT and MDR-1 transfected cell lines were both sensitive to idarubicin when added at nanomolar levels, however, the *in vivo* results indicate that the free drug and the liposomal drug were not significantly active when the maximum effective dose was defined as 1 mg/kg. Although there were substantial increases in idarubicin plasma concentrations at 4 hours post-injection when comparing plasma levels in mice dosed with the optimized liposomal formulation as opposed to free drug, there was < 6% of the injected dose 24 hours post-injection which may not be sufficient to provide adequate delivery of a drug to extravascular regions within the tumor. This argument makes the assumption that liposome-mediated drug delivery to tumors is critical for achieving improve therapy and this could be achieved by identification of other factors that may further increase idarubicin retention (blood levels) in the administered liposomes or possibly by using repeated doses.

Perhaps disappointing, but not unexpected given the lack of activity of the liposomal drug in the MDA435/LCC6 WT xenograft model, the liposomal formulation exhibited even less activity in the multidrug resistant variant of this cell line. Clinical interest in idarubicin is due, in part, because multidrug resistant cells appear to be less resistant to idarubicin when compared to other anthracycline family members. The MDA435/LCC6 multidrug resistant cell line, for example, was 12-fold less sensitive to doxorubicin when compared to activity in the WT cell line (see Table 6.3) but was only 3-fold less sensitive to idarubicin. As suggested previously, if a more effective dosing strategy can be identified using the MDA435/LCC6 WT tumor xenograft model, then it will be worth revisiting the activity of the liposomal formulation in a resistant cell line.

In vitro cytotoxicity studies with P388 cells indicated that these cells were 10-fold more sensitive to idarubicin than the MDA435/LCC6 cells and from these data alone one would predict improved activity in the P388 murine model. This was observed (see Figure 6.5) for both free drug and liposomal idarubicin-treated tumor bearing mice. Not unexpectedly, there was little activity observed in the P388 multidrug resistant variant which was 373-fold less sensitive to the drug than the WT cell line. Studies by others have indicated that idarubicin can achieve high intracellular concentrations in multidrug resistant cells overexpressing p-glycoprotein, attributed to its higher passive diffusion and lipophilicity [238, 239]. However, P388 ADR cells that have become resistant by exposure to doxorubicin exhibit multiple forms of resistance including overexpression of p-glycoprotein, alterations in topoisomerase II alpha and glutathione-S-transferase enzymes as well as increased onset DNA repair mechanisms [240, 241]. Idarubicin is an inhibitor of topoisomerase II activity and thus alterations in this enzyme (in multidrug resistant cell lines) would significantly reduce the drug's cytotoxic effect.

The antitumor effects observed in the P388 WT model are encouraging and suggest that further optimization of this formulation is warranted. As suggested in this discussion, optimization will be achieved by following two strategies. The first will involve further characterization of the cholesterol-free liposomes and factors that may lead to even further improvements in idarubicin retention. The second strategy will concern its use in treating models of cancer. Optimization of dosing schedules is an obvious parameter to evaluate; further improvements in therapeutic activity will more likely be achieved after consideration of idarubicin's specific use in the clinic. It will be important to focus future efficacy studies on drug-sensitive AML models and perhaps additional breast and ovarian tumor models given an emerging interest in the use of idarubicin in advanced breast and ovarian cancers. Perhaps even

more importantly, it needs to be recognized that drugs like idarubicin are not used in the clinic as single agents. Thus, the antitumor activity of liposomal formulation of idarubicin in combination with liposomal gemcitabine was evaluated in the following chapter.

CHAPTER 7

ACHIEVING SYNERGISTIC ANTITUMOR ACTIVITY IN VIVO: COMBINATION TREATMENT WITH LIPOSOMAL FORMULATIONS OF IDARUBIN AND GEMCITABINE

7.1. Introduction

Cancer is considered to be a manageable chronic disease. While local disease is amenable to surgery and radiation, systemic disease is most often treated with a “cocktail” of chemotherapeutic drugs. Combination regimens can significantly reduce the emergence of multidrug resistance (MDR) that can either be inherent or acquired, rendering the surviving malignant cells insensitive to further therapeutic interventions. Combination drug treatments can achieve a greater therapeutic response than obtained when individual drugs are administered as single agents. In view of these observations, the objectives for this study were two-fold: to design a liposomal formulation of gemcitabine and, in turn, to evaluate the antitumor activity of a combination treatment consisting of liposomal gemcitabine and liposomal idarubicin.

Gemcitabine is 2'2'-difluoro-deoxycytidine analogue, bears structural similarity to cytosine arabinoside [242]. The prodrug gemcitabine becomes activated following phosphorylation by deoxycytidine kinase. The di-phosphorylated derivative of gemcitabine, dFdCDP, has been shown to be a strong inhibitor of ribonucleotide reductase leading to a decrease of the deoxyribonucleotide pools for DNA synthesis [243, 244]. The tri-phosphorylated derivative, dFdCTP, is incorporated into DNA during the synthesis (S) phase of the cell cycle, inhibiting the action of DNA polymerases (α and ϵ) leading to a block in DNA synthesis [245]. Primer extension assays indicated that one nucleotide is added subsequent to the addition of gemcitabine into a newly synthesized DNA strand, rendering gemcitabine less susceptible to removal by the exonuclease function of DNA polymerases [245].

Gemcitabine has antitumor activity in both haematological and solid tumor models [246], including leukemia [247], lung (non small cell) [248], pancreatic [249], breast [250], ovarian [251] and bladder [252, 253]. In comparison to cytosine arabinoside, gemcitabine is more cytotoxic [254, 255], has longer retention times in tumor tissue [255], higher accumulation within leukemia cells [254], and a higher binding affinity for deoxycytidine kinase [255].

Gemcitabine is relatively well-tolerated; the dose limiting toxicity is myelosuppression and this is short lived with no need for haematopoietic growth factors. Other transient adverse side effects include fever, rash and elevated liver function tests including the aspartate aminotransferase (AST) and alanine aminotransferase (ALT) enzymes [256, 257]. Gemcitabine's non-overlapping toxicities with many other drug classes make it an ideal candidate for combination therapy, often without the need for dose reduction.

Gemcitabine is currently licensed as frontline therapy for the treatment of non small cell lung [248] and pancreatic cancers [249]. It is important to note that although gemcitabine has reasonable response rates when administered alone, higher response rates were observed when gemcitabine was combined with other classes of drugs. For example, in non small cell lung cancer activity a dose of 800 - 1250 mg/m² achieved overall response rates ranging from 20% (when used as a single agent) [258, 259] to 50% when used in combination with cisplatin, with median survival times of greater than 1 year [260]. More recently, the combination of doxorubicin and gemcitabine for the treatment of advanced breast cancer has shown favourable complete response rates in clinical trials [261].

It is anticipated that the encapsulation of gemcitabine within liposomes will (i) enhance cytotoxic activity by prolonged drug exposure of this cell cycle specific drug, (ii) protect the drug from degradation by extracellular deoxycytidine deaminase enzymes, and (iii) facilitate

improved delivery to sites of cancer growth which would, in turn, combine to improve the therapeutic effect. Similar effects have already been observed for cytosine arabinoside when encapsulated within a liposome [15], but the use of liposome for delivery of gemcitabine delivery has not been exploited previously.

Comparable to drug combinations used by oncologists, the combination of idarubicin and gemcitabine was selected on the basis of characteristics such as (i) non-overlapping toxicities, (ii) different mechanisms of elimination, (iii) distinct mechanisms for antitumor activity, suggesting that the combination of the two drugs may have additive or synergistic effects, and (iv) lack of cross resistance (gemcitabine was not sensitive to doxorubicin-resistant P388 cells [262]). Given the improved antitumor activity of liposomal idarubicin against P388 leukemia (summarized in Chapter 6) and the realization that further development of this liposomal drug may depend on its therapeutic potential when used in combination. Using in vitro and in vivo anti-cancer screening assays, the therapeutic activity of free and liposomal forms of gemcitabine and idarubicin and combinations thereof were evaluated in a murine leukemia model.

7.2. Hypothesis

Encapsulation of gemcitabine in lipid-based carriers will result in a formulation that exhibits an improved therapeutic index when used in combination with liposomal idarubicin that will, in turn, result in additive or supra-additive antitumor activity. It is anticipated that this effect will be attributed to non-overlapping toxicities and distinct mechanisms of antitumor activity exhibited by idarubicin and gemcitabine.

7.3. Results

7.3.1. P388 lymphocytic leukemia cytotoxicity of gemcitabine and idarubicin used alone, and in combination

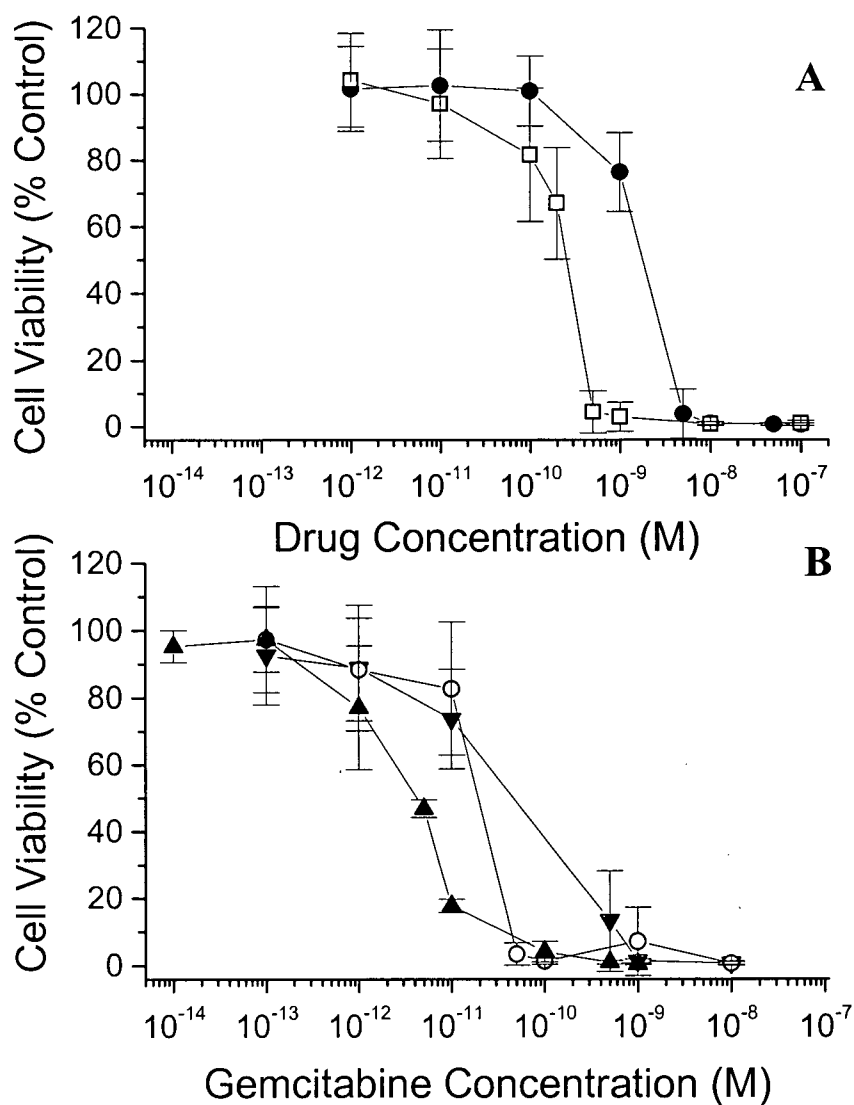
Cytotoxic activity was assessed by a standard MTT assay (as described in Chapter 2), and demonstrated that gemcitabine ($IC_{50} = 2.6 \times 10^{-10}$ M) was approximately 10-fold more cytotoxic than idarubicin ($IC_{50} = 1.8 \times 10^{-9}$ M) as shown in Figure 7.1A. The IC_{50} concentrations (concentration required to achieve 50% cell kill) of the individual drugs were used to define the fixed molar ratio for combination studies. Thus one molar ratio studied was set at 1:10 (GEM / IDA). In addition, 1:1 and 10:1 GEM / IDA fixed molar ratio drug combinations were also included to assess whether drug interactions were dependent on the drug molar ratio.

Cytotoxicity curves of the fixed ratio combinations of gemcitabine and idarubicin shown in Figure 7.1B demonstrated a shift to the left in the cytotoxicity curves when compared to use of gemcitabine as a single agent. This result suggested that a lower concentration of gemcitabine was required to achieve the similar cell kill. This effect is more apparent in Figure 7.2A, which summarizes the drug concentration required to achieve a 90% cell kill (fraction affected = 0.9) for the different treatments consisting of gemcitabine or idarubicin administered alone or in combination. For single treatment with either gemcitabine or idarubicin, the IC_{90} drug concentrations were 0.9 nM and 5.7 nM, respectively. When P388 cells were treated with GEM / IDA at a 1:10 fixed molar ratio, less of each drug was required to achieve 90% cell kill when compared to individual treatments. The fold reduction in drug concentration, also referred to as the dose reduction index (DRI), was 14 and 8.5 for gemcitabine and idarubicin, respectively. There was a moderate decreased in drug concentrations required to achieve a

Figure 7.1

Cytotoxic activity of gemcitabine and idarubicin and combinations thereof on P388 lymphocytic leukemia cells

Cells were treated with varying concentrations of (A) idarubicin (●) and gemcitabine (□) and (B) combinations thereof. Fixed molar drug ratios were chosen based on the IC_{50} of each individual treatment; and consist of GEM / IDA 1:10 molar ratio; 1:1 molar ratio, (○); 10:1 molar ratio; (▼). Cytotoxicity was evaluated by a standard MTT assay as described in Chapter 2. Each value represents the mean \pm S.D. for at least three independent experiments performed in triplicate.



fraction effect level of 0.9, when a 1:1 GEM / IDA fixed molar ratio, the DRI at this drug ratio was 1.8 and 11.8 for gemcitabine and idarubicin, respectively. There was a 180-fold reduction in idarubicin concentration when administered in 10:1 GEM / IDA fixed ratio as compared to single administration.

Dose titrations of gemcitabine and idarubicin administered alone, and in combinations added at fixed ratios were analyzed by the median effect equation by Chou and Talalay [109] to determine the combination index (CI) as a function of fraction affected (represents the fraction of non-viable cells), as shown in Figure 7.2B. A CI value of < 1 represents synergy while a CI value of 1 or > 1 indicated additive effects and antagonism, respectively. A 1:10 (GEM / IDA) fixed molar ratio, as well as the other ratios (not shown), demonstrated moderate to very strong synergism, over a broad range of effective doses. This result is consistent with other reports suggesting that gemcitabine interacts synergistically with anthracyclines [263].

7.3.2. Liposome encapsulation and plasma elimination of gemcitabine

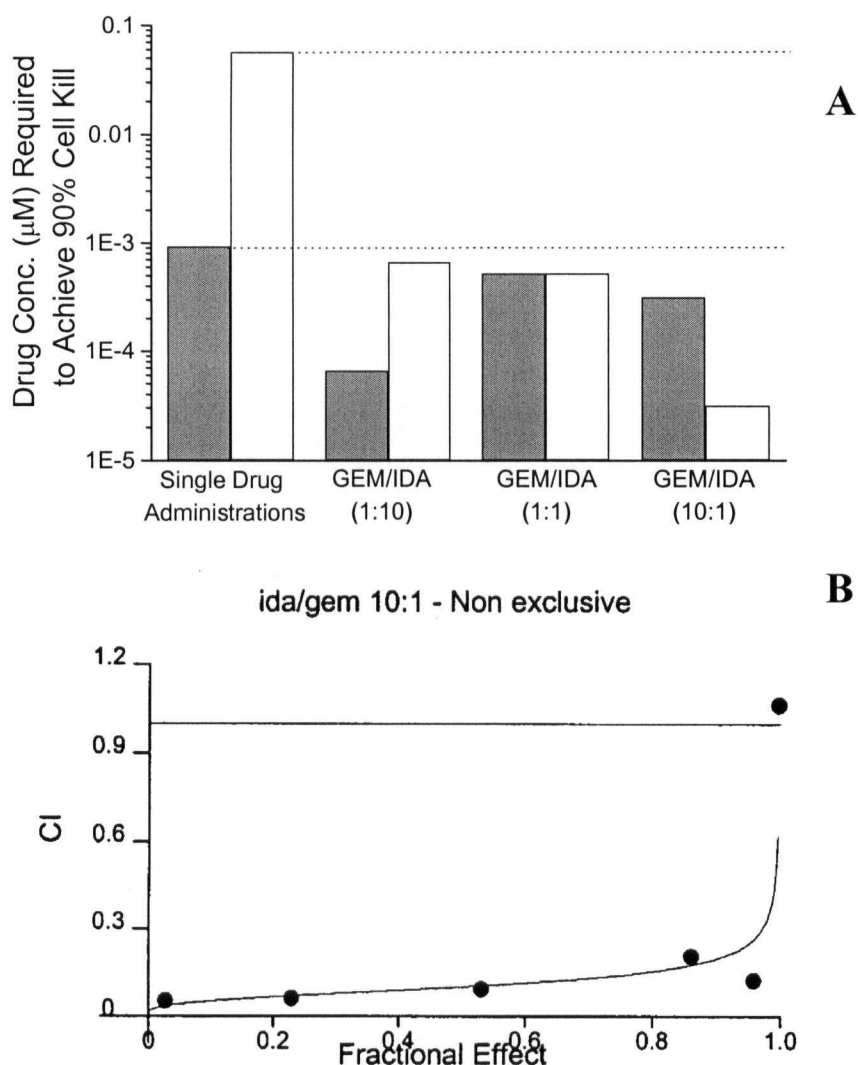
Previous studies indicated that liposomal idarubicin improved the median survival of mice inoculated i.p. with P388 leukemia cells as compared to controls and free idarubicin (refer to Chapter 6). To this point, gemcitabine's sensitivity to P388 leukemia has been demonstrated in vitro. The next objective was to encapsulate gemcitabine in a lipid-based carrier to assess whether the drug's therapeutic activity could be improved in vivo when compared to the free drug administered at levels that engender comparable levels of toxicity.

Gemcitabine was passively loaded into three different liposomal formulations; DSPC / DSPE-PEG₂₀₀₀ (95:5 mole ratio), DSPC / CH (55:45 mole ratio) and DSPC / CH / PEG (50:45:5 mole ratio). In brief, lipid films were rehydrated with 167 mM gemcitabine (dissolved in

Figure 7.2

Dose reduction index analysis at an IC_{90} of idarubicin (IDA) and gemcitabine (GEM) used alone or in combination and the combination index of GEM/IDA (1:10) fixed molar ratio

(A) The drug concentrations required to achieve 90% cell kill (IC_{90} , fraction affected = 0.9) of gemcitabine (grey bars) and idarubicin (white bars) and 1:10, 1:1 and 10:1 GEM/IDA fixed molar ratios. Data was plotted as a function of effect by the median effect equation by Chou and Talalay. The cytotoxicity data obtained from dose titrations of the different drug treatments was evaluated by a standard MTT assay (see Chapter 2). (B) Cytotoxicity curves of IDA / GEM combinations were evaluated by median effect equation by Chou and Talalay and CI index (CI) was plotted as a function fractional affected for 1:10 GEM/IDA fixed molar ratio. A CI value of < 1 , is synergistic, $= 1$ is additive and > 1 is antagonistic. Strong synergism is indicated by CI values of 0.1 – 0.3 and values of 0.3 – 0.7 are considered to indicate strong and moderate synergism, respectively. All combinations of idarubicin and gemcitabine evaluated were between moderate to strong synergism.



HEPES buffered saline, pH 7.4) at 40°C for 60 min. The samples were extruded through 2 stacked 100 nm polycarbonate filters to generate unilamellar liposomes. Two parameters were measured including liposome size by the quasielastic light scattering (QELS) technique and encapsulation efficiency following separation of free and encapsulated gemcitabine by size exclusion chromatography. For both cholesterol-containing formulations, the mean liposome diameter ranged between 100 and 130 nm. The mean liposome diameter (57.6 nm) and encapsulation efficiency (1.8%) were significantly lower for the preparations consisting of DSPC / DSPE-PEG₂₀₀₀ (95:5 mole ratio). These data have been summarized in Table 7.1. Under the conditions used here, final drug-to-lipid mole ratios of 0.1 were obtained for the cholesterol-containing formulations, however, the DSPC / CH / PEG (50:45:5 mole ratio) liposome formulations consistently exhibited higher levels of entrapment (~ 10% improvement). Since the cholesterol-free liposomal formation was not effective at encapsulating gemcitabine, this formulation was not studied further.

A second criteria for choosing a liposome formulation was based on liposome-mediated increases in gemcitabine blood residence time. Free and liposomal gemcitabine formulations were administered to female Balb/c mice at a dose of 16.5 μ mole gemcitabine/kg (5 mg/kg) and 165 μ mole total lipid/kg. At various time points post-drug administration, blood samples were taken to measure gemcitabine and liposomal lipid plasma concentrations, and these data have been summarized in Figure 7.3. Gemcitabine plasma concentrations were modeled using pharmacokinetic software, indicating a close fit with an i.v. bolus one compartment model. The pharmacokinetic parameters (Table 7.2) demonstrated that DSPC / CH / PEG (50:45:5 mole ratio) liposomes increased plasma circulation longevity of gemcitabine more than free or liposomal DSPC / CH (55:45 mole ratio) gemcitabine. Both mean plasma area-under-the-curve

Table 7.1

Effect of lipid composition on the drug-to-lipid mole ratio and encapsulation efficiency of passively loaded gemcitabine

Liposome Composition (mole ratio)	Lipid Conc. (mM)	Drug Conc. (mM)	Liposomes size (nm)^a	Drug-to- Lipid Ratio^b	Encapsulation Efficiency (%)^c
DSPC/PEG (95:5)	100	167	57.6 (2.8)	0.030	1.8
DSPC/CH (55:45)	100	167	107.0 (9.4)	0.096	5.7
DSPC/CH/PEG (50:45:5)	100	167	101.1 (5.7)	0.114	6.8

^a Liposome size was determined by quasielastic light scattering (QELS) technique, S.D. for three experiments are indicated in parentheses. The standard deviations for a given liposome population was between 25 – 32 nm.

^b Drug to lipid molar ratio (mol/mol) following separation of free and encapsulated gemcitabine on mini Sephadex G-50 columns. Gemcitabine was assayed by lysing the liposomes in OGP and measuring absorbance at 268 nm (see Chapter 2) and liposomal lipid was measured through use of ³[H]-CHE label.

^c Encapsulation efficiency was determined as the percentage of drug-to-lipid molar ratio after removal divided by initial drug-to-lipid mole ratio

Figure 7.3

Plasma elimination of free and liposomal gemcitabine in Balb/c mice

Free (■) and liposomal gemcitabine formulations radiolabeled with tracer quantities of ^3H -gemcitabine and / or ^{14}C -cholesteryl hexadecyl ether were administered intravenously via the dorsal tail vein of female Balb/c mice. The total lipid dose administered for the liposomal formulations DSPC / CH (55:45 mole ratio, ▲) and DSPC / CH / DSPE-PEG₂₀₀₀ (55:45:5 mole ratio, ●) was 165 $\mu\text{mole/kg}$. The gemcitabine dose administered was 16.5 $\mu\text{mole/kg}$. Blood was collected at 1, 2, 4 and 24 hours by cardiac puncture. An aliquot of plasma was used to determine liposomal lipid and gemcitabine content as described in Chapter 2. Each data point represents the mean \pm S.D. for 4 mice.

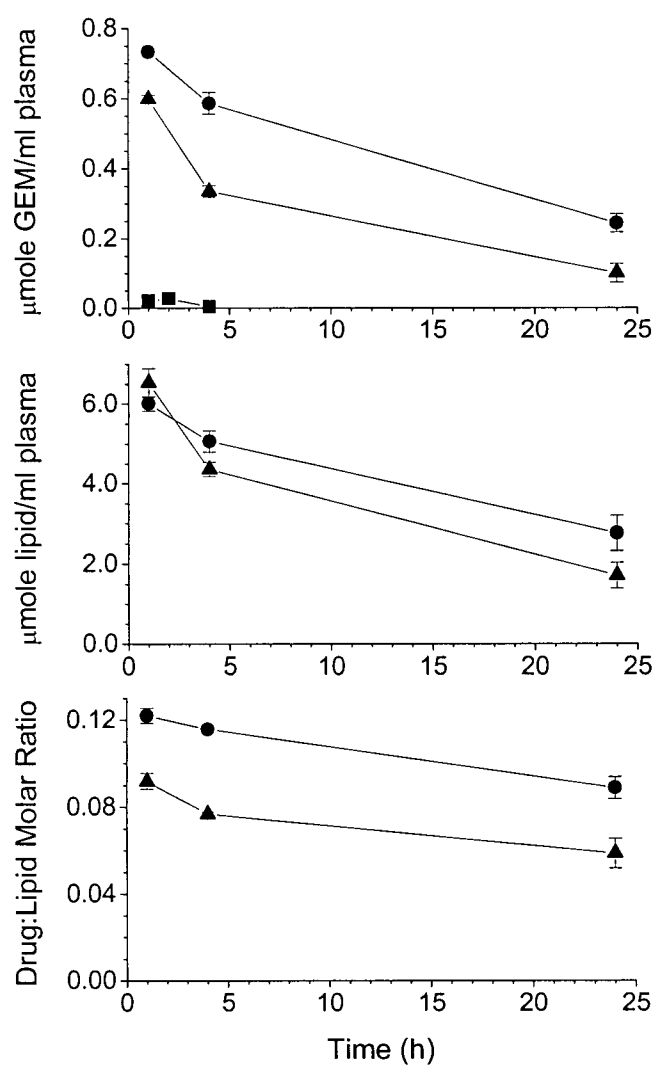


Table 7.2
Summary of pharmacokinetic parameters of free and liposomal gemcitabine

Sample	AUC _{0-t} ^a (μmole·h·ml ⁻¹)	T _{1/2} (h)	Cl (ml·h ⁻¹)	AUMC (μmole·h ² ·ml ⁻¹)	MRT _{last} (h)
GEM	0.1 ^b	2.1	6.12	0.3	3.1
DSPC/CH (50:45:5)	4.3 ^c	4.4	0.16	27.1	6.3
DSPC/CH/PEG (50:45:5)	15.4 ^c	14.3	0.05	319.0	20.7

^a AUC was calculated using the trapezoidal rule (0-Tlast)

^b Tlast was 4 hours

^c Tlast was 24 hours

^d All pharmacokinetic elimination profiles were fit to iv-bolus one compartment model using WinNonlin Version 1.5 pharmacokinetic software. R², goodness of fit statistic for one compartment model was 0.756, 0.987 and 0.994 for free gemcitabine and liposomal gemcitabine formulations DSPC / CH and DSPC / CH / PEG, respectively.

(AUC) and plasma half-life ($T_{1/2}$) increased 135-fold ($15.4 \mu\text{mole h ml}^{-1}$) and 8-fold (14.3 h), respectively, when encapsulated in DSPC / CH / PEG (50:45:5 mole ratio) as compared to free gemcitabine.

7.3.3. Antitumor activity of free and liposomal gemcitabine in P388 murine leukemia

There are numerous benefits to encapsulation of gemcitabine in lipid carriers that may not be reflected in the pharmacokinetic parameters such as protection from degradation by cytidine deaminase, prolongation of circulation longevity in order to increase exposure to malignant cells, sustained drug release, and accumulation within the tumor site. To investigate the effect of encapsulation of gemcitabine (DSPC / CH / PEG; 55:45:5 mole ratio) on therapeutic activity, efficacy experiments were performed in the P388 murine leukemia model. Initial dose-range finding studies performed in non-tumor bearing BDF-1 mice indicated that the maximum tolerable dose was 500 mg/kg and 5 mg/kg of free and liposomal gemcitabine, respectively. These data indicated that liposome encapsulation mediated a 100-fold dose reduction of gemcitabine.

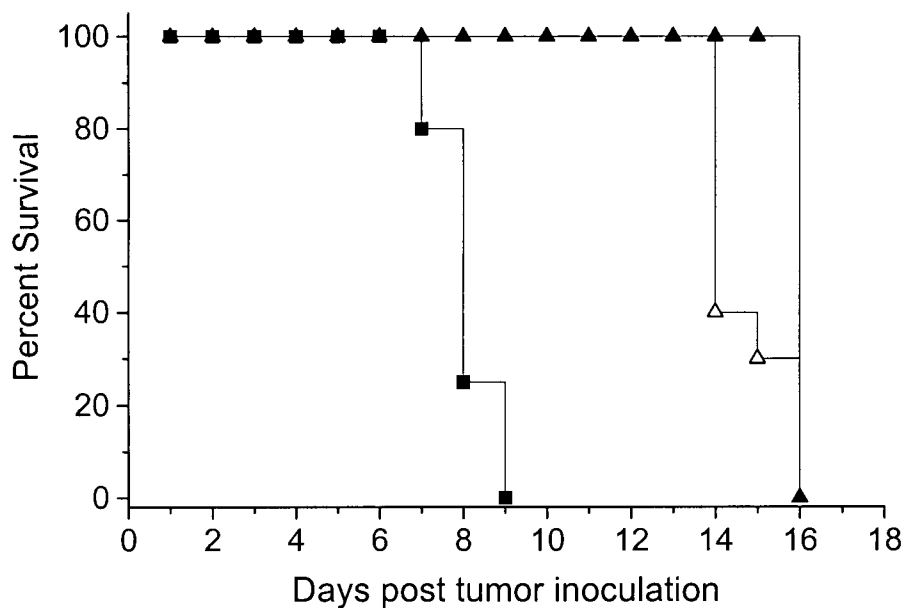
At the maximum tolerable dose, 100% increase in life span (median survival time; 16 days) was obtained in mice receiving a dose of 5 mg/kg liposomal gemcitabine shown in Figure 7.4. A 75 % ILS (median survival time; 14 days) was obtained when mice were treated with free gemcitabine at its maximum tolerated dose (500 mg/kg). At the MTD, the liposomal gemcitabine (5 mg/kg) had a significantly longer median survival time than free gemcitabine (500 mg/kg) ($p = 0.0015$). In summary, a longer median survival time was observed for liposomal gemcitabine at a dose that was approximately 100-fold less than free drug, albeit at a dose exhibiting equivalent toxicity.

In view of these results, assessment of the therapeutic activity free and liposomal

Figure 7.4

P388 antitumor activity of a single i.v. bolus injection of free and liposomal gemcitabine administered at the maximum tolerated dose (MTD)

Survival curves were derived for control (saline, ■, n = 20), 500 mg/kg free gemcitabine (△, n = 10) and 5 mg/kg liposomal gemcitabine (▲, n = 6) groups administered to BDF-1 female mice inoculated i.p. with 10^6 P388 cells and treated 24 hours later.



gemcitabine in combination with liposomal idarubicin was warranted. In vitro studies demonstrated that combinations of gemcitabine and idarubicin engendered synergistic P388 cytotoxicity when added at fixed ratios. However, it is not clear how best to use this information to characterize drug combinations in vivo. It has been argued that it will be important to define and maintain certain fixed drug ratios following administration of drug combinations in order to ensure that the synergistic potential of the drugs will be captured. It is anticipated that drug carriers will play a crucial role in maintaining fixed ratios following i.v. administration. However in the studies reported here, a general approach to set the initial drug-to-drug ratio was used. Mice were treated with the combined drugs based on a ratio defined by 66% of the individual drug's maximum tolerated dose (MTD). In this regard, dose combinations of free gemcitabine and free idarubicin were 334 mg/kg (1115 μ mole/kg) and 2 mg/kg (3.8 μ mole/kg), respectively, and this fixed drug molar ratio was maintained all doses administered. For liposomal formulations, 3.4 mg/kg (11.4 μ mole/kg) and 2 mg/kg (3.8 mg/kg) of gemcitabine and idarubicin were administered, respectively, and dose titrations maintained the same drug ratio. The results of these studies have been summarized in Table 7.3.

The survival of mice administered combinations of idarubicin / gemcitabine (IDA / GEM) and liposomal idarubicin / liposomal gemcitabine (LIDA / LGEM) are illustrated by the data shown in Figure 7.5. An increase in median survival times was observed for mice administered the liposomal drug combination, 30 days (281 % ILS), as compared to the free drug combination, 18 days (125 % ILS). Drug-induced weight loss was less than 5% in both of these treatments. The data shown in Table 7.3 indicates that free gemcitabine combined with LIDA (2 mg/kg) resulted in improved therapeutic effects, but effect was 50% less of that noted when compared with the combination of liposomal drugs. Similar conclusions can be made

Table 7.3

**Antitumor activity of combinations of free and liposomal idarubicin / gemcitabine
in BDF-1 mice bearing P388 ascitic tumors**

Group	Drug Dose (mg/kg)		%Weight Change, day 5	MST ^a (days)	%ILS ^b	Cell Kill ^c (LOG ₁₀)	Survivors
	IDA	GEM					
Control	-	-	11.8	8.0	-	N/A	0/20
IDA	0.5		13.6	9	13	0.6	0/12
	1		2.1	12	50	2.3	0/12
	2		-1.4	17	113	5.1	1/12
LIDA	0.5		2.7	11	38	1.7	0/14
	1		2.4	14.5	81	3.7	0/14
	2		-1.9	20.5	156	≥ 6	2/14
GEM		100	0.4	13	63	2.9	0/6
		200	3.0	14.5	81	3.7	0/6
		300	2.3	14.5	81	3.7	0/6
		400	1.8	15	88	4.0	0/6
		500	0.0	14	75	3.4	0/10
LGEM		1.0	-4.2	13	63	2.9	0/6
		2.5	3.3	14	75	3.4	0/6
		5.0	1.9	16	100	4.6	0/6
IDA/GEM	0.5	83.5	0.2	14	75	3.4	0/6
	1.0	167	-0.4	17	113	5.1	0/6
	2.0	334	-6.2	18	125	≥ 6	0/6
LIDA/GEM	0.5	83.5	-2.4	14	75	3.4	0/6
	1.0	167	-2.8	16.5	106	4.9	0/6
	2.0	334	-1.2	20.5	156	≥ 6	1/6
IDA/LGEM	0.5	0.85	1.8	14	75	3.4	0/6
	1.0	1.7	1.4	18	125	4.9	0/6
	2.0	3.4	0.5	19.5	144	≥ 6	1/6
LIDA/LGEM	0.5	0.85	1.7	16.5	106	4.9	0/6
	1.0	1.7	3.9	19	138	≥ 6	0/6
	2.0	3.4	1.8	30	281	≥ 6	1/6

^a MST, median survival time

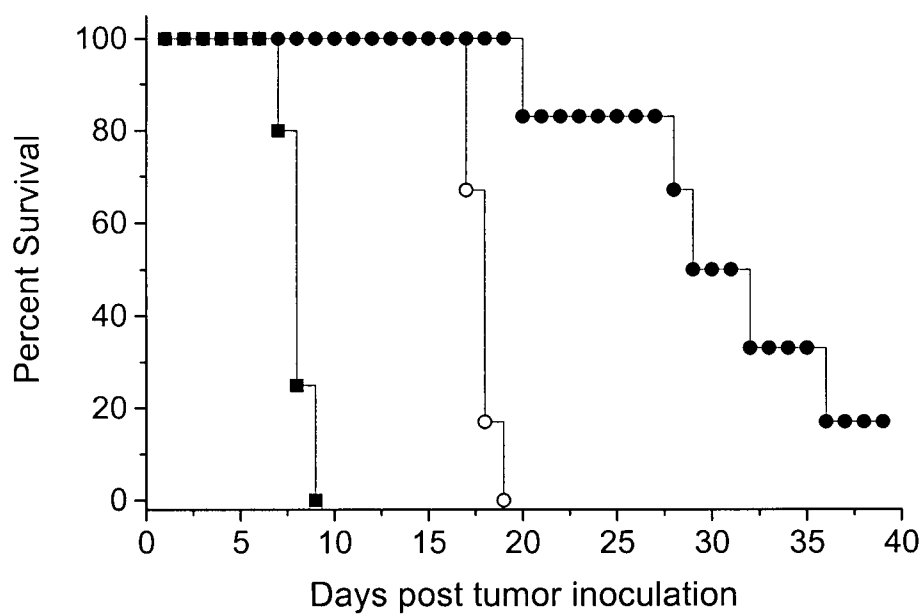
^b Percent increase in lifespan (ILS) values were determined from median survival times comparing treated and saline control groups

^c Log cell kill, represents the number of cells killed from treatment based on median survival. The correlation between median survival and number of inoculated cells were determined in a separate study. For efficacy studies mice were inoculated with 10⁶ P388 cells, treatment commenced 24 hours following inoculation. Thus a log cell kill ~ 4 indicates 10² cells remaining.

Figure 7.5

Antitumor activity of free and liposomal idarubicin and gemcitabine combination treatment

Survival curves were derived for control (saline, ■, n = 20), GEM / IDA (334/2 mg/kg, ○, n = 6) and liposomal GEM / liposomal IDA (3.4/2 mg/kg, ●, n = 6) administered to BDF-1 female mice inoculated i.p. with 10^6 P388 cells and treated 24 hours later.



when comparing the % ILS values observed at the highest doses of free IDA / GEM combinations (% ILS = 125), liposomal idarubicin / free gemcitabine (% ILS = 156) and free idarubicin / liposomal gemcitabine (% ILS = 144).

A study was also completed in order to gain a more quantitative understanding of the drug effects. In this study mice were infected with varying numbers of P388 cells and median survival time was recorded. The results indicated that mice injected with 10^6 , 10^5 , 10^4 , 10^3 , 10^2 and 10 cells had median survival times of 8, 10.5, 11, 12, 15 and 17.5 days. By correlating median survival times from mice administered treatments, the log cell kill may be calculated (Table 7.3). This analysis was not of substantial value except that it demonstrated that treatment groups that had 1 or more long term survivors required a log cell kill ≥ 6 .

7.4. Discussion

The selection of drug combination regimens for the treatment of cancer has, for the most part, been derived empirically. In recent years, there has been a concerted effort to identify therapeutically beneficial drug combinations within the laboratory setting, well before the clinical trials of the approved agents have been completed. Still many of these studies are based on cell culture analyses. Although in vitro studies are extremely valuable, application of in vivo models of cancer may be better predictors of therapeutically successful combinations. The studies performed within this chapter demonstrated two significant achievements that warrant further discussion and include the encapsulation of gemcitabine in liposomes and the combination of liposomal gemcitabine with liposomal idarubicin in mediating synergistic antitumor activity.

The pharmacokinetic analysis comparing liposomal (DSPC / CH / DSPE-PEG₂₀₀₀;

50:45:5 mole ratio) and free gemcitabine indicated that significant increases in the mean plasma area-under-the curve (AUC), and plasma half-life ($T_{1/2}$), area-under-the-moment curve (AUMC) and mean residence time (MRT), while total plasma clearance (Cl) was reduced. Both mean plasma AUC_{0-24h} and plasma half-life increased 154-fold and 6.8-fold, respectively upon encapsulation in liposomes. Antitumor activity of liposomal gemcitabine in P388 murine model demonstrated marginal improvements in median survival time at a 100-fold lower dose (compared to free drug). Similarly, Moog *et al.* encapsulated (33% entrapped, 67% free) gemcitabine in vesicular phospholipid gels (VPG) and reported a dose reduction (40 to 60-fold) as compared to free drug [264]. Dose reductions may often be attributed to increased toxicity, however, the results indicate that liposomal gemcitabine, administered at a 100-fold lower dose than free gemcitabine, did not significantly increase weight loss or compromise therapeutic activity, and resulted in an increase in median survival time as compared to free drug. Reasons for such a significant increase in dose sensitivity may be attributed to the protection of the encapsulated agent from degradation by cytidine deaminase or may be due to alterations in biodistribution. The promising antitumor activity demonstrated by liposomal gemcitabine warranted the further evaluation of combinations with liposomal idarubicin.

The studies summarized here provide at least one approach to evaluate drug combinations in vivo. The approach chosen resembled the process used by clinicians, in which drug combination regimens are chosen based on non-overlapping toxicities, complementary mechanisms of action, and proven efficacy. The initial validation of drug sensitivity was demonstrated by a standard MTT cytotoxicity study. Following validation, drug interactions were assessed using fixed drug ratios, as required by the Chou and Talalay median effect equation [109]. Dose titrations of single agents and fixed drug ratios were analyzed and the

results demonstrated that the simultaneous administration of idarubicin and gemcitabine exhibited synergistic interactions as judged by measured combination index (CI) values of less than 1 for a broad range of effective doses and over a broad range of fixed drug ratios.

Dose range finding studies were performed in mice lacking tumors, to identify the maximum tolerable dose in which 66% of the MTD was chosen as the treatment dose and was combined with dose titrations. At the highest doses, the ratio was 2 mg/kg (3.8 μ mole/kg) idarubicin and 334 mg/kg (1115 μ mole/kg) gemcitabine or 2 mg/kg (3.8 μ mole/kg) liposomal idarubicin and 3.4 mg/kg (6.4 μ mole/kg) liposomal gemcitabine. Thus the fixed dose ratio of GEM / IDA was 167:1 wt/wt ratio and 298:1 mol/mol ratio. In turn, the fixed dose ratio of LGEM / LIDA was 1.7:1 wt/wt ratio and 3.0:1 mol/mol ratio.

It is important to consider how a drug ratio is defined in the context of the experiments described here. Of course, a focus on the drug ratio is predicted by a belief that drug interactions which lead to optimal therapeutic results are dependent on the ratio of the drugs used, as well as the effect of levels measured. This belief is consistent with the methods developed of Chou and Talalay, which stress the importance of both effect level and drug ratio when using two or more drugs in combination. The importance of those factors is emphasized by a number of publications that provide data demonstrating that the observed degree of synergism (or antagonism) is dependent on the drug-to-drug ratio [265]. This is less apparent in studies summarized here, where synergistic interactions were observed over a broad range of drug ratios.

Using a method based on 66% of the MTD, the ratio of free-to-liposomal drug would be different than the ratio of free-to-free drug or liposomal-to-liposomal drug. It can be argued that the most relevant ratio to consider in the development of drug combinations is that which is

delivered to the tumor cells, and this was not measured in the study. It can also be argued, however, that drug delivery vehicles, such as liposomes, can provide an ideal way in which to control the delivery of two or more agents. Due to the inability to control the pharmacokinetics and biodistribution of two drugs administered in free form, it can be anticipated that the extent of drug delivery to the tumor cell will be dependent on plasma drug levels, distribution, metabolism and excretion of each individual agent. This, in turn, would suggest that following administration of free drugs in combination, all possible ratios are achievable.

It has been proposed that one way to better control the drug ratio would be through use of liposomal formulations of the two drugs, as described in this chapter. In this case, the liposomal carrier, the rate of drug release from the carrier, as well as the rate and extent of a liposome accumulation in the site of disease development will dictate the pharmacokinetics. In this regard, it's worth noting that the two liposomal formulations used here exhibit comparable lipid plasma elimination behaviour (~ 20% of the injected lipid dose remained 24 hours after administration), however, the rate of GEM release from DSPC / CH / PEG formulation was slower (~ 50% of the injected drug dose was released over 24 hours) than observed for the optimized liposomal idarubicin formulation developed in this thesis (where > 95% of the injected drug dose was released over 24 hours). Investigating alternative loading methodologies, such as metal complexation [266], may allow the co-encapsulation of gemcitabine and idarubicin in a single liposome formulation.

Based on these studies, it was demonstrated that gemcitabine may be useful as a treatment for leukemia, but the observations need to be expanded to a number of other models. Further, given the considerable interest to optimize multiple dosing schedules of idarubicin and

gemcitabine combination therapy for treatment of solid tumors including lung, pancreatic, breast and ovarian cancers, it may be interesting to consider the combination of the liposomal gemcitabine and liposomal idarubicin, formulations that appear to provide significantly increased therapeutic activity and, perhaps, better control over the biodistribution of the combined drugs.

CHAPTER 8

SUMMARIZING DISCUSSION

The work presented in this thesis tested the hypothesis that liposomes prepared without cholesterol could be of value as intravenous drug carriers. These formulations proved to be biologically stable upon the incorporation of PEG-lipids and, in turn, these formulations improved the retention of idarubicin, a hydrophobic anthracycline antibiotic, over that found for a cholesterol-containing formulation. Several aspects of cholesterol-free liposomes and liposomal idarubicin were discerned throughout the course of the thesis and are reviewed here, with a particular focus on future directions.

The major findings of the thesis are addressed below. It was determined that cholesterol-free liposomes composed of DSPC and ≤ 5 mol% PEG-lipids could form large unilamellar liposomes with narrow size distributions. The liposomal lipid had long circulation lifetimes that were strongly dependent on the presence of PEG-lipids in the formulation. It was established that PEG-lipids played a role in preventing liposome - liposome aggregation and did not reduce plasma protein binding. Idarubicin was encapsulated in DSPC / DSPE-PEG₂₀₀₀ liposomes by the remote loading procedure, and studies indicated that idarubicin was present both as a precipitate in the aqueous core of the liposome and partitioned in the lipid bilayer. Idarubicin was encapsulated in liposomes at incubation temperatures below the phase transition, but was quickly released from the liposomes at temperatures above the phase transition temperature. Less hydrophobic drugs, such as doxorubicin, could not be loaded at temperatures below the phase transition temperature of the liposome and thus ethanol was added as a permeability enhancer to increase drug loading rates. By this method, 100% encapsulation efficiency was achieved within a 1 hour incubation time.

Idarubicin was better retained in cholesterol-free liposomes than in cholesterol-containing liposomes as judged by pharmacokinetic analyses. The plasma elimination half-life was 1.44 h. The liposome formulation was optimized by altering lipid composition and drug loading parameters. In the optimized lipid formulation, PEG content was reduced to 2 mol% and the internal citrate concentration was reduced to 150 mM, a concentration that was iso-osmotic with the external buffer. The latter observation demonstrated that cholesterol-free liposomes are osmotically sensitive. The plasma elimination half-life of idarubicin in the optimized formulation, DSPC / DSPE-PEG₂₀₀₀ (98:2 mole ratio) increased 4-fold (5.9 h). Efficacy studies in i.p. P388 murine leukemia demonstrated that extending the blood circulation lifetime of idarubicin by encapsulation within liposomes facilitated an increase in therapeutic activity as compared to free drug administered at equivalent doses. Further improvements in therapeutic activity were observed when liposomal idarubicin was combined with liposomal gemcitabine. Both drugs have not been previously formulated in a liposome. A supra-additive therapeutic effect was observed when liposomal formulations of idarubicin and gemcitabine were combined, this result was not obtained when free idarubicin and free gemcitabine were used in combination.

These results raise a number of important issues concerning our current understanding of liposomal drug delivery systems, the use of PEG as a stabilizing lipid, as well as the identification of new areas of research that may result in improved anti-cancer therapeutics that would be enabled by the use of a liposomes.

The first objective of the thesis was to develop a liposomal preparation, without cholesterol, consisting of 1,2-distearoyl-*sn*-phosphatidylcholine (DSPC) and PEG-conjugated lipids. It is known that the addition of cholesterol to a lipid matrix of gel phase lipids

(phospholipids with \geq C18 fatty acid chains) increases the permeability of lipid membranes below the T_c of the bulk phospholipids species used, and thus it is predicted that cholesterol-free formulations would retain encapsulated contents in vivo. From studies performed in Chapter 3 and 4, the biological stability of cholesterol-free liposomes was shown to be dependent on the presence of PEG-lipids, but it is worth asking the question as to what role PEG played with an eye to the selection of other materials that may also engender stability of these formulations. PEG's role in surface stabilization and prevention of surface-surface interactions, including prevention of plasma protein adsorption at grain boundaries and aggregation of liposomes, is essential for cholesterol-free liposomes. However, it is important to recognize that PEG-lipids had a significant impact on liposome structure; large unilamellar vesicles (LUVs) were formed when 0.5 to 5 mol% PEG-lipids were incorporated into a lipid matrix consisting of DSPC. At concentrations > 10 mol% PEG-lipids, mixed micelles and bilayer disks were formed as evidenced by cryo-transmission electron microscopy studies (Chapter 4). Although these structures were not investigated further, it is possible that mixed micelles may serve as drug delivery vehicles for hydrophobic or amphipathic molecules. It could be argued that the detergent-like effects of PEG-lipids may be due to the large area occupied by the hydrophilic head group compared to the area occupied by the acyl chains. It would be interesting to know whether increases in acyl chain area would allow increased incorporation levels without micelle or disk formation.

In Chapter 4, the role of PEG-lipids in liposomes was revisited in cholesterol-free liposomes. To date the rôle of PEG-lipids has not been fully elucidated. Although many studies cite PEG's role in surface stabilization by inhibiting plasma protein adsorption, growing evidence has indicated that PEG may not reduce plasma protein adsorption. There is conclusive

evidence that PEG engrafted on solid surfaces (such as artificial organs, prosthetic limbs, and contact lenses), reduces protein binding, however, the kinetic behaviour of PEG grafted in liquid-crystalline and gel phase lipids may be different. One of the main problems encountered when trying to identify liposome-associated plasma proteins is related to the separation technique. In the studies performed within the thesis, size exclusion chromatography was used, which subjected the liposomes to non-equilibrium conditions and thus it is believed that only tightly adsorbed proteins remain bound following separation. Clearly novel equilibrium techniques need to be employed to investigate both tightly and loosely bound plasma proteins to the liposome surface. In addition, novel methods to clearly identify proteins, such as MALDI-TOF spectroscopy and protein microarrays, should be utilized. It is still very important to develop improved methods for characterizing liposome-associated plasma proteins. Two specific roles of this methodology would include (i) assessments of inter-species differences in plasma protein binding and (ii) identification of proteins that serve to enhance the biological stability of liposomes. The former would help to clarify why observations made in some animals, such as rats, are not seen in others. The latter may help resolve the role of putative dysopsonins. Regardless of the broader implications of protein-liposome interactions, results presented here clearly add to the growing body of literature which argues that the surface-grafted PEGs do not prevent protein binding to the extent previously thought.

The studies within the thesis clearly demonstrated that idarubicin was better retained in cholesterol-free liposomes compared to cholesterol-containing liposomes. The reasons for the difference in retention for the various lipid compositions are not clearly understood. It was evident that upon encapsulation of idarubicin by remote loading, a precipitate was formed (Chapter 3) and yet, a significant proportion of the drug had also partitioned into the lipid

bilayer (Chapter 5) of cholesterol-free liposomes. The latter parameter may also explain why a significant proportion of idarubicin was released when the incubation temperature was 65°C, a temperature higher than the phase transition temperature of cholesterol-free liposomes. Clearly the effect of drug release on drug distribution within the liposome, including drug partitioned within the lipid bilayer and precipitated within the aqueous core, needs further examination. It would be interesting to determine whether drug partitioning into the membrane affects drug release attributes in a manner that would increase or decrease permeability.

Results provided in this thesis suggest that both drug uptake and release were dependent on the relative hydrophobicity of each drug. For example idarubicin, the most hydrophobic of the anthracyclines tested, had a faster loading rate but was also more quickly released from the liposomes *in vivo*. Conversely, doxorubicin (the least hydrophobic of the anthracyclines tested), had a slower loading rate and was slowly released from lipid carriers. With this in mind, studies presented in chapter 5 used ethanol, as a permeability enhancer, to increase doxorubicin loading rates. Ethanol was removed prior to administration, and therefore did not affect the release rate of doxorubicin *in vivo*. Ethanol-enhanced drug loading rates could be utilized for loading drugs into cholesterol-free liposomes composed of phospholipids containing longer acyl chains such as DAPC ($T_c = 65^\circ\text{C}$) and DBPC ($T_c = 74^\circ\text{C}$). Alternatively, it is conceivable that the addition of biological compounds could be pursued, following loading of hydrophobic agents in order to reduce membrane permeability and, in turn, to improve drug retention.

There are currently only three anthracyclines approved for human use: a daunorubicin formulation (DaunoXome[®]) and two doxorubicin formulations (Doxil[®], Myocet[®]). It has been suggested that this is due to the fact that liposome encapsulation moderates the cardiac toxicity of these drugs. Idarubicin, however, is less cardiotoxic and thus improvements in the overall

therapeutic activity would have to rely on the ability of lipid-based carriers to facilitate improvements in antitumor efficacy, which could arise due to localized delivery of the carrier-associated drug to the tumor site. The antitumor studies of liposomal idarubicin performed in Chapters 6 and 7, demonstrated that increased circulation longevity of the drug yielded small, albeit, significant improvements in median survival time in ascitic P388 WT leukemia model as compared to free drug. The value of the formulation developed during the course of these investigations was more fully realized by use in combination with a second complementary agent, gemcitabine.

Improved therapeutic activity of liposomal idarubicin was observed when it was used in combination with liposomal gemcitabine in the treatment of ascitic P388 (Chapter 7). Three lipid compositions were chosen to entrap gemcitabine, among them, passive loading into DSPC / CH / DSPE-PEG₂₀₀₀ (50:45:5 mole ratio) yielded the highest encapsulation efficiency and resulted in a simple formulation that achieved significant improvements in drug blood residence time. For the passive loading technique, the encapsulation efficiency was low (approximately 10%) and a large portion of the drug needed to be removed. The combination of gemcitabine and idarubicin demonstrated the greatest improvements in median survival times in ascitic P388 leukemia when encapsulated in liposomes. Although additional pharmacokinetic studies assessing biodistribution and metabolism should be performed to understand the specific mechanism by which liposome encapsulation mediated improvements in therapeutic activity, it is clear from the in vitro studies that simultaneous addition of idarubicin and gemcitabine to cancer cells can result in therapeutic effects far better than anticipated based on additive activity. Future studies should examine the combination of liposomal formulations of gemcitabine and idarubicin in other cancers including breast, pancreatic, lung and ovarian.

Cytotoxicity studies in multidrug resistance cells indicated that idarubicin enhanced cell kill in MDR1 transfected MDA435/LCC6 breast cancer cells (as compared to doxorubicin), while no difference was observed in P388 cells that were selected in media with low levels of doxorubicin (ADR) and exhibited multiple mechanisms of drug resistance. Previous studies have shown that due to idarubicin's hydrophobicity, it can permeate cell membranes more efficiently than other less hydrophobic anthracyclines and allow for higher accumulation within malignant cells, even those expressing p-glycoprotein. However, idarubicin's enhanced cytotoxicity against MDA435/LCC6 MDR1 breast cancer cells did not translate to a substantially improve the therapeutic response in this model (Chapter 6). These results may be improved by selecting a different dosing schedule and may improve when using a multiple dosing schedule. Further investigation of liposomal idarubicin treatment in a variety of other solid and haematological tumor models should be assessed.

Although many achievements were discovered throughout the course of this thesis work, clearly there are many controversial issues that were addressed. Cholesterol is often included in liposome formulations to increase retention of encapsulated contents. The addition of cholesterol to lipid formulations composed of gel phase lipids (such as DSPC) can actually cause significant increases in membrane permeability, depending on the drug used. Within the literature most references stating that cholesterol is an essential component of liposome formulations incorporate liquid-crystalline phospholipids such as egg PC or DMPC, and thus the role of cholesterol in governing membrane stability in vivo may be more important for these lipid compositions. It is now possible, when desired, to use of PEG-lipids to aid in the design of the lipid formulations that do not contain cholesterol. Thus, cholesterol is no longer an essential requirement in all lipid formulations.

Clearly the role of PEG-lipids in liposome formulations is open to interpretation. It was demonstrated that the addition of PEG-lipids to DSPC liposomes prevents aggregation which may, in turn, prolong circulation lifetimes. However, direct evidence for liposome aggregation in serum and subsequent elimination was not obtained, and may in fact be difficult to demonstrate. It is plausible that the aggregates are readily removed by the body or that the shear forces within the blood vessels may break apart the aggregates, but if this were true then one may anticipate that PEG's effects may be more important in liposome stability in solution prior to i.v. administration. As there has been little direct evidence of inhibition of plasma protein binding by PEG-lipids, either based on charge or hydrophilicity, the direct role of PEG-lipids in extending blood circulation lifetimes must be revisited.

Doxorubicin was loaded into cholesterol-free liposomes at temperatures below the T_c by addition of small amounts of ethanol. The optimal amount of ethanol did not interfere with the liposome size, structure, permeability or the imposed pH gradient; however, it did facilitate the permeation of doxorubicin through the lipid bilayer such that 100% encapsulation efficiency could be obtained after incubation at 40°C for 60 min. The asymmetric distribution theory, which suggested that ethanol at the concentrations used was distributed in the lipid bilayer asymmetrically, is speculative. This concept can only be proven if it is known that ethanol is present on the inside of the liposome-something that is difficult to demonstrate.

The general idea that liposomal agents reduce toxicity is best exemplified by liposomal doxorubicin, and has not been observed for many other drugs. Studies from this thesis on the encapsulation of idarubicin and gemcitabine in liposomes, demonstrated life-limiting toxicities at doses equal to or less than observed for the free drug. Importantly, new toxicities were not observed, and the liposomal drugs were more efficacious than the free drugs. This is clear

evidence in support of the observation that the liposomal drug exhibited an increased therapeutic index.

In conclusion, lipid-based carrier technology has been shown to improve the pharmacological attributes of chemotherapeutic agents. The versatility of liposomes, in particular, to provide a vehicle for delivery of co-encapsulated agents is currently being explored. Our increasing knowledge of tumor biology has translated into the approval of several rational and biologically targeted therapies that include small molecule inhibitors, monoclonal antibodies, proteins, peptides and cytokines, all of which are anticipated to greatly benefit from lipid-based carrier technology.

REFERENCES

1. Nowell, P. C. (1976). The clonal evolution of tumor cell populations. *Science* 194(4260): 23-28.
2. Hanahan, D., and Weinberg, R. A. (2000). The hallmarks of cancer. *Cell* 100(1): 57-70.
3. Goodman, L. S., Wintrobe, M. M., Dameshek, W., Goodman, J. J., and Gilman, A. (1946). Nitrogen mustard therapy. Use of methyl-bis (β -chloroethyl)amine hydrochloride and tris (β -chloroethyl)amine hydrochloride for Hodgkin's disease, lymphosarcoma, leukemia and certain allied and miscellaneous disorders. *JAMA* 132:126-132.
4. Goldie, J. H. (2001). Drug resistance in cancer: a perspective. *Cancer Metastasis Rev* 20(1-2): 63-68.
5. Mapara, M. Y., and Sykes, M. (2004). Tolerance and cancer: mechanisms of tumor evasion and strategies for breaking tolerance. *J Clin Oncol* 22(6): 1136-1151.
6. Pinel, S., Barberi-Heyob, M., Cohen-Jonathan, E., Merlin, J. L., Delmas, C., Plenat, F., and Chastagner, P. (2004). Erythropoietin-induced reduction of hypoxia before and during fractionated irradiation contributes to improvement of radioresponse in human glioma xenografts. *Int J Radiat Oncol Biol Phys* 59(1): 250-259.
7. Okuno, M., Kojima, S., Matsushima-Nishiwaki, R., Tsurumi, H., Muto, Y., Friedman, S. L., and Moriwaki, H. (2004). Retinoids in cancer chemoprevention. *Curr Cancer Drug Targets* 4(3): 285-298.
8. Gately, S., and Li, W. W. (2004). Multiple roles of COX-2 in tumor angiogenesis: A target for antiangiogenic therapy. *Semin Oncol* 31(2 Suppl 7): 2-11.
9. Edelstein, M. L., Abedi, M. R., Wixon, J., and Edelstein, R. M. (2004). Gene therapy clinical trials worldwide 1989-2004-an overview. *J Gene Med* 6(6): 597-602.
10. Gorre, M. E., Mohammed, M., Ellwood, K., Hsu, N., Paquette, R., Rao, P. N., and Sawyers, C. L. (2001). Clinical resistance to STI-571 cancer therapy caused by BCR-ABL gene mutation or amplification. *Science* 293(5531): 876-880.
11. Bangham, A. D., Standish, M. M., and Watkins, J. C. (1965). Diffusion of univalent ions across the lamellae of swollen phospholipids. *J Mol Biol* 13(1): 238-252.
12. Bangham, A. D., Morley, C. J., and Phillips, M. C. (1979). The physical properties of an effective lung surfactant. *Biochim Biophys Acta* 573(3): 552-556.
13. Gregoriadis, G., Leathwood, P. D., and Ryman, B. E. (1971). Enzyme entrapment in liposomes. *FEBS Lett* 14(2): 95-99.
14. Reddi, E. (1997). Role of delivery vehicles for photosensitizers in the photodynamic therapy of tumours. *J Photochem Photobiol B* 37(3): 189-195.
15. Allen, T. M., Mehra, T., Hansen, C., and Chin, Y. C. (1992). Stealth liposomes: an improved sustained release system for 1-beta-D-arabinofuranosylcytosine. *Cancer Res* 52(9): 2431-2439.
16. Webb, M. S., Harasym, T. O., Masin, D., Bally, M. B., and Mayer, L. D. (1995). Sphingomyelin-cholesterol liposomes significantly enhance the pharmacokinetic and therapeutic properties of vincristine in murine and human tumour models. *Br J Cancer* 72(4): 896-904.
17. Torchilin, V. P., Omelyanenko, V. G., Papisov, M. I., Bogdanov, A. A., Trubetskoy, V. S., Herron, J. N., and Gentry, C. A. (1994). Poly(ethylene glycol) on the liposome surface: on the mechanism of polymer-coated liposome longevity. *Biochim Biophys Acta*

- 1195(1): 11-20.
18. Scott, M. D., and Murad, K. L. (1998). Cellular camouflage: fooling the immune system with polymers. *Curr Pharm Des* 4(6): 423-438.
19. Lusse, S., and Arnold, K. (1996). The interaction of poly(ethylene glycol) with water studied by ^1H and ^2H NMR relaxation time measurements. *Macromolecules* 29(12): 4251-4257.
20. Lee, J. H., Lee, H. B., and Andrade, J. D. (1995). Blood compatibility of polyethylene oxide surfaces. *Progress in Polymer Science* 20(6): 1043-1079.
21. Ingham, K. C., and Atha, D. H. (1984). Protein precipitation with poly(ethylene glycol). *Methods Enzymol* 104: 351-356.
22. Polson, A., Potgieter, G. M., Largier, J. F., Mears, G. E., and Joubert, F. J. (1964). The Fractionation of Protein Mixtures by Linear Polymers of High Molecular Weight. *Biochim Biophys Acta* 82:463-475.
23. Abuchowski, A., McCoy, J. R., Palczuk, N. C., van Es, T., and Davis, F. F. (1977). Effect of covalent attachment of poly(ethylene glycol) on immunogenicity and circulating life of bovine liver catalase. *J Biol Chem* 252(11): 3582-3586.
24. Veronese, F. M. (2001). Peptide and protein PEGylation: a review of problems and solutions. *Biomaterials* 22(5): 405-417.
25. Tsunoda, S., Ishikawa, T., Yamamoto, Y., Kamada, H., Koizumi, K., Matsui, J., Tsutsumi, Y., Hirano, T., and Mayumi, T. (1999). Enhanced antitumor potency of poly(ethylene glycol)ylated tumor necrosis factor- α : a novel polymer-conjugation technique with a reversible amino-protective reagent. *J Pharmacol Exp Ther* 290(1): 368-372.
26. Veronese, F. M., Caliceti, P., Schiavon, O., and Sergi, M. (2002). Poly(ethylene glycol)-superoxide dismutase, a conjugate in search of exploitation. *Adv Drug Deliv Rev* 54(4): 587-606.
27. Vega, J., Ke, S., Fan, Z., Wallace, S., Charsangavej, C., and Li, C. (2003). Targeting doxorubicin to epidermal growth factor receptors by site-specific conjugation of C225 to poly(L-glutamic acid) through a poly(ethylene glycol) spacer. *Pharm Res* 20(5): 826-832.
28. Parr, M. J., Ansell, S. M., Choi, L. S., and Cullis, P. R. (1994). Factors influencing the retention and chemical stability of poly(ethylene glycol)-lipid conjugates incorporated into large unilamellar vesicles. *Biochim Biophys Acta* 1195(1): 21-30.
29. Allen, T. M., Hansen, C., Martin, F., Redemann, C., and Yau-Young, A. (1991). Liposomes containing synthetic lipid derivatives of poly(ethylene glycol) show prolonged circulation half-lives in vivo. *Biochim Biophys Acta* 1066(1): 29-36.
30. Conover, C. D., Zhao, H., Longley, C. B., Shum, K. L., and Greenwald, R. B. (2003). Utility of poly(ethylene glycol) conjugation to create prodrugs of amphotericin B. *Bioconjug Chem* 14(3): 661-666.
31. Greenwald, R. B., Zhao, H., Xia, J., Conover, C. D., Longley, C. B., and Shum, K. L. (2003). Tripartate poly(ethylene glycol) prodrugs of the open lactone form of camptothecin. *Bioorg Med Chem* 11(12): 2635-2639.
32. Senior, J., Delgado, C., Fisher, D., Tilcock, C., and Gregoriadis, G. (1991). Influence of surface hydrophilicity of liposomes on their interaction with plasma protein and clearance from the circulation: studies with poly(ethylene glycol)-coated vesicles. *Biochim Biophys Acta* 1062(1): 77-82.

33. Sou, K., Endo, T., Takeoka, S., and Tsuchida, E. (2000). Poly(ethylene glycol)-modification of the phospholipid vesicles by using the spontaneous incorporation of poly(ethylene glycol)-lipid into the vesicles. *Bioconj Chem* 11(3): 372-379.
34. Uster, P. S., Allen, T. M., Daniel, B. E., Mendez, C. J., Newman, M. S., and Zhu, G. Z. (1996). Insertion of poly(ethylene glycol) derivatized phospholipid into pre-formed liposomes results in prolonged in vivo circulation time. *FEBS Lett* 386(2-3): 243-246.
35. Yoshioka, H. (1991). Surface modification of haemoglobin-containing liposomes with poly(ethylene glycol) prevents liposome aggregation in blood plasma. *Biomaterials* 12(9): 861-864.
36. Hashizaki, K., Taguchi, H., Itoh, C., Sakai, H., Abe, M., Saito, Y., and Ogawa, N. (2003). Effects of poly(ethylene glycol) (PEG) chain length of PEG-lipid on the permeability of liposomal bilayer membranes. *Chem Pharm Bull (Tokyo)* 51(7): 815-820.
37. Webb, M. S., Saxon, D., Wong, F. M., Lim, H. J., Wang, Z., Bally, M. B., Choi, L. S., Cullis, P. R., and Mayer, L. D. (1998). Comparison of different hydrophobic anchors conjugated to poly(ethylene glycol): effects on the pharmacokinetics of liposomal vincristine. *Biochim Biophys Acta* 1372(2): 272-282.
38. Holland, J. W., Cullis, P. R., and Madden, T. D. (1996). Poly(ethylene glycol)-lipid conjugates promote bilayer formation in mixtures of non-bilayer-forming lipids. *Biochemistry* 35(8): 2610-2617.
39. de Gennes, P. G. (1987). Polymers at an interface: a simplified view. *Advances Colloid Interface Sci* 27:189-209.
40. de Gennes, P. G. (1980). Conformation of polymers attached to an interface. *Macromolecules* 13:1069-1075.
41. Hristova, K., and Needham, D. (1995). Phase behavior of a lipid/polymer-lipid mixture in aqueous medium. *macromolecules* 28:991-1002.
42. Allen, C., Dos Santos, N., Gallagher, R., Chiu, G. N., Shu, Y., Li, W. M., Johnstone, S. A., Janoff, A. S., Mayer, L. D., Webb, M. S., and Bally, M. B. (2002). Controlling the physical behavior and biological performance of liposome formulations through use of surface grafted poly(ethylene glycol). *Biosci Rep* 22(2): 225-250.
43. Papahadjopoulos, D., and Miller, N. (1967). Phospholipid model membranes. I. Structural characteristics of hydrated liquid crystals. *Biochim Biophys Acta* 135(4): 624-638.
44. Cullis, P. R., and de Kruijff, B. (1979). Lipid polymorphism and the functional roles of lipids in biological membranes. *Biochim Biophys Acta* 559(4): 399-420.
45. Papahadjopoulos, D., Jacobson, K., Nir, S., and Isac, T. (1973). Phase transitions in phospholipid vesicles. Fluorescence polarization and permeability measurements concerning the effect of temperature and cholesterol. *Biochim Biophys Acta* 311(3): 330-348.
46. Demel, R. A., and De Kruijff, B. (1976). The function of sterols in membranes. *Biochim Biophys Acta* 457(2): 109-132.
47. Ladbroke, B. D., Williams, R. M., and Chapman, D. (1968). Studies on lecithin-cholesterol-water interactions by differential scanning calorimetry and X-ray diffraction. *Biochim Biophys Acta* 150(3): 333-340.
48. Senior, J. H. (1987). Fate and behavior of liposomes in vivo: a review of controlling factors. *Crit Rev Ther Drug Carrier Syst* 3(2): 123-193.

49. Lim, H. J., Parr, M. J., Masin, D., McIntosh, N. L., Madden, T. D., Zhang, G., Johnstone, S., and Bally, M. B. (2000). Kupffer cells do not play a role in governing the efficacy of liposomal mitoxantrone used to treat a tumor model designed to assess drug delivery to liver. *Clin Cancer Res* 6(11): 4449-4460.
50. Daemen, T., Hofstede, G., Ten Kate, M. T., Bakker-Woudenberg, I. A., and Scherphof, G. L. (1995). Liposomal doxorubicin-induced toxicity: depletion and impairment of phagocytic activity of liver macrophages. *Int J Cancer* 61(5): 716-721.
51. Bally, M. B., Nayar, R., Masin, D., Hope, M. J., Cullis, P. R., and Mayer, L. D. (1990). Liposomes with entrapped doxorubicin exhibit extended blood residence times. *Biochim Biophys Acta* 1023(1): 133-139.
52. Allen, T. M., and Chonn, A. (1987). Large unilamellar liposomes with low uptake into the reticuloendothelial system. *FEBS Lett* 223(1): 42-46.
53. Gabizon, A., and Papahadjopoulos, D. (1988). Liposome formulations with prolonged circulation time in blood and enhanced uptake by tumors. *Proc Natl Acad Sci U S A* 85(18): 6949-6953.
54. Klivanov, A. L., Maruyama, K., Torchilin, V. P., and Huang, L. (1990). Amphipathic polyethyleneglycols effectively prolong the circulation time of liposomes. *FEBS Lett* 268(1): 235-237.
55. Blume, G., and Cevc, G. (1990). Liposomes for the sustained drug release in vivo. *Biochim Biophys Acta* 1029(1): 91-97.
56. Allen, T. M., and Hansen, C. (1991). Pharmacokinetics of stealth versus conventional liposomes: effect of dose. *Biochim Biophys Acta* 1068(2): 133-141.
57. Woodle, M. C., Matthay, K. K., Newman, M. S., Hidayat, J. E., Collins, L. R., Redemann, C., Martin, F. J., and Papahadjopoulos, D. (1992). Versatility in lipid compositions showing prolonged circulation with sterically stabilized liposomes. *Biochim Biophys Acta* 1105(2): 193-200.
58. Huang, S. K., Lee, K. D., Hong, K., Friend, D. S., and Papahadjopoulos, D. (1992). Microscopic localization of sterically stabilized liposomes in colon carcinoma-bearing mice. *Cancer Res* 52(19): 5135-5143.
59. Wu, N. Z., Da, D., Rudoll, T. L., Needham, D., Whorton, A. R., and Dewhirst, M. W. (1993). Increased microvascular permeability contributes to preferential accumulation of Stealth liposomes in tumor tissue. *Cancer Res* 53(16): 3765-3770.
60. Gabizon, A., Catane, R., Uziely, B., Kaufman, B., Safra, T., Cohen, R., Martin, F., Huang, A., and Barenholz, Y. (1994). Prolonged circulation time and enhanced accumulation in malignant exudates of doxorubicin encapsulated in polyethylene-glycol coated liposomes. *Cancer Res* 54(4): 987-992.
61. Papahadjopoulos, D., Allen, T. M., Gabizon, A., Mayhew, E., Matthay, K., Huang, S. K., Lee, K. D., Woodle, M. C., Lasic, D. D., Redemann, C., and *et al.* (1991). Sterically stabilized liposomes: improvements in pharmacokinetics and antitumor therapeutic efficacy. *Proc Natl Acad Sci U S A* 88(24): 11460-11464.
62. Gabizon, A. A. (1992). Selective tumor localization and improved therapeutic index of anthracyclines encapsulated in long-circulating liposomes. *Cancer Res* 52(4): 891-896.
63. Boman, N. L., Masin, D., Mayer, L. D., Cullis, P. R., and Bally, M. B. (1994). Liposomal vincristine which exhibits increased drug retention and increased circulation longevity cures mice bearing P388 tumors. *Cancer Res* 54(11): 2830-2833.
64. Jain, R. K. (1997). Delivery of molecular and cellular medicine to solid tumors. *Adv*

Drug Deliv Rev 26(2-3): 71-90.

65. Gregoriadis, G., Wills, E. J., Swain, C. P., and Tavill, A. S. (1974). Drug-carrier potential of liposomes in cancer chemotherapy. *Lancet* 1(7870): 1313-1316.
66. Li, X., Cabral-Lilly, D., Janoff, A. S., and Perkins, W. R. (2000). Complexation of internalized doxorubicin into fiber bundles affects its release rate from liposomes. *Journal of Liposome Research* 10(1): 15-27.
67. Li, X., Hirsh, D. J., Cabral-Lilly, D., Zirkel, A., Gruner, S. M., Janoff, A. S., and Perkins, W. R. (1998). Doxorubicin physical state in solution and inside liposomes loaded via a pH gradient. *Biochim Biophys Acta* 1415(1): 23-40.
68. Harrigan, P. R., Wong, K. F., Redelmeier, T. E., Wheeler, J. J., and Cullis, P. R. (1993). Accumulation of doxorubicin and other lipophilic amines into large unilamellar vesicles in response to transmembrane pH gradients. *Biochim Biophys Acta* 1149(2): 329-338.
69. Mayer, L. D., Tai, L. C., Bally, M. B., Mitlenes, G. N., Ginsberg, R. S., and Cullis, P. R. (1990). Characterization of liposomal systems containing doxorubicin entrapped in response to pH gradients. *Biochim Biophys Acta* 1025(2): 143-151.
70. Lasic, D. D., Frederik, P. M., Stuart, M. C., Barenholz, Y., and McIntosh, T. J. (1992). Gelation of liposome interior. A novel method for drug encapsulation. *FEBS Lett* 312(2-3): 255-258.
71. Abraham, S. A., Edwards, K., Karlsson, G., MacIntosh, S., Mayer, L. D., McKenzie, C., and Bally, M. B. (2002). Formation of transition metal-doxorubicin complexes inside liposomes. *Biochim Biophys Acta* 1565(1): 41-54.
72. Cheung, B. C., Sun, T. H., Leenhouts, J. M., and Cullis, P. R. (1998). Loading of doxorubicin into liposomes by forming Mn²⁺-drug complexes. *Biochim Biophys Acta* 1414(1-2): 205-216.
73. Boroujerdi, M. (2002) *Pharmacokinetics: principles and applications*, McGraw-Hill Companies, Inc., New York.
74. Hwang, K. J. (1987) Liposome Pharmacokinetics. In *Liposomes: from biophysics to therapeutics* (Ostro, M. J., ed) pp. 109-156, Marcel Dekker, New York.
75. Abra, R. M., and Hunt, C. A. (1981). Liposome disposition in vivo. III. Dose and vesicle-size effects. *Biochim Biophys Acta* 666(3): 493-503.
76. Gabizon, A., and Papahadjopoulos, D. (1992). The role of surface charge and hydrophilic groups on liposome clearance in vivo. *Biochim Biophys Acta* 1103(1): 94-100.
77. Scherphof, G., Van Leeuwen, B., Wilschut, J., and Damen, J. (1983). Exchange of phosphatidylcholine between small unilamellar liposomes and human plasma high-density lipoprotein involves exclusively the phospholipid in the outer monolayer of the liposomal membrane. *Biochim Biophys Acta* 732(3): 595-599.
78. Damen, J., Regts, J., and Scherphof, G. (1982). Transfer of [14C]phosphatidylcholine between liposomes and human plasma high density lipoprotein. Partial purification of a transfer-stimulating plasma factor using a rapid transfer assay. *Biochim Biophys Acta* 712(3): 444-452.
79. Damen, J., Regts, J., and Scherphof, G. (1981). Transfer and exchange of phospholipid between small unilamellar liposomes and rat plasma high density lipoproteins. Dependence on cholesterol content and phospholipid composition. *Biochim Biophys Acta* 665(3): 538-545.
80. Allen, T. M. (1981). A study of phospholipid interactions between high-density

- lipoproteins and small unilamellar vesicles. *Biochim Biophys Acta* 640(2): 385-397.
81. Scherphof, G., Roerdink, F., Waite, M., and Parks, J. (1978). Disintegration of phosphatidylcholine liposomes in plasma as a result of interaction with high-density lipoproteins. *Biochim Biophys Acta* 542(2): 296-307.
 82. Lalanne, F., and Ponsin, G. (2000). Mechanism of the phospholipid transfer protein-mediated transfer of phospholipids from model lipid vesicles to high density lipoproteins. *Biochim Biophys Acta* 1487(1): 82-91.
 83. Senior, J., Gregoriadis, G., and Mitropoulos, K. A. (1983). Stability and clearance of small unilamellar liposomes. Studies with normal and lipoprotein-deficient mice. *Biochim Biophys Acta* 760(1): 111-118.
 84. Raff, M. (1998). Cell suicide for beginners [news]. *Nature* 396(6707): 119-122.
 85. Kirby, C., Clarke, J., and Gregoriadis, G. (1980). Cholesterol content of small unilamellar liposomes controls phospholipid loss to high density lipoproteins in the presence of serum. *FEBS Lett* 111(2): 324-328.
 86. Chonn, A., Semple, S. C., and Cullis, P. R. (1995). Beta 2 glycoprotein I is a major protein associated with very rapidly cleared liposomes in vivo, suggesting a significant role in the immune clearance of "non-self" particles. *J Biol Chem* 270(43): 25845-25849.
 87. Loughrey, H. C., Bally, M. B., Reinish, L. W., and Cullis, P. R. (1990). The binding of phosphatidylglycerol liposomes to rat platelets is mediated by complement. *Thromb Haemost* 64(1): 172-176.
 88. Richards, R. L., Gewurz, H., Siegel, J., and Alving, C. R. (1979). Interactions of C-reactive protein and complement with liposomes. II. Influence of membrane composition. *J Immunol* 122(4): 1185-1189.
 89. Rossi, J. D., and Wallace, B. A. (1983). Binding of fibronectin to phospholipid vesicles. *J Biol Chem* 258(5): 3327-3331.
 90. Papahadjopoulos, D., and Gabizon, A. (1990). Liposomes designed to avoid the reticuloendothelial system. *Prog Clin Biol Res* 343:85-93.
 91. Allen, T. M., Hansen, C., and Rutledge, J. (1989). Liposomes with prolonged circulation times: factors affecting uptake by reticuloendothelial and other tissues. *Biochim Biophys Acta* 981(1): 27-35.
 92. Hsu, M. J., and Juliano, R. L. (1982). Interactions of liposomes with the reticuloendothelial system. II: Nonspecific and receptor-mediated uptake of liposomes by mouse peritoneal macrophages. *Biochim Biophys Acta* 720(4): 411-419.
 93. Kao, Y. J., and Juliano, R. L. (1981). Interactions of liposomes with the reticuloendothelial system. Effects of reticuloendothelial blockade on the clearance of large unilamellar vesicles. *Biochim Biophys Acta* 677(3-4): 453-461.
 94. Patel, H. M., Tuzel, N. S., and Ryman, B. E. (1983). Inhibitory effect of cholesterol on the uptake of liposomes by liver and spleen. *Biochim Biophys Acta* 761(2): 142-151.
 95. Moghimi, S. M., and Szebeni, J. (2003). Stealth liposomes and long circulating nanoparticles: Critical issues in pharmacokinetics, opsonization and protein-binding properties. *Progress in Lipid Research* 42(6): 463-478.
 96. Liang, E., and Hughes, J. A. (1998). Membrane fusion and rupture in liposomes: effect of biodegradable pH-sensitive surfactants. *J Membr Biol* 166(1): 37-49.
 97. Adlakha-Hutcheon, G., Bally, M. B., Shew, C. R., and Madden, T. D. (1999). Controlled destabilization of a liposomal drug delivery system enhances mitoxantrone antitumor activity. *Nat Biotechnol* 17(8): 775-779.

98. Weinstein, J. N., Magin, R. L., Yatvin, M. B., and Zaharko, D. S. (1979). Liposomes and local hyperthermia: selective delivery of methotrexate to heated tumors. *Science* 204(4389): 188-191.
99. Hope, M. J., Bally, M. B., Webb, G., and Cullis, P. R. (1985). Production of large unilamellar vesicles by a rapid extrusion procedure. Characterization of size distribution, trapped volume and ability to maintain a membrane potential. *Biochim Biophys Acta* 812:55-65.
100. Olson, F., Hunt, C. A., Szoka, F. C., Vail, W. J., and Papahadjopoulos, D. (1979). Preparation of liposomes of defined size distribution by extrusion through polycarbonate membranes. *Biochim Biophys Acta* 557(1): 9-23.
101. Bally, M. B., Mayer, L. D., Hope, M. J., and Nayar, R. (1993) Pharmacodynamics of liposomal drug carriers: methodological considerations. In *Liposome Technology* (Gregoriadis, G., ed) Vol. 3 pp. 27-41, CRC Press
102. Derksen, J. T., Morselt, H. W., and Scherphof, G. L. (1987). Processing of different liposome markers after in vitro uptake of immunoglobulin-coated liposomes by rat liver macrophages. *Biochim Biophys Acta* 931(1): 33-40.
103. Redelmeier, T. E., Mayer, L. D., Wong, K. F., Bally, M. B., and Cullis, P. R. (1989). Proton flux in large unilamellar vesicles in response to membrane potentials and pH gradients. *Biophys J* 56(2): 385-393.
104. Almgren, M., Edwards, K., and Karlsson, G. (2000). Cryo transmission electron microscopy of liposomes and related structures. *Colloids and Surfaces A: Physicochemical and Engineering Aspects* 174(1-2): 3-21.
105. Almgren, M., Edwards, K., and Gustafsson, J. (1996). Cryo-transmission electron microscopy of thin vitrified samples. *Curr Opin. Colloid Interface Sci.* 1:270-278.
106. Wessel, D., and Flugge, U. I. (1984). A method for the quantitative recovery of protein in dilute solution in the presence of detergents and lipids. *Anal Biochem* 138(1): 141-143.
107. Mayer, L. D., Bally, M. B., and Cullis, P. R. (1986). Uptake of adriamycin into large unilamellar vesicles in response to a pH gradient. *Biochim Biophys Acta* 857(1): 123-126.
108. Alley, M. C., Scudiero, D. A., Monks, A., Hursey, M. L., Czerwinski, M. J., Fine, D. L., Abbott, B. J., Mayo, J. G., Shoemaker, R. H., and Boyd, M. R. (1988). Feasibility of drug screening with panels of human tumor cell lines using a microculture tetrazolium assay. *Cancer Res* 48(3): 589-601.
109. Chou, T. C., and Talalay, P. (1984). Quantitative analysis of dose-effect relationships: the combined effects of multiple drugs or enzyme inhibitors. *Adv Enzyme Regul* 22:27-55.
110. Corbett, T. H., Roberts, B. J., Trader, M. W., Laster, W. R., Jr., Griswold, D. P., Jr., and Schabel, F. M., Jr. (1982). Response of transplantable tumors of mice to anthracenedione derivatives alone and in combination with clinically useful agents. *Cancer Treat Rep* 66(5): 1187-1200.
111. Pastan, I., Gottesman, M. M., Ueda, K., Lovelace, E., Rutherford, A. V., and Willingham, M. C. (1988). A retrovirus carrying an MDR1 cDNA confers multidrug resistance and polarized expression of P-glycoprotein in MDCK cells. *Proc Natl Acad Sci U S A* 85(12): 4486-4490.
112. Bittman, R., and Blau, L. (1972). The phospholipid-cholesterol interaction. Kinetics of

- water permeability in liposomes. *Biochemistry* 11(25): 4831-4839.
113. Kirby, C., Clarke, J., and Gregoriadis, G. (1980). Effect of the cholesterol content of small unilamellar liposomes on their stability in vivo and in vitro. *Biochem J* 186(2): 591-598.
 114. Senior, J., and Gregoriadis, G. (1982). Stability of small unilamellar liposomes in serum and clearance from the circulation: the effect of the phospholipid and cholesterol components. *Life Sci* 30(24): 2123-2136.
 115. Papahadjopoulos, D., Cowden, M., and Kimelberg, H. (1973). Role of cholesterol in membranes. Effects on phospholipid-protein interactions, membrane permeability and enzymatic activity. *Biochim Biophys Acta* 330(1): 8-26.
 116. Semple, S. C., Chonn, A., and Cullis, P. R. (1996). Influence of cholesterol on the association of plasma proteins with liposomes. *Biochemistry* 35(8): 2521-2525.
 117. Gregoriadis, G., and Davis, C. (1979). Stability of liposomes in vivo and in vitro is promoted by their cholesterol content and the presence of blood cells. *Biochem Biophys Res Commun* 89(4): 1287-1293.
 118. Lim, H. J., Masin, D., Madden, T. D., and Bally, M. B. (1997). Influence of drug release characteristics on the therapeutic activity of liposomal mitoxantrone. *J Pharmacol Exp Ther* 281(1): 566-573.
 119. Boman, N. L., Mayer, L. D., and Cullis, P. R. (1993). Optimization of the retention properties of vincristine in liposomal systems. *Biochim Biophys Acta* 1152(2): 253-258.
 120. Lippert, J. L., and Peticolas, W. L. (1971). Laser Raman investigation of the effect of cholesterol on conformational changes in dipalmitoyl lecithin multilayers. *Proc Natl Acad Sci U S A* 68(7): 1572-1576.
 121. Li, W. M., Xue, L., Mayer, L. D., and Bally, M. B. (2001). Intermembrane transfer of poly(ethylene glycol)-modified phosphatidylethanolamine as a means to reveal surface-associated binding ligands on liposomes. *Biochim Biophys Acta* 1513(2): 193-206.
 122. Rodriguez, W. V., Klimuk, S. K., Pritchard, P. H., and Hope, M. J. (1998). Cholesterol mobilization and regression of atheroma in cholesterol-fed rabbits induced by large unilamellar vesicles. *Biochim Biophys Acta* 1368(2): 306-320.
 123. Maruyama, K., Yuda, T., Okamoto, A., Ishikura, C., Kojima, S., and Iwatsuru, M. (1991). Effect of molecular weight in amphipathic polyethyleneglycol on prolonging the circulation time of large unilamellar liposomes. *Chem Pharm Bull (Tokyo)* 39(6): 1620-1622.
 124. Maruyama, K., Yuda, T., Okamoto, A., Kojima, S., Suganaka, A., and Iwatsuru, M. (1992). Prolonged circulation time in vivo of large unilamellar liposomes composed of distearoyl phosphatidylcholine and cholesterol containing amphipathic poly(ethylene glycol). *Biochim Biophys Acta* 1128(1): 44-49.
 125. Woodle, M. C., Newman, M. S., and Cohen, J. A. (1994). Sterically stabilized liposomes: physical and biological properties. *J Drug Target* 2(5): 397-403.
 126. Edwards, K., Johnsson, M., Karlsson, G., and Silvander, M. (1997). Effect of polyethyleneglycol-phospholipids on aggregate structure in preparations of small unilamellar liposomes. *Biophys J* 73(1): 258-266.
 127. Kenworthy, A. K., Simon, S. A., and McIntosh, T. J. (1995). Structure and phase behavior of lipid suspensions containing phospholipids with covalently attached poly(ethylene glycol). *Biophys J* 68(5): 1903-1920.
 128. Bedu-Addo, F. K., Tang, P., Xu, Y., and Huang, L. (1996). Effects of

- polyethyleneglycol chain length and phospholipid acyl chain composition on the interaction of polyethyleneglycol-phospholipid conjugates with phospholipid: implications in liposomal drug delivery. *Pharm Res* 13(5): 710-717.
129. Casazza, A., Di Marco, A., Bonadonna, G., Bonfante, V., Bertazzoli, C., Bellini, O., Pratesi, G., Sala, L., and Ballerini, L. (1980) Effects of modifications in position 4 of the chromophore or in position 4' of the aminosugar, on the antitumor activity and toxicity of daunorubicin and doxorubicin. In *Anthracyclines: current status and new developments* (Crooke, S., and Reich, S., eds) pp. 403-430, Academic Press, Inc., New York.
 130. Allen, T. M., and Cleland, L. G. (1980). Serum-induced leakage of liposome contents. *Biochim Biophys Acta* 597(2): 418-426.
 131. Yatvin, M. B., Weinstein, J. N., Dennis, W. H., and Blumenthal, R. (1978). Design of liposomes for enhanced local release of drugs by hyperthermia. *Science* 202(4374): 1290-1293.
 132. Maruyama, K., Unezaki, S., Takahashi, N., and Iwatsuru, M. (1993). Enhanced delivery of doxorubicin to tumor by long-circulating thermosensitive liposomes and local hyperthermia. *Biochim Biophys Acta* 1149(2): 209-216.
 133. Unezaki, S., Maruyama, K., Takahashi, N., Koyama, M., Yuda, T., Suginaka, A., and Iwatsuru, M. (1994). Enhanced delivery and antitumor activity of doxorubicin using long-circulating thermosensitive liposomes containing amphipathic poly(ethylene glycol) in combination with local hyperthermia. *Pharm Res* 11(8): 1180-1185.
 134. Kenworthy, A. K., Hristova, K., Needham, D., and McIntosh, T. J. (1995). Range and magnitude of the steric pressure between bilayers containing phospholipids with covalently attached poly(ethylene glycol). *Biophys J* 68(5): 1921-1936.
 135. Blume, G., and Cevc, G. (1993). Molecular mechanism of the lipid vesicle longevity in vivo. *Biochim Biophys Acta* 1146(2): 157-168.
 136. Du, H., Chandaroy, P., and Hui, S. W. (1997). Grafted poly-(ethylene glycol) on lipid surfaces inhibits protein adsorption and cell adhesion. *Biochim Biophys Acta* 1326(2): 236-248.
 137. Nikolova, A. N., and Jones, M. N. (1996). Effect of grafted PEG-2000 on the size and permeability of vesicles. *Biochim Biophys Acta* 1304(2): 120-128.
 138. Mori, A., Klivanov, A. L., Torchilin, V. P., and Huang, L. (1991). Influence of the steric barrier activity of amphipathic poly(ethyleneglycol) and ganglioside GM1 on the circulation time of liposomes and on the target binding of immunoliposomes in vivo. *FEBS Lett* 284(2): 263-266.
 139. Scherphof, G., Morselt, H., Regts, J., and Wilschut, J. C. (1979). The involvement of the lipid phase transition in the plasma-induced dissolution of multilamellar phosphatidylcholine vesicles. *Biochim Biophys Acta* 556(2): 196-207.
 140. De Kruffy, B., Van Dijck, P. W., Demel, R. A., Schuijff, A., Brants, F., and Van Deenen, L. L. (1974). Non-random distribution of cholesterol in phosphatidylcholine bilayers. *Biochim Biophys Acta* 356(1): 1-7.
 141. Casazza, A. M. (1979). Experimental evaluation of anthracycline analogs. *Cancer Treat Rep* 63(5): 835-844.
 142. Gallois, L., Fiallo, M., and Garnier-Suillerot, A. (1998). Comparison of the interaction of doxorubicin, daunorubicin, idarubicin and idarubicinol with large unilamellar vesicles. Circular dichroism study. *Biochim Biophys Acta* 1370(1): 31-40.

143. Mayer, L. D., Wong, K. F., Menon, K., Chong, C., Harrigan, P. R., and Cullis, P. R. (1988). Influence of ion gradients on the transbilayer distribution of dibucaine in large unilamellar vesicles. *Biochemistry* 27(6): 2053-2060.
144. Storm, G., ten Kate, M. T., Working, P. K., Bakker-Woudenberg, I. A., Daemen, T., Hofstede, G., and Scherphof, G. L. (1998). Doxorubicin entrapped in sterically stabilized liposomes: effects on bacterial blood clearance capacity of the mononuclear phagocyte system. *Clin Cancer Res* 4(1): 111-115.
145. Hristova, K., Kenworthy, A. K., and McIntosh, T. J. (1995). Effect of bilayer composition on the phase behavior of liposomal suspensions containing poly(ethylene glycol)-lipids. *Macromolecules* 28:7693-7699.
146. Needham, D., McIntosh, T. J., and Lasic, D. D. (1992). Repulsive interactions and mechanical stability of polymer-grafted lipid membranes. *Biochim Biophys Acta* 1108(1): 40-48.
147. Woodle, M. C., and Lasic, D. D. (1992). Sterically stabilized liposomes. *Biochim Biophys Acta* 1113(2): 171-199.
148. Bartucci, R., Pantusa, M., Marsh, D., and Sportelli, L. (2002). Interaction of human serum albumin with membranes containing polymer-grafted lipids: spin-label ESR studies in the mushroom and brush regimes. *Biochim Biophys Acta* 1564(1): 237-242.
149. Mori, Y., Nagaoka, S., Takiuchi, H., Kikuchi, T., Noguchi, N., Tanzawa, H., and Noishiki, Y. (1982). A new antithrombogenic material with long polyethyleneoxide chains. *Trans Am Soc Artif Intern Organs* 28:459-463.
150. Li, W. M., Mayer, L. D., and Bally, M. B. (2002). Prevention of antibody-mediated elimination of ligand-targeted liposomes by using poly(ethylene glycol)-modified lipids. *J Pharmacol Exp Ther* 300(3): 976-983.
151. Chiu, G. N., Bally, M. B., and Mayer, L. D. (2001). Selective protein interactions with phosphatidylserine containing liposomes alter the steric stabilization properties of poly(ethylene glycol). *Biochim Biophys Acta* 1510(1-2): 56-69.
152. Hope, M. J., Wong, K. F., and Cullis, P. R. (1989). Freeze-fracture of lipids and model membrane systems. *J Electron Microscop Tech* 13(4): 277-287.
153. Ickenstein, L. M., Arfvidsson, M. C., Needham, D., Mayer, L. D., and Edwards, K. (2003). Disc formation in cholesterol-free liposomes during phase transition. *Biochim Biophys Acta* 1614(2): 135-138.
154. Johnstone, S. A., Masin, D., Mayer, L., and Bally, M. B. (2001). Surface-associated serum proteins inhibit the uptake of phosphatidylserine and poly(ethylene glycol) liposomes by mouse macrophages. *Biochim Biophys Acta* 1513(1): 25-37.
155. Chonn, A., Semple, S. C., and Cullis, P. R. (1992). Association of blood proteins with large unilamellar liposomes in vivo. Relation to circulation lifetimes. *J Biol Chem* 267(26): 18759-18765.
156. Chonn, A., Semple, S. C., and Cullis, P. R. (1991). Separation of large unilamellar liposomes from blood components by a spin column procedure: towards identifying plasma proteins which mediate liposome clearance in vivo. *Biochim Biophys Acta* 1070(1): 215-222.
157. Bedu-Addo, F. K., and Huang, L. (1995). Interaction of PEG-phospholipid conjugates with phospholipid: implications in liposomal drug delivery. *Advanced Drug Delivery Reviews* 16:235-247.
158. Ahl, P. L., Bhatia, S. K., Meers, P., Roberts, P., Stevens, R., Dause, R., Perkins, W. R.,

- and Janoff, A. S. (1997). Enhancement of the in vivo circulation lifetime of L-alpha-distearoylphosphatidylcholine liposomes: importance of liposomal aggregation versus complement opsonization. *Biochim Biophys Acta* 1329(2): 370-382.
159. Kirpotin, D., Hong, K., Mullah, N., Papahadjopoulos, D., and Zalipsky, S. (1996). Liposomes with detachable polymer coating: destabilization and fusion of dioleoylphosphatidylethanolamine vesicles triggered by cleavage of surface-grafted poly(ethylene glycol). *FEBS Lett* 388(2-3): 115-118.
 160. Rupert, L. A., Engberts, J. B., and Hoekstra, D. (1988). Effect of poly(ethylene glycol) on the Ca²⁺-induced fusion of didodecyl phosphate vesicles. *Biochemistry* 27(21): 8232-8239.
 161. Bonte, F., and Juliano, R. L. (1986). Interactions of liposomes with serum proteins. *Chem Phys Lipids* 40(2-4): 359-372.
 162. Swaney, J. B. (1980). Mechanisms of protein-lipid interaction. Association of apolipoproteins A-I and A-II with binary phospholipid mixtures. *J Biol Chem* 255(18): 8791-8797.
 163. Chonn, A., Semple, S. C., and Cullis, P. R., eds (1994) *Protein-membrane interactions in the biological milieu* Vol. 82
 164. Price, M. E., Cornelius, R. M., and Brash, J. L. (2001). Protein adsorption to poly(ethylene glycol) modified liposomes from fibrinogen solution and from plasma. *Biochimica et Biophysica Acta Biomembranes* 1512(2): 191-205.
 165. Blunk, T., Luck, M., Calvor, A., Hochstrasser, D. F., Sanchez, J. C., Muller, B. W., and Muller, R. H. (1996). Kinetics of plasma protein adsorption on model particles for controlled drug delivery and drug targeting. *European Journal of Pharmaceutics & Biopharmaceutics* 42(4): 262-268.
 166. Turbill, P., Beugeling, T., and Poot, A. A. (1996). Proteins involved in the Vroman effect during exposure of human blood plasma to glass and polyethylene. *Biomaterials* 17(13): 1279-1287.
 167. Cuypers, P. A., Willems, G. M., Hemker, H. C., and Hermens Th, W. (1987). Adsorption kinetics of protein mixtures. A tentative explanation of the Vroman effect. *Annals of the New York Academy of Sciences* 516(pp 244-252):
 168. Slack, S. M., Bohnert, J. L., and Horbett, T. A. (1987). The effects of surface chemistry and coagulation factors on fibrinogen adsorption from plasma. *Annals of the New York Academy of Sciences* 516(pp 223-243):
 169. Vroman, L. (1987). Methods of investigating protein interactions on artificial and natural surfaces. *Ann N Y Acad Sci* 516:300-305.
 170. Oja, C. D., Semple, S. C., Chonn, A., and Cullis, P. R. (1996). Influence of dose on liposome clearance: critical role of blood proteins. *Biochim Biophys Acta* 1281(1): 31-37.
 171. Laverman, P., Brouwers, A. H., Dams, E. T., Oyen, W. J., Storm, G., van Rooijen, N., Corstens, F. H., and Boerman, O. C. (2000). Preclinical and clinical evidence for disappearance of long-circulating characteristics of poly(ethylene glycol) liposomes at low lipid dose. *J Pharmacol Exp Ther* 293(3): 996-1001.
 172. Park, Y. S., and Huang, L. (1993). Effect of chemically modified GM1 and neoglycolipid analogs of GM1 on liposome circulation time: evidence supporting the dysopsonin hypothesis. *Biochim Biophys Acta* 1166(1): 105-114.
 173. Moghimi, S. M., Muir, I. S., Illum, L., Davis, S. S., and Kolb-Bachofen, V. (1993).

- Coating particles with a block co-polymer (poloxamine-908) suppresses opsonization but permits the activity of dysopsonins in the serum. *Biochim Biophys Acta* 1179(2): 157-165.
174. Blunk, T., Hochstrasser, D. F., Sanchez, J. C., Muller, B. W., and Muller, R. H. (1993). Colloidal carriers for intravenous drug targeting: plasma protein adsorption patterns on surface-modified latex particles evaluated by two-dimensional polyacrylamide gel electrophoresis. *Electrophoresis* 14(12): 1382-1387.
 175. Gao, Z., Lukyanov, A. N., Chakilam, A. R., and Torchilin, V. P. (2003). PEG-PE/phosphatidylcholine mixed immunomicelles specifically deliver encapsulated taxol to tumor cells of different origin and promote their efficient killing. *J Drug Target* 11(2): 87-92.
 176. Krishnadas, A., Rubinstein, I., and Onyuksel, H. (2003). Sterically stabilized phospholipid mixed micelles: in vitro evaluation as a novel carrier for water-insoluble drugs. *Pharm Res* 20(2): 297-302.
 177. Lasic, D. D. (1992). Mixed micelles in drug delivery. *Nature* 355(6357): 279-280.
 178. Mulder, H. S., Dekker, H., Pinedo, H. M., and Lankelma, J. (1995). The P-glycoprotein-mediated relative decrease in cytosolic free drug concentration is similar for several anthracyclines with varying lipophilicity. *Biochem Pharmacol* 50(7): 967-974.
 179. Gallois, L., Fiallo, M., Laigle, A., Priebe, W., and Garnier-Suillerot, A. (1996). The overall partitioning of anthracyclines into phosphatidyl-containing model membranes depends neither on the drug charge nor the presence of anionic phospholipids. *Eur J Biochem* 241(3): 879-887.
 180. Papahadjopoulos, D., Nir, S., and Oki, S. (1972). Permeability properties of phospholipid membranes: effect of cholesterol and temperature. *Biochim Biophys Acta* 266(3): 561-583.
 181. Nicholas, A. R., Scott, M. J., Kennedy, N. I., and Jones, M. N. (2000). Effect of grafted poly(ethylene glycol) (PEG) on the size, encapsulation efficiency and permeability of vesicles. *Biochim Biophys Acta* 1463(1): 167-178.
 182. Silvander, M., Johnsson, M., and Edwards, K. (1998). Effects of PEG-lipids on permeability of phosphatidylcholine/cholesterol liposomes in buffer and in human serum. *Chem Phys Lipids* 97(1): 15-26.
 183. Van Echteld, C. J., De Kruijff, B., Mandersloot, J. G., and De Gier, J. (1981). Effects of lysophosphatidylcholines on phosphatidylcholine and phosphatidylcholine/cholesterol liposome systems as revealed by ³¹P-NMR, electron microscopy and permeability studies. *Biochim Biophys Acta* 649(2): 211-220.
 184. Komatsu, H., and Okada, S. (1996). Ethanol-enhanced permeation of phosphatidylcholine/ phosphatidylethanolamine mixed liposomal membranes due to ethanol-induced lateral phase separation. *Biochim Biophys Acta* 1283(1): 73-79.
 185. Komatsu, H., and Okada, S. (1995). Increased permeability of phase-separated liposomal membranes with mixtures of ethanol-induced interdigitated and non-interdigitated structures. *Biochim Biophys Acta* 1237(2): 169-175.
 186. Zeng, J., Smith, K. E., and Chong, P. L. (1993). Effects of alcohol-induced lipid interdigitation on proton permeability in L-alpha-dipalmitoylphosphatidylcholine vesicles. *Biophys J* 65(4): 1404-1414.
 187. Ueno, M. (1987). Asymmetric disposition of detergents within vesicle bilayer and its effect on ion permeation through the membrane. *Biochim Biophys Acta* 904(1): 140-144.

188. Trandum, C., Westh, P., Jorgensen, K., and Mouritsen, O. G. (2000). A thermodynamic study of the effects of cholesterol on the interaction between liposomes and ethanol. *Biophys J* 78(5): 2486-2492.
189. Barry, J. A., and Gawrisch, K. (1994). Direct NMR evidence for ethanol binding to the lipid-water interface of phospholipid bilayers. *Biochemistry* 33(26): 8082-8088.
190. Slater, S. J., Ho, C., Taddeo, F. J., Kelly, M. B., and Stubbs, C. D. (1993). Contribution of hydrogen bonding to lipid-lipid interactions in membranes and the role of lipid order: effects of cholesterol, increased phospholipid unsaturation, and ethanol. *Biochemistry* 32(14): 3714-3721.
191. Centeno, J. A., and O'Leary, T. J. (1990). Interactions of short-chain alcohols with dimyristoylphosphatidylethanolamine bilayers: a calorimetric and infrared spectroscopic investigation. *Biochemistry* 29(31): 7289-7296.
192. Rottenberg, H. (1992). Probing the interactions of alcohols with biological membranes with the fluorescent probe Prodan. *Biochemistry* 31(39): 9473-9481.
193. Chiou, J. S., Kuo, C. C., Lin, S. H., Kamaya, H., and Ueda, I. (1991). Interfacial dehydration by alcohols: hydrogen bonding of alcohols to phospholipids. *Alcohol* 8(2): 143-150.
194. Tuitou, E., Dayan, N., Bergelson, L., Godin, B., and Eliaz, M. (2000). Ethosomes - novel vesicular carriers for enhanced delivery: characterization and skin penetration properties. *J Control Release* 65(3): 403-418.
195. Wagner, A., Vorauer-Uhl, K., Kreismayr, G., and Katinger, H. (2002). Enhanced protein loading into liposomes by the multiple crossflow injection technique. *J Liposome Res* 12(3): 271-283.
196. Semple, S. C., Klimuk, S. K., Harasym, T. O., Dos Santos, N., Ansell, S. M., Wong, K. F., Maurer, N., Stark, H., Cullis, P. R., Hope, M. J., and Scherrer, P. (2001). Efficient encapsulation of antisense oligonucleotides in lipid vesicles using ionizable aminolipids: formation of novel small multilamellar vesicle structures. *Biochim Biophys Acta* 1510(1-2): 152-166.
197. Bailey, A. L., and Sullivan, S. M. (2000). Efficient encapsulation of DNA plasmids in small neutral liposomes induced by ethanol and calcium. *Biochim Biophys Acta* 1468(1-2): 239-252.
198. Ahl, P. L., Chen, L., Perkins, W. R., Minchey, S. R., Boni, L. T., Taraschi, T. F., and Janoff, A. S. (1994). Interdigitation-fusion: a new method for producing lipid vesicles of high internal volume. *Biochim Biophys Acta* 1195(2): 237-244.
199. Szoka, F., Jr., and Papahadjopoulos, D. (1978). Procedure for preparation of liposomes with large internal aqueous space and high capture by reverse-phase evaporation. *Proc Natl Acad Sci USA* 75(9): 4194-4198.
200. Charrois, G. J., and Allen, T. M. (2004). Drug release rate influences the pharmacokinetics, biodistribution, therapeutic activity, and toxicity of pegylated liposomal doxorubicin formulations in murine breast cancer. *Biochim Biophys Acta* 1663(1-2): 167-177.
201. Lagerquist, C., Beigi, F., Karlen, A., Lennernas, H., and Lundahl, P. (2001). Effects of cholesterol and model transmembrane proteins on drug partitioning into lipid bilayers as analysed by immobilized-liposome chromatography. *J Pharm Pharmacol* 53(11): 1477-1487.
202. Komatsu, H., and Rowe, E. S. (1991). Effect of cholesterol on the ethanol-induced

- interdigitated gel phase in phosphatidylcholine: use of fluorophore pyrene-labeled phosphatidylcholine. *Biochemistry* 30(9): 2463-2470.
203. Harrigan, P. R., Hope, M. J., Redelmeier, T. E., and Cullis, P. R. (1992). Determination of transmembrane pH gradients and membrane potentials in liposomes. *Biophys J* 63(5): 1336-1345.
 204. Connor, J., Yatvin, M. B., and Huang, L. (1984). pH-sensitive liposomes: acid-induced liposome fusion. *Proc Natl Acad Sci U S A* 81(6): 1715-1718.
 205. Davidsen, J., Jorgensen, K., Andresen, T. L., and Mouritsen, O. G. (2003). Secreted phospholipase A(2) as a new enzymatic trigger mechanism for localised liposomal drug release and absorption in diseased tissue. *Biochim Biophys Acta* 1609(1): 95-101.
 206. Jorgensen, K., Davidsen, J., and Mouritsen, O. G. (2002). Biophysical mechanisms of phospholipase A2 activation and their use in liposome-based drug delivery. *FEBS Lett* 531(1): 23-27.
 207. Needham, D., Anyarambhatla, G., Kong, G., and Dewhirst, M. W. (2000). A new temperature-sensitive liposome for use with mild hyperthermia: characterization and testing in a human tumor xenograft model. *Cancer Res* 60(5): 1197-1201.
 208. Madden, T. D., Harrigan, P. R., Tai, L. C., Bally, M. B., Mayer, L. D., Redelmeier, T. E., Loughrey, H. C., Tilcock, C. P., Reinish, L. W., and Cullis, P. R. (1990). The accumulation of drugs within large unilamellar vesicles exhibiting a proton gradient: a survey. *Chem Phys Lipids* 53(1): 37-46.
 209. Dubey, A. K., Eryomin, V. A., Taraschi, T. F., and Janes, N. (1996). Alcohol binding to liposomes by ²H NMR and radiolabel binding assays: does partitioning describe binding? *Biophys J* 70(5): 2307-2315.
 210. Vierl, U., Lobbecke, L., Nagel, N., and Cevc, G. (1994). Solute effects on the colloidal and phase behavior of lipid bilayer membranes: ethanol-dipalmitoylphosphatidylcholine mixtures. *Biophys J* 67(3): 1067-1079.
 211. Mou, J., Yang, J., Huang, C., and Shao, Z. (1994). Alcohol induces interdigitated domains in unilamellar phosphatidylcholine bilayers. *Biochemistry* 33(33): 9981-9985.
 212. Nambi, P., Rowe, E. S., and McIntosh, T. J. (1988). Studies of the ethanol-induced interdigitated gel phase in phosphatidylcholines using the fluorophore 1,6-diphenyl-1,3,5-hexatriene. *Biochemistry* 27(26): 9175-9182.
 213. Jain, M. K., Gleeson, J., Upreti, A., and Upreti, G. C. (1978). Intrinsic perturbing ability of alkanols in lipid bilayers. *Biochim Biophys Acta* 509(1): 1-8.
 214. Simon, S. A., and McIntosh, T. J. (1984). Interdigitated hydrocarbon chain packing causes the biphasic transition behavior in lipid/alcohol suspensions. *Biochim Biophys Acta* 773(1): 169-172.
 215. Vanderkooi, J. M. (1979). Effect of ethanol on membranes: a fluorescent probe study. *Alcohol Clin Exp Res* 3(1): 60-63.
 216. Heerklotz, H. (2001). Membrane stress and permeabilization induced by asymmetric incorporation of compounds. *Biophys J* 81(1): 184-195.
 217. Northfelt, D. W., Martin, F. J., Working, P., Volberding, P. A., Russell, J., Newman, M., Amantea, M. A., and Kaplan, L. D. (1996). Doxorubicin encapsulated in liposomes containing surface-bound poly(ethylene glycol): pharmacokinetics, tumor localization, and safety in patients with AIDS-related Kaposi's sarcoma. *J Clin Pharmacol* 36(1): 55-63.
 218. Gill, P. S., Wernz, J., Scadden, D. T., Cohen, P., Mukwaya, G. M., von Roenn, J. H.,

- Jacobs, M., Kempin, S., Silverberg, I., Gonzales, G., Rarick, M. U., Myers, A. M., Shepherd, F., Sawka, C., Pike, M. C., and Ross, M. E. (1996). Randomized phase III trial of liposomal daunorubicin versus doxorubicin, bleomycin, and vincristine in AIDS-related Kaposi's sarcoma. *J Clin Oncol* 14(8): 2353-2364.
219. Arcamone, F., Bernardi, L., Giardino, P., Patelli, B., Marco, A., Casazza, A. M., Pratesi, G., and Reggiani, P. (1976). Synthesis and antitumor activity of 4-demethoxydaunorubicin, 4-demethoxy-7,9-diepidaunorubicin, and their beta anomers. *Cancer Treat Rep* 60(7): 829-834.
 220. Ames, M. M., and Spreafico, F. (1992). Selected pharmacologic characteristics of idarubicin and idarubicinol. *Leukemia* 6(Suppl 1): 70-75.
 221. Ross, D. D., Doyle, L. A., Yang, W., Tong, Y., and Cornblatt, B. (1995). Susceptibility of idarubicin, daunorubicin, and their C-13 alcohol metabolites to transport-mediated multidrug resistance. *Biochem Pharmacol* 50(10): 1673-1683.
 222. Kuffel, M. J., Reid, J. M., and Ames, M. M. (1992). Anthracyclines and their C-13 alcohol metabolites: growth inhibition and DNA damage following incubation with human tumor cells in culture. *Cancer Chemother Pharmacol* 30(1): 51-57.
 223. Roovers, D. J., van Vliet, M., Bloem, A. C., and Lokhorst, H. M. (1999). Idarubicin overcomes P-glycoprotein-related multidrug resistance: comparison with doxorubicin and daunorubicin in human multiple myeloma cell lines. *Leuk Res* 23(6): 539-548.
 224. Testi, R., Mattii, L., Di Simone, D., Zaccaro, L., Malvaldi, G., Grassi, B., and Petrini, M. (1995). Evaluation of resistance index of several anti-cancer agents on parental and resistant P-388 cell lines. *Leuk Res* 19(4): 257-261.
 225. Berman, E., and McBride, M. (1992). Comparative cellular pharmacology of daunorubicin and idarubicin in human multidrug-resistant leukemia cells. *Blood* 79(12): 3267-3273.
 226. Wiernik, P. H., Banks, P. L., Case, D. C., Jr., Arlin, Z. A., Periman, P. O., Todd, M. B., Ritch, P. S., Enck, R. E., and Weitberg, A. B. (1992). Cytarabine plus idarubicin or daunorubicin as induction and consolidation therapy for previously untreated adult patients with acute myeloid leukemia. *Blood* 79(2): 313-319.
 227. Berman, E., Heller, G., Santorsa, J., McKenzie, S., Gee, T., Kempin, S., Gulati, S., Andreeff, M., Kolitz, J., Gabrilove, J., and *et al.* (1991). Results of a randomized trial comparing idarubicin and cytosine arabinoside with daunorubicin and cytosine arabinoside in adult patients with newly diagnosed acute myelogenous leukemia. *Blood* 77(8): 1666-1674.
 228. Martoni, A., Piana, E., Guaraldi, M., Cilenti, G., Farris, A., Saccani, F., Becchi, G., and Pannuti, F. (1990). Comparative phase II study of idarubicin versus doxorubicin in advanced breast cancer. *Oncology* 47(5): 427-432.
 229. Broggini, M., Italia, C., Colombo, T., Marmonti, L., and Donelli, M. G. (1984). Activity and distribution of iv and oral 4-demethoxydaunorubicin in murine experimental tumors. *Cancer Treat Rep* 68(5): 739-747.
 230. Penco, S., Casazza, A. M., Franchi, G., Barbieri, B., Bellini, O., Podesta, A., Savi, G., Pratesi, G., Geroni, C., Di Marco, A., and Arcamone, F. (1983). Synthesis, antitumor activity, and cardiac toxicity of new 4-demethoxyanthracyclines. *Cancer Treat Rep* 67(7-8): 665-673.
 231. Mayer, L. D., Nayar, R., Thies, R. L., Boman, N. L., Cullis, P. R., and Bally, M. B. (1993). Identification of vesicle properties that enhance the antitumour activity of

- liposomal vincristine against murine L1210 leukemia. *Cancer Chemother Pharmacol* 33(1): 17-24.
232. Mayer, L. D., Tai, L. C., Ko, D. S., Masin, D., Ginsberg, R. S., Cullis, P. R., and Bally, M. B. (1989). Influence of vesicle size, lipid composition, and drug-to-lipid ratio on the biological activity of liposomal doxorubicin in mice. *Cancer Res* 49(21): 5922-5930.
 233. Mayer, L. D., Cullis, P. R., and Bally, M. B. (1994). The use of transmembrane pH gradient-driven drug encapsulation in the pharmacodynamic evaluation of liposomal doxorubicin. *Journal of Liposome Research* 4(1): 529-553.
 234. Mui, B. L., Cullis, P. R., Evans, E. A., and Madden, T. D. (1993). Osmotic properties of large unilamellar vesicles prepared by extrusion. *Biophys J* 64(2): 443-453.
 235. Shabbits, J. A., and Mayer, L. D. (2002). P-glycoprotein modulates ceramide-mediated sensitivity of human breast cancer cells to tubulin-binding anti-cancer drugs. *Mol Cancer Ther* 1(3): 205-213.
 236. Mosmann, T. (1983). Rapid colorimetric assay for cellular growth and survival: application to proliferation and cytotoxicity assays. *J Immunol Methods* 65(1-2): 55-63.
 237. Lim, H. J., Masin, D., McIntosh, N. L., Madden, T. D., and Bally, M. B. (2000). Role of drug release and liposome-mediated drug delivery in governing the therapeutic activity of liposomal mitoxantrone used to treat human A431 and LS180 solid tumors. *J Pharmacol Exp Ther* 292(1): 337-345.
 238. Bogush, T., and Robert, J. (1996). Comparative evaluation of the intracellular accumulation and DNA binding of idarubicin and daunorubicin in sensitive and multidrug-resistant human leukaemia K562 cells. *Anti-cancer Res* 16(1): 365-368.
 239. Bennis, S., Faure, P., Chapey, C., Hu, Y. P., Fourche, J., El Yamani, J., and Robert, J. (1997). Cellular pharmacology of lipophilic anthracyclines in human tumor cells in culture selected for resistance to doxorubicin. *Anti-cancer Drugs* 8(6): 610-617.
 240. Deffie, A. M., Alam, T., Seneviratne, C., Beenken, S. W., Batra, J. K., Shea, T. C., Henner, W. D., and Goldenberg, G. J. (1988). Multifactorial resistance to adriamycin: relationship of DNA repair, glutathione transferase activity, drug efflux, and P-glycoprotein in cloned cell lines of adriamycin-sensitive and -resistant P388 leukemia. *Cancer Res* 48(13): 3595-3602.
 241. McPherson, J. P., Deffie, A. M., Jones, N. R., Brown, G. A., Deuchars, K. L., and Goldenberg, G. J. (1997). Selective sensitization of adriamycin-resistant P388 murine leukemia cells to antineoplastic agents following transfection with human DNA topoisomerase II alpha. *Anti-cancer Res* 17(6D): 4243-4252.
 242. Hertel, L. W., Kroin, J. S., Misner, J. W., and Tustin, J. M. (1988). Synthesis of 2-deoxy-2,2-difluoro-D-ribose and 2-deoxy-2,2-difluoro-D-ribofuranosyl nucleosides. *J Org Chem* 53:2406-2409.
 243. Heinemann, V., Xu, Y. Z., Chubb, S., Sen, A., Hertel, L. W., Grindey, G. B., and Plunkett, W. (1990). Inhibition of ribonucleotide reduction in CCRF-CEM cells by 2',2'-difluorodeoxycytidine. *Mol Pharmacol* 38(4): 567-572.
 244. Gandhi, V., and Plunkett, W. (1990). Modulatory activity of 2',2'-difluorodeoxycytidine on the phosphorylation and cytotoxicity of arabinosyl nucleosides. *Cancer Res* 50(12): 3675-3680.
 245. Huang, P., Chubb, S., Hertel, L. W., Grindey, G. B., and Plunkett, W. (1991). Action of 2',2'-difluorodeoxycytidine on DNA synthesis. *Cancer Res* 51(22): 6110-6117.
 246. Merriman, R. L., Hertel, L. W., Schultz, R. M., Houghton, P. J., Houghton, J. A.,

- Rutherford, P. G., Tanzer, L. R., Boder, G. B., and Grindey, G. B. (1996). Comparison of the antitumor activity of gemcitabine and ara-C in a panel of human breast, colon, lung and pancreatic xenograft models. *Invest New Drugs* 14(3): 243-247.
247. Steinherz, P. G., Seibel, N. L., Ames, M. M., Avramis, V. I., Krailo, M. D., Liu-Mares, W., Reid, J. M., Safgren, S. L., and Reaman, G. H. (2002). Phase I study of gemcitabine (difluorodeoxycytidine) in children with relapsed or refractory leukemia (CCG-0955): a report from the Children's Cancer Group. *Leuk Lymphoma* 43(10): 1945-1950.
248. Comella, P., Panza, N., Manzione, L., De Cataldis, G., Cioffi, R., Maiorino, L., Lorusso, V., Lamberti, A., Micillo, E., Natale, M., Bilancia, D., Nicoletta, G., Di Nota, A., Mancarella, S., Frasci, G., and Comella, G. (2000). Interim analysis of a phase III trial comparing cisplatin, gemcitabine, and vinorelbine vs. either cisplatin and gemcitabine or cisplatin and vinorelbine in advanced non small-cell lung cancer. A Southern Italy Cooperative Oncology Group Study. *Clin Lung Cancer* 1(3): 202-207; discussion 208.
249. Novarino, A., Chiappino, I., Bertelli, G. F., Heouaine, A., Ritorto, G., Addeo, A., Bellone, G., Merlano, M., and Bertetto, O. (2004). Phase II study of cisplatin, gemcitabine and 5-fluorouracil in advanced pancreatic cancer. *Ann Oncol* 15(3): 474-477.
250. Brodowicz, T., Kostler, W. J., Moslinger, R., Tomek, S., Vaclavik, I., Herscovici, V., Wiltshcke, C., Steger, G. G., Wein, W., Seifert, M., Kubista, E., and Zielinski, C. C. (2000). Single-agent gemcitabine as second- and third-line treatment in metastatic breast cancer. *Breast* 9(6): 338-342.
251. Mutch, D. G. (2003). Gemcitabine combination chemotherapy of ovarian cancer. *Gynecol Oncol* 90(2 Pt 2): S16-20.
252. von der Maase, H., Hansen, S. W., Roberts, J. T., Dogliotti, L., Oliver, T., Moore, M. J., Bodrogi, I., Albers, P., Knuth, A., Lippert, C. M., Kerbrat, P., Sanchez Rovira, P., Wersall, P., Cleall, S. P., Roychowdhury, D. F., Tomlin, I., Visseren-Grul, C. M., and Conte, P. F. (2000). Gemcitabine and cisplatin versus methotrexate, vinblastine, doxorubicin, and cisplatin in advanced or metastatic bladder cancer: results of a large, randomized, multinational, multicenter, phase III study. *J Clin Oncol* 18(17): 3068-3077.
253. Hertel, L. W., Boder, G. B., Kroin, J. S., Rinzel, S. M., Poore, G. A., Todd, G. C., and Grindey, G. B. (1990). Evaluation of the antitumor activity of gemcitabine (2',2'-difluoro-2'-deoxycytidine). *Cancer Res* 50(14): 4417-4422.
254. Bouffard, D. Y., Momparler, L. F., and Momparler, R. L. (1991). Comparison of antineoplastic activity of 2',2'-difluorodeoxycytidine and cytosine arabinoside against human myeloid and lymphoid leukemic cells. *Anti-cancer Drugs* 2(1): 49-55.
255. Heinemann, V., Hertel, L. W., Grindey, G. B., and Plunkett, W. (1988). Comparison of the cellular pharmacokinetics and toxicity of 2',2'-difluorodeoxycytidine and 1-beta-D-arabinofuranosylcytosine. *Cancer Res* 48(14): 4024-4031.
256. Possinger, K. (1995). Gemcitabine in advanced breast cancer. *Anti-cancer Drugs* 6 Suppl 6(55-59).
257. Pollera, C. F., Ceribelli, A., Crecco, M., and Calabresi, F. (1994). Weekly gemcitabine in advanced or metastatic solid tumors. A clinical phase I study. *Invest New Drugs* 12(2): 111-119.
258. Gatzemeier, U., Shepherd, F. A., Le Chevalier, T., Weynants, P., Cottier, B., Groen, H. J., Rosso, R., Mattson, K., Cortes-Funes, H., Tonato, M., Burkes, R. L., Gottfried, M., and Voi, M. (1996). Activity of gemcitabine in patients with non-small cell lung cancer:

- a multicentre, extended phase II study. *Eur J Cancer* 32A(2): 243-248.
259. Anderson, H., Lund, B., Bach, F., Thatcher, N., Walling, J., and Hansen, H. H. (1994). Single-agent activity of weekly gemcitabine in advanced non-small-cell lung cancer: a phase II study. *J Clin Oncol* 12(9): 1821-1826.
 260. Abratt, R. P., Bezwoda, W. R., Goedhals, L., and Hacking, D. J. (1997). Weekly gemcitabine with monthly cisplatin: effective chemotherapy for advanced non-small-cell lung cancer. *J Clin Oncol* 15(2): 744-749.
 261. Jassem, J. (2003). Gemcitabine and anthracyclines in breast cancer. *Semin Oncol* 30(2 Suppl 3): 11-14.
 262. Waud, W. R., Gilbert, K. S., Grindey, G. B., and Worzalla, J. F. (1996). Lack of in vivo crossresistance with gemcitabine against drug-resistant murine P388 leukemias. *Cancer Chemother Pharmacol* 38(2): 178-180.
 263. Peters, G. J., van der Wilt, C. L., van Moorsel, C. J., Kroep, J. R., Bergman, A. M., and Ackland, S. P. (2000). Basis for effective combination cancer chemotherapy with antimetabolites. *Pharmacol Ther* 87(2-3): 227-253.
 264. Moog, R., Burger, A. M., Brandl, M., Schuler, J., Schubert, R., Unger, C., Fiebig, H. H., and Massing, U. (2002). Change in pharmacokinetic and pharmacodynamic behavior of gemcitabine in human tumor xenografts upon entrapment in vesicular phospholipid gels. *Cancer Chemother Pharmacol* 49(5): 356-366.
 265. Chou, T. C., Motzer, R. J., Tong, Y., and Bosl, G. J. (1994). Computerized quantitation of synergism and antagonism of taxol, topotecan, and cisplatin against human teratocarcinoma cell growth: a rational approach to clinical protocol design. *J Natl Cancer Inst* 86(20): 1517-1524.
 266. Abraham, S. A., McKenzie, C., Masin, D., Ng, R., Harasym, T. O., Mayer, L. D., and Bally, M. B. (2004). In vitro and in vivo characterization of doxorubicin and vincristine coencapsulated within liposomes through use of transition metal ion complexation and pH gradient loading. *Clin Cancer Res* 10(2): 728-738.